CONCRETE BEAMS WITH STIRRUPS

SUBJECT TO

TORSION, SHEAR AND BENDING

by

OTHMAN AHMAD A JOLLA

Thesis submitted for the degree of
Doctor of Philosophy

Department of Civil Engineering
The University of Aston in Birmingham

September 1980

TO MY MOTHER AND FAMILY

SUMMARY

by

OTHMAN AHMAD A JOLLA

for

The Degree of Doctor of Philosophy

1980

This thesis examines experimentally and theoretically the behaviour and ultimate strength of rectangular reinforced concrete members under combined torsion, shear and bending.

The experimental investigation consists of the test results of 38 longitudinally and transversely reinforced concrete beams subjected to combined loads, ten beams of which were tested under pure torsion and self weight. The behaviour of each test beam from application of the first increment of load until failure is presented. The effects of concrete strength, spacing of the stirrups, the amount of longitudinal steel and the breadth of the section on the ultimate torsional capacity are investigated.

Based on the skew-bending mechanism, compatibility, and linear stress-strain relationship for the concrete and the steel, simple rational equations are derived for the three principal modes of failure for the following four types of failure observed in the tests:

TYPE I   Yielding the reinforcement, at failure, before crushing the concrete.
TYPE II Yielding of the web steel only, at failure, before crushing the concrete.
TYPE III Yielding of the longitudinal steel only, at failure, before crushing the concrete.
TYPE IV Crushing of the concrete, at failure, before yielding of any of the reinforcement.

This investigation shows that the interaction equation, $(T/T_u)^2 + (V/V_u)^2 + M/M_u = 1$, describes the ultimate capacity adequately only where the complete yielding of the reinforcement occurs

For the types of failure above other than yielding the concrete in the shear compression zone is involved. The stresses in this zone are combined using Cowan's simplified failure criterion for concrete under combined stresses. This criterion is simplified further in order to obtain a relationship between resultant shear torsional stresses, f_v, and cylinder compression strength of concrete, f_c', independent of the bending stress, f_m, as $f_v = \xi.f_c'$.

The theoretical solutions are compared with 515 test beams, including the author's and reasonable agreement is obtained.

Keywords: beams; stirrups; torsion; shear; bending

ACKNOWLEDGEMENTS

THE AUTHOR

The author graduated from the Department of Civil Engineering
at the University of Sulaimaniyah, Sulaimaiy, Iraq in 1973. He
spent the following year as a construction and building materials
engineer. Since September 1975 the author has been engaged as a
postgraduate research student in the Department of Civil Engineering
at the University of Aston in Birmingham, and the work presented
in this thesis has been carried out during this period.

No part of this work has been submitted in support of an
application for another degree or qualification.

LIST OF CONTENTS

LIST OF TABLES

LIST OF FIGURES

LIST OF PLATES

Subscripts

    1 refers to mode 1 failure.

    2 refers to mode 2 failure.

    3 refers to mode 3 failure.

    y refers to complete yield.

    w refers to yielding of web steel only.

    ℓ refers to yielding of longitudinal steel only.

    c refers to crushing of the concrete.

    i refers to inclined to the actual orientation.

A_b half of the total area of the longitudinal reinforcement near the bottom face of the section.

A_r angular rotation.

A_s half of the total area of the longitudinal reinforcement in one of the sides of the section.

A_t half of the total area of the longitudinal reinforcement near the top face of the section.

A_w area of one leg of the web reinforcement.

b   breadth of the section.

$C_{(1,2,3)}$ a parameter which relates the reinforcement ratio to the inclination of the failure surface for different modes.

$d_{(1,2,3)}$ effective depth to the tension reinforcement for different modes.

d_m deflection.

$dn_{(1,2,3)}$ depth of shear-compression zone for different modes.

e   eccentricity of the torsional load.

$e_{(1,2,3)}$ an arbitrary point in the tension zone through which moment is considered.

E_c modulus of elasticity of concrete.

E_s modulus of elasticity of steel.

f_b actual direct stress in the bottom longitudinal bars.

f_{by} yield strength of the bottom longitudinal bars.

f'_c uniaxial cylinder crushing strength of concrete.

f_{cu} characteristic concrete cube crushing strength.

$fm_{(1,2,3)}$ direct bending stress in the concrete due to the flexural moment for different modes.

$fm_{i(1,2,3)}$ skew-bending stress in the concrete due to flexural torsion and shear for different modes.

f_r modulus of rupture of the concrete.

f_s actual direct stress of the longitudinal bars in the highly tensioned side of the beam.

f_{sp} cylinder splitting tensile strength of concrete.

f_{sy} yield strength of the side longitudinal bars.

f_t actual direct stress in the top longitudinal bars.

f_{ty} yield strength of the top longitudinal bars.

$fv_{(1,2,3)}$ resultant shear stress in the concrete due to torsion and shear for different modes.

$F_{i(i,2,3)}$ compressive force of the concrete normal to the θ-plane in the shear-compression zone for different modes.

$F'_{i(1,2,3)}$ tensile force of the reinforcement normal to θ-plane in the tension zone for different modes.

h height of the section.

Kd a factor associated with cracking of the section.

Km direct bending stress distribution coefficient for the concrete in the shear-compression zone.

Km_i bending stress distribution coefficient for the concrete, normal to the θ-plane.

K_s depth to the resultant force coefficient for concrete in the shear-compression zone.

K_v average shear stress distribution coefficient for the concrete in the shear-compression zone.

m modular ratio.

M applied bending moment in the presence of torsion and shear.

P applied bending load.

$r_{(1,2,3)}$ ratio of the force on the web steel to the force in the longitudinal bars in the tension zone for different modes.

$R_{(1,2,3)}$ the lever arm to the resultant shear force in the shear-compression zone for different modes.

s centre to centre spacing of the closed stirrups, measured along the longitudinal axis of the beam.

S_t experimental torsional stiffness of the member.

T applied torsional moment in the presence of bending and shear.

V shear force in the beam in presence of bending and torsion.

x width of the closed stirrup.

y depth of the closed stirrup.

$\alpha_{(1,2,3)}$ angle of inclination of tensile cracks of the failure section for different modes of types of failure other than yielding.

δ applied shear force to torsional moment (V/T).

θ angle of inclination of the shear-compression zone in the concrete.

ξ combined stress coefficient varying between 0.20-0.25.

$\rho_{(1,2,3)}$ tension steel ratio for different modes.

ψ applied bending moment to torsional moment ratio (M/T).

CHAPTER ONE

REVIEW OF PREVIOUS WORK

1.1 INTRODUCTION

The rapid development in modern technology, advance in science and a reduction in load factors, makes it less justifiable for a structural engineer to consider torsion as a secondary effect in design.

Since the beginning of the second half of this century, a considerable amount of experimental data has been accumulated and different empirical and rational expressions have been introduced in relation to concrete members subjected either to pure torsion or in combined torsion, bending and shear. The information required for the design of structures subject to torsion, still remains incomplete.

The establishment of ACI-Committee 438, Torsion, in 1958 by the American Concrete Institute undoubtedly stimulated more concern by researchers and engineers. Two very beneficial contributions by this committee were the publication of "Torsion of Structural Concrete', SP-18 [1] in 1968, and the review of code of practice by committee members Fisher and Zia [2] in 1964. They reviewed the code of practice for 22 countries and showed the scarcity of knowledge on torsion requirements for the design of concrete members.

Various theories are available in the current literature to check the strength and behaviour of concrete members subject to torsion. They can be classified mainly into three categories. The first category is "empirical formulas", which enable the strength to be determined, based on experimental observations. This method

was initiated by Turner and Davies [3] in 1934. The fact that the establishment of these formulae depends on very limited experimental tests affects their reliability in practice [4]. The second category is "Rational methods" or sometimes described as "Stress methods". The common agreement between these theories is that the torsional strength of a reinforced concrete member is the sum of the torque resisted by the concrete based on the elastic theory, and the torque resisted by the transverse steel. The main disagreement in these theories is the proportion of the torque which is carried by the concrete and the proportion resisted by the reinforcement. A criticism of this method is that it does not take care of the continual readjustments of strains in the internal equilibrium brought about by continual propagation of the cracks in the member [5]. Anderson [6] was the first to introduce this method. The third category is the "Analytical method" or alternatively known as the "Failure-mechanism method", which includes the "Truss-analogy method". One approach in this method considers the equilibrium conditions of the external and internal loads at a failure section, assuming the yielding of all reinforcement crossing this section. This assumption contradicts with many experimental results reported in literature [6, 7, 8, 9, 10 and 11]. This approach was introduced in 1958 by Lessig [8] in the Soviet Union. A different approach, however, was developed in 1929 by a German engineer called Rausch [12]. This approach corresponds to the space truss-analogy concept, where the reinforcement act as the tension members and the concrete struts between the cracks act as compression diagonals. Again the customary assumption of yielding the reinforcement at failure section is assumed in this approach.

2

In order to obtain a clear knowledge of the state of research in this field, therefore, a literature review of the previous work has been carried out. The plain concrete beams in torsion will be discussed briefly, not because they occur in practice but becuase they provide the basis for many of the existing torsional theories. This will be followed by concrete beams reinforced with longitudinal steel only. The case of fully reinforced rectangular concrete beams under torsion alone and in conjunction with other loads is reviewed in some detail later, and is the main concern of this thesis.

1.2 PLAIN CONCRETE RECTANGULAR BEAMS

When a plain concrete beam is subjected to pure torsion, failure occurs when the maximum torsional shear stress exceeds maximum tensile strength of the concrete. There are however different opinions about the distribution of the stress in the section at failure. Marshall [13] in 1944, proposed that the perfectly plastic stress distribution could be used to determine these stresses in the concrete section. Cowan [14] in 1950 recommended that the elastic theory, based on St Venant's hypothesis and stress distribution, could be applied to evaluate these stresses.

In general the plastic theory overestimates and the elastic theory underestimates the strength of plain concrete members in torsion, since the concrete behaviour is neither fully plastic nor linearly elastic. To account for elasto-plastic behaviour of concrete, Turner and Davies [3] in 1934 developed a theory on the basis of idealized non-linear stress-strain relationship for concrete in compression. They analysed circular cross sections and modified the analysis for rectangular concrete sections later.

3

Iyengar and Rangan [15] assumed that the torque resisted by the concrete was simply the mean value of the torque capacities as given by both elastic and fully-plastic theories.

Zia [4] has shown, however, that the Turner and Davies theory is not valid for rectangular sections when the ratio of the height to width exceeds 2.5. After comparing the strength obtained from test results and the stress calculated by plastic and elastic theories, Hall and Archer [16] stated that the plastic theory allowed failure to be predicted in terms of stress parameters which were approximately constant for a given concrete.

In the theories above the failure surface is described as tensile cracks with a fracture forming a helix around the sides at an inclination of 45° to the longitudinal axis of the beam. However Hsu [17] from his experimental observations concluded that failure of rectangular plain concrete section in pure torsion was one of bending on a skewed failure plane rather than one of torsion, with a compression hinge forming on a larger side. This type of failure was first recognized by Lessig [8] for reinforced concrete members subject to torsion. That conclusion lead Hsu to develop a theory, assuming a linear stress distribution on the inclined failure surface, to predict the torsional strength of plain concrete rectangular beams. Hsu found that the minimum value of the torsional capacity would occur when the angle of inclination of the failure surface was 45° with the longitudinal axis of the beam.

Martin [18] in 1973 extended the above theory, using compatibility stress-strain relationship, and resolving moment of forces about the neutral axis at the failure section derived an equation for plain concrete rectangular beams in torsion.

4

The various equations for pure torsion obtained by the different investigators mentioned above can be written in one single familiar form for torsional shear stress for concrete τ with variation only in the value of torsional factor β for different investigators as follows:

$$\tau = T_p/\beta \cdot B^2 D \qquad\qquad (1.1)$$

where

τ = maximum torsional shear stress

T_p = the ultimate torsional strength of plain concrete

B = width of the section

D = depth of the section

β = torsional factor

Marshal [13] suggested that the value of torsional factor β varies from 0.333-0.500, depending on the ratio of D/B, and can be calculated from the expression $\beta_p = 1/2 \cdot (1-B/3D)$. Cowan [14] used St Venant's factor, which varies from 0.200 to 0.333 depending on the ratio of D/B. Turner and Davies [3], however, presented an expression which gives a value for this factor lower than obtained by plastic and higher than obtained by elastic theories. It is a function of St Venant's torsional factor, and can be approximated by the expression $\beta_{ep} \simeq 1.491 \cdot \beta_e$. Hsu [17] found β theoretically to be a constant and equal to 0.333. But Martin [18] again theoretically showed that this factor is a function of the ratio of D/B, and can be found from the expression $\beta_m = 1/(3 + \sqrt{B/D})$.

Any particular value of torsional factor β, given by a particular investigator above, appears to be valid, as long as a reasonable value can be obtained for ultimate torsional strength τ.

5

Classical theories interpretate τ as maximum principal tensile stress, which is approximately equal to the uniaxial tensile strength of concrete f_t. Iyenger and Rangan using a failure criterion for concrete under compressive-tensile stresses found a relation between τ and f_t which was a function of the ratio of f'_c/f_t. Hsu however used reduced modulus of rupture $(0.85 \cdot f_r)$. Since modulus of rupture tests are rarely performed in practice, therefore, he latter expressed f_r in terms of compressive strength f'_c. To obtain the relationship, he performed a more elaborate approach, by making use of the straight-line simplification of Mohr's theory, and some of his test results. The expression is a function of the dimension of the cross-section as well as f'_c. The nature of it is complicated and needs to be revised in a more logical way. Martin believes that the failure of a plain concrete section will occur when τ reaches the modulus of rupture of the concrete.

It seems there are still different conceptions concerning the magnitude and the distribution of ultimate stress at failure. A logical equation, therefore, which gives a value of torsional strength of a rectangular plain concrete member higher than the value obtained by the elastic theory and lower than that obtained by the plastic theory will be acceptable.

Cowan [7] appears to be the first to consider the strength of plain concrete rectangular section under combined action of bending and torsion. Assuming the maximum tensile stress criterion for failure, the elasto-plastic stress distribution for moments, and a full plastic stress distribution for torsion, he developed a theory which considered the interaction of bending and torsion. This interaction equation can be written in the following general

6

non-dimensional form;

$$(T/T_p)^2 + (M/M_p)^2 = 1 \tag{1.2}$$

where

    T = torsional moment in combined torsion and bending

    T_p = ultimate torsional strength for plain concrete rectangular

        section, in pure torsion, using fully plastic theory.

    M = flexural moment in combined torsion and bending.

    M_p = ultimate flexural strength of plain concrete rectangular

        section in pure bending, which is equal to $1/4.23BD^2f_t$.

Walsh et al [19] in 1966, using plastic stress distribution
for both torsion and bending, compared some of their test results
with the principal tensile stress and principal shear stress
criteria. They concluded that the principal tensile stress
criterion was an adequate failure criterion for concrete under tor-
sion and bending, and suggested the following interaction formula;

$$(T/T_p)^2 + M/M_p = 1 \tag{1.3}$$

Zia [4] showed theoretically that for plain concrete members
the presence of torsion reduces the bending capacity, and like-
wise, the torsional capacity is rapidly reduced by the simultaneous
action of bending.

Using skew-failure mechanism, Martin [18] appears to be the
first to derive theoretical equations for the three modes of
failure, namely modes 1, 2 and 3 for rectangular plain concrete
members in combined torsion and bending. The interaction equation
obtained by Martin is in the same form as Equation (1.2), but
with different values for T_p and M_p. Martin obtained a reasonable
agreement between the strength predicted by his theory and those
recorded from the experiment for a considerable number of test

7

results.

1.3 CONCRETE MEMBERS WITH LONGITUDINAL STEEL ONLY

Many investigators [3, 6, 14, 15, 19, 20] deduced that the
strength of rectangular concrete members reinforced with longitudinal
steel only, and subject to pure torsion, was no different from
those of plain concrete beams. In some cases higher strength [21,
22] for reinforced members have been reported. Hsu [23] suggested
that beams reinforced with longitudinal steel only may be conserv-
ately considered as plain concrete members when calculating the
strength. This suggestion, however, appears to be unsafe, since
lower strength is also apparent [24]. Cowan [14] suggested that,
by adding the transformed area of the reinforcement to the concrete
area, the higher strength may be accounted for. Iyengar and Rangan
[15] showed that the capacity increased only by 12%, and therefore
suggested that the contribution of the longitudinal steel to the
torsional capacity of the member was small.

The first series of experimental results and theoretical
solution in torsion and bending for longitudinally reinforced
beams was presented by Nylander [25] in 1945. In this work, he
assumed that the applied torsional moment was resisted partly by
the concrete in the uncracked zone of the section, and partly by
transverse shear forces in the longitudinal steel. He also assumed
that at failure the steel reached its yield strength under the
action of combined stresses produced by shear stress due to torsion
and direct stress due to bending. Nylander combined these stresses
according to Huber-Beltramis' criterion. This theory in some cases
overestimates the torsional strength because the condition is not
always guaranteed.

Gesund and Boston [22] deduced from the examination of their tests that failure of concrete members without web reinforcement occurred due to dowel action. The effect of this dowel force is to spall the concrete cover to the steel at the corners, and eventually to produce failure. The theoretical solution was complex, and is applicable only to the type of beams containing the type of steel used in their tests. Difficulties were experienced in determining the spalling force, which is an important factor in their equation.

Failing to obtain a rational method to calculate the torsional capacity of members with longitudinal steel only, in combined torsion and bending, Walsh et al [19] in 1966 confirmed that the torsional strength, for design purposes, could be estimated by their empirical equation for plain concrete proposed earlier [26]. The equation can be written in imperial units as follows;

$$T = 1.75 \cdot B^2 \cdot (D-B/3) \cdot \sqrt{f'_c} \tag{1.4}$$

Hsu [27] in 1968 developed an interaction curve for torsion and bending empirically. He found that interaction between torsion and bending occurred in the range of $0.5 < M/M_u \leq 1.0$, particularly for square sections. Hsu, therefore, defined the interaction curve for concrete beams without web steel, conservatively by three straight-lines, as:

$$T/T_u = 1.0 \qquad \text{for } M/M_u \leq 0.5$$

$$T/T_u + 1.4 \cdot (M/M_u) = 1.7 \qquad \text{for } 0.5 < M/M_u \leq 1.0 \tag{1.5}$$

$$M/M_u = 1.0 \qquad \text{for } T/T_u < 0.3$$

Where T_u was the ultimate strength in pure torsion and calculated from his equation for plain concrete [17]. M_u was the

ultimate strength in pure bending, obtained from the ACI Code 318-63 equation for rectangular beams with tension reinforcement only.

Analysing a large number of quarter-scale test results, Mirza and McCutcheon [28] decided that for rectangular members under bending and torsion the shape of interaction curve depended on the proportion of longitudinal steel. Also this interaction may be enveloped by a rectangular curve as $T/T_u = 1.0$, and $M/M_u = 1.0$.

Martin [18], using skew-failure mechanism method and adopting two different approaches, obtained a rational interaction relationship between torsional and bending moments for this type of concrete member . In the first approach he assumed that the failure was controlled by the reduced compressive strength due to combined flexural stress and torsional shear stress. A dowel force was assumed to act at a right angle to the tension steel to balance shear force due to torsional shear stress in the compression zone. Later he combined the direct bending stress and the torsional shear stress using Cowan's failure criterion of concrete in compression. The resulting general interaction equation can be expressed for mode one as:

$$(T_1/T_{u1})^2 + (2M_1/M_{u1})^2 - (3M_1/M_{u1}) = 1 \qquad (1.6)$$

where

M_{u1} = ultimate bending moment in pure bending, which is
equal to $(2/3)$ $B \cdot dn_1 \cdot la_1 \cdot f'_c$

T_{u1} = ultimate torsional moment in pure torsion, and is
equal approximately to $0.2 \cdot M_{u1}$

Involved in Equation (1.6) is the depth of compression zone dn_1. By resolving the forces in the skew failure plane, assuming

linear stress distribution and linear stress-strain relationship
for both the steel and the concrete, he obtained an expression to
find dn . Comparing this equation with some test results, he
obtained a mean value of T_{test}/T_{theory} of 1.01 with coefficient
of variation of 5%.

An alternative form of failure was based on the yielding of
the reinforcement. He assumed that failure occurred when the
steel reached its definite yield strength. In this approach
account was taken of moment of forces about two perpendicular
axes passing through a point in the concrete compression zone,
assuming that the tension steel is subjected to a direct stress
due to flexure and a shear stress produced by the dowel action in
the steel. Using the Huber-Von Mises-Hencky shear distortion
strain energy criterion for steel, he combined these two stresses,
and obtained an equation which related torsion to bending. The
final general non-dimensional interaction form in mode 1 was
expressed as:

$$(T_1/T_{y1})^2 + (M_1/M_{y1})^2 = 1 \qquad\qquad (1.7)$$

where

M_{y1} = ultimate bending capacity in pure bending, and is
equal to $2 \cdot A\ell \ f\ell_y \cdot La_{y1}$.

T_{y1} = ultimate torsional capacity in pure torsion, and can
be obtained by $M_{y1}/\sqrt{3}$

Comparing this equation with 14 test results he obtained a
mean value of T_{test}/T_{theory} of 1.17 with coefficient of variation
of 11%.

When torsion is predominant, however, the torsional load does

not increase beyond the value of the first crack, but decreases gradually as more cracks develop. Therefore he suggested that it was reasonable to calculate the ultimate torsional strength of concrete members without web steel, using the ultimate strength equation for plain concrete members in pure torsion, as in section 1.2.

Series of beams were designed and tested in combined torsion, bending and shear by Birkeland [21] in 1965 to supplement Nylander's work. Using a more practical reinforcement ratio, and varying the beam length, he studied the effect of shear span to depth ratio as well as the effect of extensive cracking on the diagonal tension failure under combined loading. He deduced from the tests that the shear span to depth ratio did not affect the existing interaction relation of torsion and shear. For members without web reinforcement, which fail by diagonal tension failure, this interaction can be described as a circular arc defined by,

$$(V/V_u)^2 + (T/T_u)^2 = 1.0 \tag{1.8}$$

where

V = applied shear force in combined torsion, bending and shear.

V_u = ultimate shear strength in combined bending and shear only.

Two years later this equation was confirmed by Mattock et al [29] after analysing a number of beams tested in torsion, bending and shear. They concluded that the strength of this type of beams in shear gradually reduced as torsion increased, and conversly the torsional strength reduced as shear increased. They also observed that the interaction between torsion and shear was

12

not influenced by the magnitude of the moment to shear ratio, and can be expressed in the same form as Equation (1.8). No expressions are given to calculate V_u or T_u, since they use direct test value for V_u and extrapolated value from the interaction curve for T_u.

Hsu [27] realized that the two-dimensional torsion shear interaction curve, proposed earlier, can not truely portray the actual combined strength behaviour of members under three different types of loads (i.e. torsion, bending and transverse shear). The interaction must, therefore, be expressed in three-dimensional rectangular coordinate system, each axis representing one type of applied load. The strength of a member exposed to a combined torsion, bending and shear force is then represented by a point on an interaction surface. This surface is defined by the three mutually perpendicular axes, representing the nondimensional para-meters, T/T_u, M/M_u and V/V_u. The intersection of this surface with T/T_u, M/M_u plane is the torsion-bending interaction curve, and with M/M_u, V/V_u plane is the combined ultimate strength equation in shear and bending proposed by ACI-ASCE Committee [30].

Having adopted torsion-bending and shear-bending interaction curves, the interaction surface is then described by a series of torsion-shear curves between these two boundaries. This enabled Hsu to express a series of interaction curves by one general equation representing the interaction surface, which can be expressed as:

$$(T/T_{ub})^m + (V/V_{cb})^n = 1.0 \tag{1.9}$$

where

    m, n = exponents to be determined from the tests

    T_{ub} = ultimate torque in combined torsion and bending

    V_{cb} = shear strength based on cracking strength in combined

13

shear and bending.

Depending on a number of other's test results, Hsu suggested a conservative interaction surface for design purposes, with $m = 2$, $n = 1$ for $M/M_u \leq 0.5$, and $m = 2$, $n = 2$ for $0.5 < M/M_u \leq 1.0$. This means the parabola for the former and the circle for the latter, with a discontinuity in the surface at the plane of $M/M_u = 0.5$. This discontinuity may be considered as a criticism.

Mirza and McCutchoen [28] deduced from the study of tests on small scale specimens that the longitudinal steel in rectangular members under that type of loading had a significant effect in increasing the flexural shear strength, whereas its effect on torsional strength was small. Following Hsu [27] they obtained an interaction surface for test results in combined torsion, bending and shear. Their conclusion, however, needs to be considered with caution, since there is always a possibility that the model specimens and full size members behave differently.

Where all the interaction equations for torsion, bending and shear are compared, Hsu's method is considered to be simple and convenient for design practice.

1.4 RECTANGULAR CONCRETE MEMBERS REINFORCED WITH LONGITUDINAL AND TRANSVERSE STEEL

1.4.1 Pure Torsion

Rausch [12] in 1929 assumed the yielding of the reinforcement, and was the first to derive a rational equation to calculate the strength of fully reinforced rectangular beams subjected to pure torsion. He employed the truss analogy method and assumed that the whole of the torque was resisted by the reinforcement and non by the concrete.

In 1937 Anderson [31] developed his equation for the torsional strength of a circular section with spiral reinforcement at 45° along the span. Later he transformed this for a rectangular section, by making use of equivalent cross-sectional area. The agreement between the theory and the tests was good, except for beams with a low percentage of spiral reinforcement. The reason for this may have been due to the assumption in which the steel resists the part of torsional shear stress in excess of the maximum stress carried by the plain concrete member. Anderson also noted that the torsional strength increased with increase in compressive strength of the concrete.

Based on the elastic concept Cowan [14] in 1950 developed a rational theory, using St. Venant stress distribution. The solution put forward by Cowan was obtained by equating the work done by the torsional moment of the strain energy stored in the beam. The total strain energy was assumed to be divided equally between the compressive strain energy of the concrete and the tensile strain energy in the reinforcement. However, he clearly pointed out that the reinforcement was elastic almost up to failure and the beam sometimes failed before the steel yielded.

Ernst [20], after testing a series of beams with vertical close stirrup in 1957, reported that for most of his beams the failure occurred by yielding both the longitudinal and transverse steel, even though the ratio of web to main reinforcement was not unity.

Adopting some of Cowan's equations and assuming that the forces in the closed stirrups alone resist the entire torsional moment, Ernst obtained an equation for the ultimate torsional resistance.

An alternative equation was proposed by Iyengar and Rangan [15] in 1968, which was similar to the previous theory. The torsional resistance of such a beam was assumed to be approximately equal to the sum of the torque resisted by the concrete plus the torque resisted by the transverse reinforcement. Adopting a failure criterion for concrete subjected to compressive and tensile stresses, and assuming that the compression zone was subjected to both torsional and direct stresses, the shear stress was related to the uniaxial tensile strength of the concrete.

The main general agreement between the above theories is that the torsional strength of a reinforced concrete member is the total of the strength carried by the concrete and the strength resisted by the reinforcement, which is expressed in the following form:

$$T_u = T_c + T_s$$

or

$$T_u = T_c + k \cdot \frac{A_s \cdot f_{sy}}{s} \cdot x \cdot y \tag{1.10}$$

where

T_u = ultimate torque

T_c = torque resisted by concrete (Plain concrete section)

T_s = torque resisted by transverse steel

k = a factor

A_s = cross-sectional area of one leg of the stirrup

f_{sy} = yield strength of the stirrup steel

s = centre to centre spacing of the stirrups

x = the smaller dimension of the stirrups

y = the larger dimension of the stirrups

The values of T_c and T_s vary for different investigators, Rausch [12] put $T_c = 0$ and $k = 2$. Anderson [31] suggested the value of 1.34 for k and permissible shear stress for T_c. Cowan [14] replaced k with 1.6 and T_c with the strength of plain concrete section. Ernst [20] found k from his test results, which varied from 1.23 to 7.96 and put $T_c = 0$. Using a mean value for elastic and fully-plastic stress distribution with a failure criterion for concrete, Iyengar and Rangan [15] obtained an expression to calculate T_c. They considered k to be unity.

Lessig [8] in 1958, from observation of her experimental tests, proposed a bending mechanism approach to check the ultimate strength of fully reinforced concrete members in torsion. She analysed the failure section by equating external moments, about an inclined axis in the compression zone, to the internal moments of yielded reinforcement. Manipulation of the equation by optimizing the angle of the failure section enabled her to obtain an expression to calculate minimum strength.

The failure section was described as spirally tensile cracks around the bottom, one of the sides and top face of the beam with compression zone on the fourth face. Failure occurred due to bending about the neutral axis in the compression zone.

This method is satisfactory providing the steel crossing the failure section yields at ultimate failure.

A series of comprehensive test results on transversely and longitudinally rectangular reinforced concrete beams in pure torsion was reported by Hsu [10] in 1968. Later he [32] used Lessig's skew bending theory, but assumed the failure plane to intersect the vertical sides at an angle of 45° and the horizontal faces at an angle of 90°. He derived a theoretical equation to

17

calculate the ultimate torsional strength for reinforced members in pure torsion.

The theoretical equation was in the form of Equation (1.10). T_c was considered to represent the torsional resistance provided by shear strength of the shear compression zone, and not as the strength of plain concrete, because the experiments on hollow concrete members showed that the concrete core of the beam did not contribute to the torsional resistance. A special technique, based partly upon the rational analysis and partly upon tentative results, was used to derive an expression for T_c. It was a function of the dimension of the cross-section as well as the compressive strength of the concrete f'_c and was expressed in imperial units as;

$$T_c = 2.4 \cdot D \cdot B^{3/2} \sqrt{f'_c} \qquad (1.11)$$

Hsu [32] found theoretically that the coefficient k in the second term of Equation (1.10) was a function of the volume of longitudinal bars to the volume of stirrups, m; the ratio of yield strength of longitudinal to stirrup steel, $f_{\ell y}/f_{sy}$; the ratio of larger to smaller dimension of the closed rectangular stirrup, and the vertical distance between the main bars, as well as their efficiency and dowel forces. The expression which combined these terms was complicated, and Hsu admitted that it did not submit to reasonable analysis, therefore, he defined the coefficient k empirically. For an under-reinforced rectangular member with a cross-sectional area of 150 in^2; and $y/x < 2.6$; m = 1, $f_{\ell y}/f_{sy} = 1$, he deduced that k = 0.66 + 0.33 y/x was applicable. Thus k varied between 0.99 - 1.52, for y/x between 1.0 and 2.6.

To ensure the applicability of the theory Hsu emphasized that the total reinforcement provided must be less than the balanced

total volume percentage (i.e. $P_{tb} = 2400 \cdot \sqrt{f'_c / f_{sy}}$), and also the balanced ratio of volume of longitudinal bar to volume of stirrups, m_b, should be within the range $0.7 < m_b < 1.5$.

Comparing the equation with 37 of the test beams [10], Hsu obtained a mean value of T_{test}/T_{theory} of 1.03 with standard deviation of 6.3%. The equation was also applied to the remaining 16 beams, which were partially and completely over-reinforced, and yielded the mean value of 1.18 for T_{test}/T_{theory} with standard deviation of 14%. He also compared his theory with 27 out of the total of 44 reinforced concrete beams tested by the investigators [3, 9, 20, 33, 35, 36 and 37]. The ratio of T_{test}/T_{theory} ranged between 0.69 - 1.29. It must be mentioned that the magnitude of the terms in the limitation, in excess of the proposed limit, were neglected during the comparison.

Hsu [10] investigated the torsional stiffness after cracking for fully reinforced concrete members. He found that the stiffness was chiefly a function of the smaller dimension; larger to smaller dimension and the total volume percentage of reinforcement P_t. Empirically he found the torsional stiffness shortly after cracking was only $0.021 \cdot P_t$ times the torsional stiffness before cracking. Empirical equations were also presented for angle of twist and cracking torque.

Considering moments of forces about the transverse and longitudinal axes of the member, and adopting Lessig's bending failure mechanism, Martin [18] derived a theoretical equation for an under-reinforced concrete member in combined bending and torsion. It reduced for the case of pure torsion, where the compression zone was in one side of the beam. It can be expressed in the form of

$$T = 2 \cdot A_2 \cdot f_{2y} \cdot L_{a2} \cdot \sqrt{r_{2y}/(1+b/d)} \qquad\qquad (1.12)$$

Where L_{a2} is the lever arm, and $r_{2y} = A_s \cdot f_{sy} \cdot d/s \cdot A_2 \cdot f_{2y}$.

To calculate the ultimate strength the exact value of the lever arm (L_{a2}) was required. Its magnitude was a function of the depth of concrete compression zone dn which Martin theoretically determined using Cowan's failure criterion for concrete. The determination of dn required the value of the inclination of the failure plane tanα, which was defined as $1/\sqrt{r_{2y}(1 + b/d)}$.

Putting L_{a2} equal to x and equating the ratio of b/d to x/y, this equation is exactly identical to the one put forward by Rausch [12].

Martin compared his theory with 38 results of under-reinforced beams mainly those of Hsu [10]. The mean value of T_{test}/T_{theory} was equal to 0.97 with a coefficient of variation of 10.2%. Based on some of Hsu's results, he also treated the case of partially yielding of the reinforcement, for which an empirical expression was developed and was in the form of Equation (1.10), where T_c and k were equal to $0.75 \cdot d \cdot b^2 \cdot \sqrt{f'_c}$ and $1/\{0.25 + 1.2 \cdot (r_{12})^{2/3}\}$ respectively. Assuming that the stresses in the stirrup steel and longitudinal steel were equal, r_{12} was reduced to $A_s \cdot b'/s \cdot A_2$. Comparing this equation with 5 of Hsu's beams resulted in the T_{test}/T_{theory} mean of 1.04 and coefficient of variation of 4.2%

The most effective and practical arrangement of torsion reinforcement is made up of a combination of vertical closed stirrups and longitudinal bars distributed evenly around the inside perimeter of the stirrups. In fact this favours the school of investigators which bases its theory on the truss analogy. The space truss assumes that the longitudinal bars act as stringers,

the stirrup legs act as posts and the concrete struts between the cracks act as compression diagonals.

In a recent paper published by Elfgren et al [38] in 1974, using the truss analogy method, a rational theory was derived. They investigated the most complicated case of combined torsion, bending and shear. For the case of pure torsion, their equation reduced to the form of Rausch's, providing that the condition of simultaneous yielding of longitudinal and web steel occurred, and the longitudinal bars distributed symmetrically round the cross-section. An identical expression, however, had been reported earlier by Lampert and Collins [39].

The equation of ultimate strength, in truss-analogy method, is independent of the concrete strength. It also estimates the ultimate strength of a hollow rectangular reinforced section, because this equation is proportional to the area enclosed by the width and the height of the close stirrup.

1.4.2 Torsion and Bending

The first to consider the action of combined torsion and bending of fully reinforced concrete members was Cowan [7] in 1953. He derived a method to calculate the torsional resistance of a member assuming that the torque was resisted partly by the uncracked concrete in the compression zone and partly by the stresses in the torsional reinforcement. The resistance of the concrete was expressed as the pure torsional capacity of the plain member, using the plastic theory. The shear stresses set up in the torsional steel, due to the remaining torque, was calculated from the stresses in the concrete adjacent to the steel using elastic theory.

He considered that the applied bending moment introduced a

direct flexural stress, as in pure bending, to the concrete in the compression zone. The relation between applied torque and bending moment was then found. Using the principal tensile stress-strain criterion for failure, where torsion was predominant, and Coulomb-Mohr internal friction theory, where bending was predominant.

Cowan made no attempt to define the inclination of the crack angles of failure section and also the failure modes. He concluded, however, that the addition of a small amount of bending moment would increase the torsional strength, while the bending strength was slightly reduced by the addition of a small torque.

Lessig's ultimate equilibrium theory [8] considered the case of bending and torsion as a particular case of the general loading arrangement of combined bending, torsion and shear. She concluded that most frequently members subjected to bending and torsion failed in mode 1, by bending about an oblique axis in the compression zone, located near the top face. The failure was due to crushing of the concrete in this zone accompanied by the yielding of reinforcement in the tensile zone. The inclination of the oblique axis was dependent mainly on the ratio of twisting moment to bending moment as well as the reinforcement.

To derive an expression to calculate the failure load for this mode, she analysed the failure section by taking moments of forces about the axis of rotation through the compression zone, and equating the internal moments to external moments. Equilibrium of forces normal to the compression zone, governed the depth of it. The external moments were the component of bending moment and the torque. The internal moments were due to the tensile forces in the bottom longitudinal steel and the bottom legs of the stirrups.

For this reason the approach enabled Lessig to introduce an
equation combining the bending moment, torsional moment, reinforcement
and shape parameters. To arrive at the final form of this equation,
she had to make some simplifications, such as the assumption of
yielding the reinforcement intersecting the failure plane. She
also assumed the inclination of the tensile cracks as straight
lines and constant around the three sides of the beam.

The forces in the vertical legs of the stirrups were ignored
by Lessig, and justified by the fact that the crack angle was
almost parallel to the steel for mode 1.

Following similar approach to that in mode 1, she derived an
expression also for mode 2, where the compression zone was on one
of the vertical sides.

Lessig did not attempt to arrive at an accurate value of
the depth of compression zone or the lever arm, and also failed
to identify the mode 3 type of failure, where the compression
hinge is near the bottom face of the beam, as reported later for
the first time by Walsh et al [19].

Later she conducted an extensive series of experiments [35] to
verify the theory, which showed that the equation was reasonably
accurate particularly in those cases where the reinforcement
reached their yield strength.

Gesund et al [40], in 1964, advanced a different theory by
attempting to include dowel action of the longitudinal steel into
the equation of ultimate strength. They divided the possible type
of failure into "Flexural failure" influenced by torsion, where
the longitudinal steel yielded before collapse, and "Torsional
failure", where the reinforcement did not yield. For the case
of bending failure, referring to the tests, they described the

intersection of compression hinge as an S shaped curve, the central
part of which was parallel to the longitudinal axis of the beam.
They considered the tensile cracks on the side faces at a constant
angle of 45°, and on the bottom face at a variable angle of θ.
Based on experimental data, θ was varied between 63.5° for $C_2 \geq 0.25$
and 90° for $C_2 < 0.25$, where C_2 was the ratio of torsional moment
to bending moment (i.e. T/M).

For the case of torsional failure, the strength was governed
either by an equilibrium equation of moments about the longitudinal
hinge near the top face or by an equation based on the dowel action
of the steel, whichever estimated the lower torsional strength at
failure.

Gesund et al concluded that when the failure was mainly one
of bending, the ultimate strength was not affected by the amount of
transverse reinforcement. This would not agree with the experimental
data.

A close study of this work leads to a conclusion that when
the failure is one of torsion, the ultimate strength is neither
influenced by the existence of bending nor by the amount of longi-
tudinal reinforcement. This does not appear to be entirely rational.

Evan and Sarkar [41], in 1965, put forward a method for the
ultimate strength design of reinforced concrete beams used in
practice, under combined bending and torsion. The base for the
theoretical approach was the experimental observation of 18 rein-
forced hollow rectangular beams.

In the analysis they employed two equilibrium equations. One
was of moments about an inclined axis through the compression zone,
in which was fixed at 45°. The other equation was of forces normal
to the compression zone, from which the depth of this zone was

determined. The reinforcement was assumed to reach yield stress at failure. The angle of inclination of tensile cracks on the bottom and the side faces α, was involved in the ultimate strength equation. Using the principal tensile stress criterion for plain concrete, assuming fully plastic distribution for shear stress and semi-plastic distribution for flexural stress, an expression was obtained to evaluate α. Unlike Lessig, this expression was entirely independent of the reinforcement parameters.

Only the bending type of failure was considered in the analysis, although, the torsional failure was recognised.

The comparison between the theory and their own tests as well as a few others was reasonable.

Maintaining Lessig's approach, Collins et al [42], in 1966, proposed a theory to predict the ultimate strength of reinforced member under combined bending and torsion. In the analysis three principal modes of failure were studied, namely modes 1, 2 (recognized first by Lessig) and 3. The third failure mode - first recognised by Walsh et al [19], occurred frequently in members containing smaller amount of the main bars in the top rather than the bottom, and subjected to a high ratio of torsion to bending moments.

In their analysis [42], only one equilibrium equation was considered. It was around the neutral axis in the compression zone. This resulted in an equation which combined bending moment, torsional moment, reinforcement and dimension parameters as well as the inclination of the compression hinge with transverse axis of the beam. This inclination was then determined for which the torsional strength was a minimum.

It was assumed that the tensile cracks around the three faces were at constant inclination to the axis of the beam. They further assumed that the depth of the compression zone was equal to a depth corresponding to that in pure bending.

Comparison of the theory with available experimental results necessitated the imposition of some restrictions.

A new parameter, r, was introduced by Collins et al [42] in their study. It was defined as the ratio of transverse to longitudinal reinforcement, which specified the limits for the applicability of their theory.

In a later paper by Walsh et al [43], the interaction behaviour for under-reinforced rectangular concrete beams in bending and torsion was studied. An interaction equation was then deduced which was in the following form;

$$(T/T_0)^2 + M/M_0 = 1.0 \tag{1.13}$$

where

T_0 = ultimate torsional capacity in pure torsion for fully reinforced concrete members.

M_0 = ultimate flexural capacity in pure bending for fully reinforced concrete members.

It could be seen from the graph of iteraction curve for torsion and bending [43] that the trend of the experimental results closely followed the curves of theoretical equations [42]. The theory also correctly predicted the substantial decreases in bending capacity induced by torsion, and vise versa.

Fairbairn and Davies [44] in 1969 made an attempt to improve the theoretical approach of Evan and Sarkar [41]. Their approach was essentially the same as later authors, except that the former

obtained an expression for the inclination of the compression fulcrum, β. The true value of β, they believed, would be a function of the flexural and torsional stresses in the compression zone, and therefore dependent on the ratio of bending moment to torsional moment. The assumption of setting β fixed at 45° as considered by Evan and Sarkar is difficult to consent.

The expression which relates the inclination of the compression zone, β, to the inclination of tensile cracks on the other three faces was not original, because that kind of relation was considered earlier by Collins et al [42].

Large discrepancies were evident between the experimental ultimate moments and those calculated, using their theory, in particular for beams 7 and 8 of their own tests.

Pandit and Warwaruk [37], in 1968, reported a theoretical and experimental study on members reinforced longitudinally and transversely, subjected to bending and torsion. The basis for the theory was the well known principle, that the torsional strength of reinforced concrete member is the sum of the strength of both concrete and reinforcement.

The observation of the tests let them to believe, that the area of the compression zone was not significantly changed by torsion. But the effect of torsion was to shift this zone from flexural compression towards the centre of the beam section. This had the effect of reducing the lever arm of the internal flexural moment.

The ultimate strength equation obtained can be expressed as;

$$T_{ultimate} = T_{concrete} + T_{steel}$$

The contribution of the concrete to the torsional strength,

they assumed, was the sum of the stresses of the concrete in the compression zone and the concrete in tension zone. The concrete in compression, they considered, was subjected to a state of biaxial stress due to combined action of bending and torsion. Using Cowan's failure criterion [7], two expressions were obtained for both cleavage and shear unit torsional failures of compressed concrete in the compression zone. The depth of this zone was assumed to be a quarter of the cross-sectional area.

Pandit and Warwaruk, however, failed to present an exact solution for the unit torsional strength of concrete in tension. They therefore, expressed their solution fluctuating between zero, for concrete in pure bending, as a lower bound limit, and the value of maximum torsional capacity of concrete in pure torsion as an upper bound limit.

The contribution of the steel to the ultimate strength was assumed to be from both categories of the reinforcement (i.e. the stirrups and the main bars). The steel was assumed to have reached its yield strength at failure, providing that enough longitudinal steel existed, both at the top and the bottom of the beam to resist the longitudinal component of diagonal tension.

As it was expected, a considerable disagreement was noticed between the calculated and the experimental values of ultimate torsional strength, because a large number of assumptions and simplifications were introduced into the theory.

A similar theoretical approach was developed by Iyengar and Rangan [15] to examine reinforced members subjected to combined stresses. They recognized two types of failure, namely torsional failure and bending failure. For torsional failure the strength was considered to be the same as the strength of reinforced

member in pure torsion - explained in section 1.2 earlier on.

In the case of bending failure they assumed that the concrete in the compression zone was subjected to direct stress due to applied bending moment and shear stress due to the applied torsional moment. They suggested that the resultant of these stresses would produce a principal compressive stress accompanied by a principal tensile stress in the tension zone of the section. Failure was assumed to have been reached, when these principal stresses satisfied the following Krishnaswamy's failure criterion for concrete under compressive-tensile stress;

$$\sigma_1/f_c' + (\sigma_2/f_t)^2 = 1.0 \qquad (1.14)$$

where

σ_1, σ_2 = principal compressive and tensile stresses respectively

f_c', f_t = uniaxial compressive and tensile strengths respectively.

Ignoring the difference in the depth of the compression zone of a member subjected to pure bending and a beam under combined bending and torsion, the bending stress was expressed in terms of the uniaxial compressive strength of concrete f_c', as $f = K \cdot f_c'$. Where f, was the bending stress for a member under bending and torsion, and K was a reduction factor of the compressive strength of concrete due to the existance of torsional shear stress.

In pure bending the flexural stress was assumed to be equal to the compressive strength f_c', therefore, K was expressed as a ratio of M_b/M_{b0}. Where M_b was ultimate flexural capacity of the beam under combined bending and torsion and M_{b0} was flexural capacity of the beam under pure bending.

The torsional shear stress was calculated, using the elastic stress distribution, because they believed that the failure occurred by crushing of the concrete and the torsional strength would be in the elastic state.

Comparison, mainly for torsional failure, between the theory and test results was good. The torsional strength was increased by increasing the bending moment, except for very high values of bending moments. Therefore, the existing interaction between bending and torsion differed considerably for those obtained by others [8, 43].

Iyengar and Rangan also considered the stiffness of members under combined bending and torsion. Approximate expressions were presented to predict the deflection and angle of twist.

Neither Pandit and Warwaruk [45], nor Iyengar and Rangan [15] mentioned the different modes of failure, because their approach was not based on the consideration of equilibrium of forces at the failure section.

Goode and Helmy [11] presented further experimental and theoretical work on longitudinally and transversely reinforced concrete beams under the action of bending and torsion. In the analysis, they considered the stresses in the reinforcement as unknowns, because the test results showed many cases of non-yield-ing. To calculate these stresses they, following Lessig [8], developed an extra equation of moment about an axis through the centre of the compression zone and perpendicular to the neutral axis.

According to Goode and Helmy, there are six modes of failure by which a beam in bending and torsion may fail. Four of these were observed in the tests and therefore considered in their analysis.

To obtain the solution for the equation, the average compressive stress was assumed to be 0.85 times the compressive strength of the concrete. The crack angles around the failure section were also assumed to be 45°, where either category of reinforcement had not yet reached its yield strength.

In the comparison of test results with theory, they favoured the graphical representation. They considered that the tabulated form was unsatisfactory, since a false picture of the correlation could be apparent. They did not impose any limitation on the application of their theory, and therefore it can be used to predict the strength of members under pure torsion, for which only fair agreement can be found.

Jackson and Estanero [46], in 1971, investigated the implication of the plastic flow law, in relation to the applicability of current method of plastic analysis, to reinforced concrete members subjected to both flexural and torsional moments. They stated that a knowledge of bending-torsion interaction curve whilst necessary, was not sufficient to enable a plastic analysis to be carried out. Adequate rotation capacity and also the associated plastic flow law of the member in the region of the plastic hinge were equally important. To study this, they tested 80 both symmetrically and unsymmetrically rectangular reinforced concrete beams under combined action of flexural and torsion without shear.

From the experiment results, they concluded that the excess of rotation beyond the proportional limit was sufficient to permit the required redistribution of moments, followed by the formation of the first plastic hinge (s), for the subsequent development of a failure mechanism. The directions of the axes of rotation

during the pseudo-plastic stage indicated that the use of the term "the axis of rotation" by many investigators – when discussing failure in combined bending and torsion, was incorrect. They believed that component rotations about an axis other than the axis of rotation indicated by the concrete crushing, must also be present to provide the resultant axes of rotation observed in their tests.

Finally, they deduced that the fundamental assumptions of plastic potential flow law which formed the basis of plastic analysis of structures was satisfied by reinforced concrete members under combined action of bending and torsional moments.

Martin [18] in 1973 presented a theoretical solution for the determination of the ultimate strength of fully reinforced concrete members in bending and torsion. In that approach the ultimate load conditions were mainly divided into two cases, depending on whether all the steel intercepting the failure section was stressed to yield. In the case of yielding the reinforcement, like Yudin [47], Martin considered moments of forces in the failure section about two perpendicular axes, one of which was parallel to the longitudinal axis of the member. But unlike Yudin, Martin determined the inclination of the cracks at the failure section from the equilibrium of forces.

To arrive at the solution of moment equations the lever arm, which depended on the value of depth of compression zone, had to be determined. For this, Martin made use of Cowan's simplified failure criterion of concrete in compression. He assumed that the compression zone was subjected to both direct flexural stress due to bending and shear stress due to torsion.

The comparison of this approach, for 72 beams which failed

in mode 1, yielded the mean value for T_{test}/T_{theory} of 1.05 with a coefficient of variation of 11.6%, the mean value of 0.97 with a coefficient of variation of 10.2% for 38 beams failed in mode 2, and a mean of 0.95 with coefficient of variation of 14.8% for 6 beams in mode 3.

For the cases other than yielding case, Martin considered both partially and completely over reinforced members. To separate the yielding from non-yielding cases, he made use of the ratio of actual to critical ratios of transverse to longitudinal steel. The member was considered to be over-reinforced, when this ratio was less than 1.0. The critical value of this ratio was obtained by restraining the tensile crack angles on the sides of the beam to be equal or less than 45°.

In the case of partially over reinforced members, he considered that since the area of transverse steel was low, therefore, it would most likely be at yield, while the longitudinal steel was still in the elastic stage. By taking moments of forces about longitudinal axis through the centroid of the compression zone, in one side of the section, fixing the crack angle at 45° and approximating the lever arm to the larger dimension of stirrup legs, Martin obtained an expression to calculate the ultimate torsional strength. The method was conservative. When compared with 120 experimental results, yielded the average value of T_{test}/T_{theory} of 1.10 with a coefficient of variation of 22.9%.

In the case of completely over reinforced concrete members, although Martin pointed out the possibility of the test results which had been reported as over-reinforced members were in fact partially over-reinforced. He presented an empirical expression for the ultimate strength of completely over-reinforced section, based

on a few experimental results by Hsu [10].

The expression was mainly a function of the root square of cylinder compressive strength of concrete, and the dimension of the section as well as the ratio of transverse to longitudinal steel.

Lacking sufficient experimental results for this case of failure, Martin was unable to verify his expression.

1.4.3 Bending, Torsion and Shear

Although the general case of combined bending, torsion and shear in reinforced concrete members is more likely to occur in practice, it has received little attention until recently. The interaction behaviour between these combined loads has not been clearly understood. None of the different theories, reviwed so far can analyse a distinctive as well as the common cases of load combination.

One of the first concerned with this problem was Lessig [8]. In 1958 she proposed a theory, based on test observation, to predict the ultimate capacity of members subjected to torsion combined with bending and shear. She concluded, also from the tests, that when a reinforced concrete beam subjected to bending and torsion with a moderate amount of transverse shear, failure was taking place by bending about a skew axis through the com-pressed zone on one of the sides - mode 2.

The theoretical equation was derived, based on the equilibrium condition of moments and forces at the failure section. With a high ratio of bending to torsional moment and small shear, failure was caused by bending about a skew axis in the top of the failure section.(i.e. mode 1). In this case shear may be ignored and the

case considered as combined bending and torsion only. The resulting equation was too complicated for practical purposes, and later she proposed a simple empirical relation between shear and torsion [34]. When shear was too high, she confirmed that the failure was one of shear, and the shear strength might be approximately expressed as;

$$V = V_0 - 3 \cdot T/b$$

For a member with moderate shear (mode 2), Lessig suggested the relationship;

$$V \cdot b/2 = T_0 - T$$

where V_0 and T_0 were the ultimate shear strength in bending and shear alone, and the torsional strength in pure torsion, respectively.

It must be recalled that the principal assumption in Lessig's approach of yielding of all reinforcement crossing the failure section is not always valid as shown by many of the reported test results [9, 10, 11].

To verify her theory, Lessig performed an extensive test programme on rectangular reinforced concrete beams under combined loading [35]. She confirmed that the recommended formula estimated the ultimate strength reasonably well, in particular when the yielding occurred. For those beams the ratio of experimental torsional strength to the calculated strength varied between 1.01 to 1.28, but for 9 of Ernst's test beams [20], this ratio was in the range of 0.72 to 1.13. The greatest inaccuracy in the theory was for certain beams in which the flexural moment was very small.

It should be noted that the limitations imposed on the theory were empirical as well as the expression for over-reinforced member to calculate the torsional resistance.

In all the test beams the horizontal and vertical legs of transverse steel were spot-welded alternatively to the longitudinal bars - i.e. not in the form of closed links.

Further tests were conducted by Laylin [9] in reinforced members under combined action of bending torsion and shear. The main objective was to determine the optimum ratio of longitudinal to transverse steel and to define empirically the steel limit at which failure of concrete occurred before the reinforcement reached the yield point. Laylin, based on one set of his test results, concluded that Lessig's theory produced satisfactory results only when the ratio of transverse to longitudinal was within specified empirical limits. He also deduced that compression in the concrete could produce failure even though none of the longitudinal steel and stirrups reached their yield strength.

In the analysis, Yudin modified Lessig's skew bending approach. He formed the theoretical equations by resolving moments of forces about the longitudinal and transverse axes of the beam, assuming constant tensile crack angle of 45° spiralling around the three faces. This assumption has been referred to as incorrect, particularly for beams tested under combined loadings with high ratio of flexural to torsional moments. An interaction between bending and torsion was then applied which produced an equation for the ultimate torque. It was essentially the same as Rausch's equation.

This equation, however, suggests that variations in the magnitude of bending moment or the amount of longitudinal steel does not affect the torsional strength of a member, whereas tests have

36

indicated that this is not true.

When shear was present, he suggested, for the purpose of design, that the shear force could be replaced by an equivalent torque equal to $V \cdot b'/2$. In order to obtain the effective total torque the equivalent torque should be added to the actual torque, then the area of steel required to resist ultimate torque could be calculated.

Yudin [48], in 1964, published the result of tests on reinforced concrete beams, designed in accordance with rules proposed by himself in the earlier paper [47]. He deduced that Lessig's design equation yielded reasonable agreement with the experimental results, although his equation provided more accurate estimations of the ultimate strength.

Collins et al [42] in a report published in mid 1966 presented a method to design rectangular reinforced concrete beams subjected to combined torsion, bending and shear. By making certain modifications to Lessig's theory, they obtained a fairly simple method for design of rectangular beams with both transverse and longitudinal steel. In that report equations were developed for two principal modes of failure (i.e. modes 1 and 2), as well as a third failure mode in which inclined tension cracks opened up across the top and side faces and failure occurred by rotation of the beam about a hinge located near the bottom face. To preserve the nomenclature of Lessig, this mode of failure was therefore called mode 3.

They deduced from the tests that mode 3 failure might be superseded in beams where there was a deficiency of top steel and subjected to predominantly torsional moment.

The final solution for their equations required the deter-

mination of the inclination of compression hinge to optimise the
ultimate torque. The resulting expression was mainly a function of
the ratio of torsional to bending moments and the reinforcement.

Their work could be well criticized analytically for the
simplifications entailed, such as ignoring the depth of compression
zone in mode 2 failure. Collins et al also ignored the contribution
of the shear force in analysing modes 1 and 3 failures. To pre-
vent types of failure other than the yielding, such as shear and
compression, empirical expressions to limit the range of applica-
bility of the theory were introduced.

To prevent a compression failure in torsion, the overall
dimensions should be such that; $T/b^2 h \cdot f'_c \leq 0.07$. To prevent
compression failure in bending, the percentage of main longitudinal
steel should not exceed that given by; $p = 0.4 \cdot f'_c / f_{\ell 1}$, where $f_{\ell 1}$
was the yield strength of longitudinal steel near the bottom
face of the beam. To prevent shear failure, the ratio of applied
shear force to the ultimate shear of the member in simple bending
as computed from ACI 318-63 Code equation, should be less or
equal to 0.5.

Furthermore, for low values of parameter r, which related
transverse to longitudinal steel, the main bars might not reach
their yield strength. In order to supervene the yielding,
Collins et al made use of an optimum design value for parameter
r, which they called r_0. Relying on a large number of tests,
which satisfied the restrictions set out above, and subjected to
bending and torsion only, Walsh et al [49] in a later paper showed
that the analysis presented by Collins et al [42] was consistent
and accurate for beams with values of r/r_0 greater than unity.

The prediction by the theory was low (i.e. conservative),

particularly for beams failing in modes 1 and 3, but generally followed the trend of the tests. Applying this method on 26 of Lessig's and Laylin's beams which satisfied the restrictions imposed on the theory and subjected to one point loading produced the mean value of T_{test}/T_{theory} of 1.28 with standard deviation of 7%. It is also interesting to note that this ratio, for 83 beams, mainly of Lessig's, which did not satisfy all the limitations, varied between 0.75-2.86 with a standard deviation of 30%.

Osburn [50] in his thesis described tests on reinforced concrete beams in bending, torsion and shear. The purpose of these tests was to assess the   behaviour of reinforced concrete beams designed in accordance with the proposals put forward by Mattock [51], and therefore ultimate strength was not considered. The test results confirmed that the proposals in the paper "How to design for torsion" [51] were reasonably conservative.

In 1970 McMullin and Warwaruk [52] presented an experimental and theoretical investigation into the behaviour and ultimate strength of rectangular reinforced concrete members subjected to torsional moment combined with bending moment and vertical shear. The tests were designed to study the effect of transverse shear on the torsional strength of reinforced beams with stirrups.

The ultimate strength analysis was based on the theory developed by Lessig in 1958. They, however, advanced this analysis by deriving an equation to predict ultimate strength for beams failing by rotation about a skew axis located in the vicinity of the bottom reinforcement (i.e. mode 3), as was recognized first by Walsh et al [19]. The ultimate torsional moment was calculated from one equilibrium equation of the internal and external moments. To find an optimum value of the torsional moment, this equation was

differentiated with respect to the longitudinal projection of the compression zone. An expression for the depth of compression zone was also obtained from the equilibrium of forces perpendicular to the inclined failure section.

Finally an iterative procedure was used to find the values of the longitudinal projection and the depth of the compression zone, and eventually the ultimate torsional moment.

They concluded that in beams subjected to point loads with constant torsional moment, mode 1 failure was critical in the region of highest bending moment, and mode 3 failure was critical in the region of lowest bending moment. Also the mode of failure predicted by the analysis agreed well with the observed mode of failure.

McMullin and Warwaruk checked the accuracy of the theory against their experimental results only, which showed good agreement. However, reasonable correlation was also obtained by Elfgren et al [53], for eleven of their tested beams.

In an attempt to obtain a reliable ultimate load method for design of rectangular reinforced concrete beams in torsion, combined with bending and shear, Swann [54] reported an experimental investigation in 1970. He adopted the hypothesis that torsion could be separated from bending and shear. It was considered to be resisted by the additional reinforcement other than that required for bending and shear by an amount equal to that which would be required for pure torsion.

He considered the ultimate torsional strength equation as in equation (1.10). T_c, representing the part of torque resisted by the concrete, was equated to zero, because Swann failed to explain

the true nature of its value. The factor k was believed to be a variable, and also it was likely to be influenced by the shape of the section and the ratio of concrete cube strength to steel yield strength. It was therefore investigated and a constant value of 1.2 was deduced from the experimental results.

In the report the validity of the design formula was not checked against the test results, which makes it difficult to assess the work. It however, is clearly shown by Martin [18] that Swann's approach in fact overestimates the torsional strength for reinforced member subjected to high bending moment. Therefore it should not be relied upon as Swann claims for design purposes, even if a material factor is introduced.

Recently a theoretical investigation of ultimate strength for members under combined loadings (i.e. torsion, bending and shear) was presented by Elfgren et al [38]. Making use of both the bending equilibrium method and the truss-analogy method, a simple and rational interaction equation for reinforced concrete beams under torsion, bending and vertical shear was developed. The three basic modes of failure were studied, and interaction equation for each failure mode was established.

In the analysis, two equilibrium equations for moments about two perpendicular axes, one of which was parallel to the longitudinal axis of the beam through the centre of the compression zone were considered. A third equation for the shear force – by resolving the external and internal forces along the vertical direction, was also established.

After simplifications and certain assumptions such as yield-ing of both reinforcement categories at failure, an interaction equation from the above three equations was derived, and arranged

41

in the following general non-dimensional form:

$$M/M_0 + (T/T_0)^2 + (V/V_0)^2 = 1.0 \qquad\qquad (1.15)$$

where

M,T,V = applied bending moment, torsional moment and
shear force respectively, under combined loadings.

M_0, T_0, V_0 = ultimate strength in pure bending, pure torsion
and shear respectively.

At failure the inclined failure section was studied. This
inclination varied from face to face due to variation in shear and
tensile stresses in the different faces of the beam. An important
point to be noticed in their analysis was that Elfgren et al [38]
had considered the inclination of the compressive struts of the
concrete between the cracks, and not the inclination of the actual
tensile cracks.

In the light of available experimental evidence, however, it
is difficult to visualize this phenomena as part of the analysis.
It is also difficult to justify the complete dependency of the
inclination of the struts on the ratio of the amount of longitudinal
reinforcement and the amount of stirrups. Again tests have shown
that the applied loads play an important part in shaping the fail-
ure section.

Elfgren et al suggested that to ensure the yielding of both
categories of reinforcement the above ratio (i.e. reinforcement
ratio) should have such a value which restrained the value of
$\cot\alpha_T$ within the range; $0.5 < \cot\alpha_T < 2.0$. No further explanation
was given into the source of the confined boundary.

The main conclusion was that the inclination surface for the

three analysed modes, namely modes 1, 2 and 3, together formed an interaction surface which governed the load-carrying capacity for a reinforced beam.

A graphical representation of a few test results was presented in the paper to check the accuracy of the analysis, which in fact was not sufficient to draw a final assessment. In general, however, the test results followed the trend of the theoretical curve.

CHAPTER TWO

EXPERIMENTAL WORK

2.1 INTRODUCTION

Literature surveys which have been carried out by many research workers in past years and by the author indicate that there is wide information on plain and reinforced concrete members, with or without web reinforcement, for the case of pure torsion or torsion combined with bending. However, for the most important and practical case of torsion combined with bending and vertical shear less information is available. The test programme, which is presented in this chapter, was designed to investigate certain strength parameters for reinforced concrete members subject to combined loading.

2.2 TEST PROGRAMME

A total of 38 simply-supported reinforced concrete beams were prepared and tested. The beams were divided into four series, all having rectangular cross-sections (square for beams D1 and DR1 of series D). An outline of test programme and the dimensions of the test beams are given in table 2.1 and figure 2.1 respectively.

Beams in SERIES A were designed and tested in order to investigate the effect of concrete strength on the ultimate capacity of a member under the combined action of torsion, bending and shear. The series was subdivided into Group A, which was comprised of nine beams and Group AR, which was comprised of three beams.

Beams of SERIES B were prepared and tested to investigate the effect of stirrup spacing and subdivided into two groups, seven beams for Group B and three beams for Group BR.

The area of the longitudinal reinforcement was investigated in

44

SERIES C, which was subdivided into two groups. Group C contained

five beams, and Group CR contained three beams.

Dimensions of the cross-section affect the stiffness chara-

cteristics and ultimate strength of the structural members, and

SERIES D was therefore designed and tested in order to study the

effect of dimension properties on torsional strength. This series

was subdivided again into two groups, five beams in Group D and

three beams in Group DR.

The main difference between the two groups of each series was

the distribution of the longitudinal reinforcement. Beams of the

first group contained an equal amount of compression and tension

steel, while beams in the second group (affixed with letter R)

contained a lower amount of compression steel, except beam CR1.

Beams in groups A, B, C and D and beams BR4, BR7 in group

BR, were loaded in combined torsion, bending and vertical shear,

according to the loading arrangement   shown in figure 2.2.

The loading system shown in figure 2.3 was applied to beams in

group AR, CR, DR and beam BR2. In order to ensure that the com-

pression zone formed in the bottom half of the beam (Mode 3), these

beams were subjected to a large torsional moment. The beams also -

as stated above - had a large amount of longitudinal reinforce-

ment in the tension side, and the bending moment and vertical

shear force was introduced by the dead load of the test beam.

It can be seen from table 2.1, that ϕ5 mm diameter steel was

used for stirrups in beams of group A, series A, but for group AR

and the remaining three series ϕ6 mm diameter mild steel bars were

used. Every possible effort was made when manufacturing the con-

crete for series B, C and D to produce a constant strength.

Series	Beam	M:T:Vh*	h mm	b mm	Longitudinal Steel bottom	Longitudinal Steel top	Stirrups Size	Stirrups Spacing	Mean Target f'$_c$ 28 days
A	A1	3:1:0.3	175	100	φ10	φ10	φ5	70	10
	A2	3:1:0.3	175	100	φ10	φ10	φ5	70	13
	A3	3:1:0.3	175	100	φ10	φ10	φ5	70	15
	A4	3:1:0.3	175	100	φ10	φ10	φ5	70	20
	A5	3:1:0.4	175	100	φ10	φ10	φ5	70	25
	A6	5:1:0.5	175	100	φ10	φ10	φ5	70	30
	A7	3:1:0.3	175	100	φ10	φ10	φ5	70	30
	A8	3:1:0.3	175	100	φ10	φ10	φ5	70	40
	A9	3:1:0.4	175	100	φ10	φ10	φ5	70	65
	AR4	0.2:1:0	175	100	φ10	φ6	φ6	80	20
	AR5	0.2:1:0	175	100	φ10	φ6	φ6	80	25
	AR9	0.1:1:0	175	100	φ10	φ6	φ6	80	65
B	B1	2:1:0.2	175	100	φ10	φ10	φ6	25	25
	B2	2:1:0.3	175	100	φ10	φ10	φ6	40	25
	B3	2:1:0.3	175	100	φ10	φ10	φ6	60	25
	B4	3:1:0.3	175	100	φ10	φ10	φ6	80	25
	B5	3:1:0.3	175	100	φ10	φ10	φ6	100	25
	B6	3:1:0.3	175	100	φ10	φ10	φ6	120	25
	B7	3:1:0.4	175	100	φ10	φ10	φ6	200	25
	BR2	0.2:1:0	175	100	φ10	φ6	φ6	40	25
	BR4	3:1:0.3	175	100	φ10	φ6	φ6	80	25
	BR7	2:1:0.2	175	100	φ10	φ6	φ6	200	25
C	C1	3:1:0.4	175	100	φ6	φ6	φ6	80	25
	C2	3:1:0.3	175	100	φ8	φ8	φ6	80	25
	C3	2:1:0.2	175	100	φ10	φ10	φ6	80	25
	C4	2:1:0.2	175	100	φ12	φ12	φ6	80	25
	C5	2:1:0.2	175	100	φ16	φ16	φ6	80	25
	CR1	0.2:1:0	175	100	φ6	φ6	φ6	80	25
	CR3	0.2:1:0	175	100	φ10	φ6	φ6	80	25
	CR5	0.2:1:0	175	100	φ16	φ6	φ6	80	25
D	D1	3:1:0.3	150	70	φ10	φ10	φ6	100	25
	D2	2:1:0.2	150	90	φ10	φ10	φ6	100	25
	D3	2:1:0.2	150	110	φ10	φ10	φ6	100	25
	D4	2:1:0.2	150	130	φ10	φ10	φ6	100	25
	D5	2:1:0.2	150	150	φ10	φ10	φ6	100	25
	DR1	0.2:1:0	150	70	φ10	φ6	φ6	100	25
	DR3	0.2:1:0	150	110	φ10	φ6	φ6	100	25
	DR5	0.2:1:0	150	150	φ10	φ6	φ6	100	25

* Approximate ratios between applied loads at mid-span

TABLE 2.1: Test programme, general outline
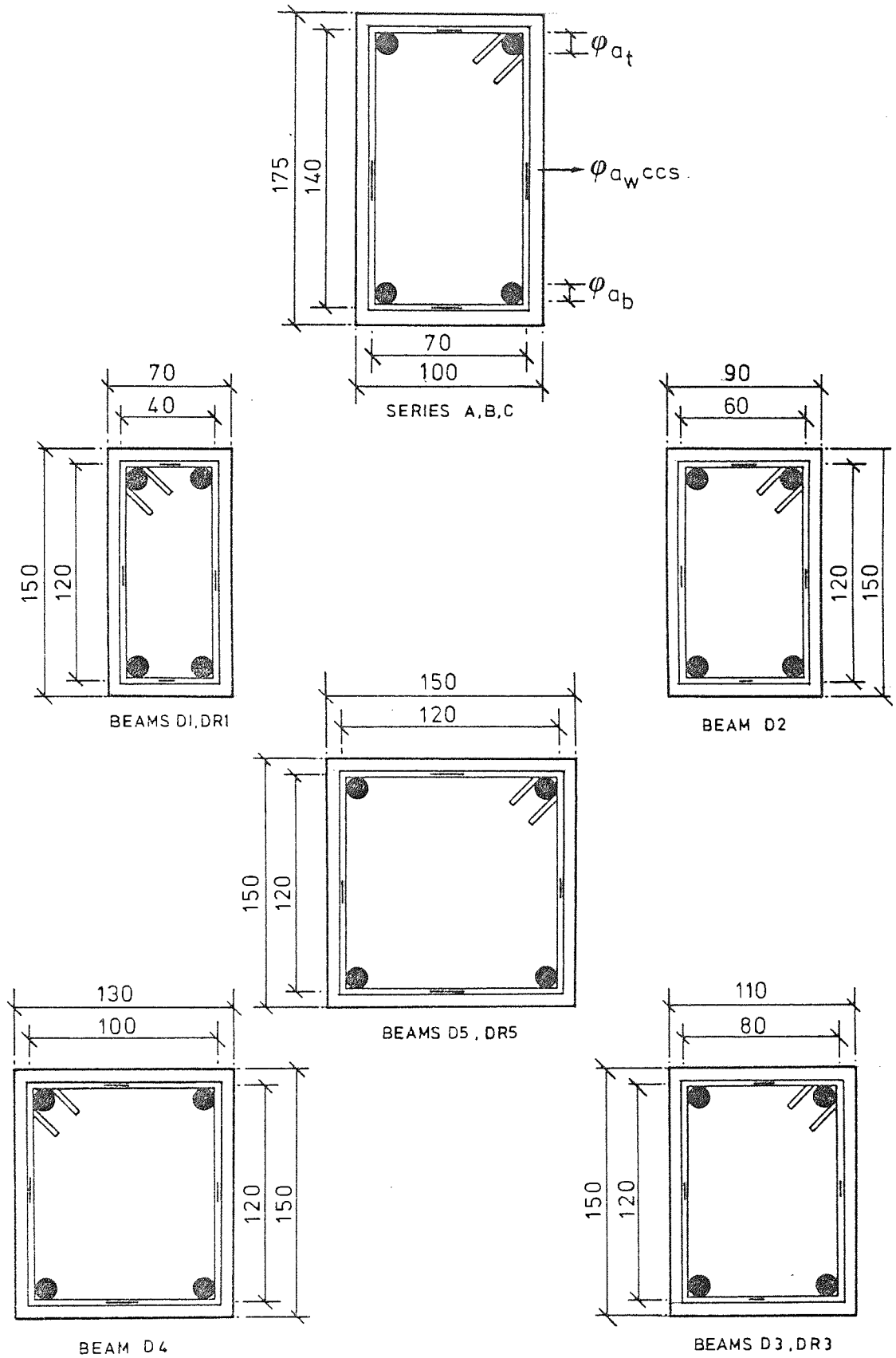
FIGURE 2.1 : Cross sections and dimensions of the test beams
(for more details see tables 2.2 and 2.3)

47
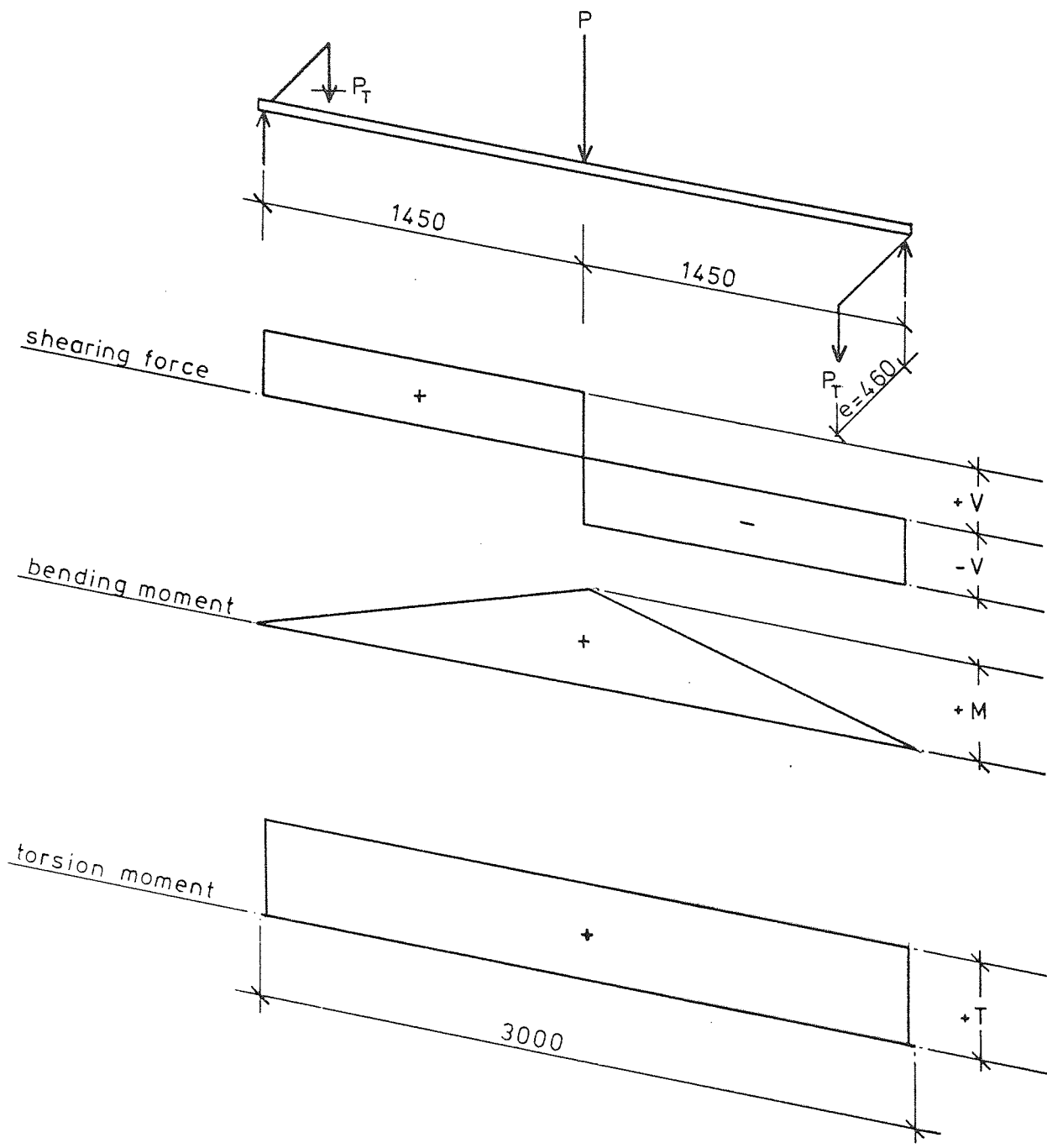
FIGURE 2.2 : Loading arrangement for groups A,B,BR(except beam BR2),C
and D.

48
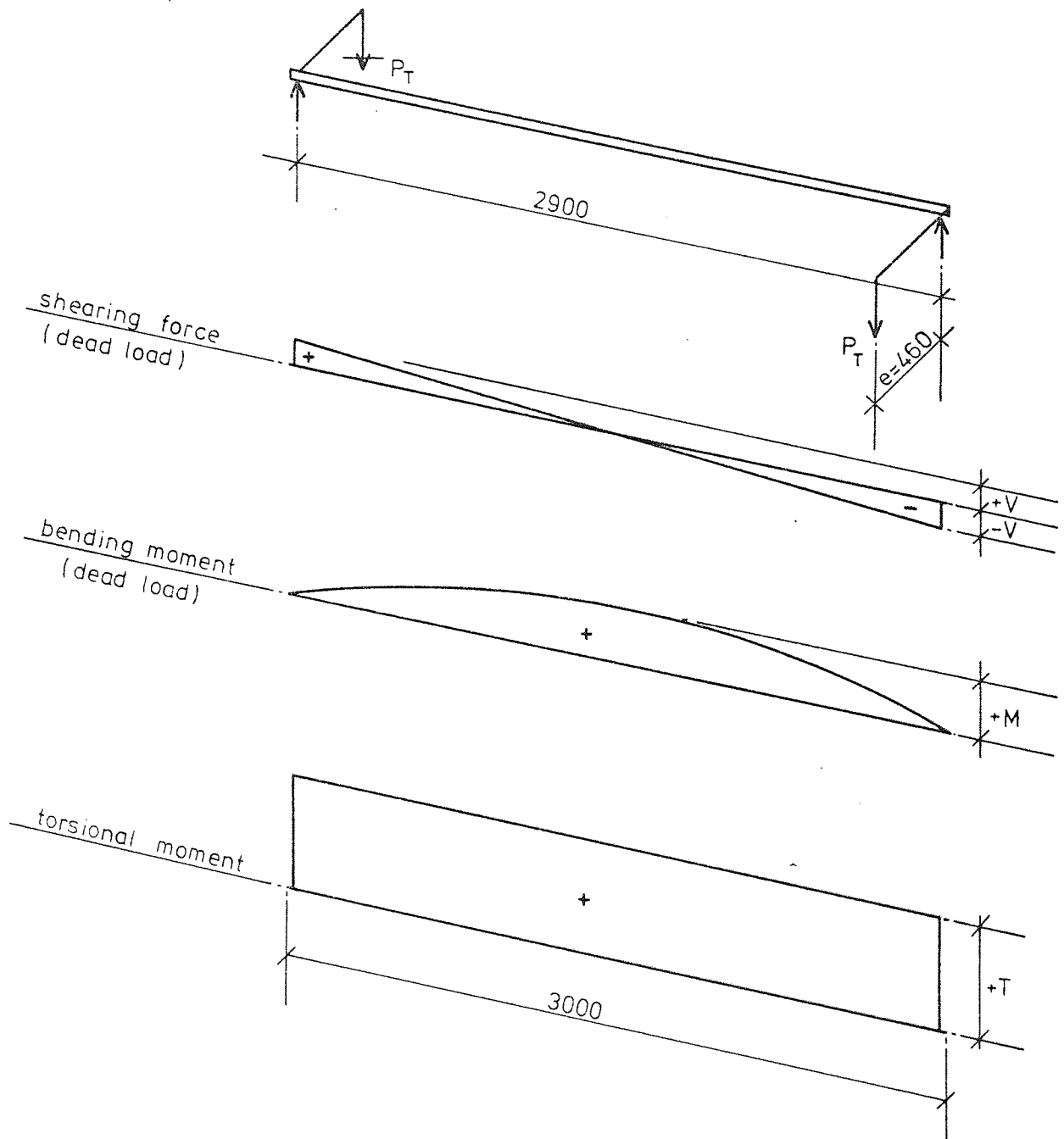
FIGURE 2.3 : Loading arrangement for groups AR, BR (beam BR 2 only)
CR and DR

2.3   MATERIAL PROPERTIES

2.3.1   Steel and Reinforcement Layout

All reinforcement used was mild steel bar. Samples were tested in accordance with the British Standard Specification (BS 1881) in order to determine the yield point and ultimate strength. An idealized stress-strain curve is presented in figure 2.4. The reinforcement properties for all the beams are given in detail in tables 2.2 and 2.3. Each reinforcement cage was made from four longitudinal bars bound together with vertical closed stirrups of a specified diameter and spacing, with one longitudinal bar in each corner, as shown in figure 2.5.

From table 2.2 it can be seen that only in beams of groups A, B, C and D the longitudinal steel was distributed symmetrically around the corners, while smaller diameter top steel was provided for beams in groups AR, BR, CR (except CR1) and DR. As mentioned earlier, only the stirrups for group A beams were made from a mild steel of low (260 N/mm^2) nominal yield strength, and only for these beams a region of 500 mm at both ends was heavily reinforced in order to avoid failure near the supports.

2.3.2   Concrete Mix and Quality Control

The concrete was proportioned for a target cylinder compressive strength of 25 N/mm^2 at 28 days, for series B, C and D, and a different compressive strength for series A (see table 2.1). The concrete used in all the test specimens was a mix from Ordinary Portland Cement, local zone 3 sand with crushed aggregate of 10 mm maximum size and tap water. To manufacture the concrete a "Linear Cumflow 1A" mixer of .25 m^3 capacity was used. From each

batch of concrete one test beam, three 100 x 100 mm cubes, three 100 x 100 x 500 mm modulus of rupture beams and four 150 x 300 mm cylinders were cast. Formica coated plywood formwork with an over-all length of 3000 mm and section dimensions as shown in figure 2.1 was used for the testing beams, and standard steel moulds for the control specimens. The concrete was vibrated during the casting using a 25 mm diameter poker vibrator, except for beams B1, D1 and DR1 and their specimens where a table vibrator was used. After 24 to 48 hours the sides of the form-work were removed leaving the beam on the base for seven days, while the moulds were stripped. The beam and the specimens were kept in the curing area (plate 2.1) under damp hessian which was automatically sprayed with water once or twice a day for approximately 25 days (except beam Al which kept for 5 days only). One to two days before testing they were removed and left in the laboratory condition, allowing the surface to dry.

The control specimens were tested according to British Standard Specification (BS 1881) on the same day as their corresponding beams. The cubes were tested to determine the cube compressive strength f_{cu}. The prismatic beams were used to determine the standard modulus of rupture f_r. Two of the four cylinders were used in order to determine the indirect tensile strength f_t (Brazilian method), and the remaining two were used to determine the cylinder compressive strength f'_c and the modulus of elasticity of the concrete E_c.

Table 2.4 presents the mix proportions for the concrete, the date of casting, the method of storing and target strength of the concrete.
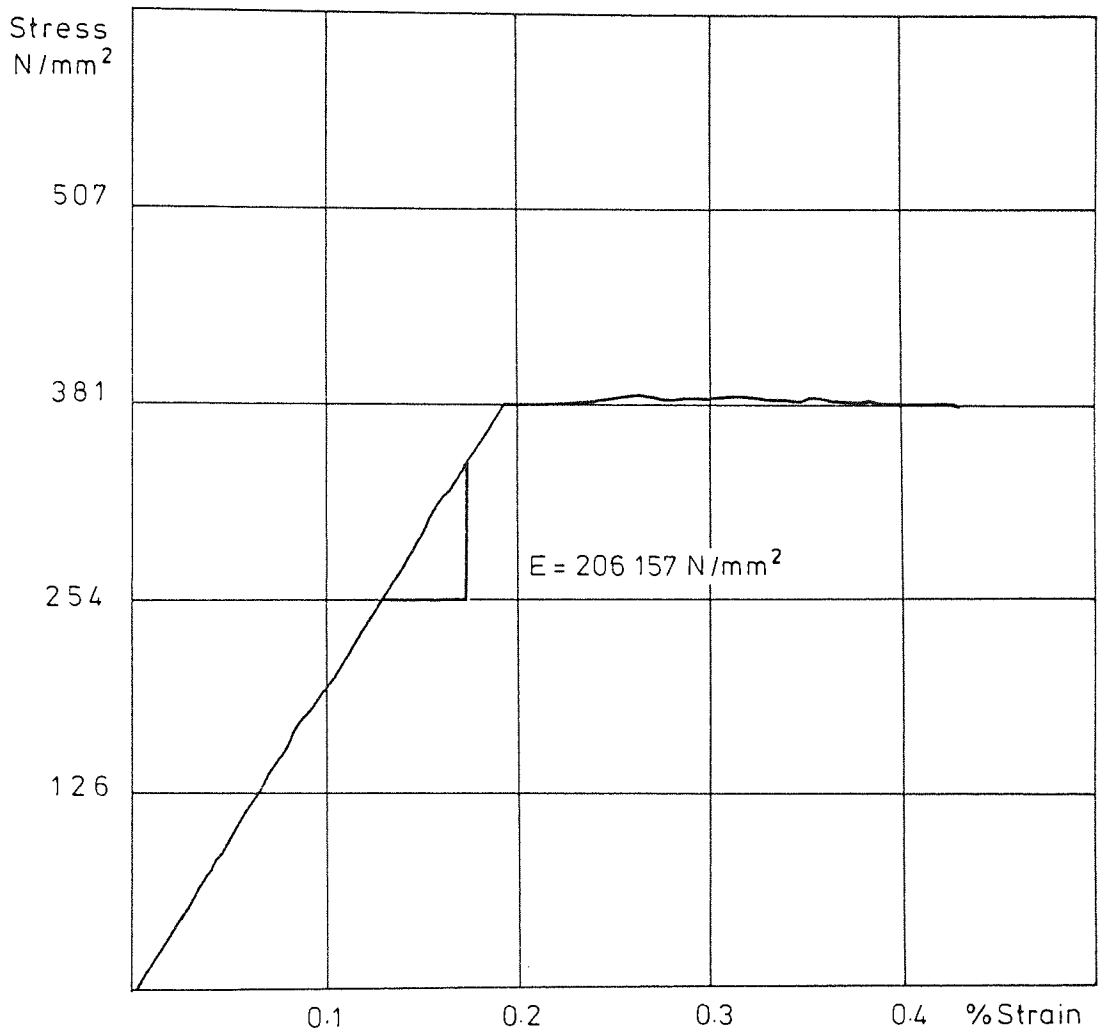
FIGURE 2.4 : An idealized stress-strain curve for φ 10mm bar.

Beam	Bottom Steel		Top Steel		Web Steel		
	ϕmm	f_{by} N/mm^2	ϕmm	f_{ty} N/mm^2	ϕmm	f_{wy} N/mm^2	s mm
A1	10*		10*		5		70
A2	10*		10*		5		70
A3	10*		10*		5		70
A4	10*		10*		5		70
A5	10*	335.26	10*	335.26	5	259.80	70
A6	10*		10*		5		70
A7	10*		10*		5		70
A8	10*		10*		5		70
A9	10*		10*		5		70
AR4	10		6		6		80
AR5	10	340.42	6	393.52	6	393.52	80
AR9	10		6		6		80
B1	10		10		6		25
B2	10		10		6		40
B3	10		10		6		60
B4	10	340.42	10	340.42	6	393.52	80
B5	10		10		6		100
B6	10		10		6		120
B7	10		10		6		200
BR2	10		6		6		40
BR4	10	340.42	6	393.52	6	393.52	80
BR7	10		6		6		200
C1	6	393.52	6	393.52	6		80
C2	8	294.78	8	294.78	6		80
C3	10	340.42	10	340.42	6	393.52	80
C4	12	325.97	12	325.97	6		80
C5	16	320.47	16	320.47	6		80
CR1	6	393.52	6		6		80
CR3	10	340.42	6	393.52	6	393.52	80
CR5	16	320.47	6		6		80
D1	10		10		6		100
D2	10		10		6		100
D3	10	340.42	10	340.42	6	393.52	100
D4	10		10		6		100
D5	10		10		6		100
DR1	10		6		6		100
DR3	10	340.42	6	393.52	6	393.52	100
DR5	10		6		6		100

* See Table 2.4

TABLE 2.2: Reinforcement details

53

Bars	Area mm^2	Yield Str. f_y (N/mm^2)**	Ulti. Str. f_{ul}. (N/mm^2)**	Mod. of El. E_s (N/mm^2)**
$\phi5^*$	.196	259.80	296.67	-
$\phi6$	.283	393.52	545.64	202.380
$\phi8$	.503	294.78	479.71	206.251
$\phi10^*$	.785	335.26	474.79	-
$\phi10$	.785	340.42	494.78	203.891
$\phi12$	1.131	325.97	499.53	204.641
$\phi16$	2.011	320.47	491.77	198.288

*   Bars used for group A only

**   The average results of three samples

TABLE 2.3: Reinforcement properties
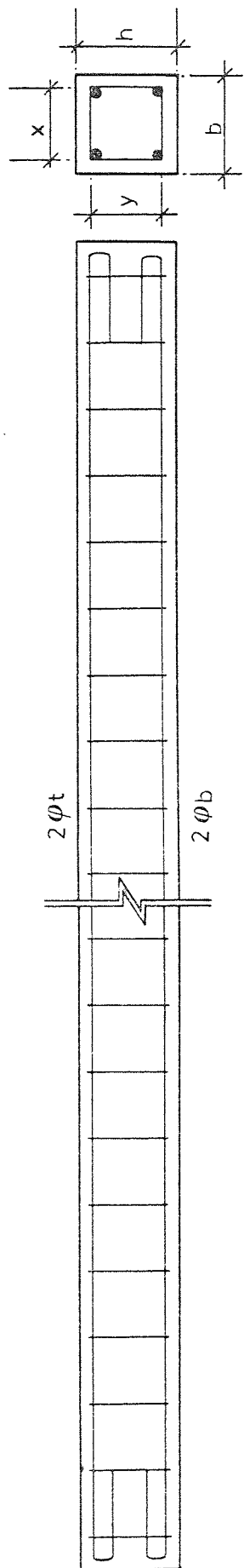
SERIES D
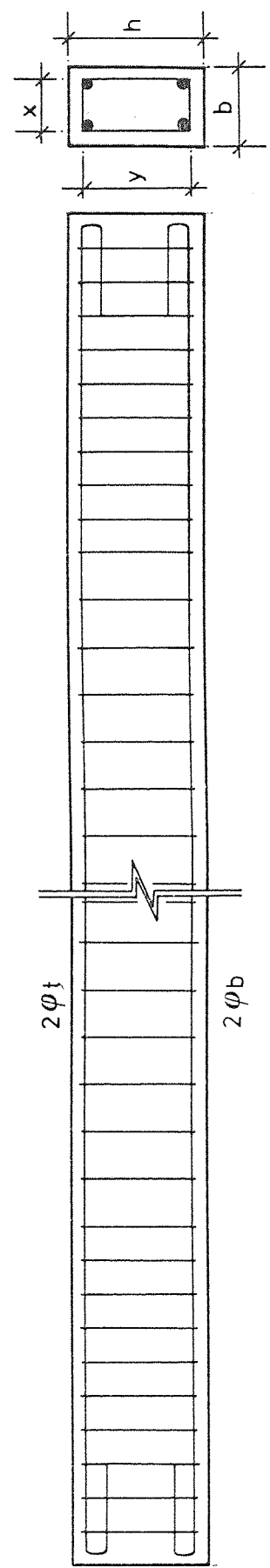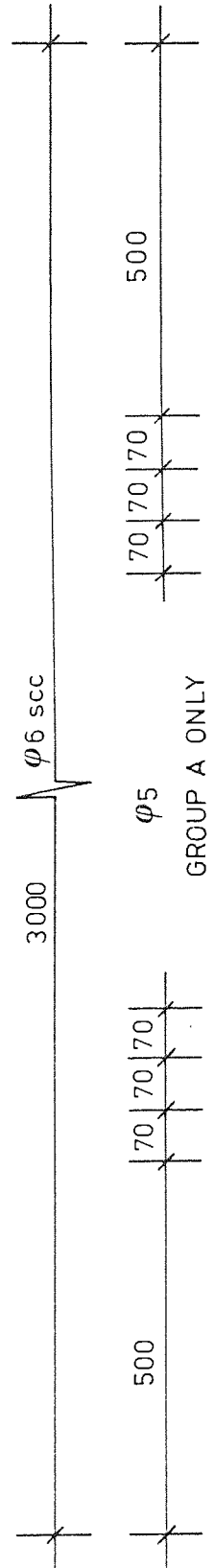
SERIES A, B and C.

FIGURE 2.5 : Reinforcement details and cages — See also figure 2·1 (for b , t and s) see table 2·2)

Beam	Design Mixes	Cement N/one batch	Date of Casting	form	damp	air	Target St. N/mm^2
A1	1:4.0:4.0:0.90	251.8	15.07.1977	1	5	1	10
A2	1:3.2:4.8:0.90	251.8	20.05.1977	1	26	1	13
A3	1:2.9:4.3:0.80	252.9	28.03.1977	1	26	1	15
A4	1:2.7:4.0:0.75	270.5	08.03.1977	1	26	1	20
A5	1:2.3:3.5:0.65	307.2	22.02.1977	1	26	1	25
A6	1:2.0:3.1:0.58	343.4	11.02.1977	2	25	1	30
A7	1:2.0:3.1:0.58	343.4	07.04.1977	1	26	1	30
A8	1:1.8:2.8:0.48	375.9	01.02.1977	2	24	2	40
A9	1:1.0:1.5:0.33	669.2	10.06.1977	4	22	2	65
AR4	1:2.7:4.0:0.75	207.5	18.05.1978	1	26	1	20
AR5	1:2.3:3.5:0.65	307.2	01.06.1978	1	26	1	25
AR9	1:1.0:1.5:0.33	669.2	15.06.1978	1	26	1	65
B1			20.12.1977				
B2			08.09.1977				
B3			25.08.1977				
B4	1:2.3:3.5:0.65	307.2	03.08.1977	1	26	1	25
B5			19.07.1977				
B6			07.07.1977				
B7			15.12.1977				
BR2			20.04.1978				
BR4	1:2.3:3.5:0.65	307.2	06.04.1978	1	26	1	25
BR7			04.05.1978				
C1			20.10.1977				
C2			05.05.1977				
C3	1:2.3:3.5:0.65	307.2	03.11.1977	1	26	1	25
C4			17.11.1977				
C5			08.11.1977				
CR1			29.06.1978				
CR3	1:2.3:3.5:0.65	307.2	01.06.1978	1	26	1	25
CR5			13.07.1978				
D1			23.03.1978				
D2			08.03.1978				
D3	1:2.3:3.5:0.65	328.7	23.02.1978	1	26	1	25
D4			09.02.1978				
D5			25.01.1978				
DR1			17.08.1978				
DR3	1:2.3:3.5:0.65	328.7	03.08.1978	1	26	1	25
DR5			27.07.1978				

TABLE 2.4: Proportion properties for the concrete mixes; date of casting, method of storing, and target strengths.

2.4 TEST PROCEDURE

The frame used for testing the beams is shown in plates 2.2 and 2.3.

At the commencement of the test the side faces of each beam were cleaned and marked from mid-span towards both ends with horizontal and vertical lines in a plane normal to the axis of the beam, in order to plot the formation of the cracks. The cracks were plotted on graph paper at the end of the test. The beam was arranged on the test rig after the torsion out-rigger arms (figure 2.6) had been clamped and secured at both ends. A general view of the rig with test beam subject to the combined action of torsion, bending and shear is shown in plate 2.2. Plate 2.3 shows a general view of the beams tested approximately in pure torsion. Then the wires, which were soldered to the leads of electrical strain gauges fixed on the reinforcement and water proofed (section 2.4.1) prior to the casting, were connected to a junction box and then to a "Peekel" box. Three mechanical deflection gauges were then placed, one at the centre of the span, and one at the end of each of the torsion arms (see plate 2.2). Just before the test started the top surface of the beam was made level.

Immediately before the test the initial deflection and strain gauge readings were recorded. The experiment was started by applying constant load increments, in accordance with the appropriate loading arrangement and sequence for each beam (see section 2.4.2) until failure occurred. Failure occurred when the limit of rotation arms had been reached and the strain gauges had reached the limit.

After considerable stability of the loads, between each two increments the deformation readings were recorded, and the crack

57

formation and extension were carefully traced. New cracks were
marked with their respective load increments on all sides of the
beam. The time needed for each single stage varied between 10
and 15 minutes.

2.4.1 Testing Equipment

The flexural shear load was applied to the beam transversely
at mid-span as a point load, using a hydraulic jack connected to
a "Losenhausen" pump. It was transmitted to the beams by means
of a 100 x 150 mm cross-section bearing pad. The bearing pad
consisted of needle bearings and roller bearings arranged in such
a way as to provide overall axial and rotational freedom.

The torsional load was introduced by means of eccentric
forces applied from a jack of 300 kN capacity (independent of the
flexural jack) to the right outrigger arm. The yokes were fixed
securely at a distance of 50 mm from the ends, using steel wedges
and bolts, and supported on a combination of bearing pads of
similar arrangement to that used at mid-span. The left outrigger
arm was secured firmly to the testing frame using a 32 mm diameter
threaded mild-steel bar, whilst the right was connected to the
torsional load jack through a 50 kN capacity and .0299 kN sensi-
tivity tensile proving ring (the calibration chart is given in
reference [55]) via a 32 mm diameter bar (figure 2.6). This system
was designed and employed by Wainwright [55]. Mechanical "Batty"
dial gauges with 2 in and 25 mm travel and sensitivity of .001 in
and .01 mm respectively, were used throughout the tests. Tokyo
Sokki Kenkyujo type PL-5-11 electrical resistance strain gauges
of 5 mm length, 120 ± .3 resistance, and of 2.05 average gauge
factor, were used to measure the strain in the reinforcement. To

obtain the strain for the concrete compressive cylinders and hence the modulus of elasticity, PL-60-11 of 60 mm gauge length, 120 ± .3 resistance, and of 2.10 average gauge factor were used. M-Bond 200 adhesive, and M-Coat Micro-Measurements product were used for glueing and water-proofing the strain gauges respectively. (The procedure is explained in detail by Alos [56]). The univer-sal "Peekel" electric strain indicator type B103U and extension box type 48U was used to record the steel and concrete strain readings throughout the test programme except beams in group BR and beam D1 for which - Intercol Systems Compulog Alpha 16 Data Logger - was used for reading the steel strain only. The detailed information about the programming is given by Cooper [57]. The Dennison compression and bending machine was used for testing the control specimens, and the Dennison tension machine was used for testing the steel samples.

The concrete was vibrated with a 25 mm diameter "TRIMIX" poker vibrator of 50 revolution per second frequency. This was used throughout, except for beams B1, D1 and DR1, where a table vibrator of changeable frequency was used.

2.4.2 Loading Scheme and Sequence

As it has already been stated in section 2.2, two types of loading arrangements were used throughout the experimental work. The schematic drawings are given in figures 2.2 and 2.3.

For beams loaded in combined torsion, bending and vertical shear (type one load system, figure 2.2), the first bending load increment of 0.981 kN was applied to the test beam, then immediately the first increment of 0.598 kN of torsional load was applied using the right-hand side outrigger arm. After the

stability of the loads the deformation readings were recorded, and the first crack formation readings were detected. The second load stage was then applied by increasing the flexural and torsional loads respectively with the same load ratio and sequence as in the first stage. This was repeated up to failure.

All the beams of group A were tested in this way except beam A6 where the bending load increment for the first three stages was 2.45 kN and 0.981 kN thereafter as for the rest of the beams in this group. The same procedure was conducted for beams in groups B, C and D and beams BR4 and BR7, except in these beams the flexural load was maintained in different stages, for different groups and different beams, as can be seen from Appendix B, whilst the torsion load was increased in stages to failure.

For those beams loaded in very high torsion (type two load system, figure 2.3), the torsional loads were increased in equal increments of 0.598 kN until failure was reached. As it is viewed in plate 2.3, in testing these beams the flexural jack was disconnected and the centre-span bearing pads were removed.

Since the self-weight of the testing beams and the attached apparatus gave rise to the applied bending and torsional loads, the correction for the influence of the dead loads was made and has been included in the reported bending and torsional loads. The change in length of the torsional lever arm when twisting of the beams occurs has been ignored, since at a maximum the error involved is 0.01%.

2.4.3 Instrumentation

All test beams were instrumented for both displacement (deflection and twist) and deformation (reinforcement strain).

60

Vertical deflection (d_m, mm) was measured directly under the bending load (i.e. at maximum moment) using a Batty dial gauge.

The angular rotation (A_r rad/1000 m) for the test beams was evaluated from the recorded measurements of the two mechanical dial gauges. Each of the dial gauges was secured in place on the outer end of the torsional arm, so that the gauge needle was touching the top surface of the grab end of the 32 mm diameter bar. A diagram is given in detail in figure 2.6. The dial gauges measured the vertical displacement at the outer end of the torsional arms. From the change in slope of the arms, the angular rotation was calculated for each stage. In those cases where the bending and torsional deflections were higher than the maximum capacity of the dial gauges, the gauges had to be reset, sometimes more than once.

All the beams were instrumented for steel strain ε_s using electrical resistance strain gauges (section 2.4.1). A total of eight strain gauges were used for each beam. Four of them were stuck on the longitudinal steel (one each) and the other four on the legs of a single stirrup. As explained in section 2.4.1, the strain reading in the steel was obtained for each particular stage by the Data Logger for beams in group BR and beam D1 only, and manually using the Peekel box for the others. The type, adhesive and coating was described in section 2.4.1 above. Their location and distance from the centre of the span are given in table 2.5.

For reason of economy, only the predicted critical (failure) region was instrumented for each beam. Concrete deformation measurements for the beams were also not taken to reduce the number of strain gauges used.

61

Beam	Location of the failure section from the C.P. (mm)	Location of the strain gauges (mm)	
		Stirrups	Longit. Steel
A1	75 RCP*	70 RCP	35 RCP
A2	0 CP	70 RCP	35 RCP
A3	15 RCP	70 RCP	35 RCP
A4	50 RCP	70 RCP	35 RCP
A5	150 RCP	70 RCP	35 RCP
A6	75 RCP	70 RCP	35 RCP
A7	60 RCP	70 RCP	35 RCP
A8	35 RCP	70 RCP	35 RCP
A9	75 RCP	70 RCP	35 RCP
AR4	1100 RCP	80 RCP	40 RCP
AR5	1100 RCP	80 RCP	40 RCP
AR9	1025 LCP*	1100 LCP	1140 LCP
B1	50 LCP	50 RCP	38 RCP
B2	75 RCP	60 RCP	80 RCP
B3	125 RCP	60 RCP	30 RCP
B4	75 RCP	40 RCP	80 RCP
B5	150 RCP	50 RCP	100 RCP
B6	600 RCP	60 RCP	120 RCP
B7	875 LCP	200 RCP	100 RCP
BR2	1150 LCP	80 RCP	60 RCP
BR4	1200 RCP	80 RCP	40 RCP
BR7	1125 LCP	200 RCP	100 RCP
C1	75 RCP	80 RCP	40 RCP
C2	70 RCP	80 RCP	40 RCP
C3	1200 RCP	80 RCP	40 RCP
C4	1325 LCP	80 RCP	40 RCP
C5	1350 RCP	80 RCP	40 RCP
CR1	300 LCP	1000 LCP	960 LCP
CR3	1100 RCP	80 RCP	40 RCP
CR5	1200 LCP	1000 LCP	960 LCP
D1	300 RCP	100 RCP	50 RCP
D2	180 RCP	100 RCP	50 RCP
D3	170 RCP	100 RCP	50 RCP
D4	150 LCP	100 RCP	50 RCP
D5	150 RCP	100 RCP	50 RCP
DR1	850 LCP	900 LCP	850 LCP
DR3	1170 LCP	1000 LCP	950 LCP
DR5	250 LCP	900 LCP	850 LCP

* RCP, LCP   Right and Left of the Central Plane respectively

TABLE 2.5:   Location of the failure section and the strain gauges
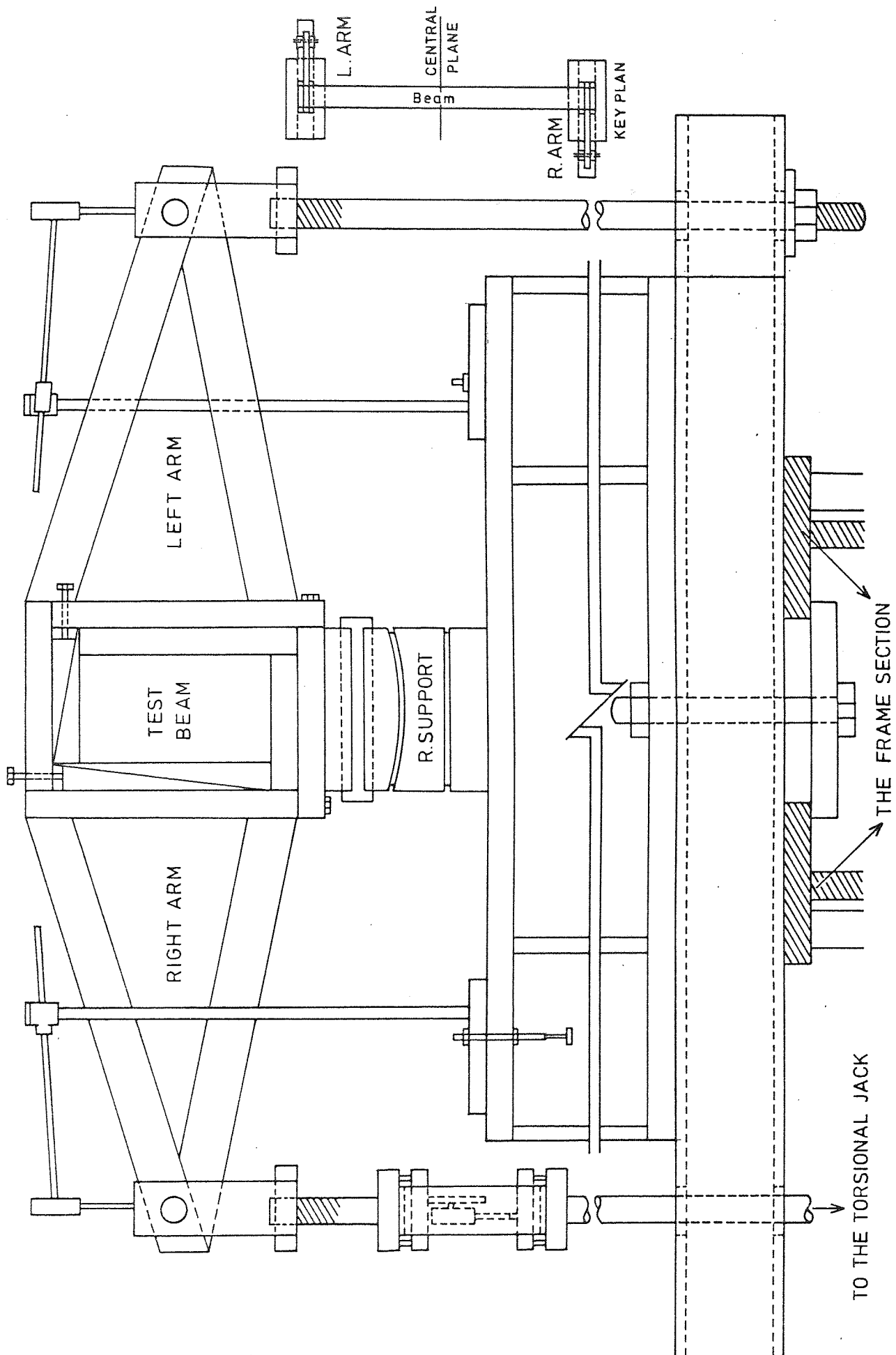
FIGURE 2.6   End elevation of the test rig

63
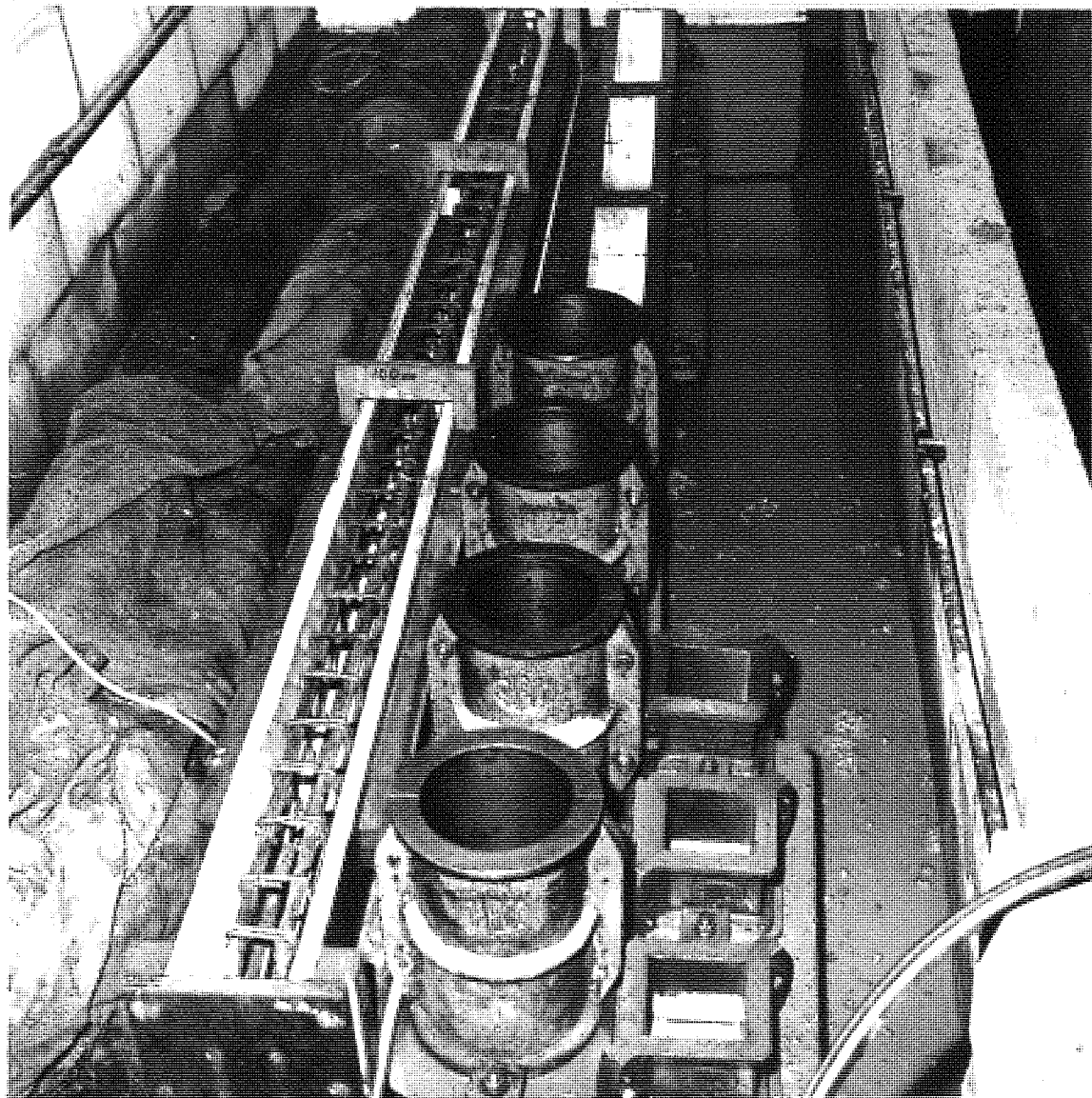
PLATE 2.1 General layout of the formwork and curing area
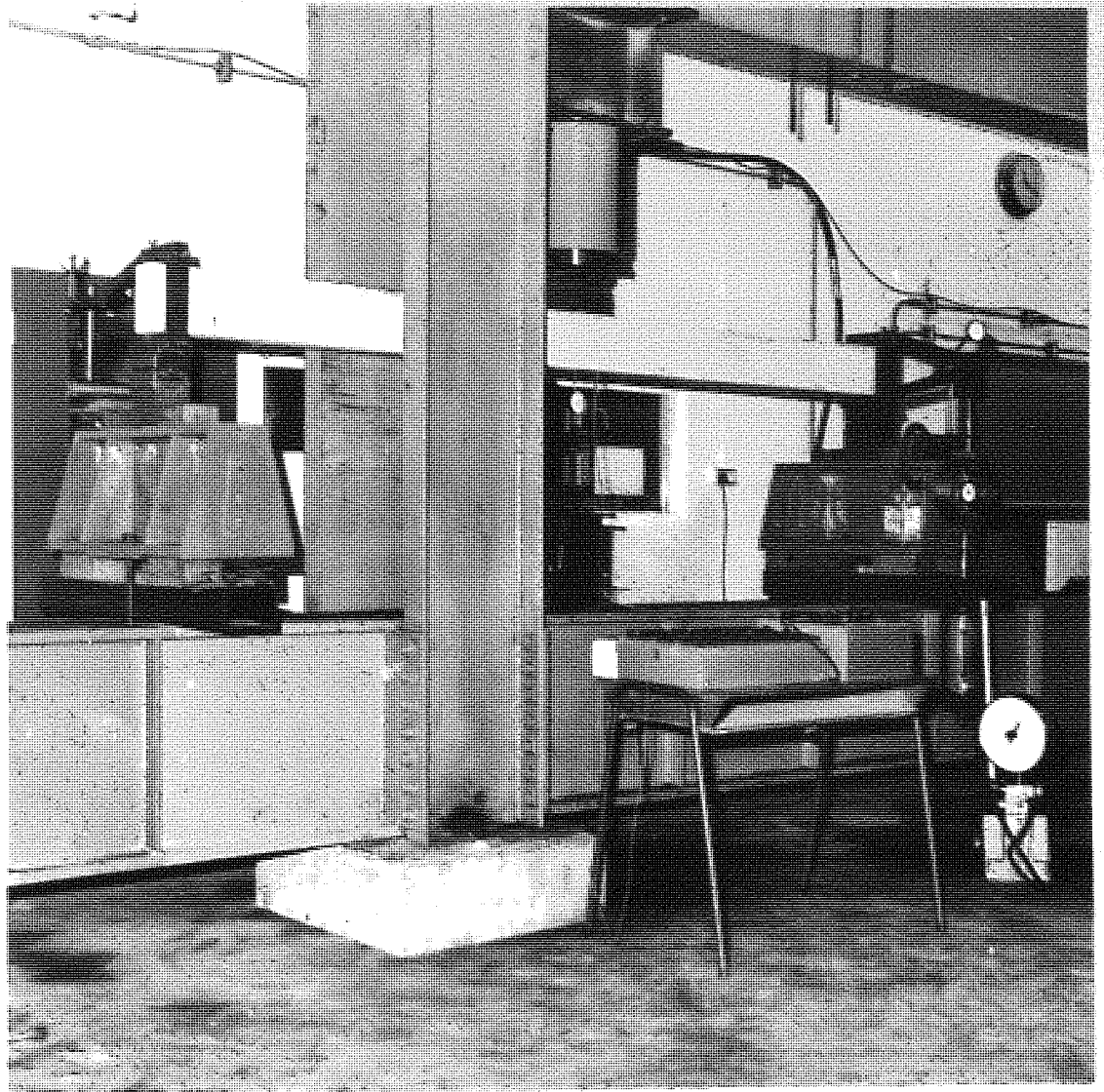
PLATE 2.2 General view of the testing rig for beams tested under
the combined action of torsion, bending and shear
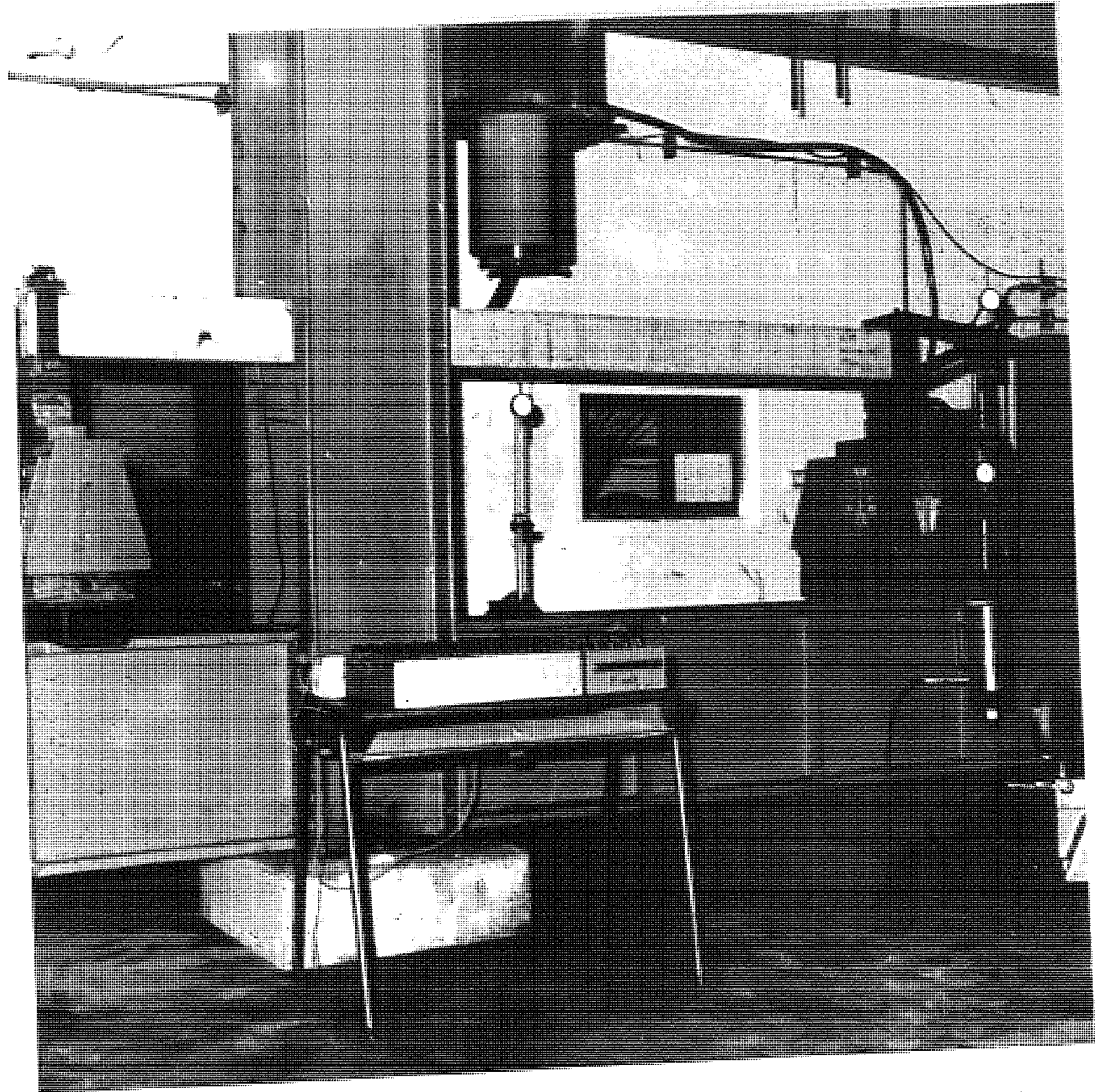
PLATE 2.3   General view of the testing rig, for beams tested in high
torsional moment

CHAPTER THREE

EXPERIMENTAL RESULTS

3.1 INTRODUCTION

Relatively little experimental work with regard to reinforced concrete beams subject to torsion, bending and shear, has been carried out in the past few years. Far less is known about the deformation behaviour and characteristics during the loading stages. Some recent works [58, 59] have, however, improved the situation, and the report by Walsh et al [19] in 1966 was one of the first to consider this matter.

The theoretical analysis of a member at ultimate load requires a detailed knowledge concerning the state of stress and deformation through various stages of loading. The detailed measurements recorded during the experimental work presented in this chapter, will be used later to develop the theory.

In this chapter the average strength of the control specimen, the loads at the first visible crack and at ultimate strength as well as the observed mode of failure are given. Deflection and rotation are plotted against both torsion and moment and also failure pattern and inclination of the cracks on the faces of the beam are considered. The behaviour of each individual beam from the first visible crack till failure is described, but over-all behaviour at various load stages is tabulated in the appendix.

3.2 PRINCIPAL TEST RESULTS

Results obtained from the experimental work can be divided into those recorded from testing the control specimens, and those for the reinforced concrete test beams.

3.2.1 Control Specimens

The characteristic strengths of the control specimens for the test beams are given in table 3.1. The values given in this table for cube compressive strength (f_{cu}), cylinder compressive strength (f_c'), splitting tensile strength (f_{sp}), modulus of rupture (f_r) and modulus of elasticity (E_c), are the average values obtained from testing 3 cubes, 2 cylinders, 2 cylinders, 3 prismatic beams and (2 cylinders) respectively, unless otherwise indicated. The method used to obtain the modulus of elasticity is explained in Appendix A.

3.2.2 Test Beams

The applied load P, bending moment M, torsional moment T and vertical shear V at first visible crack and at ultimate load in the mid-span are given in table 3.2. The observed mode of failure is also stated in this table. In some cases it was not possible to specify the exact failure mode from the appearance of the beam at failure, and therefore two modes are reported, with the most pre-dominant one first.

The applied torsional moment and measured bending moment and vertical shear, at the failure section, are presented in table 3.3.

The location of failure section (table 2.5) is measured from the mid-span (i.e. central plane - which is normal to the longi-tudinal axis of the beam at the mid-span), to the failure section (i.e. plane of critical section - which is parallel to the central plane through the failure section). Table 3.3 also contains values of the vertical deflection d_m at mid-span, angular rotation A_r and torsional stiffness S_t for all the test beams at failure.

The estimated dead loads are included in the values reported

Beam	f_{cu} N/mm^2	f_c' N/mm^2	f_{sp} N/mm^2	f_r N/mm^2	E_c N/mm^2 Initial	E_c N/mm^2 Secant
A1	13.08	10.56	1.42	2.33	-	-
A2	23.21	15.61	1.69	2.99	20597	10298
A3	28.28	19.81	2.47	2.97	21930	10965
A4	29.75	25.10	2.52	3.46	27142	13571
A5	40.83	32.82	2.72	3.69	-	-
A6	44.78	31.63	2.91	4.09	-	-
A7	45.14	28.19	3.19	3.02	-	-
A8	50.67	38.48	3.82	5.71	-	-
A9	59.89	44.51	4.11	5.24	42162	21081
AR4	31.94	23.41	2.22	3.01	27500	13750
AR5	41.42	25.00	2.25	3.04	27055	13528
AR9	66.62	55.61	3.90	4.86	50846	25423
B1	27.26	19.53	2.17	2.73	-	-
B2	26.49	19.78	1.78	2.76	26378	13189
B3	30.60	23.24	2.46	2.94	31024	15512
B4	31.71	23.22	1.74	2.82	-	-
B5	31.58	19.33	2.43	2.95	30678	15339
B6	35.96	26.03	2.46	3.70	31171	15585
B7	28.77	23.39	2.29	2.99	28167	14083
BR2	32.23	22.45	1.71	3.32	26382	13191
BR4	26.05	21.75	1.89	3.18	22432	11216*
BR7	35.06	26.11	1.91	2.59	24031	12016*
C1	28.89	23.57	1.57	2.94	28292	14146
C2	35.19	29.51	2.58	3.08	-	-
C3	31.90	22.70	2.43	2.86	29355	14677
C4	31.81	25.17	2.12	3.00	30903	15451
C5	30.05	26.92	2.16	2.55	27219	13610
CR1	35.66	25.03	2.84	3.04	29335	14668
CR3	31.94	23.41	2.22	3.01	27500	13750
CR5	37.27	28.94	2.24	3.41	33958	16979
D1	28.70	20.34	2.52	2.95	21770	10885*
D2	39.42	28.11	2.62	3.44	27622	13811*
D3	38.62	25.81	2.48	3.15	28047	14023
D4	33.25	24.42	2.38	3.09	30454	15227*
D5	31.61	24.83	2.39	3.01	28964	14482
DR1	40.53	23.59	2.46	3.67	29379	14689*
DR3	38.28	30.97	2.48	3.35	30884	15442
DR5	39.31	32.33	2.51	3.64	32859	16430

* Calculated from one specimen

TABLE 3.1: The average strength of the control specimen

Beam	P KN	Cracking loads			Ultimate loads			Obse. mode of failure
		M kN.m	T KN.m	V KN	M KN.m	T KN.m	V KN	
A1	6.353	2.007	0.694	1.084	4.140	1.382	2.555	1
A2	6.353	2.007	0.694	1.084	4.140	1.409	2.555	1
A3	7.334	2.718	0.969	1.574	4.518	1.657	3.045	1
A4	8.315	2.718	0.969	1.574	5.562	1.794	3.536	1
A5	9.295	2.718	0.969	1.574	6.273	2.207	4.026	1
A6	9.295	2.362	0.419	1.329	6.273	1.519	4.026	1
A7	9.295	2.718	0.969	1.574	6.273	2.207	4.026	1
A8	10.276	3.429	1.244	2.065	6.984	2.345	4.516	1
A9	11.257	3.429	1.244	2.065	7.695	2.620	5.007	1
AR4	1.244	0.436	1.794	–	0.436	2.345	–	3
AR5	1.244	0.436	1.794	–	0.436	2.441	–	3
AR9	1.244	0.436	2.895	–	0.436	3.514	–	3
B1	8.315	3.423	1.244	2.065	5.562	2.936	3.536	1
B2	8.315	2.718	0.969	1.574	5.562	2.276	3.536	1
B3	8.315	2.007	0.694	1.084	5.562	2.413	3.536	1
B4	8.315	2.718	0.969	1.574	5.562	2.207	3.536	1
B5	8.315	2.007	0.694	1.084	5.562	2.001	3.536	1
B6	8.315	2.718	0.969	1.574	5.562	1.932	3.536	2
B7	7.334	2.718	0.969	1.574	4.851	1.588	3.045	2
BR2	1.244	0.436	2.070	–	0.436	2.661	–	3, 2
BR4	8.315	2.718	0.969	1.574	5.562	2.386	3.536	3, 2
BR7	4.392	2.007	0.694	1.084	2.718	1.519	1.574	2
C1	6.353	2.007	0.694	1.084	4.140	1.244	2.555	1
C2	6.353	2.007	0.694	1.084	4.140	1.519	2.555	1
C3	6.353	2.718	0.969	1.574	4.140	1.932	2.555	2
C4	6.353	2.718	0.969	1.574	4.140	2.400	2.555	2
C5	6.437	4.169	1.519	2.555	4.169	2.345	2.555	–
CR1	1.244	0.436	1.794	–	0.436	2.001	–	2
CR3	1.244	0.436	1.794	–	0.436	2.345	–	3
CR5	1.244	0.436	1.794	–	0.436	2.592	–	3
D1	5.856	1.833	0.694	1.084	3.966	1.313	2.555	–
D2	7.051	1.907	0.694	1.084	4.751	2.028	3.045	1
D3	7.263	1.982	0.694	1.084	4.826	2.372	3.045	1
D4	7.476	2.057	0.694	1.084	4.901	3.032	3.045	1
D5	7.690	2.132	0.694	1.084	4.976	2.413	3.045	1
DR1	0.953	0.262	0.969	–	0.262	1.244	–	3
DR3	1.379	0.411	1.794	–	0.411	2.042	–	2
DR5	1.806	0.561	2.620	–	0.561	3.280	–	2

TABLE 3.2:   The applied loads at cracking, and at ultimate with observed mode of failure.

| Beam | Load ratio M:T:Vh at ultimate | Loads at failure section | | | Displacement | | Stiffness |
		M KN.m	T KN.m	V KN	d_m mm	A_r rad/1000m	S_t KN.m^2/rad
A1	2.810:1.0:0.328	3.883	1.382	2.594	7.52	38.00	36.368
A2	2.938:1.0:0.317	4.140	1.409	2.555	8.81	29.36	47.990
A3	2.897:1.0:0.322	4.801	1.657	3.051	12.92	72.97	22.708
A4	2.993:1.0:0.347	5.370	1.794	3.557	15.82	74.21	24.175
A5	2.548:1.0:0.324	5.624	2.207	4.090	15.55	70.14	31.467
A6	3.916:1.0:0.468	5.949	1.519	4.058	7.92	23.45	64.776
A7	2.725:1.0:0.321	6.013	2.207	4.052	21.54	77.52	28.470
A8	2.906:1.0:0.341	6.815	2.345	4.572	23.08	64.05	36.612
A9	2.785:1.0:0.337	7.297	2.620	5.039	26.04	31.12	84.190
AR4	0.045:1.0:0.035	0.105	2.345	0.472	-2.18	55.02	42.621
AR5	0.043:1.0:0.034	0.105	2.441	0.472	0.50	74.08	32.951
AR9	0.036:1.0:0.022	0.128	3.514	0.440	-1.02	61.98	56.696
B1	1.829:1.0:0.212	5.370	2.936	3.557	17.83	101.69	28.872
B2	2.317:1.0:0.274	5.274	2.276	3.568	14.48	70.03	32.500
B3	2.107:1.0:0.260	5.083	2.413	3.590	23.38	78.87	30.595
B4	2.390:1.0:0.283	5.274	2.207	3.568	23.23	78.62	28.072
B5	2.492:1.0:0.315	4.987	2.001	3.600	27.85	37.36	53.560
B6	1.687:1.0:0.344	3.260	1.932	3.793	21.98	42.86	45.077
B7	1.212:1.0:0.377	1.924	1.588	3.420	10.46	62.57	25.380
BR2	0.034:1.0:0.032	0.090	2.661	0.493	-4.24	61.33	43.388
BR4	0.402:1.0:0.297	0.959	2.386	4.051	9.88	99.60	23.956
BR7	0.401:1.0:0.237	0.609	1.519	2.057	7.49	67.06	22.651
C1	3.156:1.0:0.364	3.926	1.244	2.587	37.72	37.82	32.893
C2	2.594:1.0:0.298	3.940	1.519	2.585	41.00	39.24	38.710
C3	0.370:1.0:0.278	0.714	1.932	3.070	7.80	70.41	27.439
C4	0.149:1.0:0.228	0.357	2.400	3.123	8.69	78.92	30.411
C5	0.123:1.0:0.237	0.288	2.345	3.173	4.67	57.15	41.032
CR1	0.173:1.0:0.011	0.346	2.001	0.129	4.29	55.59	35.996
CR3	0.045:1.0:0.035	0.105	2.345	0.472	-2.18	55.02	42.621
CR5	0.029:1.0:0.035	0.075	2.592	0.515	-4.55	74.31	34.881
D1	2.395:1.0:0.301	3.145	1.313	2.632	14.05	102.48	12.812
D2	2.052:1.0:0.230	4.161	2.028	3.105	16.48	109.53	18.515
D3	1.796:1.0:0.197	4.260	2.372	3.114	24.21	79.08	29.995
D4	1.449:1.0:1.154	4.393	3.032	3.117	18.14	81.60	37.157
D5	1.849:1.0:0.194	4.461	2.413	3.128	29.95	51.98	46.422
DR1	0.143:1.0:0.023	0.217	1.244	0.219	-0.10	45.90	27.102
DR3	0.039:1.0:0.035	0.079	2.042	0.474	-1.12	37.41	54.584
DR5	0.141:1.0:0.006	0.464	3.280	0.138	-1.22	34.99	93.741

TABLE 3.3: Failure loads at the critical section; and measured displacement

in table 3.2 and 3.3. An average unit weight of 23.7 kN/m^3 for the concrete was used for all the test beams, except beam C5 for which 25.3 kN/m^3 was used [60].

3.3 GENERAL OBSERVATIONS AND MODES OF FAILURE

Loading sequence is described in section 2.4.2. The crack pattern and behaviour of the individual beams, from first observed crack till failure, are given in detail in section 3.7. In this section, a general observed failure pattern of the beams during the experimentation is described with reference to the three idealized failure modes, namely modes 1, 2 and 3.

In all of the modes the two ends of a major tension crack, spiralling around three faces of the beam, joined together through the compression hinge near the fourth face. Failure occurred when the beam rotated about an axis in the critical zone accompanied by crushing of the concrete. The failure is referred to as mode 1 when the compression zone was near the top, mode 2 when near one of the sides or mode 3 when near the bottom face of the beam. The failure mechanism was first observed and described by Lessig [8]. She concluded that, at failure, the steel crossing the failure section reached the yield strength.

3.3.1 Mode One Failure

Beams which failed in this mode were mainly those which were subjected to a high ratio of bending to torsion moment ψ, in accordance to type one load system (see section 2.4.2).

The first crack was observed to form after the load stage 2 for most of these beams. These cracks were fine flexural cracks in the region of maximum bending moment. They originated at the bottom of the side faces and travelled across the bottom face.

Immediately after cracking the strain in the reinforcement increased considerably, associated with an increase in the rotation. With increasing load the cracks spread upward at approximately constant inclination towards the right support, on the north face, where the torsion and shear stress were opposite, and towards the left support on the south face, where the shear stresses were coincident. Meanwhile, more cracks developed around the three faces.

The crack slope decreased beyond the mid-height of the side faces in the vicinity of the central plane. Near the supports cracks were almost non-existent. This description confirms that the bending to torsion ratio (ψ) largely affects the inclination of the cracks at the failure section in beams subjected to combined loading.

When further load increments were applied, more cracks initiated around the three faces in the region of high bending moment. The existing tensile cracks widened and spread upward almost to the top face with constant inclination. Failure was observed to occur by extensive crushing of the concrete at the top face accompanied by a principal tensile crack spiralling at different inclinations on the other three faces.

At failure the stiffness was very small and the beam experienced a large increase in both global and local deformation.

3.3.2 Mode Two Failure

This mode of failure occurred mainly in the beams tested with low ratios of ψ. For beams which failed in this mode cracks also started at the region of high bending moment but at a later stage than the beams in mode 1. After cracking, due to subsequent load-

73

ing the existing cracks, mainly on the highly stressed side (the side in which the torsional and shear stresses were additive), gradually spread upwards. At the same time torsional (diagonal tension) cracks formed around the bottom, highly stressed side and on the top faces along the central part of the span, independently of the flexural cracks. In the final load stage, one or two of the spiralling tensile cracks widened extensively on the three faces. The beam failed by crushing of the concrete on the fourth face (the face in which the torsional and shear stresses were subtractive) and by rotation of the segments of the beam about an axis in the critical section.

3.3.3 Mode Three Failure

Mode 3 failure occurred in those beams which were tested under almost pure torsional moment (i.e. very small values of ψ). In these beams cracks were first observed at a load stage close to failure. The cracks were torsional - at an inclination of approximately 45° - spiralling around the four faces along the span. As the load was increased, some newly formed cracks appeared and the existing cracks widened and extended to join the ends forming a complete rectangular helix. The cracks were more numerous on these beams faces in comparison with the beams which failed in the earlier modes. At failure one or two of these tensile diagonal cracks near the support opened followed by crushing of the concrete in the bottom face.

In some cases with particularly small ratios of ψ, the crushing of the concrete was not apparent, and it was assumed that the concrete failed by cleavage.

3.4 VERTICAL SHEAR

The effect of vertical shear force on the behaviour and ultimate strength of the beams in combined torsion and bending was significant in particular those beams which failed in mode 2. In this case the applied shear force prevented the diagonal tensile cracks from propagating on the lowly stressed side (the side on which the stresses due to torsion and shear were in opposite sign). Consequently, as the load increased mode 1 failure changed to mode 2.

In general the applied vertical shear reduced the ultimate capacity of the beams, and also affected the development and inclination of the cracks, particularly on the sides of those beams which failed in modes 1 and 3. This resulted in the different crack angles on the side faces.

3.5 DISPLACEMENT OF THE BEAMS

This section is concerned with both the vertical deflection and angular rotation of the test beams.

In both sets of bending-deflection and torque-twist curves the values of the loads at first observed cracks are indicated by a small dash with a letter c above, located just to the right of the open dots, which indicated the load stage.

At some loading stage, (as explained previously) the bending load was maintained constant while the torsional load was increased to failure. The stage at which the load was maintained is indicated by a horizontal dash - marked with the symbol of the load, located just to the left of the curve. In plotting these curves, the applied loads only were considered i.e. the dead loads were ignored.

3.5.1   Deflection d_m (mm)

The vertical mid-span deflection for all the test beams was measured.   The load-deflection curves for groups A, B, C and D are shown in figures 3.1, 3.2, 3.3 and 3.4; and for groups AR, BR, CR and DR are presented in figures 3.5, 3.6, 3.7 and 3.8, respectively.

Beams tested in bending, torsion and shear deflected downwards, as the load was applied.   Whilst beams tested under pure torsion and self-weight, with weak top steel - such as beams AR4, AR5, AR9, BR2, CR3, CR5, DR3 and DR5, showed upward deflection upon increasing the torsional load.

Maximum downward deflection of 41.00 mm was recorded for beam C2 - tested under the load ratio M:T:Vh of 3:1:0.3, and the maximum upward deflection of -4.55 mm was recorded for beam CR5.

The upward deflection may be explained by the phenomena that, after the propagation of the torsional cracks around the beam, the weaker reinforcement (located near the top in these beams) reached a higher strain, and consequently when a higher load was applied, the beam failed in mode 3.

There are no clear differences in the slope of the bending-deflection curves for beams within groups A, B and D.   In general, they ascend smoothly through loading stages till close to failure, where, for some beams, the deflection increases considerably for a small increase in the applied load.

Load-deflection curves for beams of group C, illustrated in figure 3.3, show that the inclination of the curve is clearly a function of the amount of longitudinal reinforcement.

It can be seen from figures 3.1, 3.2 and 3.4 that the concrete quality, the amount of transverse steel, and the cross-

section dimension appears to have little effect on the slope of bending-deflection curves before cracking.

3.5.2 Rotation A_r (rad/1000 m)

The angle of twist for the beams in the main groups (i.e. A, B, C and D) was measured over a half length of the span, while those for beams in the secondary groups - i.e. AR, BR (beam BR2 only), CR and DR, was measured over the full length. The torque-twist curves for groups A, B, C, D, AR, BR, CR and DR are shown in figures 3.9, 3.10, 3.11, 3.12, 3.13, 3.14, 3.15 and 3.16, respectively.

The shape of torque-twist curves for beams tested in high torsion can be described as a linear curve ascending from the origin until the cracking torque is reached. Beyond the cracking torque a distinct reduction in the slope is apparent, and terminates with a flat region associated with failure. This sudden change in the slope is not so apparent for the curves of beams tested under combined loadings.

It must be remembered, however, that these latter curves represent values over the half length of the beams which were subjected to variable bending moments. It is difficult, therefore, to generalize concerning the influence of different ψ ratios on the inclination of the torque-twist curves.

The maximum angle of twist recorded was 109.53 rad/1000 m for beam D2; while the minimum twist angle was 23.45 rad/1000 m for beam A6.

3.6 LOCAL DEFORMATIONS

3.6.1 Reinforcement Strain ε_s

The strain in the legs of one stirrup and the four longi-
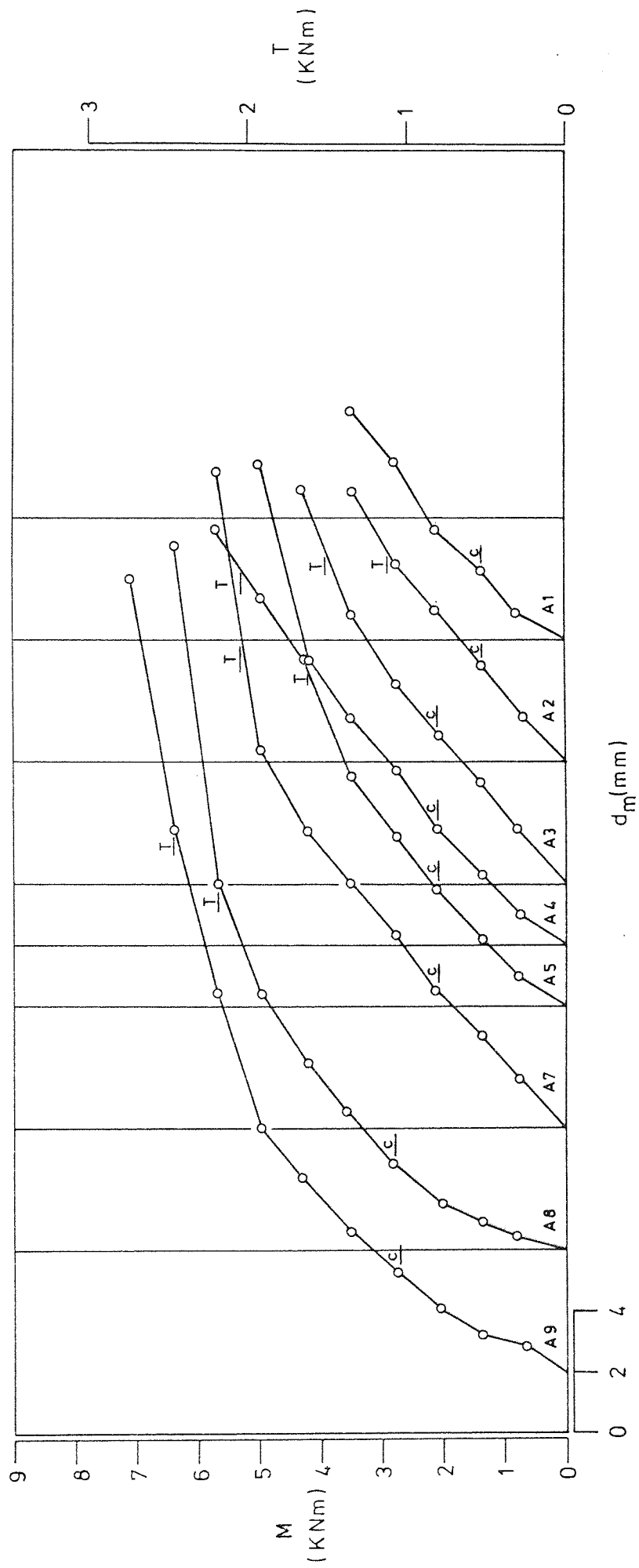
FIGURE 3.1 : Applied bending, torsion - central deflection curves for beams in group A
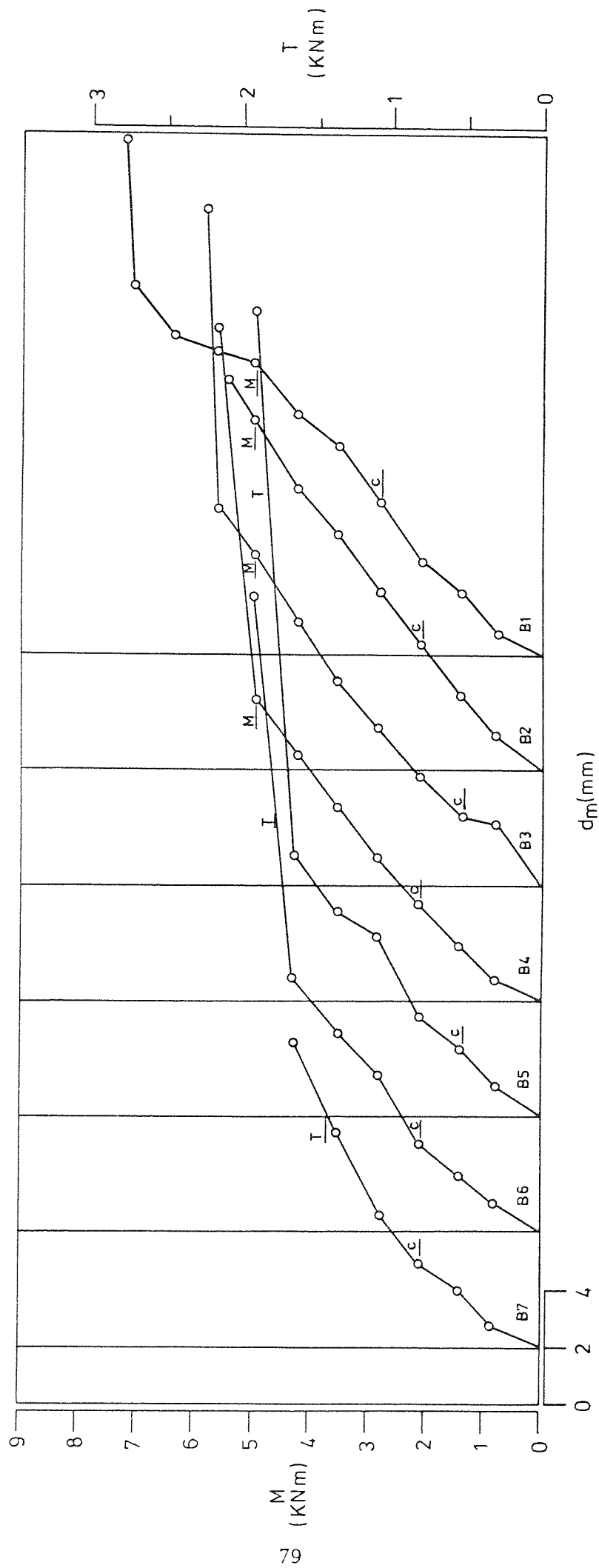
FIGURE 3.2 : Applied bending ; torsion-central deflection curves for beams in group B
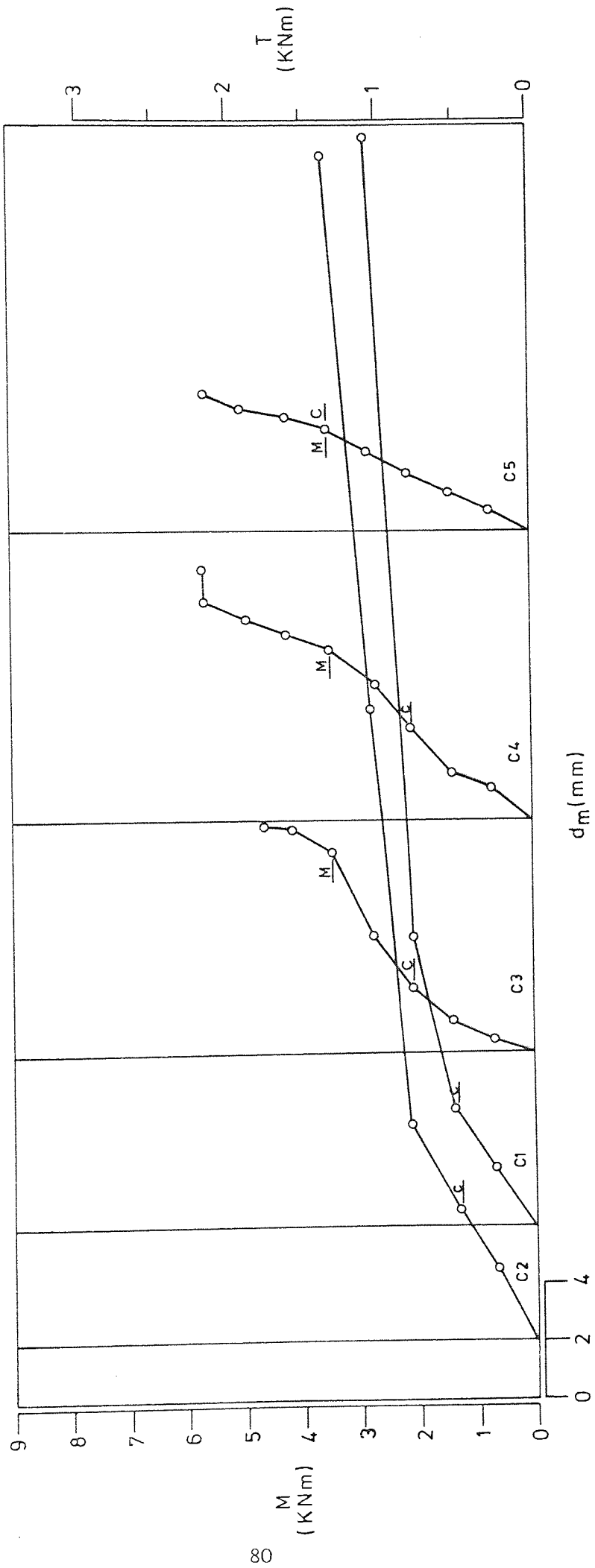
FIGURE 3.3 : Applied bending ;torsion - central deflection curves for beams in group C
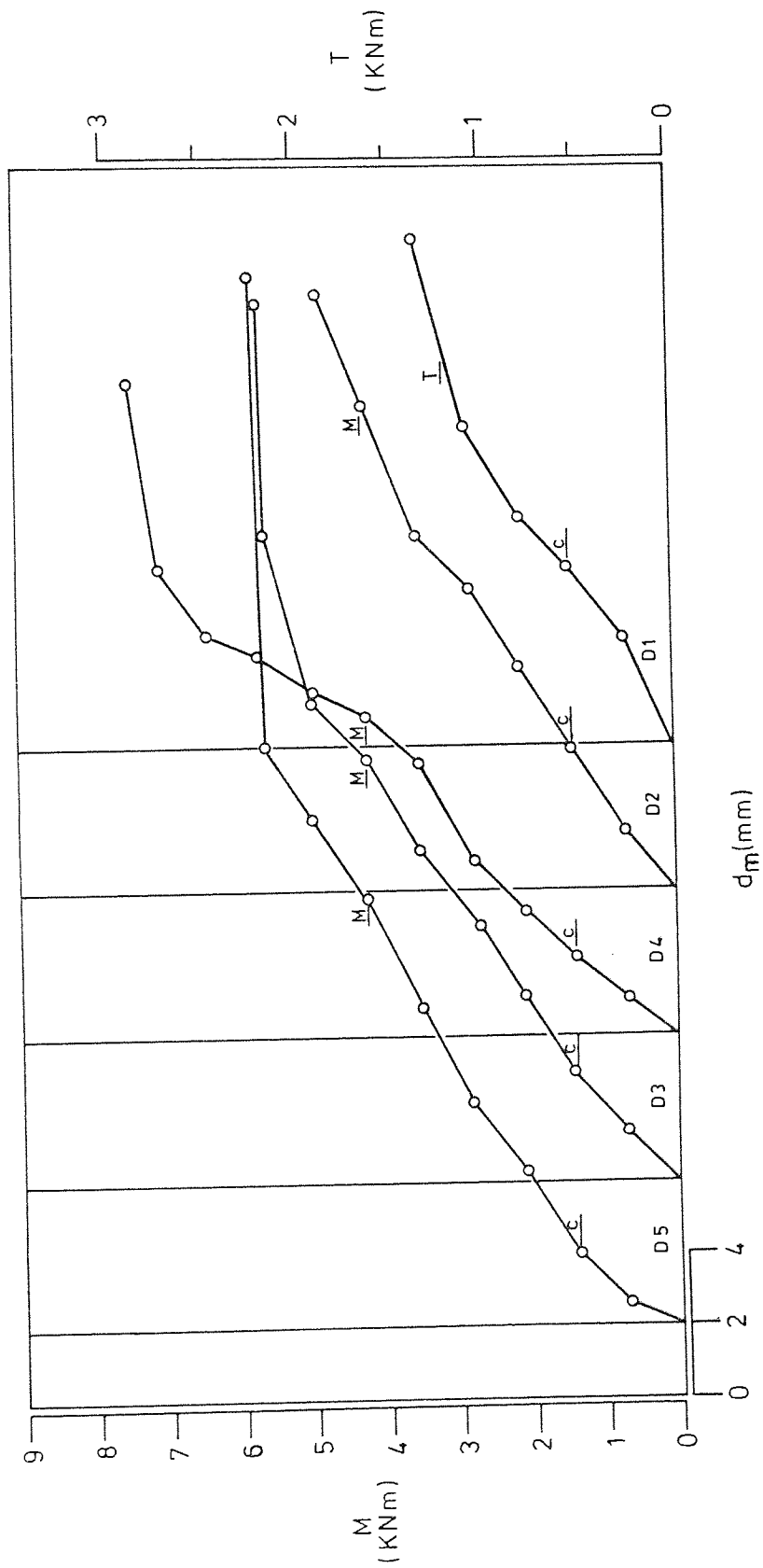
FIGURE 3.4 : Applied bending ; torsion – central deflection curves for beams in group D
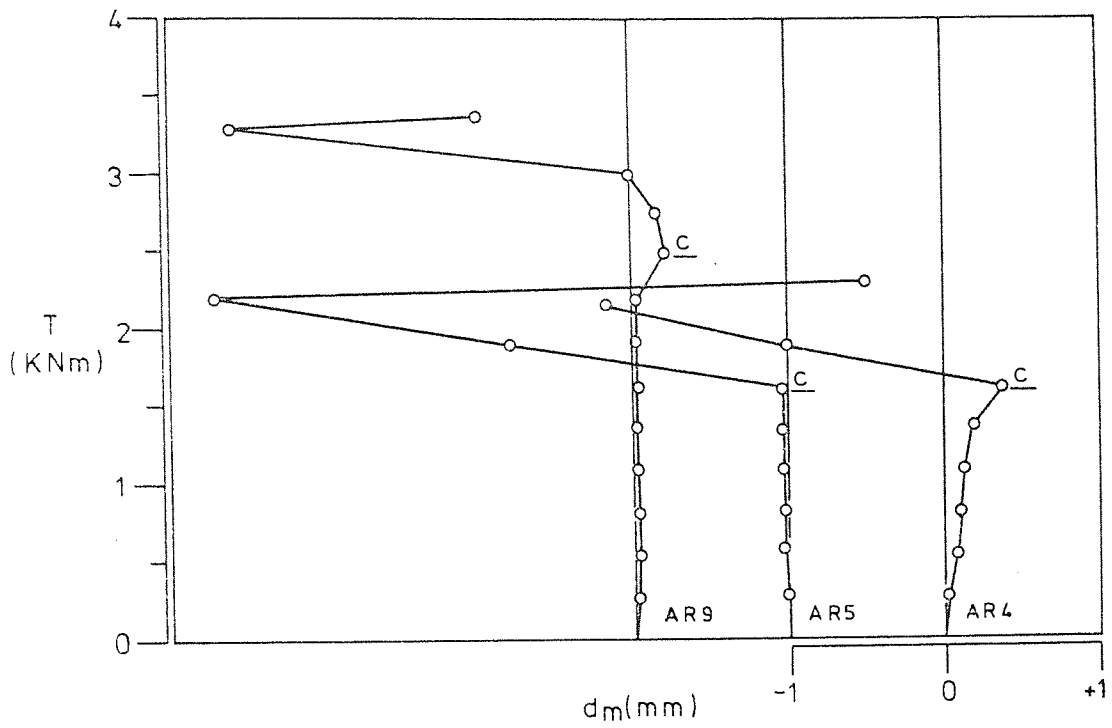
FIGURE 3.5 : Applied torsion - central deflection curves

for beams in group AR.
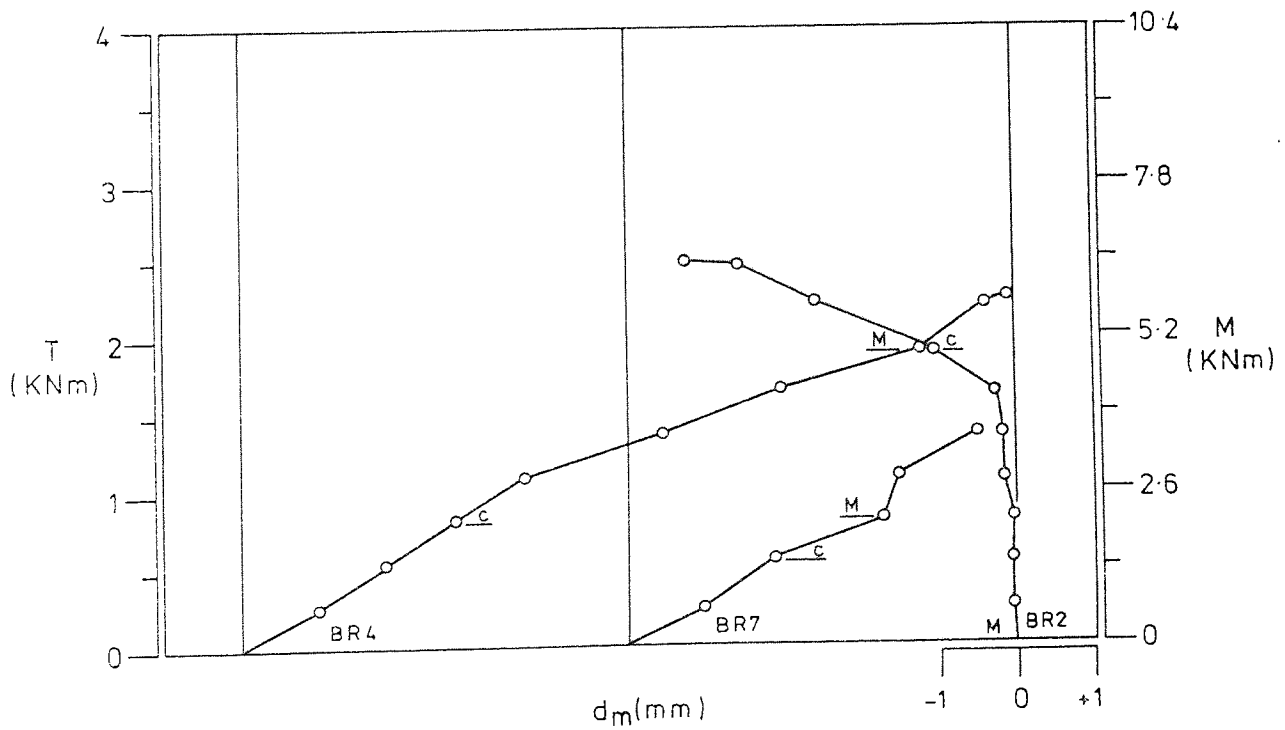
FIGURE 3.6 : Applied bending, torsion - central deflection

curves for beams in group BR.
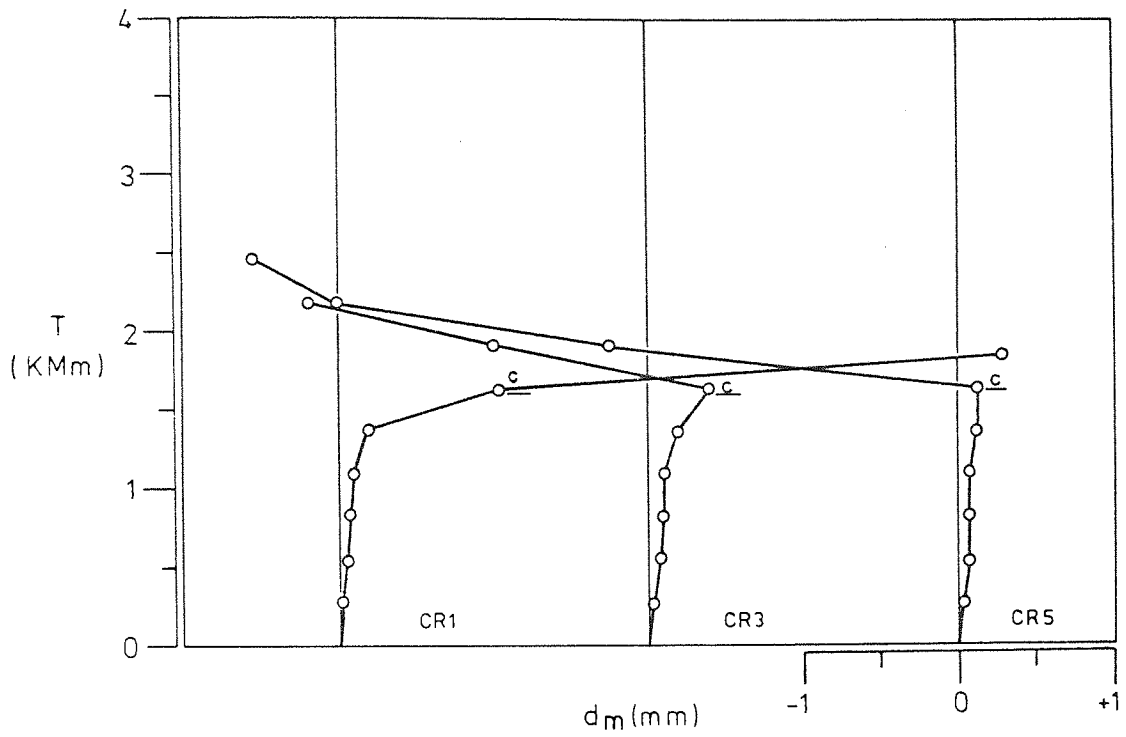
FIGURE 3.7 : Applied torsion – central deflection curves

for beams in group CR
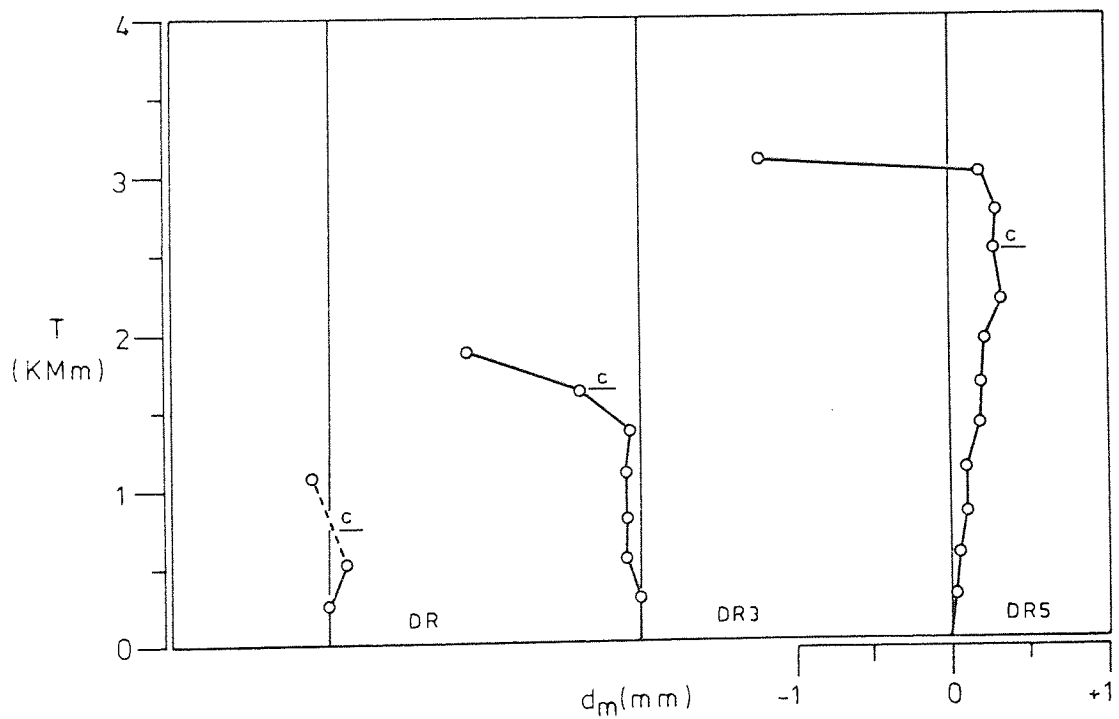
FIGURE 3.8 : Applied torsion – central deflection curves

for beams in group DR
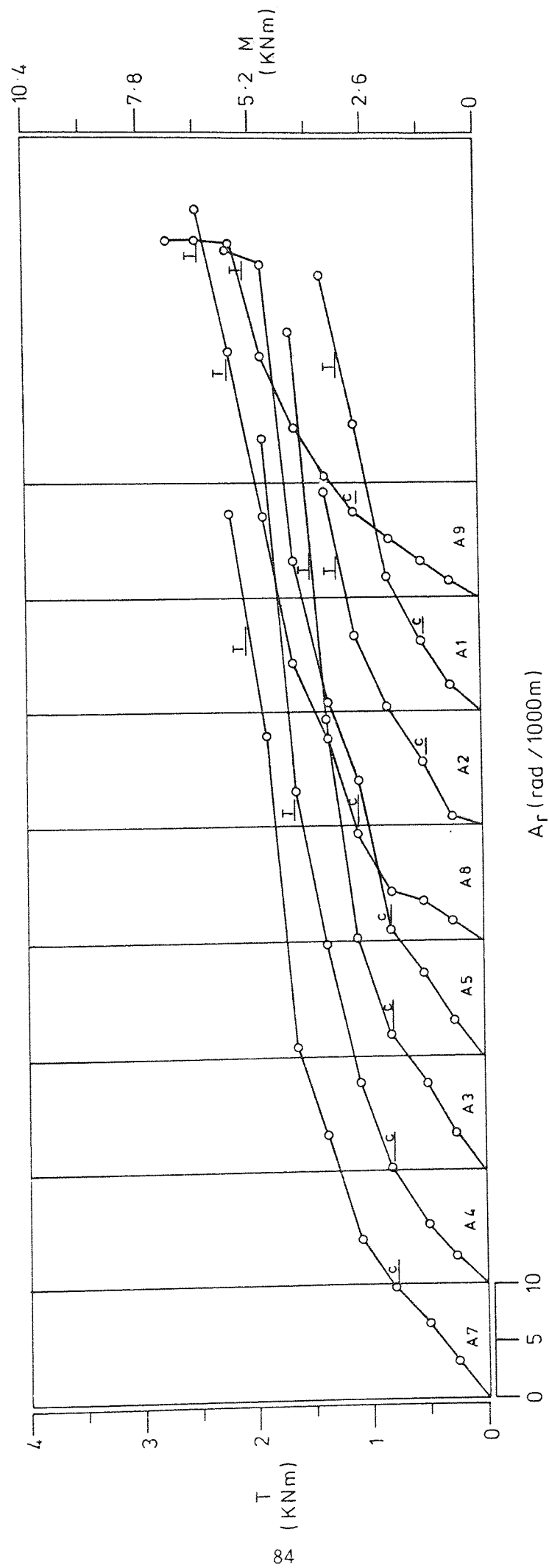
FIGURE 3.9 : Applied torsion ; bending-rotation (over half length of the span) curves for beams in group A
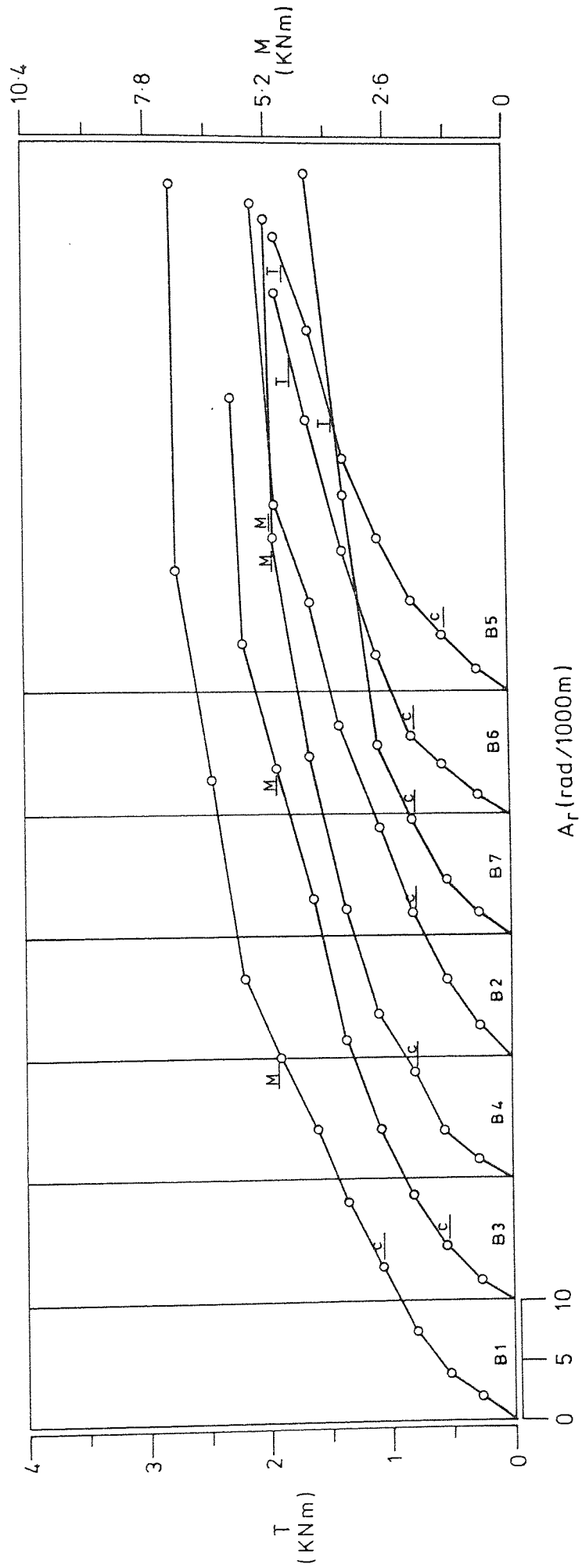
FIGURE 3.10 : Applied torsion ; bending-rotation (over half length of the span) curves for beams in group B
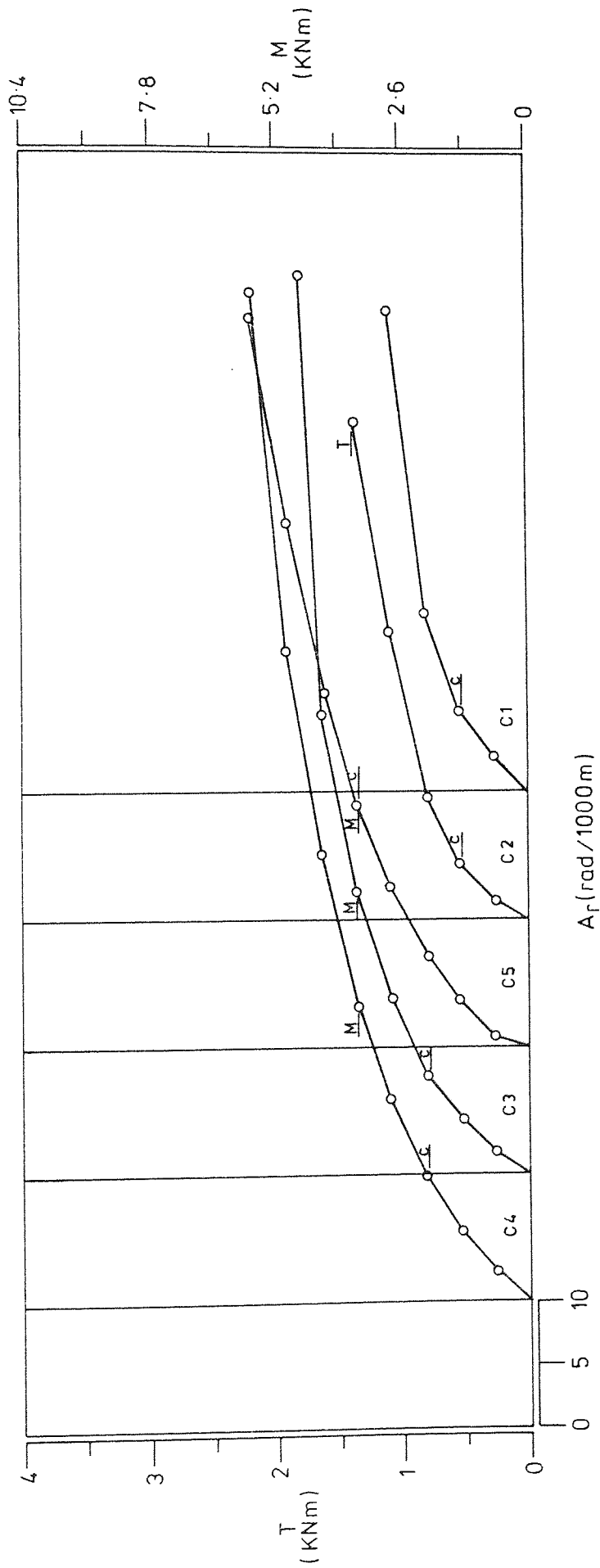
FIGURE 3.11 : Applied torsion, bending-rotation (over half length of the span) curves for beams in group C
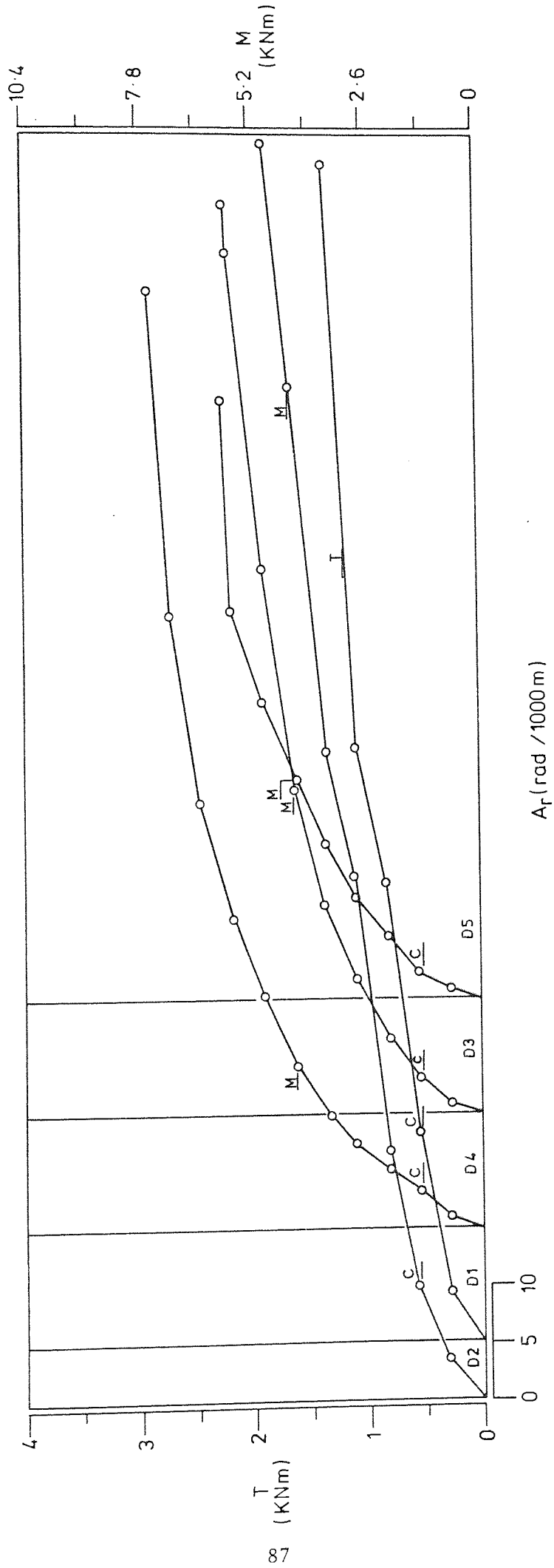
FIGURE 3.12 : Applied torsion ; bending - rotation (over half length of the span) curves for beams in group D.
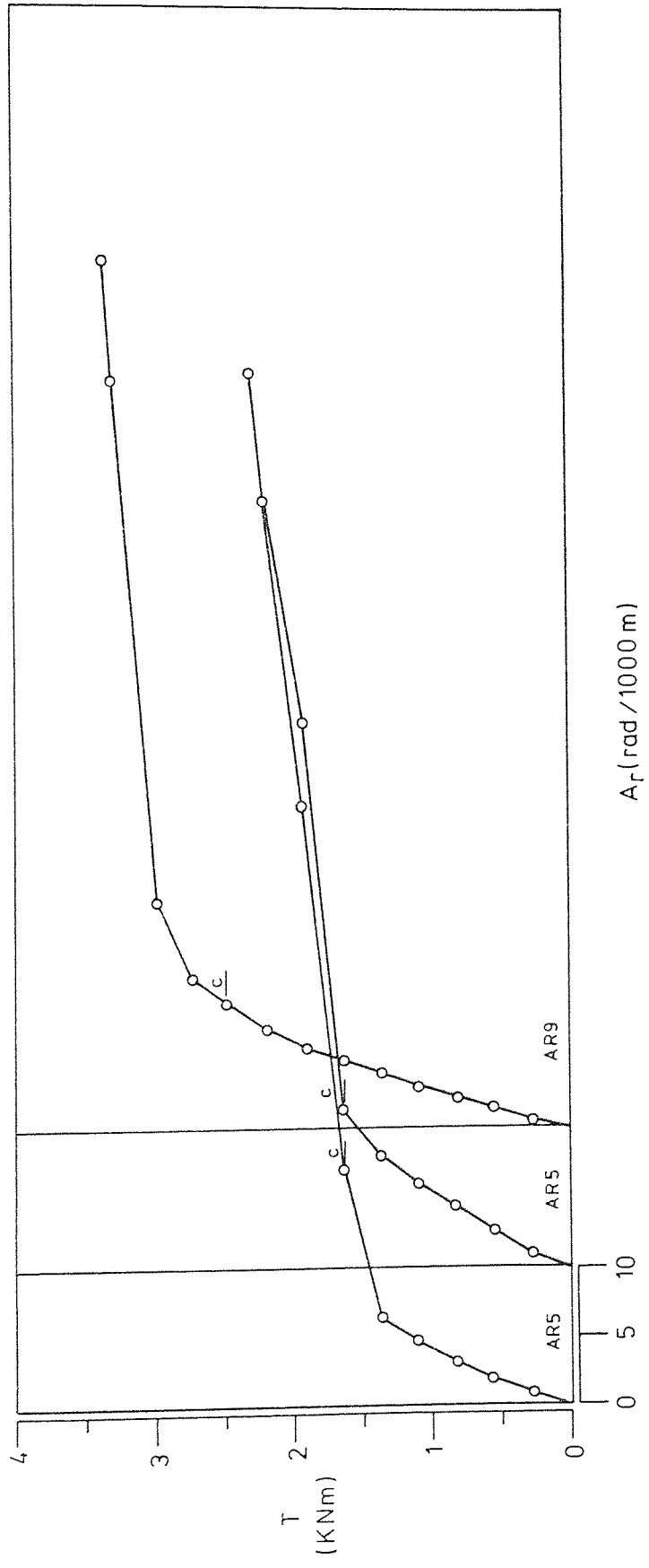
FIGURE 3.13 : Applied torsion-rotation (over full length of the span) curves for beams in group AR
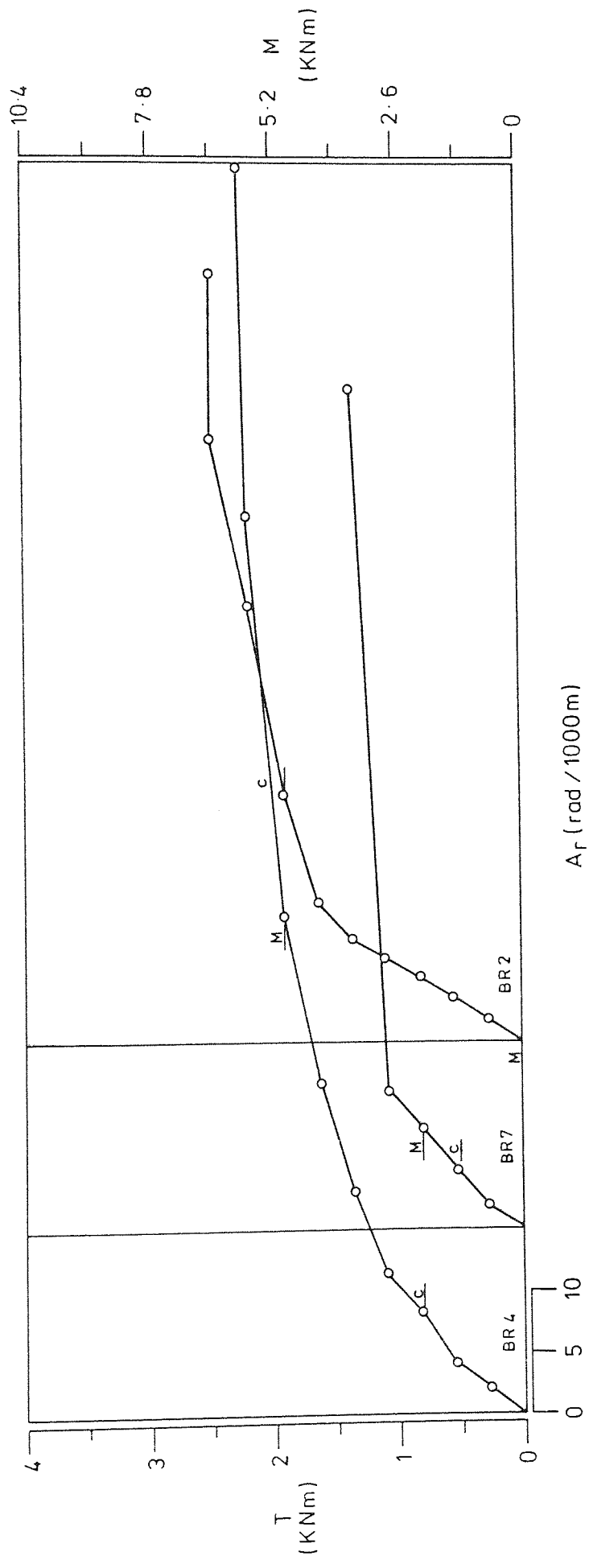
FIGURE 3.14 : Applied torsion ; bending-rotation (over the full length of the span for BR 2 only) curves

for beams in group BR.
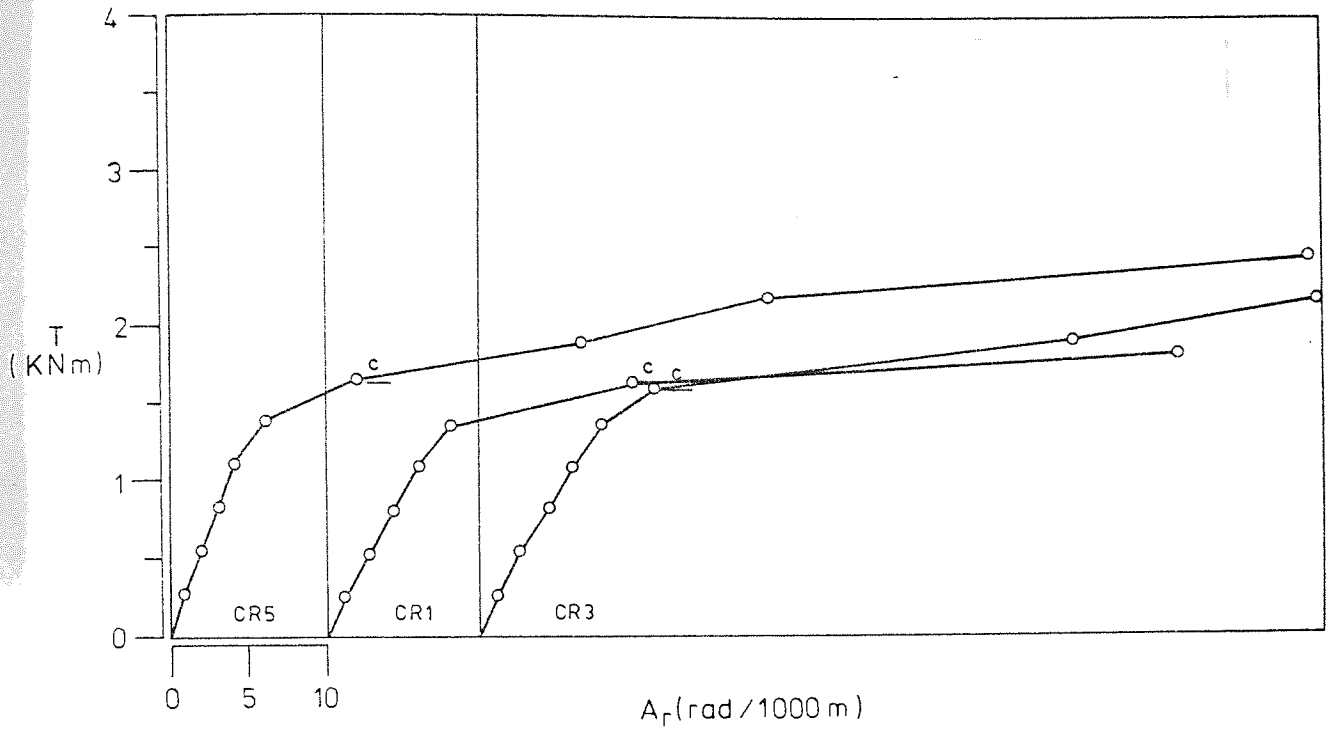
FIGURE 3.15 : Applied torsion–rotation (over full length of the span) curves

for beams in group CR.
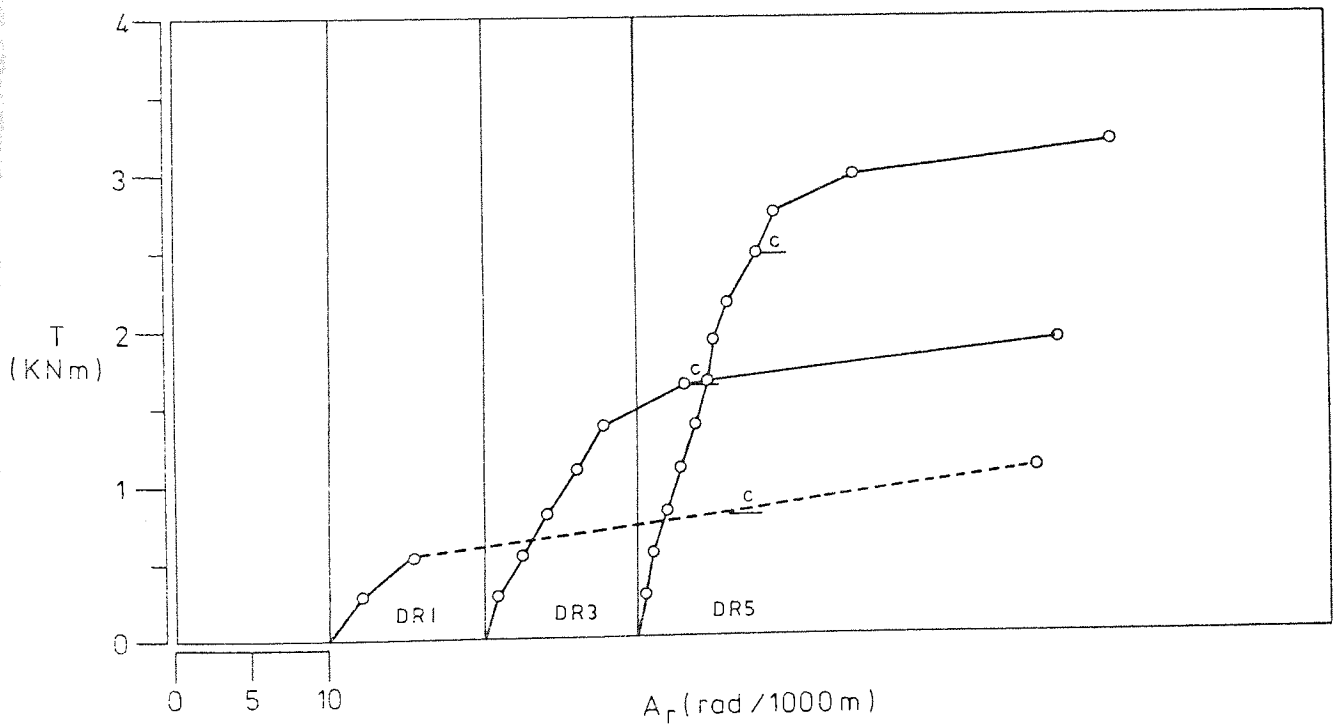
FIGURE 3.16 : Applied torsion–rotation (over full length of the span)

curves for beams in group DR

Beam	Stresses in the long. steel N/mm^2				Stresses in the stirrups N/mm^2			
	1	2	3	4	5	6	7	8
A1	-29	yield	yield	-	34	6	54	54
A2	-	219	230	-223	-	-98	6	45
A3	-153	yield	190	26	yield	157	161	49
A4	-22	263	206	-140	84	130	65	132
A5	-113	286	273	-120	51	137	104	122
A6	-66	267	216	-47	3	0	1	-2
A7	-64	yield	269	-27	37	70	yield	20
A8	-8	295	268	-109	10	-5	12	73
A9	-8	yield	-	-51	-21	189	yield	37
AR4	-19	164	20	196	98	71	16	191
AR5	132	94	96	254	108	-3	140	74
AR9	yield	216	149	275	-6	-1	308	73
B1	-13	yield	309	-104	39	91	40	83
B2	-194	244	yield	-11	-118	56	28	97
B3	-51	-	200	-26	-197	241	89	53
B4	-50	yield	214	-61	49	334	369	9
B5	-90	133	137	-105	-77	208	-	69
B6	-56	283	209	-57	160	84	41	49
B7	-48	238	214	-	106	24	14	54
BR2	-	-	-	-	-	-	-	-
BR4	-	-	-	-	-	-	-	-
BR7	-	-	-	-	-	-	-	-
C1	-155	yield	186	-369	304	4	133	17
C2	-294	151	130	-86	-	-	30	38
C3	-8	176	185	-20	34	63	9	3
C4	-31	166	218	-12	94	41	23	yield
C5	-147	40	75	-25	103	128	146	100
CR1	274	102	78	167	46	47	120	239
CR3	-19	164	20	196	98	71	16	191
CR5	yield	-	-105	296	-141	-273	-30	-
D1	-	-	-	-	-	-	-	-
D2	-155	yield	269	-67	316	-111	-	53
D3	-	-	-	-	-	-	-	-
D4	-91	294	yield	-340	30	13	40	51
D5	-64	246	yield	-200	-260	23	82	288
DR1	282	56	-290	-	yield	-73	193	-80
DR3	46	90	77	119	135	80	11	-57
DR5	35	-80	-	184	-21	-221	-58	8

TABLE 3.4: The stresses in the reinforcement at ultimate

tudinal bars of each test beam was measured at what was thought to be a critical region, using electrical strain gauges (see section 2.4.3). The position of the gauges and the locations of failure sections are presented in table 2.5.

The stress at ultimate in the reinforcement for the test beams are given in table 3.4. They were obtained using a linear stress-strain relationship with the nominal value of 200 kN/mm^2 for the modulus of elasticity of steel. The detailed stress development during the loading stages is tabulated in Appendix B.

The recorded maximum strains are frequently less than the yield strain. This may be because the tensile failure cracks did not intersect the reinforcement at the position of the strain gauges. In many cases, however, the strain gauges were at the failure section and the yield strain of the steel had not been reached at failure. This may indicate that the yield criterion as a failure mechanism is not always valid.

In some of the beams the strain measurement was not recorded due to the malfunction of the gauge instruments.

3.7 BEHAVIOUR OF THE INDIVIDUAL BEAMS

Overall description of the observed behaviour and crack pattern for each individual test beam is presented in this section. The recorded measurements for every beam from the first stage of loading until ultimate failure are given in Appendix B.

The appearance of beams, CR5, DR1, DR3 and DR5, at the failure section, are shown in plates 3.1, 3.2, 3.3 and 3.4, respectively; and the crack pattern for all the tested beams at the vicinity of failure section are shown in Appendix C. They are presented as a developed surface to make the crack pattern more

92

visible. The numerals alongside the cracks refer to the load stage at which the part of the crack was visible.

3.7.1 Beams of Series A - Group A

Each beam of this group was subjected to torsion and a mid-span transverse load which produced the bending and shear force on the beam, as explained in section 2.4.2. The torsion and bending loads were applied simultaneously until failure in equal increments.

Beam A1

The first flexural crack was observed just after load stage 2, in the bottom face, close to central plane. By the end of load stage 4, the crack had widened and extended into the mid-height of both side faces, at almost vertical inclination. An inclined crack was also visible just to the left of central plane (i.e. CP), on the north-bottom corner. At load stage 5, the existing cracks suddenly changed their inclinations from vertical to about 30°. A number of inclined cracks also developed on the south, bottom and north faces. The concrete in the top of the beam, next to the loading cell, precipitated crushing.

Finally, the beam failed in mode 1, with a loading ratio of bending moment to torsional moment to shear M:T:Vh of 2.810:1.0: 0.328 at the failure section. Maximum recorded strain was indicated by the yielding of bottom longitudinal bars only. The strain in the stirrup legs was well below yield at failure.

Beam A2

Cracks were observed immediately after load stage 2, in different locations on the south, bottom and north faces of the beam. With increasing the load, these cracks extended around the

faces and some newly formed cracks were also visible. Soon after load stage 6, the beam failed in mode 1 at the region of maximum bending moment, by crushing of the concrete at the top face. For this beam the loading ratio of bending to torsion to shear, M:T:Vh was 2.938:1.0:0.317.

Beam A3

In this beam the first crack developed soon after the application of load stage 3. The propagation of the cracks was quite similar to beam A2 except that for this beam more cracking was apparent. In load stage 7, it failed by yielding of both categories of the steel and crushing of the concrete near the top face. Failure was in the region of maximum bending moment, and the load ratio at failure section, M:T:Vh was 2.897:1.0:0.322.

Beam A4

Cracks were first seen after load stage 3 on the bottom of the north face close to the maximum bending region, and they were essentially flexural cracks. By load stage 4, the extent of the cracking had increased considerably with almost constant inclination. At the same time other cracks developed in the bottom and south faces of the beam, and some appreciable change in the inclination of the cracks was noticed after load stage 5. The crushing of the compressed concrete took place at the top of the beam soon after the application of the bending load at stage 7 and the beam failed in mode 1. The bending to torsion to shear ration, M:T:Vh was 2.993:1.0:0.347. (The yield strain for the north-bottom corner longitudinal bar was recorded at failure).

Beam A5

Cracking started at load stage 3 on the bottom of the north face very close to the mid-span. In load stage 4, a transverse crack was noticed on the bottom face, at about 150 mm to the right of mid-span. An inclined crack also was observed on the south face in this region. By load stage 5, the transverse crack at the bottom face had extended well into both south and north faces, while some torsional cracks, on the three faces along the span towards the right support were noticed. With increasing the load the existing cracks extended to the full depth of the beam, and some newly formed cracks were also observed. By load stage 8 the ultimate strength of the beam was reached and the concrete at the top face crushed. The load ratio, M:T:Vh for this beam at failure, was 2.548:1.0:0.324.

Steel strain, close to yield, was recorded for the longitudinal bar in the south-bottom corner where the shear stresses due to torsion and shear force were additive.

Beam A6

The application of the load for this beam was considerably different from the rest of the beams in this group. The flexural loading scale for the first three stages were 2.5 times the loading scale for the other tested beams. After load stage 3 the loading progressed in the same load increments as the rest of the beams in this group until failure occurred.

Beam A5 was prepared identical to beam A6 and tested in the same loading sequence as the rest of the beams in this group.

The crack patterns for these two beams were similar except in beam A6 where the first cracks were observed around south, bottom

and north faces, during the application of load stage 1, in a region very close to the mid-span. By load stage 2 these cracks had penetrated to the upper half of both sides. By load stage 6, the crushing of the concrete at the top face had initiated faulure.

The loading ratio, M:T:Vh, at the failure section was 3.916:1.0:0.468. The maximum strain recorded was again for the south-bottom corner longitudinal bar but it was lower than that of beam A5.

Beam A7

While applying the load in stage 3 some inclined cracks were detected in different locations at the vicinity of the maximum flexural region. Upon increasing the load these cracks extended to the upper halves of the sides with sudden change in their inclination just above the mid-height of the side faces. The change of slope was more distinct on the north face than the south face, and was probably due to the influence of the high bending stress and low shear stresses from torsion and shear of opposite signs on the north face, in this region. Yield strain in the south-bottom corner bar was registered by the end of load stage 5. By load stage 6, the bottom leg of the instrumented stirrup legs showed appreciable strain. During load stage 8, the beam failed through extensive crushing of the concrete at the top with yielding of only one longitudinal bar and the bottom leg of the stirrup.

The load ratio, at failure, of bending moment to torsional moment to shear, M:T:Vh, was 2.725:1.0:0.321.

Beam A8

The propagation of the cracks and their pattern in this beam were similar to beam A7 except that the first crack did not form

until the end of load stage 4. This was probably due to a better concrete quality in this beam. Failure occurred during the application of the bending load in stage 9 by crushing of the concrete at the top of the beam.

At failure the load ratio of M:T:Vh was 2.906:1.0:0.341. The maximum steel strain recorded was below yield for both categories of reinforcement.

Beam A9

This beam was of high concrete quality, and cracks were first observed after load stage 4 on the bottom face as well as the bottom of both side faces. The cracks were inclined on the bottom and south faces, but vertical on the north face. They extended well into the upper half of the sides by load stage 6. During load stage 7, some new inclined cracks formed in different locations along the span, and extended across the full depth. The first sign of crushing of the concrete was noticed after load stage 8, at the top quarter of both sides. During load stage 10 this beam exhibited mode 1 type failure, by crushing of the concrete at the top. The load ratio M:T:Vh for beam A9 was 2.785:1.0:0.337.

A yield strain for the south-bottom corner bar and the bottom leg of the stirrup were recorded in stages 8 and 9 respectively.

3.7.2 Beams of Series A - Group AR

Beams in this group were identical to their respective beams in group A, except for top longitudinal steel. They were tested in pure torsion and the dead weight only, as explained in section 2.4.2.

Beam AR4

The behaviour of this beam was quite different to that of its

identical in group A. Inclined cracks were observed to form just after load stage 6 (i.e. T = 1.794 KN.m), on the south face. These cracks were over the full depth of the face. By load stage 7 (i.e. T = 2.07 KN.m) extensive cracking had occurred and resulted in a large number of closely spaced cracks spiralling around all faces of the beam, inclined at about 45° to the vertical. During load stage 8 a number of new cracks formed along the span and were more extensive in a region close to the right support. These with the already existing cracks in the region formed a plane of weakness in the beam. Finally, failure was caused at ultimate torque of 2.345 KN.m, by opening a spiral crack around the south, top and north faces of the beam with clear cleavage at the bottom face. The failure, therefore, was identical to a mode 3 cleavage failure.

The recorded strain in the reinforcement was well below yield. It must be realized, however, that the failure section was not at the position of the instrumented reinforcement (see table 2.5).

Beam AR5

The behaviour of this beam was very similar to beam AR4. Cracking was noticed soon after load stage 6 (i.e. at twisting moment of 1.794 KN.m). Through the load stages the development of the cracks and also the pattern of failure section were identical to the above beam, except beam AR5 failed at a slightly higher torque (i.e. 2.44⊦ KN.m). The reason for this was believed to be the better quality of the concrete.

Beam AR9

No cracks were observed in this beam until three stages before failure (i.e. at the torsional moment of 2.895 KN.m). The cracks

were mainly in a region close to the left support (i.e. restrained end), and they were on the top, north and bottom faces. During load stage 10 these cracks widened and a few other cracks also formed. By load stage 12 a large number of closely spaced spiral cracks around the four faces along the span had developed. This caused a considerable reduction in the torsional capacity and finally the beam failed at ultimate torsional moment of 3.514 kN.m.

The pattern of the failure surface was not distinct and was between modes 2 and 3. However, one may deduce from the reinforcement strain readings that the mode 3 type of failure was more critical.

3.7.3 Beam of Series B - Group B

The seven beams of this group were tested in combined torsion, bending and vertical shear with one point load in the mid-span. For these beams, the bending load was maintained at a particular stage of the loading and the torsional load increased until the failure of the beam was reached. The stage at which the bending load was maintained was the seventh in this group, but in some cases failure occurred before reaching the stage.

Beam B1

After increasing the applied loads in stage 4, crack appeared around south, bottom and north faces in different locations but mainly in the vicinity of maximum bending moment. They were on the north face flexural cracks, on the bottom and south faces tended to have an inclination with the vertical. The application of the loads in stage 5 caused the change in the inclination of the cracks as well as the propagation of new torsional cracks along the span towards the right support (i.e. the end through which the torsional

99

load was applied). By load stage 10 the cracks extended to the top face - from both sides. In stage 11, during the application of the torsional load a sudden reduction in the torsional capacity accompanied by considerable crushing of the concrete at the top. Failure took place in accordance with mode 1 type of failure.

The yield strain for the south-bottom corner bar was recorded in load stage 8 while the strain in the stirrup legs was well below yield.

The bending moment to torsional moment to vertical shear, M:T:Vh, ratio for this beam at failure was 1.829:1.0:212.

Beam B2

The behaviour and crack pattern for this beam was similar to that of beam B1 except that in beam B2 the first cracks were seen at an early stage (i.e. stage 3) and were on the south and bottom faces only. After load stage 8, some crushing of the concrete was apparent on the top face - right of the central plane, but the beam still maintained its stiffness. It was during the begining of load stage 9 when the beam failed indicating a typical mode 1 failure.

The load ratio, M:T:Vh, at failure for this beam was 2.317: 1.0:0.274. The strain in the stirrup legs was comparable to that of beam B1. The yield strain was recorded for the north-bottom corner bar in beam B2.

Beam B3

In this beam, a small flexural crack was first seen on the south face at the end of load stage 2. During load stage 3 another bending crack was observed on the north face under the vertical load while the other crack extended with a significant change in

its direction towards the left support. By load stage 8 a number of parallel inclined cracks mainly on the north and south faces across the depth were evident. In the final stage of loading a wide torsional crack opened on the south face and penetrated well into the bottom face, and at the same time crushing of the concrete took place at the top and the beam failed again in mode 1.

The loading ratio, M:T:Vh, for this beam was 2.107:1.0:0.260, at failure.

Beam B4

Inclined cracks were first seen after the application of the load at stage 3 at a small distance to the right of mid-span. The cracks were on the south, bottom and north faces of the beam. Load stage 4 produced an extension of the cracks on both side faces. It also produced some new cracks along the span on both sides of the central plane. At higher loads, these and other tensile cracks spread across the bottom and well into the top of the side faces with a steeper inclination on the south face - the face on which the directions of the shear and torsional stresses were additive. By load stage 7 the first sign of the crushing was observed. During the application of load stage 8 the main tensile cracks around the beam faces widened and at the same time the final crushing of the concrete took place. Thus the beam failed in mode 1 type of failure with the compression zone at the top.

This beam failed under the load ratio of bending to torsion to vertical shear, M:T:Vh of 2.390:1.0:0.283.

The strain measurement recorded for this beam during the test showed yielding of the south-bottom corner bar and close to yield for both the south and bottom legs of the stirrup at failure.

Beam B5

At the end of load stage 2 a tensile crack appeared at the bottom face and extended across the width into the side faces at almost vertical inclination. The crack on the north face penetrated to the mid-height at load stage 3 while at the same time other cracks, mainly flexural and at the region of maximum bending moment, were also being noticed. These and other cracks extended over the full height of the sides with the first indication of concrete crushing at load stage 6. Load stage 7 was the final in which the failure of the beam occurred by crushing of the concrete at the top face.

At failure, the load ratio of M:T:Vh was 2.492:1.0:0.315.

Beam B6

A flexural crack was first observed to form at load stage 3. The crack was on the north face, and in the region of high bending moment to the right of mid-span. By load stage 5 a number of closely spaced torsional cracks were visible on the south, bottom and north face, along the span, mainly towards the right support. Just after load stage 6, one of the cracks - at about the middle of the right half of the span immediately widened and extended over the full height of the south face as well as the top and bottom. faces. Failure of the beam occurred during the application of load stage 7, due to the crushing of the concrete in the north face - the face on which the shear and torsional shear stresses were sub-tractive.

Apparently a typical mode 2 type of failure was clearly visualized at failure. The load ratio for this beam was 1.687: 1.0:0.344.

Beam B7

The behaviour of this beam was similar to that of beam B6.

The first crack was observed during load stage 3. At stage 4 other inclined cracks formed along the span, mainly on the south face towards the right support. During load stage 5 a tensile crack inclined at an angle greater than 45° to the vertical axis suddenly opened on the north face and extended into both the top and bottom faces in the left half of the span. During the application of the torque in stage 6, a considerable crushing of the concrete on the north face caused the beam to fail in typical mode 2 as in the previous beam. The crushing took place again in the side where the stress due to shear and the stress due to torsion were subtractive.

The load ratio of M:T:Vh for this beam at failure in the critical section was 1.212:1.0:0.377.

In both of the latter two beams (i.e. B6 and B7) the failure section did not coincide with the instrumented section for strain measurement in the reinforcement.

3.7.4 Beam of Series B - Group BR

Beams in this group had smaller longitudinal bars at the top and were tested under different values of bending moment to torsional moment ratio ψ.

Beam BR2

This beam was tested under very small value of ψ.

Initial cracking for Beam BR2 did not take place until load stage 7 where by then the torque was 2.07 KN.m. These cracks took the form of torsional cracks around the four faces along the span.

At load stage 8 the cracking became more extensive and some of the already existing cracks extended further. During load stage 9 the first indication of a critical section was observed just to the right of the restrained end of the beam. Soon after the application of load stage 10 the torsional capacity of the beam dramatically dropped and the beam failed with ultimate torsional moment T of 2.661 kN.m. The pattern of the failure section was difficult to analyse, and the mode of failure was thought to be between modes 3 and 2.

Beam BR4

Beam BR4 was tested under a moderate ratio of ψ.

Cracking started at load stage 3 in this beam well before that of the previous beam. The cracks were mainly flexural on the bottom of the south face and extended onto the bottom face. By load stage 8 the number of the cracks had increased, particularly in the region of high bending moment. Other inclined tensile cracks were also apparent on the bottom, south and top faces, in a region close to the right support. Suddenly, in this region, a wide crack opened on the north face and also one on the bottom face. Finally, the beam failed with bending to torsion to shear ratio, M:T:Vh, of 0.402:1.0:0.297.

The mode of failure was not easy to distinguish but from the appearance of the failure section modes 3 and 2 are critical.

Beam BR7

This beam was tested under a low ratio of ψ.

The first tensile crack was seen soon after load stage 2. It was in the form of bending crack across the bottom face which

extended into the bottom of the sides, to the right of mid-span.

Another crack with approximately the same distance but to the left of mid-span was also apparent on the lower half of the north face and extended to the mid-width of the north face. At load stage 3 these cracks extended further upward and inclined towards the right support on the north face, and the left (restrained) support on the south face. A number of other tensile cracks were also traced, mainly on the north face in the region of high bending moment, with spacing approximately equal to the spacing of the stirrups. At load stage 5 the crushing of the concrete on the south face, accompanied by a major spiralling crack on the other three faces, eventually caused the beam to fail in mode 2.

The failure of this beam was sudden and occurred in a region close to the restrained support where no initial cracks were traced before failure. The load ratio M:T:Vh for this beam at failure section was 0.401:1.0:0.237.

3.7.5 Beam of Series C - Group C

Beams in this group were tested under combined bending, torsion and shear with a variation only in the amount of longitudinal reinforcement for each individual beam. The bending moment was held constant at load stage 5 for this group.

Beam C1

Cracks were sighted after load stage 2. They were mainly flexural, and in the region of high bending moment on all faces except the top. By load stage 4, these cracks had extended almost to the top face. At this stage three planes of weakness were evident, and upon increasing the bending load increment at stage 5,

a wide tensile crack opened in the top face and ultimately the beam failed. The crack pattern at failure did not show a distinct type of failure, although mode 1 was suggested from the recorded strain for the main bars. Bending to torsion to shear, M:T:Vh, ratio, for this beam at failure was 3.156:1.0:0.364. The yield strain for only the south-bottom corner bar was registered at failure.

Beam C2

The bahaviour and crack pattern for this beam were quite similar to those of beam C1. Beam C2, however, resisted a higher torque at ultimate failure.

The ratio of bending to torsion to shear for this beam was 2.594:1.0:0.298.

Unlike beam C1 none of the reinforcement had reached its yield strain in this beam.

Beam C3

A crack was first observed to form on the bottom of the south face just after load stage 3. It was in the region of maximum moment and just to the right of mid-span. By load stage 3 the number of the cracks had increased. These cracks were torsional and extended over the width of the bottom face as well as the full height of the sides. A tensile crack was also apparent on the top face close to the right support. During load stage 7 an inclined crack opened wide on the bottom face just to the left of the restrained support accompanied by some crushing of the concrete on the north face. These with the existing tensile cracks in that region formed a critical plane. The beam failed in this section with the M:T:Vh ratio of 0.370:1.0:0.278 indicating mode 2 failure.

Beam C4

The appearance and propagation of the first crack as well as
the subsequent cracks were similar to beam C3 until a few stages
before failure. During load stage 8 (a stage before failure) a
plane of weakness suddenly formed just to the right of the restrained
support by opening a spiral crack around the four faces of the
beam. Some crushing of the concrete was also apparent.on the south
face in the region. Soon after the application of load stage 9 the
beam experienced a sudden loss in its torsional capacity and con-
sequently failed with the M:T:Vh ratio of 0.149:1.0:0.228. The mode
in which the beam failed was not clear, but possibly mode 2 was
predominant.

Beam C5

The crack did not appear in this beam until well after load
stage 5 where an inclined crack was sighted on the north face, just
to the right of mid-span. When the load was increased the number
of the cracks increased and extended over the full height on the
sides. By the end of load stage 8 an extensive crushing of the
concrete on the bottom face next to the right support had taken
place accompanied by a wide tensile crack at the top face. A hybrid
of tensile-compressive cracks was also evident on the north face
in this region. Finally, the torsional capacity reduced suddenly
and the beam failed with the load ratio M:T:Vh of 0.123:1.0:0.237.

Failure in beams C3, C4 and C5, however, seemed to have occurred
prematurely because in each of these beams the failure section was
close to one of the supports.

3.7.6 Beam of Series C - Group CR

Beams in this group were identical to their respective numbers

107

in beams of group C except that these beams contain a smaller amount of top longitudinal steel. They were tested under fairly large torsional moment.

Beam CR1

In this beam initial cracks had not formed until the application of load stage 6 where the torsional moment was 1.794 KN.m. At this stage extensive cracking occurred which resulted in a number of torsional cracks spiralling around all faces of the beam. The cracks were only along the left half of the span while along the right half no cracks were seen. The inclinations of the cracks were approximately normal to the direction of principal strain. At load stage 7 the four faces of the right half of the span cracked approximately at the same inclination and number as for the other half in stage 6. At the same time some other inclined cracks on the latter half were also apparent. Those with the other existing cracks formed a critical section in a region just to the left of mid-span. The beam failed at an ultimate torsional moment of 2.001 KN.m.

The mode in which this beam failed was not clear but some crashing of the concrete on the north face was visible which indicated mode 2.

Beam CR3

This beam was exactly the same as beam AR4, listed here to complete the group.

Beam CR5

The developed appearance of this beam at the failure region is shown in plate 3.1.

As in beam CR1 initial cracking started after load stage 6 in this beam, but they were few inclined cracks on the north, top and south faces. By load stage 8 the number of cracks spiralling around the faces had increased. In this stage a plane of weakness with some widely opened cracks on the north, top and south faces could be seen in a region close to the restrained support. It was during load stage 9 when other wide tensile cracks on all faces opened in this region, the torsional capacity dropped suddenly and ultimately the beam failed. Again the mode of failure was difficult to distinguish. From the recorded steel strain and the appearance of the beam at failure, mode 3 form of failure is critical.

The ultimate torsional moment for this beam at failure was 2.592 KN.m.

Yield strain for the south top corner bar was recorded at failure.

3.7.7 Beams of Series D - Group D

These beams were symmetrically reinforced and tested under combined torsion, bending and shear. The major differences among the beams of this group was the width to height ratio. The target load stage for the sustained bending moment was 6. Beam D1, however, failed one stage earlier.

Beam D1

Cracks were visible in this beam soon after load stage 2. They extended along the right half of the span and on all faces except the top. The cracks were in the form of torsional cracks on the bottom face and bending cracks on the side faces. At load stage 3 the number of inclined cracks increased along the span. By load stage 4 some of these cracks extended almost to the top

face. Also in this stage some other tensile cracks opened across the full depth of the sides mainly on the south face. They were inclined at an angle greater than $45°$ to the vertical and mainly along the right half of the span. During load stage 5 the width of one of those cracks close to the mid-span increased considerably and initiated the failure section.

Eventually the beam failed with bending to torsion to shear, M:T:Vh ratio of 2.395:1.0:0.301. Although some crashing on the top face was apparent the mode of failure was not clear.

Beam D2

After load stage 2 cracks were seen on the bottom of both the north and south faces and also on the bottom face. The cracks were in the region of high bending moment just to the right of mid-span. In stage 3 of loading the crack on the north face extended toward the top and other cracks on the three faces along the span were also seen. By load stage 4 some cracks were also evident on the top face while the existing cracks on the sides extended well across the full depth. By load stage 6 the cracks along the span and on the four faces were quite numerous. It was during load stage 7 that the beam lost its resistance to the applied torque and failed with M:T:Vh ratio of 2.052:1.0:0.230.

The failure section was close to the mid-span on the right and the failure seemed to be mode 1 tensile (cleavage) failure. Yield strain for south-bottom corner bar was registered at failure.

Beam D3

Mainly flexural cracks were first seen on both sides after load stage 2 and torsional cracks were observed on the bottom face to the right of mid-span. As the load was increased the cracks

on the sides extended towards the top face with some change in their direction under the influence of the torsional moment. The change in inclination was towards the right support on the north face and the left on the south face. By load stage 7 a number of tensile cracks spread along the span and around the three faces. By load stage 8 a considerable crushing was apparent on the top face close to the mid-span from the right. At load stage 9 extensive crushing took place in the region accompanied by a wider tensile crack at the bottom face and the beam failed in mode 1 by crushing of the concrete.

The load ratio M:T:Vh at failure section was 1.796:1.0:0.197.

Beam D4

Stage 2 was again the initial cracking load stage for this beam. The initial crack was a small flexural crack across the bottom face into the bottom of the south face. At load stage 3 some more cracking occurred mainly along the central region of the span on the south, bottom and north faces. By load stage 10 the amount of cracking had increased considerably on the faces and during load stage 11 a region of weakness formed just to the left of the central plane. Finally, the beam failed in mode 1 by a hybrid of compressive tensile action of the concrete in the top.

Bending to torsion to shear, M:T:Vh ratio at failure was 1.449:1.0:0.154.

Yield strain for only the north-bottom corner longitudinal bar was recorded at failure. The strain in the legs of instrument stirrup was well below yield.

Beam D5

Like the other beams in this group cracking in this beam

started at load stage 2 with a crack across the bottom face into the sides in a region right of the mid-span. At load stage 3 the crack on the north face extended upward with a change in direction towards the right support. Other cracks at some distance apart opened on the bottom face and on both sides mainly in the central region of the span. On increasing the load the cracks on the sides extended farther towards the top and other cracks also formed. By the end of load stage 8 a critical section had been clearly identified at the region of initial cracking. It was at the begining of load stage 9 when the concrete crushed on the top face, and the beam failed in mode 1.

This beam failed with load ratio M:T:Vh of 1.849:1.0:0.194, and the recorded strain in the reinforcement indicated yielding for the south-bottom corner bar after load stage 4.

The ultimate resistance for this beam at failure was considerably lower than that for beam D4 although it was greater in width.

3.7.8 Beam of Series D - Group DR

Beams in this group were tested under a high torsional moment and were identical to some of the beams in group D, except for the amount of top steel.

Beam DR1

The developed appearance of the failure section for this beam at failure is given in plate 3.2.

Cracking started in this beam during load stage 3 with numerous cracks spiralling around all four faces along the span. By load stage 4 the number of the cracks had increased considerably.

Upon the application of load stage 5 the torsional stiffness suddenly reduced and consequently the beam failed with an ultimate torsional moment of 1.244 KN.m.

The failure section, which was at the middle of the left half of the span, distorted due to a redistribution of the stresses and horizontal cracks appeared along the longitudinal axis of the beam. The failure mode was not clearly defined but a compressive-tensile mode 3 failure was possible based on the measured strain in the reinforcement.

A yield strain was recorded for the top leg of the instrumented stirrup at failure.

Beam DR3

Plate 3.3 shows the developed appearance of the failure region at failure.

A crack was not noticed in this beam until the end of load stage 6 when the torsional moment was 1.794 KN.m. The cracks were torsional and around the four faces in a region at some distance from the restrained support. During load stage 7 other torsional cracks appeared around the faces along both sides of the span. Those close to the left support suddenly widened and produced failure by crushing of the concrete in the north face. Mode 2 type failure seemed to be more critical.

The maximum torque resisted by this beam, at failure, was 2.042 KN.m.

Beam DR5

A developed view for this beam at the failure section is shown in plate 3.4.

The first crack was seen after load stage 9 in a region some distance from the left support and in the form of torsional cracks around the side faces and also on the top. By load stage 11 a few other similar cracks had formed along the left half of the span. Soon after load stage 12 the beam started to fail by opening the tensile cracks on the top, south and bottom faces, in a region to the left of mid-span. The maximum torque registered for this beam at failure was 3.280 KN.m.

TF

NF

BF

SF
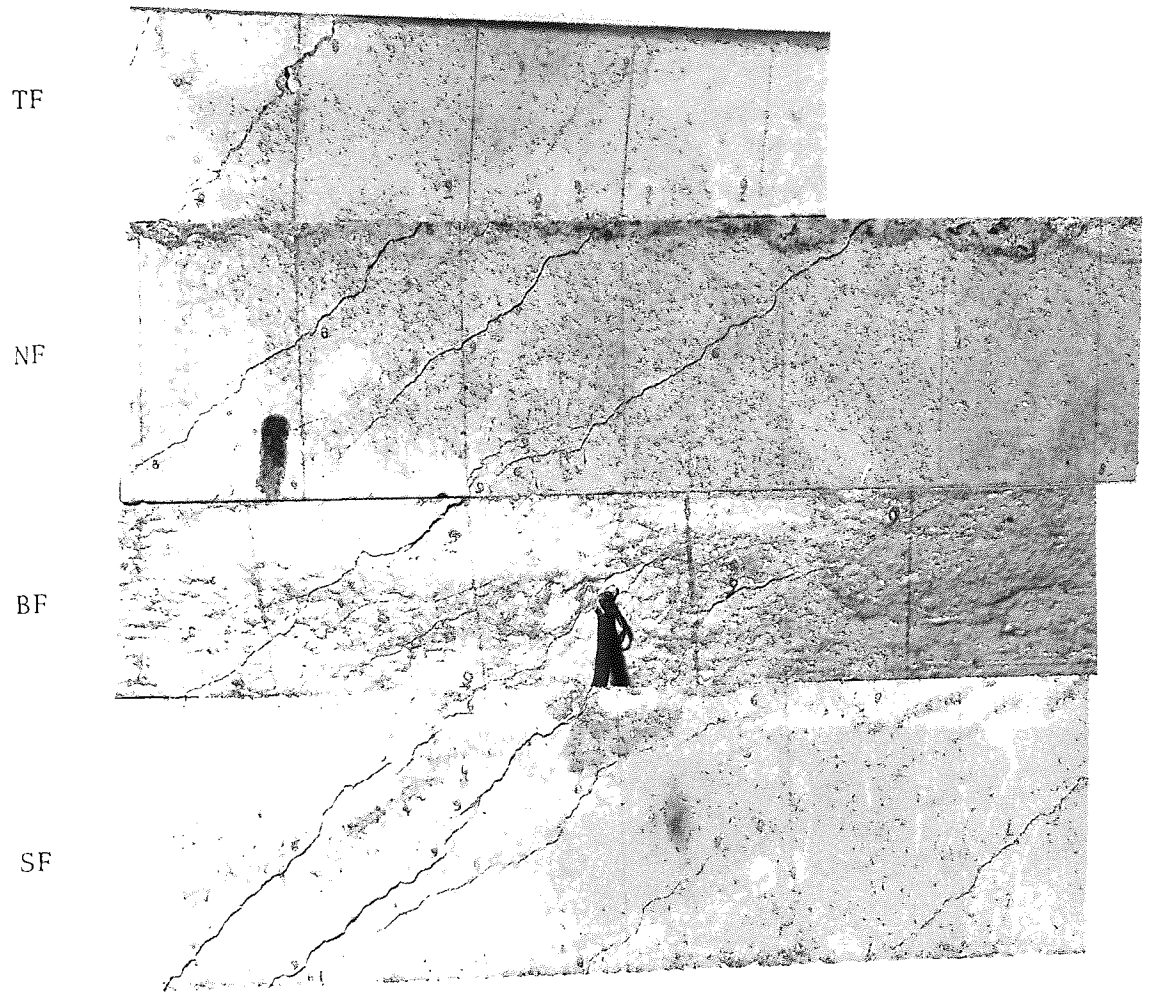
PLATE 3.1: A developed view of beam CR5, at the critical section, after failure

TF

NF

BF

SF
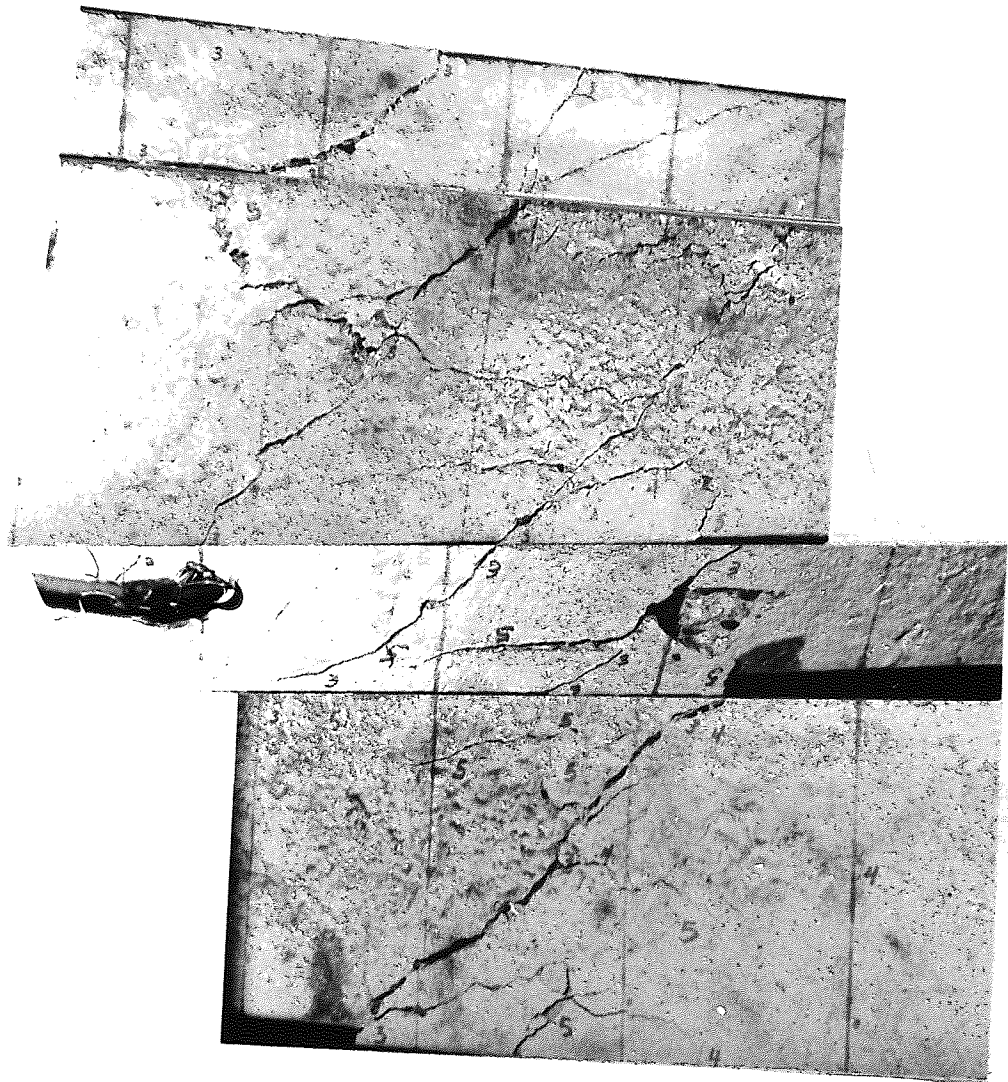
PLATE 3.2: A developed view of beam DR1, at the critical
section, after failure

TF

NF

BF

SF
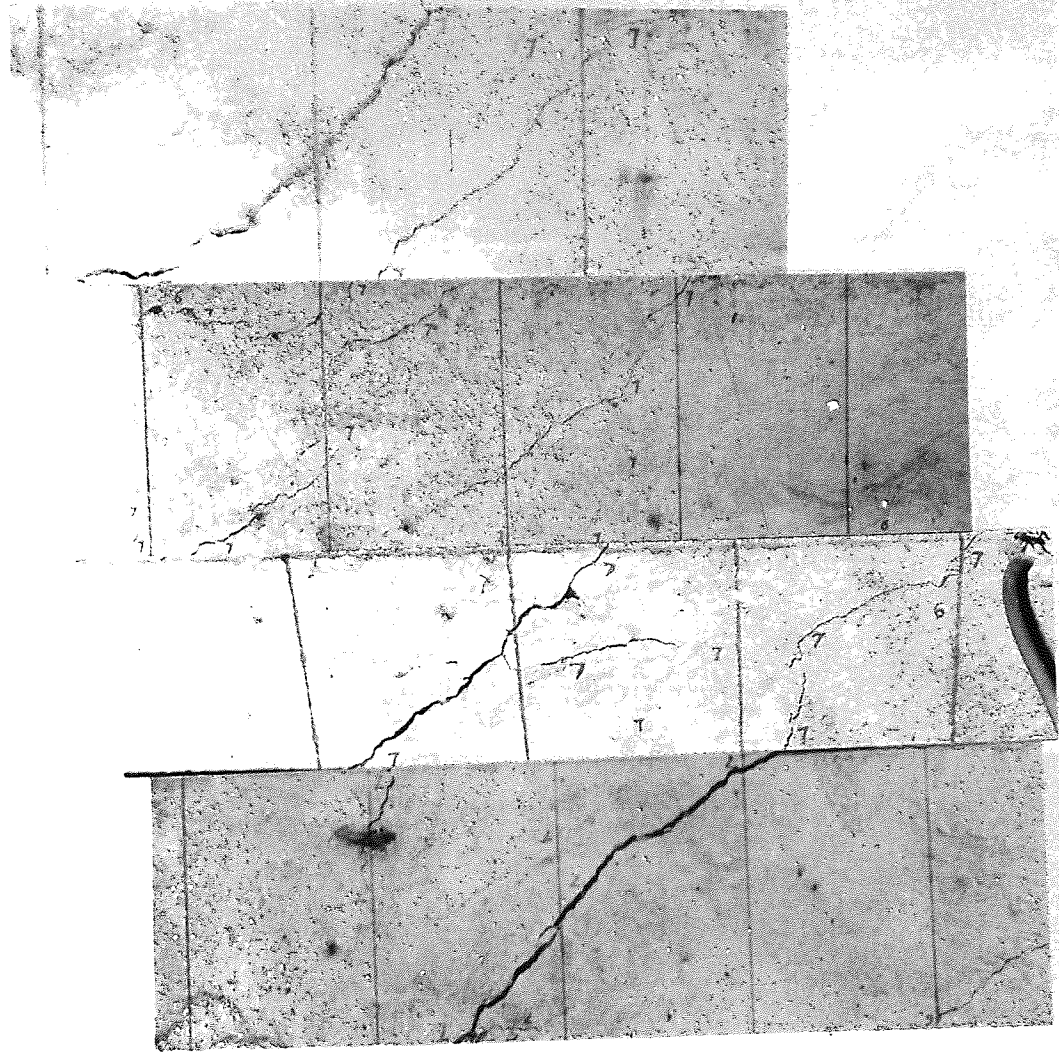
PLATE 3.3: A developed view of beam DR3, at the critical
            section, after failure

TF

NF

BF

SF
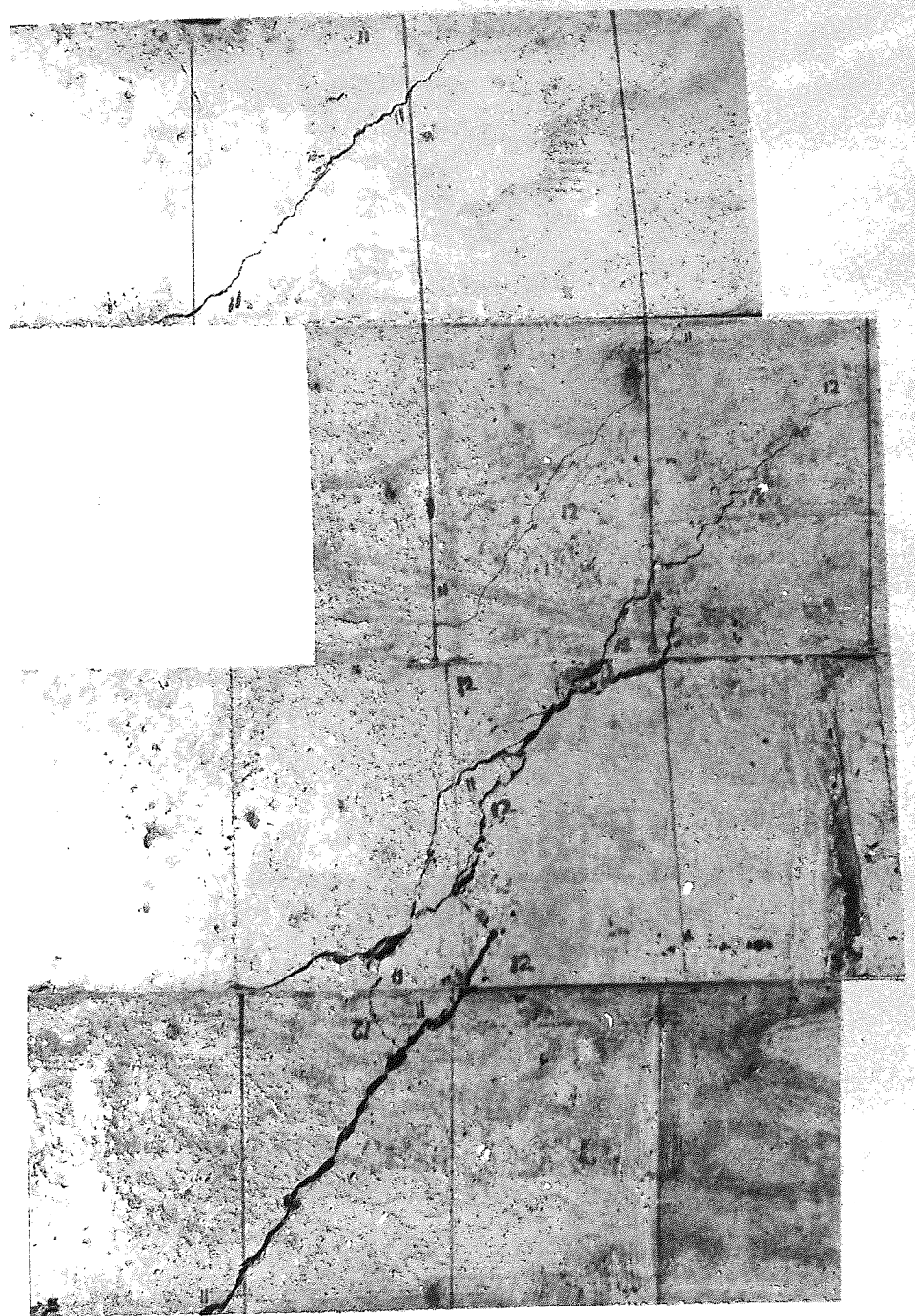
PLATE 3.4:   A developed view of beam DR5, at the critical
section, after failure

CHAPTER FOUR
THE ULTIMATE STRENGTH ANALYSIS

4.1 INTRODUCTION

In this chapter, the ultimate strength of longitudinally and
transversely reinforced concrete rectangular members under the
combined action of torsion, bending and vertical shear are analysed.
The ultimate strength of members under torsion alone, or combined
torsion and bending, however, are considered as special cases of
the theory.

The theoretical analysis is based on the 'skew bending' mech-
anism approach, commonly used for determining the ultimate capacity
of reinforced concrete members in torsion. Although the skew-
bending theory usually assumes yielding of both the longitudinal
and the transverse steel upon failure, the present approach
analyses the strength of under-reinforced, partially over-reinforced,
and completely over-reinforced members alike. Obviously this is
an advantage of the theory, since experimental evidence from the
strain measurements in the reinforcement by many investigators and
by the author indicate a large number of non-yielding cases. In
practice non- or partial yielding cases are likely to occur because
a beam is generally designed for one critical section, and the same
steel is inserted at other sections along the span.

Simple rational equations, capable of predicting not only the
ultimate strength but also the characteristics and modes of fail-
ure, have been developed for four types of failure observed during
the experimental work.

From the test observations it is possible that failure occurs
in accordance with one of the following categories:

a) Yielding of both longitudinal bars and stirrups before crushing of the concrete at failure.

b) Yielding of the stirrups only (not the longitudinal bars) before crushing of the concrete at failure.

c) Yielding of the longitudinal bars only (not the stirrups) before crushing of the concrete at failure.

d) Crushing of the concrete before yielding of any of the reinforcement at failure.

Similar categories of failure have been observed in tests and described earlier by Goode and Helmy [61], and also by Hsu [32], but satisfactory rational equations have not been developed.

For each type of failure above, the three principal modes - namely mode 1, 2 and 3 are considered. A beam is considered to fall in mode 1 when the compression zone is near the top face; mode 2, when the compression zone is near one of the sides; and mode 3, when this zone forms near the bottom face, depending on the ratio of bending moment to torsional moment ψ, and the distribution of the longitudinal bars and also the dimensions of the section.

The theoretical solution proposed in the analysis is based on the equilibrium of a cracked-section, ignoring the effect of any dowel action. For the first type of failure - i.e. yielding of both categories of reinforcement - two moment equilibrium equations about two perpendicular axes through the centroid of the compression zone are developed, as well as an equilibrium equation for the transverse forces.

In the remaining three types of failure - i.e. where failure occurs prior to yielding of the reinforcement, failure of the concrete in the compression zone is involved. Therefore in the

analysis involves the concrete compression zone, and this zone is subjected to compressive stresses due to bending moment, and shear stresses due to the torsional moment and the shear force. These stresses are combined using Cowan's [7] failure criterion, which has been used successfully by other investigators [62, 63, 64]. Since all or part of the steel does not yield at failure, it is assumed that the skew-bending linear elastic analysis may be used to obtain the depth of the compression zone.

The inclination of the tensile cracks of the failure section is controlled by the equilibrium of forces when all the steel yields. When partial yielding occurs or the beam is over-reinforced, this inclination is controlled by the cracking of the concrete. At initial cracking this inclination on the three tensile faces may be determined by $\tan \alpha = \rho + \sqrt{\rho^2 + 1}$ [41], where ρ is mainly a function of the ratio of applied bending moment to torsional moment. Close to ultimate load, however, numerous cracks form which are interconnected in various directions, but are assumed to be characterised by $\tan \alpha = 1$. This assumption has the merits of producing simple equations which are reasonably accurate.

4.2 TYPE I FAILURE-YIELDING OF BOTH SETS OF REINFORCEMENT

This type of failure occurs in beams containing a relatively low percentage of both transverse and longitudinal reinforcement (i.e. under reinforced). It is assumed, therefore, that all steel intercepting the failure section has yielded at ultimate load.

From the tests it was observed that when bending was predominant the bottom steel yielded and the compression concrete crushed near the top face at ultimate resulting in a mode ly form of failure. For beams tested under a moderate amount of torsional

121

moment with or without shear, at failure the reinforcement yielded
on one vertical side and the compression zone formed on the opposite
side - i.e. the side in which the torsional and shear stresses are
opposed, resulting in a mode 2y form of failure. When torsion was
predominant in lightly top reinforced beams, at failure the com-
pression zone formed near the bottom face, and the reinforcement
at the top yielded, resulting in a mode 3y form of failure.

On the bases of the observations above theoretical equations
will be derived for the three principal modes: 1y, 2y and 3y of
which the lowest torsional capacity is the critical. Since both
categories of the reinforcement yield at failure, the contribution
of the concrete in the compression zone to the ultimate resistance
of the member is believed to be very small for modes 1y and 3y, and
therefore, it is ignored in the analysis of this type of failure -
i.e. type I.

4.2.1 Mode 1y Failure

This mode of failure is critical when the ratio of bending
moment to torsional moment ψ is high and the longitudinal bars
are distributed symmetrically around the cross-section. At
ultimate load the reinforcement near the bottom face reaches the
yield strength and finally the beam fails by bending about an
axis in the compression zone - which is near the top face in this
case.

The failure surface resulting from this mode of failure (i.e.
mode 1y) can be seen in figure 4.1(a). The failure surface is
bounded by spiral tensile cracks around the north, bottom and
south faces with the compression zone located near the top face
joining the ends. To simplify the analysis it is assumed that the

tensile cracks defining the failure surface are straight lines, making different angles of inclination on the faces with the transverse axis.

For a member loaded in combined torsion, bending and vertical shear, the inclination of the cracks in the sides is assumed to be controlled by two independent parameters, $\tan\alpha_{1y}$ for predominantly torsion failure control, and $\tan\gamma_{1y}$ for predominantly shear failure control. To produce equilibrium in the failure section, in a beam under combined loads, these two parameters are additive on one vertical side of the section and subtractive on the other.

The different inclinations for mode 1y resulting from this summation on the north, bottom and south faces with the transverse axis are $(\tan\alpha_{1y} - \tan\gamma_{1y})$, $\tan\alpha_{1y}$ and $(\tan\alpha_{1y} + \tan\gamma_{1y})$ respectively. The angle of inclination of the compression zone which joins the ends of the tensile cracks near the top is denoted as θ_{1y}. To simplify the analysis, the centroid of the concrete compression zone is considered to be located approximately at the level of the stirrups in the top of the section. It is further assumed that the distance from the stirrup legs in the bottom to the neutral axis, and the lever arm to the bottom longitudinal bars are approximately equal to y.

From equilibrium of the external and internal moments about an axis parallel to the longitudinal axis of the beam, through the centroid of the compression zone - see figure 4.1(b), the following equation can be developed

$$T_{1y} = A_w \cdot f_{wy} \cdot \frac{y}{s} \cdot (\tan\alpha_{1y} - \tan\gamma_{1y}) \cdot \frac{x}{2} + A_w \cdot f_{wy} \cdot \frac{y}{s} \cdot (\tan\alpha_{1y} + \tan\gamma_{1y}) \cdot \frac{x}{2}$$

$$+ A_w \cdot f_{wy} \cdot \frac{x}{s} \cdot \tan\alpha_{1y} \cdot y$$

In the equation above the first and the second terms of the right hand side are the forces in the vertical legs of the stirrups intercepting the failure section, multiplied by the lever arm x/2. The third is the forces in the bottom legs of the yielded stirrups crossing the failure section, multiplied by the lever arm y.

Rearranging

$$T_{1y} = 2 \cdot A_w \cdot f_{wy} \cdot \frac{x \cdot y}{s} \cdot \tan\alpha_{1y} \tag{4.1}$$

Equation 4.1 involves $\tan\alpha_{1y}$ and to form an expression to determine its value two other equilibrium equations are considered. One equation is obtained by taking moments of forces about an axis through the centroid of the compression zone, normal to the longitudinal axis of the beam, and the other by resolving forces in the vertical direction.

Equating the moment of the external forces to that of the internal forces about an axis through the centroid of the concrete compression zone, in a direction perpendicular to the longitudinal axis of the beam, the following equation is produced.

$$M_{1y} + V_{1y} \cdot \ell_1 = 2 \cdot A_b \cdot f_{by} \cdot y - A_w \cdot f_{wy} \cdot \frac{y}{s} \cdot (\tan\alpha_{1y} - \tan\gamma_{1y}) \cdot$$

$$[\frac{1}{2} \cdot (x+y) \cdot \tan\alpha_{1y} + \frac{1}{2} \cdot y \cdot \tan\gamma_{1y}]$$

$$- A_w \cdot f_{wy} \cdot \frac{y}{s} \cdot (\tan\alpha_{1y} + \tan\gamma_{1y}) \cdot$$

$$[\frac{1}{2} \cdot (x+y) \cdot \tan\alpha_{1y} - \frac{1}{2} \cdot y \cdot \tan\gamma_{1y}] \tag{4.2}$$

The first term in the right hand side of equation 4.2 is the force induced in the two bottom longitudinal bars at yield,

multiplied by the lever arm y - assuming that the line of action of the main bars to be at the same level as the bottom leg of the stirrups. The second and the third terms are the forces in the vertical leg of the stirrups on the north and south faces, multiplied by their lever arms $[\frac{1}{2} \cdot (x+y) \cdot \tan\alpha_{1y} + \frac{1}{2} \cdot y \cdot \tan\gamma_{1y}]$, and $[\frac{1}{2} \cdot (x+y) \cdot \tan\alpha_{1y} - \frac{1}{2} \cdot y \cdot \tan\gamma_{1y}]$ respectively. The second term in the left hand side of the equation above is the existing shear force in the section, multiplied by the horizontal dislocation, ℓ_1, of its line of action from the moment axis (i.e. the centroid of the compression zone), along the longitudinal axis of the beam.

From the geometry of figure 4.1(b), ℓ_1 can be found in terms of the known parameters as

$$\ell_1 = \frac{y}{2} \cdot (\tan\alpha_{1y} - \tan\gamma_{1y}) + \frac{x}{2} \cdot \tan\alpha_{1y} + \frac{y}{2} \cdot (\tan\alpha_{1y} + \tan\gamma_{1y})$$

$$- [y \cdot (\tan\alpha_{1y} - \tan\gamma_{1y}) + \frac{x}{2} \cdot \tan\alpha_{1y}]$$

Rearranging

$$\ell_1 = y \cdot \tan\gamma_{1y}$$

Equating the external shear force to the internal forces in the stirrup legs in the sides, along the transverse direction, ignoring the contribution of the concrete in the compression zone to the shear resistance, another equation can be obtained as,

$$V_{1y} = A_w \cdot f_{wy} \cdot \frac{y}{s} \cdot (\tan\alpha_{1y} + \tan\gamma_{1y}) - A_w \cdot f_{wy} \cdot \frac{y}{s} \cdot (\tan\alpha_{1y} - \tan\gamma_{1y})$$

The two terms in the right hand side of the above equation are the forces in the yielded stirrup legs in the south and north face respectively.

Rearranging

$$V_{1y} = 2.A_w.f_{wy}.\frac{y}{s}.\tan\gamma_{1y} \qquad\qquad (4.3)$$

Combining equations 4.1 and 4.3 with equation 4.2, after substituting for ℓ_1 from the expression, the following interaction equation can be deduced,

$$\left(\frac{T_{1y}}{Tu_{1y}}\right)^2 + \left(\frac{V_{1y}}{Vu_{1y}}\right)^2 + \frac{M_{1y}}{Mu_{1y}} = 1 \qquad\qquad (4.4)$$

The form of equation 4.4 for mode 1 has been produced previously by Elfgren et al [38], using truss-analogy method.

In Eqn 4.4

$$Mu_{1y} = 2.A_b.f_{by}.y$$

$$Tu_{1y} = 2.Mu_{1y}.\sqrt{r_{1y}/(1+y/x)}$$

$$Vu_{1y} = 2.Mu_{1y}.\sqrt{r_{1y}/(x.y)}$$

and

$$r_{1y} = \frac{A_w.f_{wy}.x}{2.A_b.f_{by}.s}$$

Equation 4.4 can be rearranged to form a quadratic equation in T_{1y}/Tu_{1y} as,

$$[1+(\delta/B_1)^2].\left(\frac{T_{1y}}{Tu_{1y}}\right)^2 + [\psi/A_1].\left(\frac{T_{1y}}{Tu_{1y}}\right) - 1 = 0$$

Solving for T_{1y}/Tu_{1y}

$$\frac{T_{1y}}{Tu_{1y}} = \frac{-\psi/A_1 \pm \sqrt{(\psi/A_1)^2 + 4.[1+(\delta/B_1)^2]}}{2.[1+(\delta/B_1)^2]} \qquad\qquad (4.5)$$

where

$$A_1 = Mu_{1y}/Tu_{1y} = (1/2).\sqrt{(1+y/x)/r_{1y}}$$

126

$$\tan \alpha_{b1} = \tan \alpha_{1y}$$

$$\tan \alpha_{n1} = \tan \alpha_{1y} - \tan \gamma_{1y}$$

$$\tan \alpha_{s1} = \tan \alpha_{1y} + \tan \gamma_{1y}$$

a) General failure surface

b) Parallel to the longitudinal axis, and north views

c) Top view
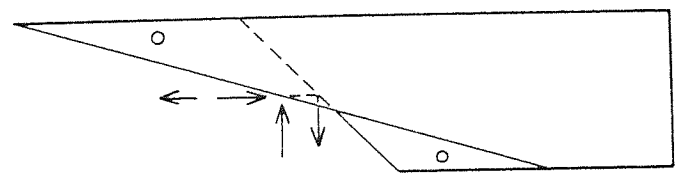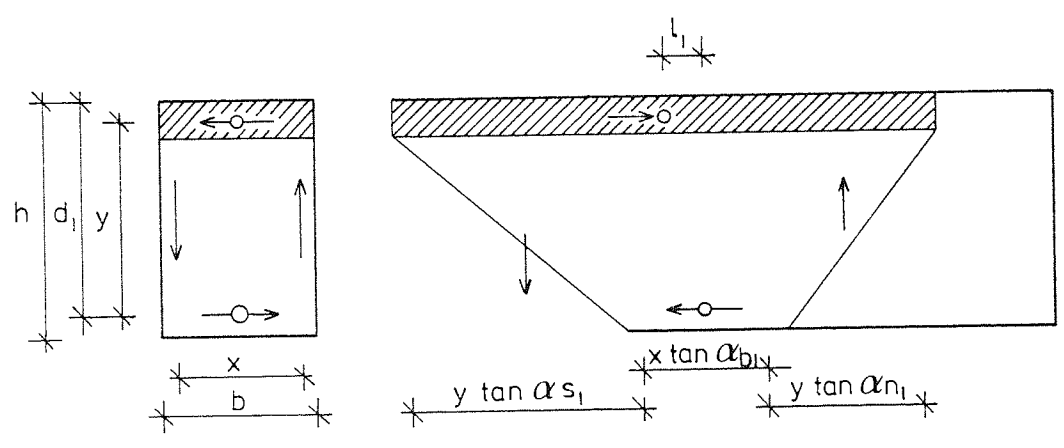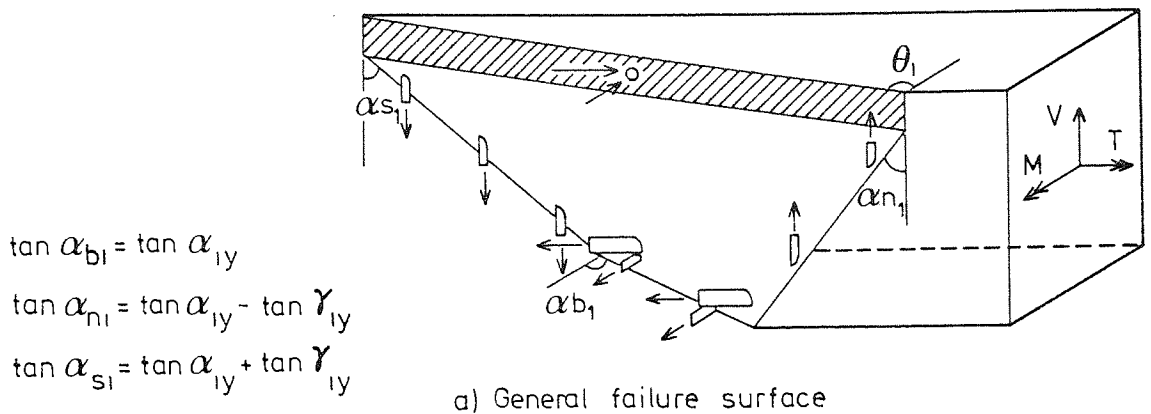
FIGURE 4.1 : Mode 1y failure mechanism for reinforced concrete beams under combined torsion, bending and shear.

$$B_1 = Vu_{1y}/Tu_{1y} = \sqrt{(1+y/x)/(x.y)}$$

Equation 4.1 can be expressed in terms of the ultimate bending strength, Mu_{1y}, for mode 1y as,

$$T_{1y} = 2.Mu_{1y}.r_{1y}.\tan\alpha_{1y} \qquad (4.6)$$

Dividing equation 4.6 by the expression for the ultimate torsional strength in pure torsion, Tu_{1y}, another relation between T_{1y} and Tu_{1y} can be found as;

$$\frac{T_{1y}}{Tu_{1y}} = 2.A_1.r_{1y}.\tan\alpha_{1y} \qquad (4.7)$$

Substituting equation 4.7 into equation 4.5 to eliminate T_{1y}/Tu_{1y} and rearranging for $\tan\alpha_{1y}$, it can be shown that

$$\tan\alpha_{1y} = \frac{-\psi+\sqrt{\psi^2+4.A_1^2.[1+(\delta/B_1)^2]}}{4.A_1^2.r_{1y}[1+(\delta/B_1)^2]} \qquad (4.8)$$

Now the ultimate torsional capacity resisted by a fully reinforced concrete member subject to combined loading and failing in mode 1y by yielding of both sets of the reinforcement can be calculated from equation 4.1, using the value for $\tan\alpha_{1y}$ obtained from equation 4.8.

The value of $\tan\alpha_{1y}$ was not defined by Elfgren et al [38]. The combination of equation 4.1 and 4.8 are considered more suitable for analysis and design than equation 4.4.

4.2.2 Mode 2y Failure

The analysis for mode 2y failure follows the same approach as that of mode 1y, although in this mode the compression zone

forms near one of the vertical sides. Figure 4.2(a) shows the general failure mechanism surface for a beam failing in mode 2y. At failure the reinforcement yield in the vertical side due to the shear stresses from torsion and shear force, and the compression zone forms on the opposite side.

From equilibrium of external and internal moments about an axis parallel to the longitudinal axis of the beam, through the centroid of the compression zone - figure 4.2(b), the following equation can be developed.

$$T_{2y} + V_{2y} \cdot \frac{x}{2} = A_w \cdot f_{wy} \cdot \frac{y}{s} \cdot (\tan\alpha_{2y} + \tan\gamma_{2y}) +$$

$$A_w \cdot f_{wy} \cdot \frac{x}{s} \cdot \tan\alpha_{2y} \cdot (\frac{y}{2} + \frac{y}{2})$$

Rearranging

$$T_{2y} + V_{2y} \cdot \frac{x}{2} = 2 \cdot A_w \cdot f_{wy} \cdot \frac{x \cdot y}{s} \cdot \tan\alpha_{2y} + A_w \cdot f_{wy} \cdot \frac{x \cdot y}{s} \cdot \tan\gamma_{2y} \qquad (4.9)$$

Assuming that only one half of the existing shear force is resisted by the yielded stirrups in the tension side, the following expression can be constructed,

$$V_{2y} = 2 \cdot A_w \cdot f_{wy} \cdot \frac{y}{s} \cdot \tan\gamma_{2y} \qquad (4.10)$$

Inserting equation 4.10 into equation 4.9, and rearranging

$$T_{2y} = 2 \cdot A_w \cdot f_{wy} \cdot \frac{x \cdot y}{s} \cdot \tan\alpha_{2y} \qquad (4.11)$$

The inclination $\tan\alpha_{2y}$ must be determined in order to obtain a solution for equation 4.11. An expression for $\tan\alpha_{2y}$ can be obtained using the same approach as in the previous mode, by equating the external moments to the moments of the internal forces around a transverse axis through the centroid of the compression zone - see figure 4.2(c).

$$M_{2y} = 2 \cdot A_s \cdot f_{sy} \cdot x - A_w \cdot f_{wy} \cdot \frac{x}{s} \cdot \tan\alpha_{2y} \cdot$$

$$[x \cdot \tan\alpha_{2y} + y \cdot (\tan\alpha_{2y} + \tan\gamma_{2y})]$$

The applied bending moment has no effect about this axis and therefore

$$2 \cdot A_s \cdot f_{sy} \cdot x = A_w \cdot f_{wy} \cdot \frac{x}{s} \cdot \tan\alpha_{2y} \cdot$$

$$[x \cdot \tan\alpha_{2y} + y \cdot (\tan\alpha_{2y} + \tan\gamma_{2y})] \tag{4.12}$$

Substituting equations 4.10 and 4.11 into equation 4.12 to eliminate $\tan\alpha_{2y}$ and $\tan\gamma_{2y}$, and rearranging, the following inter-action equation for mode 2y can be obtained,

$$(\frac{T_{2y}}{Tu_{2y}})^2 + \frac{T_{2y}}{Tu_{2y}} \cdot \frac{V_{2y}}{Vu_{2y}} = 1 \tag{4.13}$$

This equation differs from that produced by Elfgren et al [38] for mode 2. The reason for this is that in forming equation 4.12 above, the difference between the forces in the bottom and the top longitudinal steel in the tension side which results from the variation of the applied bending moment along the failure section, was ignored.

In Eq? 4.13

$$Tu_{2y} = 2 \cdot Mu_{2y} \cdot \sqrt{r_{2y}/(1+x/y)}$$

$$Vu_{2y} = 2 \cdot Mu_{2y} \cdot \sqrt{r_{2y} \cdot (1+x/y)/x^2}$$

$$Mu_{2y} = 2 \cdot A_s \cdot f_{sy} \cdot x$$

and

$$r_{2y} = \frac{A_w \cdot f_{wy} \cdot y}{2 \cdot A_s \cdot f_{sy} \cdot s}$$

Rearranging equation 4.13 for T_{2y}/Tu_{2y} results in

130

$$\tan \alpha t_2 = \tan \alpha_{2y}$$

$$\tan \alpha s_2 = \tan \alpha + \tan \gamma_{2y}$$

$$\tan \alpha b_2 = \tan \alpha_{2y}$$
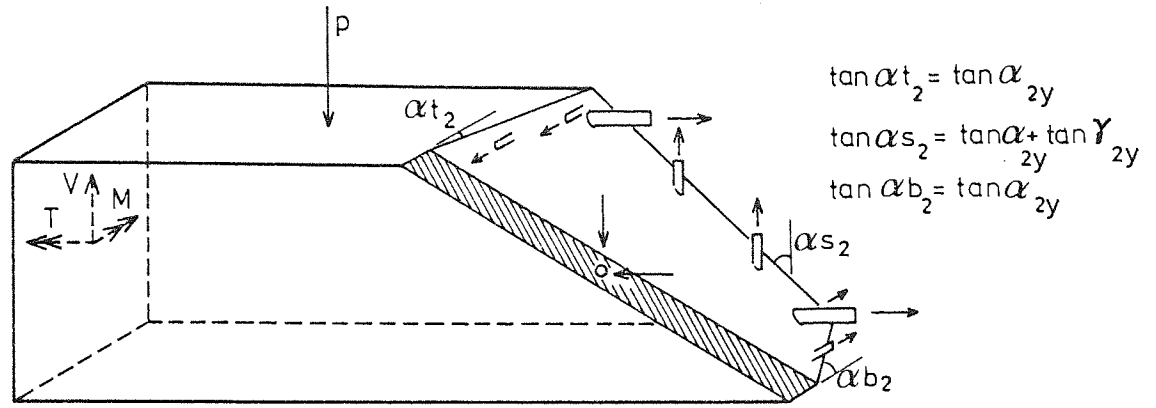
a) General failure surface
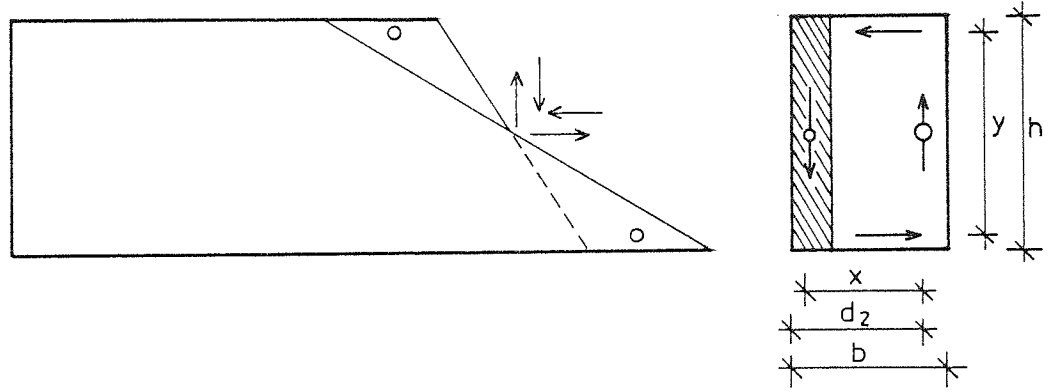
b) North and parallel to the longitudinal axis view
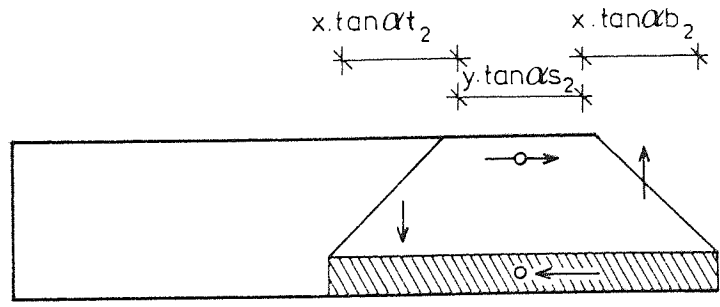
c) Top view

FIGURE 4.2 : Mode 2y failure mechanism for reinforced concrete beams under combined torsion, bending and shear.

$$\frac{T_{2y}}{Tu_{2y}} = \frac{1}{\sqrt{1+ (\delta/B_2)}} \qquad (4.14)$$

where

$$B_2 = Vu_{2y}/T_{u2y} = (1 + x/y)/x$$

Equation 4.11 can be rearranged in terms of the ultimate bending strength, Mu_{2y}, for mode 2y as

$$T_{2y} = 2 \cdot Mu_{2y} \cdot r_{2y} \cdot \tan\alpha_{2y} \qquad (4.15)$$

Dividing equation 4.15 by the expression for ultimate torsional strength in pure torsion, Tu_{2y}, for mode 2y, another relation between T_{2y} and Tu_{2y} can be found as,

$$\frac{T_{2y}}{Tu_{2y}} = 2 \cdot A_2 \cdot r_{2y} \cdot \tan\alpha_{2y} \qquad (4.16)$$

where

$$A_2 = Mu_{2y}/Tu_{2y} = \frac{1}{2} \cdot \sqrt{(1+x/y)/r_{2y}}$$

Combining equation 4.14 with equation 4.16 to eliminate T_{2y}/Tu_{2y}, and rearranging for $\tan\alpha_{2y}$, it can be shown that

$$\tan\alpha_{2y} = \frac{1}{2 \cdot A_2 \cdot r_{2y} \cdot \sqrt{1+\delta/B_2}} \qquad (4.17)$$

4.2.3 Mode 3y Failure

This mode of failure occurs when the ratio of bending moment to torsional moment ψ is small or zero. The equation for this mode gives a lower failure torque for members where the amount of the longitudinal steel in the top of the section is less than that in the bottom. At failure the reinforcement in the top yields,

132

and the compression concrete crushes near the bottom. The appearance of the idealized failure surface for this mode is shown in figure 4.3(a).

Equilibrium of internal and external moments about an axis through the centroid of the compression zone, and parallel to the longitudinal axis of the beam , see figure 4.3(b), results in the following equation;

$$T_{3y} = A_w \cdot f_{wy} \cdot \frac{y}{s} \cdot (\tan\alpha_{3y} + \tan\gamma_{3y}) \cdot \frac{x}{2} +$$

$$A_w \cdot f_{wy} \cdot \frac{y}{s} \cdot (\tan\alpha_{3y} - \tan\gamma_{3y}) \cdot \frac{x}{2} +$$

$$A_w \cdot f_{wy} \cdot \frac{x}{s} \cdot \tan\alpha_{3y} \cdot y$$

Rearranging

$$T_{3y} = 2 \cdot A_w \cdot f_{wy} \cdot \frac{x \cdot y}{s} \cdot \tan\alpha_{3y} \qquad (4.18)$$

A solution for equation 4.18 can be obtained only when the inclination $\tan\alpha_{3y}$ is known. An expression for determining $\tan\alpha_{3y}$ can be obtained following the same approach as in mode 1y.

From the equilibrium of the external and internal moments about an axis perpendicular to the longitudinal axis of the beam, through the centroid of the compression zone - see figure 4.3(c), the following equation can be obtained,

$$M_{3y} - V_{3y} \cdot \ell_3 = -2 \cdot A_t \cdot f_{ty} \cdot y + A_w \cdot f_{wy} \cdot \frac{y}{s} \cdot (\tan\alpha_{3y} + \tan\gamma_{3y}) \cdot$$

$$[\frac{1}{2} \cdot (x+y) \cdot \tan\alpha_{3y} - \frac{1}{2} \cdot y \cdot \tan\gamma_{3y}]$$

$$+A_w \cdot f_{wy} \cdot \frac{y}{s} \cdot (\tan\alpha_{3y} - \tan\gamma_{3y}) \cdot [\frac{1}{2} \cdot (x+y) \cdot \tan\alpha_{3y} + \frac{1}{2} \cdot y \cdot \tan\gamma_{3y}] \qquad (4.19)$$

It can be shown in the same way as in mode 1y that:

$$\ell_3 = y \cdot \tan\gamma_{3y}$$

and

$$V_{3y} = 2 \cdot A_w \cdot f_{wy} \cdot \frac{y}{s} \cdot \tan\gamma_{3y}$$

Substituting for ℓ_3 and V_{3y} in equation 4.19 and combining with equation 4.18 to eliminate $\tan\alpha_{3y}$ and $\tan\gamma_{3y}$, the following inter-action equation for mode 3y can be obtained,

$$(\frac{T_{3y}}{Tu_{3y}})^2 + (\frac{V_{3y}}{Vu_{3y}})^2 - \frac{M_{3y}}{Mu_{3y}} = 1 \qquad (4.20)$$

The same form of equation 4.20 was produced previously by Elfgren et al [38] for mode 3, using truss-analogy method.

In Eqn 4.20

$$Mu_{3y} = 2 \cdot A_t \cdot f_{ty} \cdot y$$

$$Tu_{3y} = 2 \cdot Mu_{3y} \cdot \sqrt{r_{3y}/(1+y/x)}$$

$$Vu_{3y} = 2 \cdot Mu_{3y} \cdot \sqrt{r_{3y}/(x \cdot y)}$$

and

$$r_{3y} = \frac{A_w \cdot f_{wy} \cdot x}{2 \cdot A_t \cdot f_{ty} \cdot s}$$

Following the same procedure as in mode 1y, an expression for $\tan_{3y}$ can now be deduced, and written as:

$$\tan_{3y} = \frac{\psi + \sqrt{\psi^2 + 4 \cdot A_3^2 [1+(\delta/B_3)^2]}}{4 \cdot A_3^2 \cdot r_{3y} \cdot [1+(\delta/B_3)^2]} \qquad (4.21)$$

where
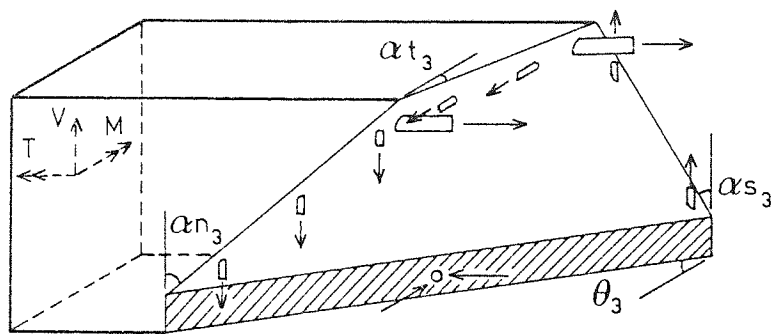
$$\tan \alpha t_3 = \tan \alpha_{3y}$$

$$\tan \alpha n_3 = \tan \alpha_{3y} + \tan \gamma_{3y}$$

$$\tan \alpha s_3 = \tan \alpha_{3y} - \tan \gamma_{3y}$$

a) General failure surface
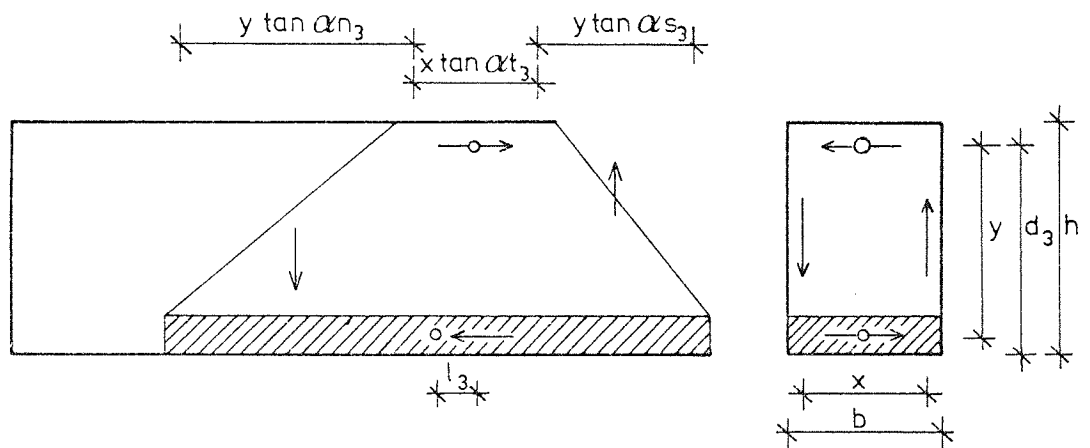
b) North and parallel to the longitudinal axis views
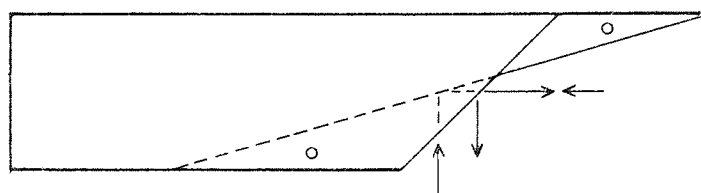
c) Top view

FIGURE 4.3 : Mode 3y failure mechanism for reinforced concrete beams under combined torsion, bending and shear.

$$A_3 = Mu_{3y}/Tu_{3y} = \frac{1}{2} \cdot \sqrt{(1+y/x)r_{3y}}$$

$$B_3 = Vu_{3y}/Tu_{3y} = \sqrt{(1+y/x)/x^2}$$

Equation 4.21 was not produced by Elfgren [38], but combined with equation 4.18 is more suitable for analysis and design.

4.3 TYPE II FAILURE - YIELDING OF THE WEB STEEL ONLY

Beams which are reinforced with heavy longitudinal steel fail when the stirrups yield at the ultimate load, while the main rein- forcement is still in elastic state. In this case the concrete in the compression zone assists in resisting the applied loads. The concrete in this zone is subjected to a direct stress due to the bending moment, and shear stresses due to both torsional moment and shear force. The direct stresses, fm, and the resultant shear stresses, fv, can be combined into Cowan's [7] failure criterion for concrete. Cowan suggested that the more complicated failure enve- lopes for the failure of concrete in compression could be replaced by a straight line tangent to the uniaxial compressive strength, as shown in figure 4.4. From the figure, an expression which rel- ates the resultant shear stresses, fv, to the cylinder compressive strength of the concrete, f'_c, can be deduced and written as:

$$fv = \frac{(1 - \sin\beta)/2}{\sqrt{1+(\frac{fm}{2 \cdot fv})^2} - (\frac{fm}{2 \cdot fv}) \cdot \sin \beta} \cdot f'_c \qquad (4.22)$$

where

β is the angle of the straight line failure envelope for concrete to the horizontal, which Cowan found to be $37°$.

The relationship between fv and fm in equation 4.22 is shown in figure 4.5. To avoid a complicated representation of the ratio
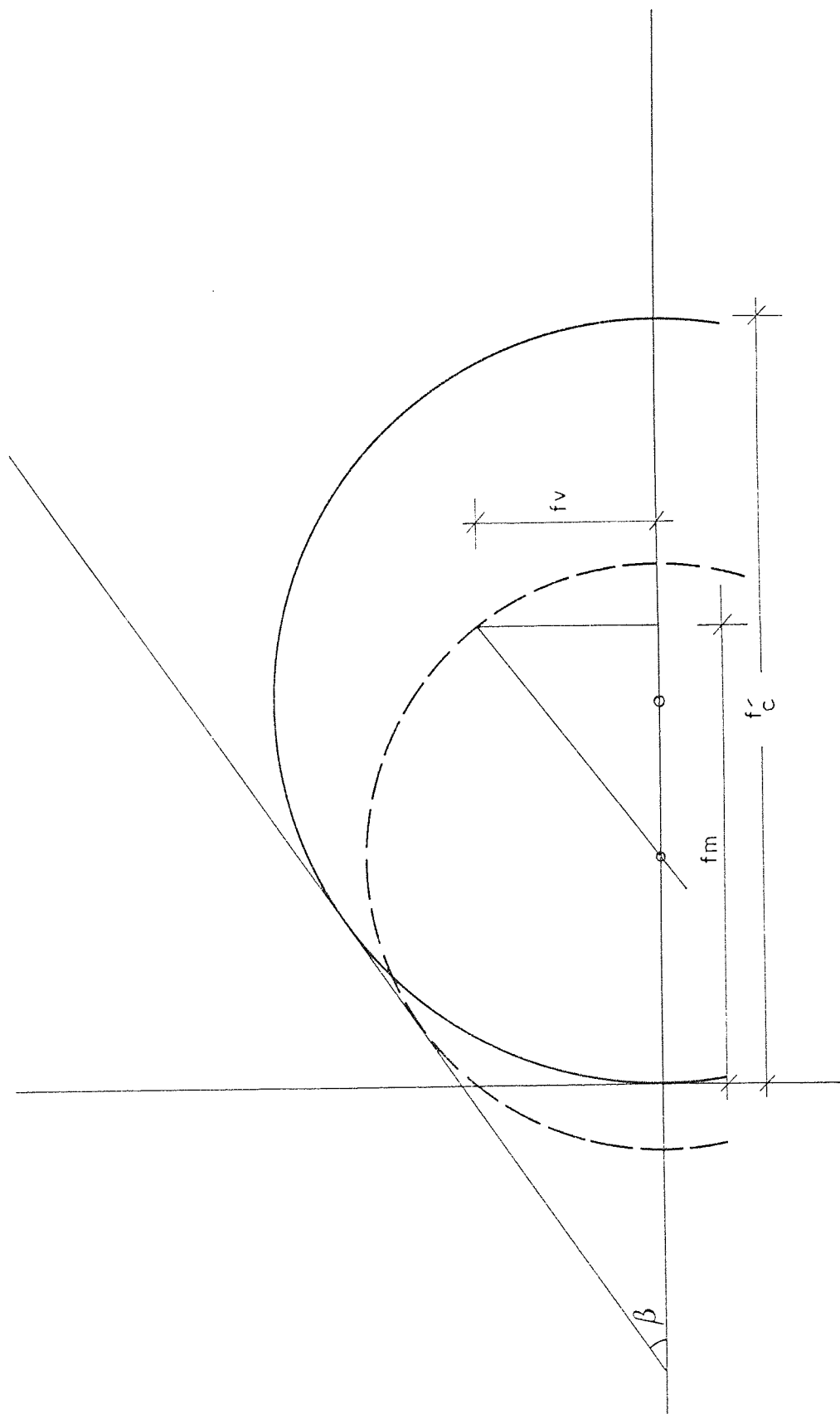
FIGURE 4.4 : Cowan's failure criterion for concrete under combined stresses
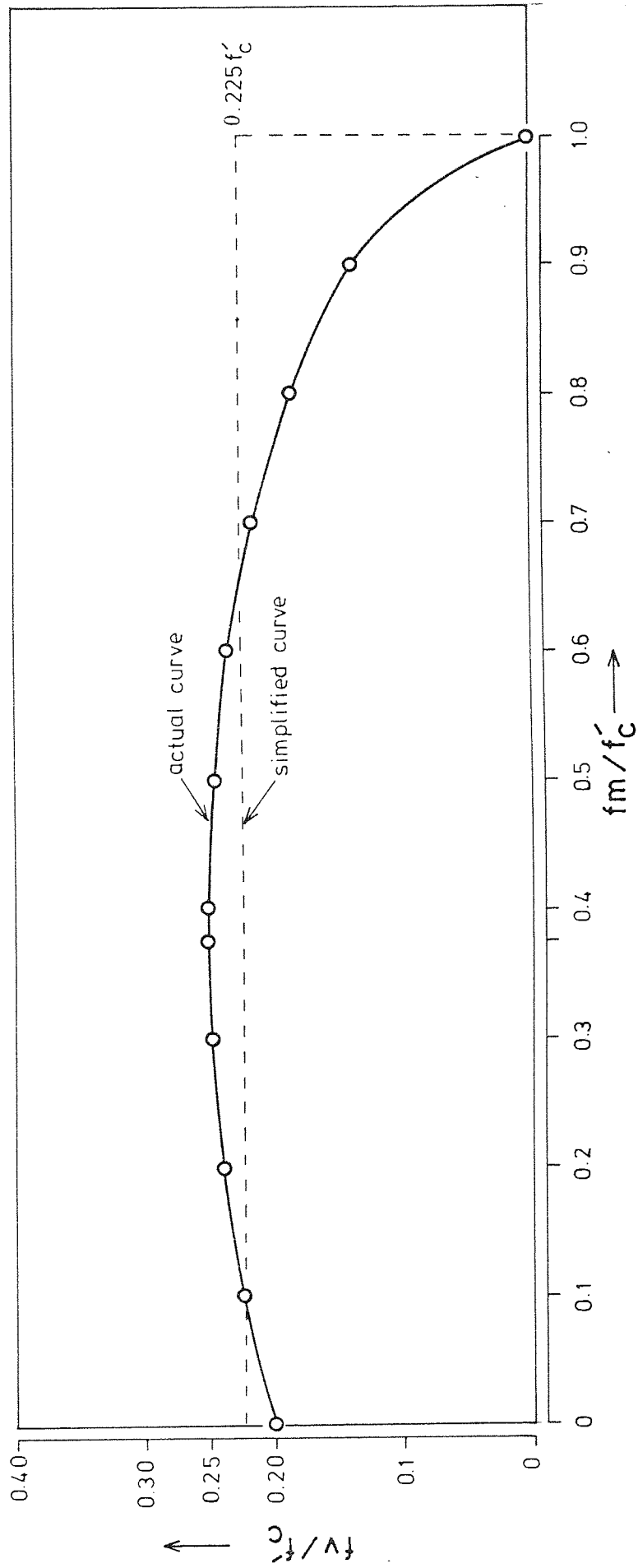
FIGURE 4.5: Actual and simplified relationship between resultant shear stresses f_v and direct compressive stress f_m.

fm/fv, a linear relationship shown as a dotted line in figure 4.5, is assumed as:

$$fv = \xi.f'_c \qquad\qquad (4.23)$$

where ξ is a coefficient varying between 0.20 to 0.25 for fm from zero to $0.75.f'_c$.

An average value for ξ therefore is 0.225, providing fm is not greater than f'_c.

As previously, in this type of failure three principal modes 1w, 2w and 3w are possible depending on the amount of longitudinal steel and the stresses induced in them from the applied loads.

4.3.1 Mode 1w Failure

This mode of failure occurs in beams subjected to a high ratio of bending to torsional moment ψ. At failure the bottom longitudinal steel reaches a high stress due to a large value of ψ and therefore crushing of the concrete takes place near the top of the section, resulting in a mode 1w failure by yielding of the stirrups. The failure surface is shown in figure 4.6(a).

Equating the external moment to the moment of the internal forces about an axis parallel to the longitudinal axis of the beam through an arbitrary point e_1 - see figure 4.6(b).

$$T_{1w} + V.\frac{x}{2} = Kv.b.dn_{1w}.fv.R_{1w} + A_w.f_{wy}.\frac{(d_1-dn_{1w})}{s}.x.\tan\alpha_{1w}$$

The first term of the right hand side of the above equation is the torsional resistance carried by the concrete in the compression zone, while the second term is the part of torque resisted by the web steel at yield.

139

Rearranging

$$T_{1w} = \frac{Kv.b.dn_{1w}.fv_{1w}.R_{1w} + A_w.f_{wy}.[(d_1-dn_{1w})/s].x.tan\alpha_{1w}}{1 + (\delta.x)/2} \qquad (4.24)$$

To solve equation 4.24, values for dn_{1w}, fv_{1w}, R_{1w} and $tan\alpha_{1w}$ must be determined.

The inclination of the tensile cracks $tan\alpha_{1w}$ of the failure surface on the three faces are assumed to be constant and - as explained previously - equal to 1.

The resultant shear stress fv_{1w} can be obtained from equation 4.23.

Other unknown quantities in equation 4.24 are dn_{1w} and R_{1w} which are inter-related. The important value is dn_{1w}.

Since the longitudinal reinforcement is still in the elastic stage, an elastic stress distribution is considered to be appropriate to determine the depth of shear compression zone. This theoretical solution involves the equilibrium of forces on a skew-bending sur-face, a linear strain distribution over the depth of the cracked section, and a linear stress-strain relationship for the concrete and the steel.

Equating the compressive force in the concrete to the tensile force in the reinforcement in a direction perpendicular to the skew compression zone - see figure 4.6(c), results in:

$$Km_i.b.dn_{1w}.fm_{1iw}/cos\theta_{1w} = 2.A_b.f_b.cos\theta_{1w} + A_w.f_{wy}.\frac{x}{s}.tan\alpha_{1w}.sin\theta_{1w} \qquad (4.25)$$

From figure 4.6(c), considering linear distribution of strain across the depth of the skew-cracked section - i.e. strain compati-bility,

$$\frac{\varepsilon_{liw}}{dn_{lw}} = \frac{\varepsilon'_{liw}}{(d_1 - dn_{lw})} \tag{4.26}$$

where

ε_{liw} is the compressive concrete strain at the top of the beam in a direction perpendicular to θ-plane

ε'_{liw} is the tensile concrete strain for an element adjacent to the bottom reinforcement in a direction perpendicular to the θ-plane.

Below et al [65] proposed that for a concrete element located on the level of bottom reinforcement, the strain in the direction perpendicular to the tensile crack should be considered as the principal tensile strain, and the tensile strain in the direction of the crack could be ignored. This proposal led to a relationship between the tensile strain of the concrete in the direction perpendicular to the θ-plane, and the direct strain in the tensile longitudinal bars, using Mohr's circle for strain. The relationship can be expressed in the form:

$$\varepsilon'_{liw} = \varepsilon_b \cdot \cos^2\theta_{lw} \cdot (1 + \tan\alpha_{lw} \cdot \tan\theta_{lw})^2 \tag{4.27}$$

Substituting equation 4.27 into equation 4.26 and combining with equation 4.25 to eliminate fm_{liw} and rearranging, the following quadratic equation in (dn_{lw}/d_1) is produced.

$$(\frac{dn_{lw}}{d_1})^2 + \frac{\rho_1 \cdot m}{Km_i} \cdot C_{lw} \cdot (\frac{dn_{lw}}{d_1}) - \frac{\rho_1 \cdot m}{Km_i} \cdot C_{lw} = 0$$

Solving for dn_{lw}/d_1

$$\frac{dn_{lw}}{d_1} = \sqrt{(\frac{1}{2} \cdot \frac{\rho_1 \cdot m}{Km_i} \cdot C_{lw})^2 + 2 \cdot \frac{\rho_1 \cdot m}{Km_i} \cdot C_{lw}} - \frac{1}{2} \cdot \frac{\rho_1 \cdot m}{Km_i} \cdot C_{lw} \tag{4.28}$$

where

$$C_{1w} = \frac{(1 + r_{1w} \cdot \tan\alpha_{1w} \cdot \tan\theta_{1w})}{(1 + \tan\alpha_{1w} \cdot \tan\theta_{1w})^2}$$

and

$$\tan\theta_{1w} = \tan\alpha_{1w} / [1 + Kd \cdot (h/b)]$$

$$r_{1w} = \frac{A_w \cdot f_{wy} \cdot x}{2 \cdot A_b \cdot f_b \cdot s}$$

In order to obtain a value for r_{1w} above, the tensile stress in bottom longitudinal bars, f_b, must be known.

Since the stirrups yield at failure, an expression which relates the stress in the longitudinal bar to the stress in the stirrup leg in the tension zone is required. A relationship proposed again by Below et al [65], which relates the tensile strain in the longitudinal direction to that in transverse direction is convenient and can be expressed as,

$$f_b = f_{wy} / \tan^2\alpha_{1w}$$

Since the exact values for torsional and shear stresses in the compression concrete is not known, the lever arm to the resultant shear force, R_{1w} can only be determined approximately. From the geometry of figure 4.6(b).

$$R_{1w} = \sqrt{(d_1 - Ks \cdot dn_{1w})^2 + (x/2)^2}$$

The ultimate torsional strength of a reinforced concrete beam subject to a combined loading, and failing in mode 1w, can be calculated from equation 4.24, incorporating the values obtained for dn_{1w}, fv_{1w} and R_{1w}.

4.3.2 Mode 2w Failure

This mode of failure takes place in reinforced beams subject

142

to moderate or low ratio of ψ with or without shear. Due to the longitudinal component of the additive stresses from the torsion and the shear on one of the vertical sides, the longitudinal steel in this latter side is subject to a relatively high strain and produce compression in the concrete in the opposite side of the section. Eventually, with increasing the load, the concrete in the latter sides crushes and the stirrups in the tensile zone yield, while the main bars are still behaving elastically. The appearance of the failure surface for this mode can be seen in figure 4.7(a).

Taking moment of external and internal forces about an axis parallel to the longitudinal axis of the beam, through point e_2 - see figure 4.7(b),

$$T_{2w} - V.\frac{X}{2} = K_v.d.dn_{2w}.fv_{2w}.R_{2w} + A_w.f_{wy}.\frac{(d_2 - dn_{2w})}{s}.y.\tan\alpha_{2w}$$

Rearranging

$$T_{2w} = \frac{K_v.d.dn_{2w}.f_{2w}.R_{2w} + A_w.f_{wy}.[(d_2 - dn_{2w})/s].y.\tan\alpha_{2w}}{1 - (\delta.x)/2} \qquad (4.29)$$

In equation 4.29 values for fv_{2w} and $\tan\alpha_{2w}$ are similar to mode 1w. An expression for dn_{2w}/d_2 can be obtained using the same strain compatibility approach as in mode 1w, and can be written as:

$$\frac{dn_{2w}}{d_2} = \sqrt{(\frac{1}{2}.\frac{\rho_2.m}{Km_i}.C_{2w})^2 + 2.\frac{\rho_2.m}{Km_i}.C_{2w}} - \frac{1}{2}.\frac{\rho_2.m}{Km_i}.C_{2w} \qquad (4.30)$$

where

$$C_{2w} = \frac{(1 + r_{2w}.\tan\alpha_{2w}.\tan\theta_{2w})}{(1 + \tan\alpha_{2w}.\tan\theta_{2w})^2}$$

and

$$\tan\theta_{2w} = \tan\alpha_{2w}/[1 + K_d.(b/h)]$$

$$r_{2w} = \frac{A_w.f_{wy}.y}{2.A_s.f_s.s}$$

143

$$f_s = f_{wy}/\tan^2\alpha_{2w}$$

The lever arm to the resultant shear force in the compression concrete in the side R_{2w}, can be approximately determined from the geometry of figure 4.7(b) as,

$$R_{2w} = \sqrt{(d_2 - Ks.dn_{2w})^2 + (y/4)^2}$$

The last term under the root in the expression above is introduced in order that the inclination of the resultant shear in the concrete compression - for which its magnitude is not known - to be accounted for and also to make the proposed approach applicable for members with narrow section.

4.3.3 Mode 3w Failure

This mode of failure occurs when ψ is low. The equation for this mode gives lower ultimate failure torque for beams with relatively less longitudinal steel at the top of the section. At failure the compression zone forms near the bottom face due to relatively higher total strain experienced by the main bars and the yielded stirrups near the top. The general view of the failure section for this mode is shown in figure 4.8(a).

Equating the external moment to the moment of internal forces about an axis parallel to the longitudinal axis of the beam, through e_3 (see figure 4.8(b)) results in:

$$T_{3w} - V.\frac{x}{2} = Kv.b.dn_{3w}.fv_{3w}.R_{3w} + A_w.f_{wy}.\frac{(d_3 - dn_{3w})}{s}.x.\tan\alpha_{3w}$$

Rearranging

$$T_{3w} = \frac{Kv.b.dn_{3w}.fv_{3w}.R_{3w} + A_w.f_{wy}.[(d_3 - dn_{3w})/s].x.\tan\alpha_{3w}}{1 - (\delta.x)/2} \qquad (4.31)$$

The values for fv_{3w} and $\tan\alpha_{3w}$ are considered to be comparable

144

a) General failure surface

c) Parallel to the compression zone view, and the strain distribution

d) Top view

b) Parallel to the longitudinal axis, and north views
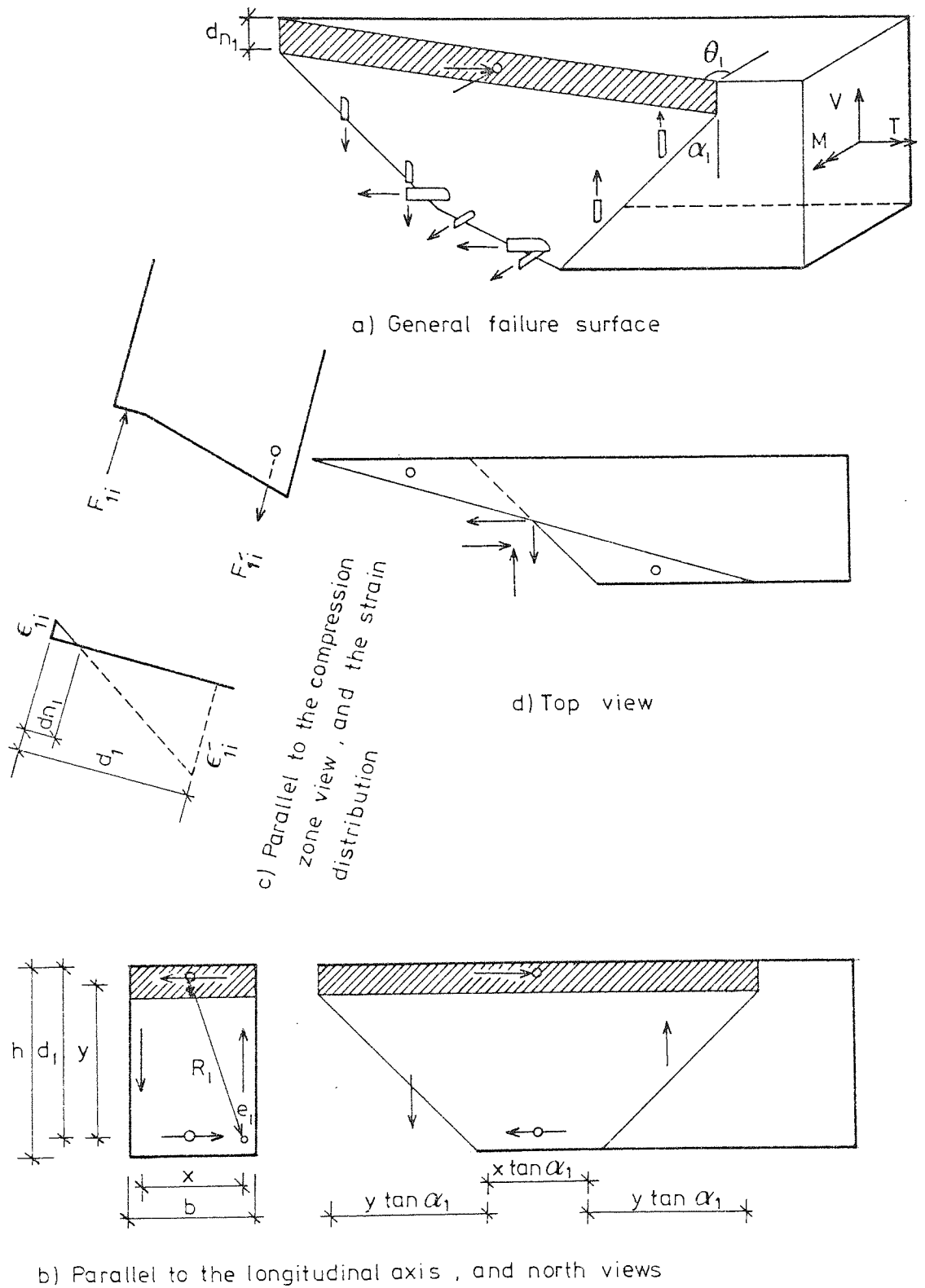
FIGURE 4.6 : Mode 1 failure mechanism for reinforced concrete
beams under combined loads (non - yielding)

145

a) General failure surface

d) Top view

c) Parallel to the compression zone view, and the strain distribution

b) North and parallel to the longitudinal axis views

FIGURE 4.7: Mode 2 failure mechanism for reinforced concrete beams under combined loads (non-yielding)

d) Top view

c) Parallel to the compression zone view and the strain distribution
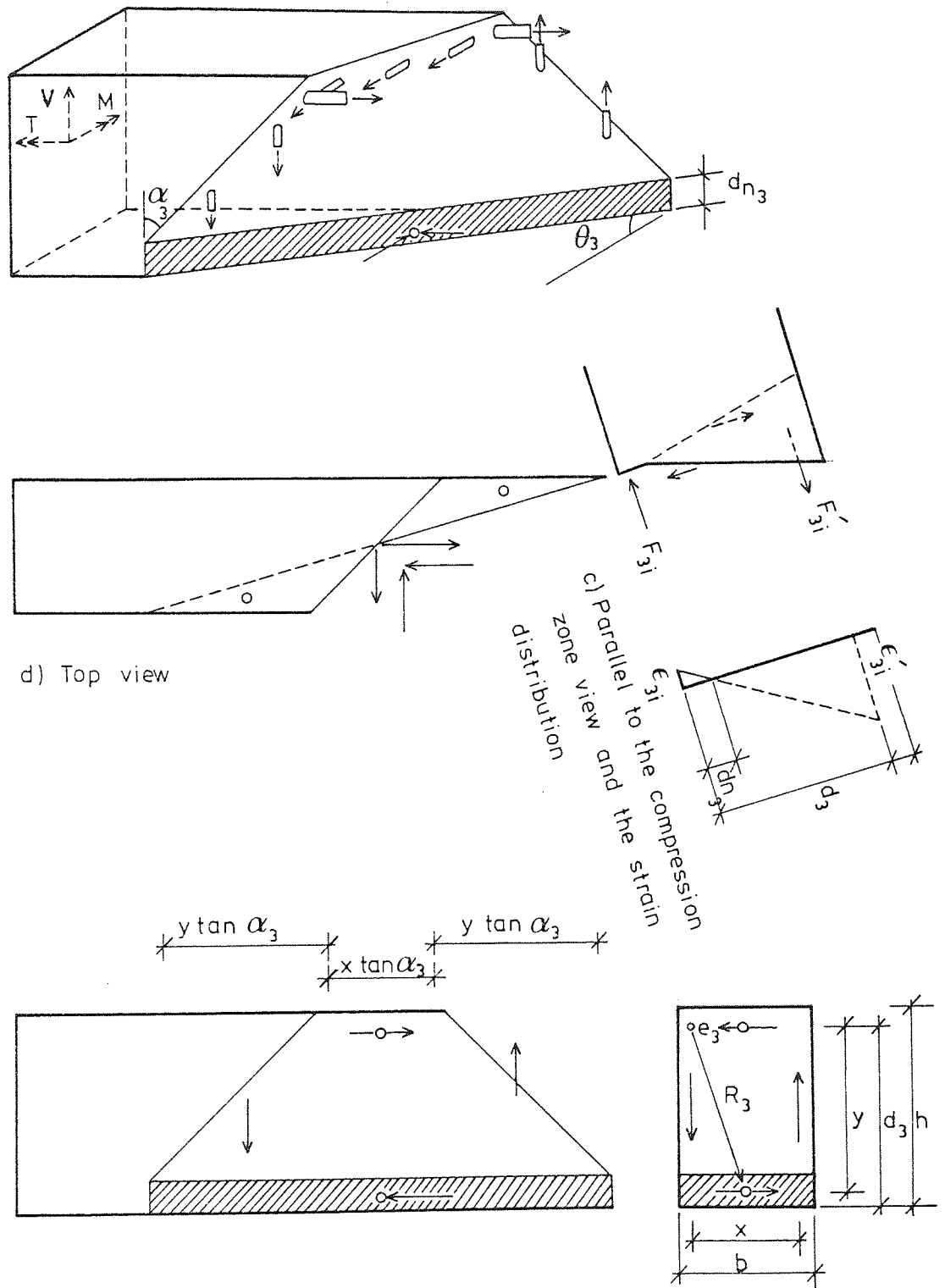
b) North and parallel to the longitudinal axis views

FIGURE 4.8 : Mode 3 failure mechanism for reinforced concrete beams under combined loads (non-yielding)

147

to the previous two modes of this type of failure.

An expression to determine a value for dn_{3w} can be produced using the same approach as for the other modes, and can be written with respect to the mode 3 effective depth, d_3 as follows:

$$\frac{dn_{3w}}{d_3} = \sqrt{(\frac{1}{2}.\frac{\rho_3.m}{Km_i}.C_{3w})^2 + 2.\frac{\rho_3.m}{Km_i}.C_{3w}} - \frac{1}{2}.\frac{\rho_3.m}{Km_i}.C_{3w} \qquad (4.32)$$

where

$$C_{3w} = \frac{(1 + r_{3w}.\tan\alpha_{3w}.\tan\theta_{3w})}{(1 + \tan\alpha_{3w}.\tan\theta_{3w})^2}$$

and

$$\tan\theta_{3w} = \tan\alpha_{3w}/[1 + Kd.(h/b)]$$

$$r_{3w} = \frac{A_w.f_{wy}.x}{2.A_t.f_t.s}$$

$$f_t = f_{wy}/\tan^2\alpha_{3w}$$

The lever arm to the resultant shear in the compression concrete R_{3w} can be determined from the geometry of figure 4.8(b), on the same principals as for the previous modes of this type.

$$R_{3w} = \sqrt{(d_3 - Ks.dn_{3w})^2 + (x/2)^2}$$

4.4 TYPE III FAILURE-YIELDING ON THE LONGITUDINAL STEEL ONLY

Failure of this type occurs in beams with a relatively large amount of stirrup steel, which at failure remains elastic while the longitudinal steel yields. As in the previous type of failure, because one category of the reinforcement does not reach its yield strength, the concrete in the compression zone crushes at ultimate load. The concrete in this zone is subjected to direct stress due to the bending moment and shear stresses due to both the torsional

moment and shear force. These stresses are combined, using Cowan's failure criterion for concrete, in the same way as in type II failure.

Depending on the ratio of bending moment to torsional moment ψ, and the distribution of the main bars, any one of the three principal modes of failure - i.e. 1ℓ, 2ℓ and 3ℓ - is possible at ultimate load.

The inclination of the tensile cracks of the failure section on the three faces are assumed to be constant and approximately equal to 1, in this type of failure.

4.4.1 Mode 1ℓ Failure

This mode is critical in beams symmetrically reinforced, and tested under a large bending moment. At failure, due to a high bending stress the longitudinal bars yield near the bottom, and the compression concrete crushes near the top face, while the stirrups are still behaving elastically. The appearance of the general view of the failure surface can be seen in figure 4.6(a).

The equation to calculate torsional capacity of a member failing in mode 1ℓ, can be obtained by equating the external moments to the moments of the internal forces about a longitudinal axis through e_1 - see figure 4.6(b),

$$T_{1\ell} + V \cdot \frac{x}{2} = Kv \cdot b \cdot dn_{1\ell} \cdot fv_{1\ell} \cdot R_{1\ell} + A_w \cdot f_w \cdot \frac{(d_1 - dn_{1\ell})}{s} \cdot x \cdot \tan\alpha_{1\ell}$$

The first term of the right hand side in the above equation, is the contribution of the concrete in the shear-compression zone - which is near the top, while the second term is the contribution of the non-yielded stirrups in one of the vertical sides.

Rearranging;

$$T_{1\ell} = \frac{Kv \cdot b \cdot dn_{1\ell} \cdot fv_{1\ell} \cdot R_{1\ell} + A_w \cdot f_w \cdot [(d_1 - dn_{1\ell})/s] \cdot x \cdot \tan\alpha_{1\ell}}{1 + (\delta \cdot x)/2} \qquad (4.33)$$

In equation 4.33, besides $dn_{1\ell}$, $fv_{1\ell}$, $R_{1\ell}$ and $\tan\alpha_{1\ell}$, the stresses in the non-yielded stirrup legs, f_w, must be known in order to obtain the solution.

Taking moments about a transverse axis, through the centroid of the compression zone (figure 4.6(b), the following equation can be obtained,

$$M_{1\ell} = 2 \cdot A_b \cdot f_{by} \cdot (d_1 - Ks \cdot dn_{1\ell}) - A_w \cdot f_w \cdot \frac{(d_1 - dn_{1\ell})}{s} \cdot x \cdot [1 + (d_1 - dn_{1\ell})/x]$$

$$\cdot \tan^2\alpha_{1\ell} \qquad (4.34)$$

Substituting equation 4.34 in equation 4.33 to eliminate f_w, and rearranging gives,

$$T_{1\ell} = \frac{Kv \cdot b \cdot dn_{1\ell} \cdot fv_{1\ell} \cdot R_{1\ell} + 2 \cdot A_b \cdot f_{by} \cdot (d_1 - Ks \cdot dn_{1\ell})/[\{1 + (d_1 - dn_{1\ell})/x\} \cdot \tan\alpha_{1\ell}]}{1 + (\delta \cdot x)/2 + \psi/[\{1 + (d_1 - dn_{1\ell})/x\} \cdot \tan\alpha_{1\ell}]}$$

$$(4.35)$$

The shear stress of the concrete in the compression zone, $fv_{1\ell}$, can be obtained using the simplified linear relation with f'_c, presented in equation 4.23.

The elastic strain distribution for cracked section can be used to derive an expression for the depth of compression zone, $dn_{1\ell}$. This is similar to type II failure, and involves the equilibrium of forces perpendicular to the θ-plane and the strain compatibility across the depth of the skew failure section

Equating the compressive force of the concrete in the compression zone, to the tensile force in the reinforcement near the bottom, in a direction perpendicular to the skew-failure section - figure 4.6(c), gives;

$$Km_i \cdot b \cdot dn_{1\ell} \cdot fm_{1i\ell}/\cos\theta_{1\ell} = 2 \cdot A_b \cdot f_{by} \cdot \cos\theta_{1\ell} + A_w \cdot f_w \cdot \frac{x}{s} \cdot \tan\alpha_{1\ell} \cdot \sin\theta_{1\ell} \qquad (4.36)$$

Considering the strain compatibility across the cracked section in the same direction - figure 4.6(c);

$$\frac{\varepsilon_{1i\ell}}{dn_{1\ell}} = \frac{\varepsilon'_{1i\ell}}{d_1 - dn_{1\ell}} \qquad (4.37)$$

Following the same approach as in type II failure, combining equation 4.36 and 4.37 to eliminate the skew-compressive stress for concrete, $fm_{1i\ell}$, and rearranging, the following expression for the depth of compression zone $dn_{1\ell}$ in respect of the effective depth d_1, will result,

$$\frac{dn_{1\ell}}{d_1} = \sqrt{\left(\frac{1}{2} \cdot \frac{\rho_1 \cdot m}{Km_i} \cdot C_{1\ell}\right)^2 + 2 \cdot \frac{\rho_1 \cdot m}{Km_i} \cdot C_{1\ell}} \; - \; \frac{1}{2} \cdot \frac{\rho_1 \cdot m}{K_{mi}} \cdot C_{1\ell} \qquad (4.38)$$

where

$$C_1 = \frac{(1 + r_{1\ell} \cdot \tan\alpha_{1\ell} \cdot \tan\theta_{1\ell})}{(1 + \tan\alpha_{1\ell} \cdot \tan\theta_{1\ell})^2}$$

and

$$\tan\theta_{1\ell} = \tan\alpha_{1\ell}/[1 + Kd \cdot (h/b)]$$

$$r_{1\ell} = \frac{A_w \cdot f_w \cdot x}{2 \cdot A_b \cdot f_{by} \cdot s}$$

$$f_w = f_{by} \cdot \tan^2\alpha_{1\ell}$$

From figure 4.6(b), the torsional lever arm $R_{1\ell}$, for this mode can, as previously, be expressed by,

$$R_{1\ell} = \sqrt{(d_1 - Ks \cdot dn_{1\ell})^2 + (x/2)^2}$$

The torsional capacity of a reinforced concrete member under the combined action of torsion, bending and shear, failing in mode 1ℓ by crushing of the concrete and yielding the longitudinal tension

bars can be calculated from equation 4.35, using the values obtained from the expressions for $dn_{1\ell}$, $fv_{1\ell}$ and $R_{1\ell}$.

4.4.2 Mode 2ℓ Failure

A symmetrically reinforced beam when subjected to a moderate or low ratio of bending moment to torsional moment, ψ, with or without shear, fails in mode 2ℓ by crushing of the concrete in one of the vertical sides and yielding of the longitudinal bars in the opposite side - as shown in figure 4.7(a). The steel yields due to the longitudinal component of the addative stresses from torsion and shear in this side. Since in this category beams are reinforced relatively heavier in transverse steel, it is considered that failure occurs before they reach their yield strength.

Taking moment of forces about an axis parallel to the longitudinal axis of the beam through point e_2 - figure 4.7(b);

$$T_{2\ell} - V \cdot \frac{x}{2} = Kv \cdot d \cdot dn_{2\ell} \cdot fv_{2\ell} \cdot R_{2\ell} + A_w \cdot f_w \cdot \frac{(d_2 - dn_{2\ell})}{s} \cdot y \cdot \tan\alpha_{2\ell} \qquad (4.39)$$

Taking moments about a transverse axis through the centroid of the compression zone - figure 4.7(d),

$$2 \cdot A_s \cdot f_{sy} \cdot (d_2 - Ks \cdot dn_{2\ell}) = A_w \cdot f_w \cdot \frac{(d_2 - dn_{2\ell})}{s} \cdot y \cdot [1 + (d_2 - dn_{2\ell})/y] \cdot \tan^2\alpha_{2\ell}$$

$$(4.40)$$

Substituting equation 4.40 into equation 4.39 to eliminate the actual stresses in the stirrups, f_w, and rearranging, the following equation is produced for determining the torsional capacity of a beam failing in this mode;

$$T_{2\ell} = \frac{Kv \cdot d \cdot dn_{2\ell} \cdot fv_{2\ell} \cdot R_{2\ell} + 2 \cdot A_s \cdot f_{sy} \cdot (d_2 - K_s \cdot dn_{2\ell}) / [\{1 + (d_2 - dn_{2\ell})/y\} \cdot \tan\alpha_{2\ell}]}{1 - (\delta \cdot x)/2}$$

$$(4.41)$$

A value can be obtained for the average shear stress of concrete $fv_{2\ell}$, using equation 4.23.

From figure 4.7(c), using the same analytical procedure as in mode 1ℓ, an expression can be formed to determine the depth of compression zone, $dn_{2\ell}$, which can be expressed in terms of effective depth d_2, as follows:

$$\frac{dn_{2\ell}}{d_2} = \sqrt{(\frac{1}{2} \cdot \frac{\rho_2 \cdot m}{Km_i} \cdot C_{2\ell})^2 + 2 \cdot \frac{\rho_2 \cdot m}{Km_i} \cdot C_{2\ell}} - \frac{1}{2} \cdot \frac{\rho_2 \cdot m}{Km_i} \cdot C_{2\ell} \qquad (4.42)$$

where

$$C_2 = \frac{(1 + r_{2\ell} \cdot \tan\alpha_{2\ell} \cdot \tan\theta_{2\ell})}{(1 + \tan\alpha_{2\ell} \cdot \tan\theta_{2\ell})^2}$$

and

$$\tan\theta_{2\ell} = \tan\alpha_{2\ell}/[1 + Kd \cdot (b/h)]$$

$$r_{2\ell} = \frac{A_w \cdot f_w \cdot y}{2 \cdot A_s \cdot f_{sy} \cdot s}$$

$$f_w = f_{sy} \cdot \tan^2\alpha_{2\ell}$$

The lever arm to the shear force of the concrete in the shear-compression zone, $R_{2\ell}$, for this mode can be obtained using the following expression - see figure 4.7(d).

$$R_{2\ell} = \sqrt{(d_2 - Ks \cdot dn_{2\ell})^2 + (y/4)^2}$$

4.4.3 Mode 3ℓ Failure

This mode is critical in beams with low percentage of top steel, and subject to a small ratio of bending moment to torsional

moment, ψ. At failure the weaker steel at the top yields and the concrete near the bottom face crushes, while the stirrups are in their elastic state. The surface of the failure mechanism for this mode is shown in figure 4.8(a).

Equating the external moment to the moment of the internal forces about a longitudinal axis through point e_3 - see figure 4.8(b);

$$T_{3\ell} -V.\frac{x}{2} = Kv.b.dn_{3\ell}.fv_{3\ell}.R_{3\ell} + A_w.f_w.\frac{(d_3-dn_{3\ell})}{s} .x.\tan\alpha_{3\ell} \qquad (4.43)$$

Equating the external moment to the moment of internal forces along a transverse axis through the centroid of the compression zone (figure 4.8(b),

$$M_{3\ell}=-2.A_t.f_{ty}.(d_3-Ks.dn_{3\ell})+A_w.f_w.\frac{(d_3-dn_{3\ell})}{s}.x.[1+(d_3-dn_{3\ell})/x]\tan^2\alpha_{3\ell}$$

$$(4.44)$$

Combining equation 4.43 and equation 4.44 to eliminate the actual stress in the stirrups, f_w, and rearranging

$$T_{3\ell}=\frac{Kv.b.dn_{3\ell}.fv_{3\ell}.R_{3\ell}+2.A_t.f_{ty}.(d_3-Ks.dn_{3\ell})/[\{1+(d_3-dn_{3\ell})/x\}.\tan\alpha_{3\ell}]}{1 - (\delta.x)/2 -\psi/[\{1+(d_3-dn_{3\ell})/x\}.\tan\alpha_{3\ell}]}$$

$$(4.45)$$

The shear stresses of the concrete $fv_{3\ell}$ can be calculated using equation 4.23.

Using the same approach as for the other modes of failure in this type, an expression to determine the depth of compression zone $dn_{3\ell}$ can be derived, and written in terms of the effective depth d_3, as follows:

$$\frac{dn_{3\ell}}{d_3} = \sqrt{(\frac{1}{2}\cdot\frac{\rho_3\cdot m}{Km_i}\cdot C_{3\ell})^2 + 2\cdot\frac{\rho_3\cdot m}{Km_i}\cdot C_{3\ell}} - \frac{1}{2}\cdot\frac{\rho_3\cdot m}{Km_i}\cdot C_{3\ell} \qquad (4.46)$$

where

$$C_3 = \frac{(1 + r_{3\ell}\cdot\tan\alpha_{3\ell}\cdot\tan\theta_{3\ell})}{(1 + \tan\alpha_{3\ell}\cdot\tan\theta_{3\ell})^2}$$

and

$$\tan\theta_{3\ell} = \tan\alpha_{3\ell}/[1 + Kd\cdot(h/b)]$$

$$r_{3\ell} = \frac{A_w\cdot f_w\cdot x}{2\cdot A_t\cdot f_{ty}\cdot s}$$

$$f_w = f_{ty}\cdot\tan^2\alpha_{3\ell}$$

The lever arm to the shear force in the compression concrete, $R_{3\ell}$, for this mode can be obtained from the geometry of figure 4.8(b),

$$R_{3\ell} = \sqrt{(d_3 - Ks\cdot dn_{3\ell})^2 + (x/2)^2}$$

4.5 TYPE IV FAILURE-CRUSHING OF THE CONCRETE

Failure of this type occurs in beams over-reinforced with both categories of reinforcement. Upon failure the ultimate compressive strain of the concrete in the compression zone will be reached, while the strain in the tension reinforcement is below the yield point. The compression concrete, therefore, is the critical zone and subjected to direct stress due to bending, and shear stresses due to both torsional moment and shear force. Cowan's failure criterion for concrete is again used to combine these stresses - as explained in section 4.3.

Three principal modes of failure, namely modes 1c, 2c and 3c are possible, depending on the distribution of the main bars and

155

the ratio of bending moment to torsional moment, ψ.

The angle of inclination of the tensile crack defining the failure surface is again assumed to be 45° with the transverse on all the three faces, in this failure type.

4.5.1 Mode 1c Failure

This mode is critical in beams subject to a high value of bending moment to torsional moment. Failure occurs by crushing of the concrete near the top of the section due to the bending moment, while the main bars and web steel are still behaving elastically at failure. The appearance of the failure surface can be seen from figure 4.6(a).

An equation for ultimate torque can be obtained by equating the external moment to the moment of the internal forces about an axis parallel to the longitudinal axis through e_1 - see figure 4.6(b).

$$T_{1c} + V.\frac{x}{2} = Kv.b.dn_{1c}.fv_{1c}.R_{1c} + A_w.f_w.\frac{(d_1-dn_{1c})}{s}.x.\tan\alpha_{1c} \qquad (4.47)$$

The first term of the equation above is the contribution of the concrete in the shear-compression zone to the ultimate torsional capacity, while the second term is the contribution of the non-yielded stirrups in one side of the section.

Equating the forces in the compression zone to the forces in the bottom leg of the stirrups crossing failure section, in a direction perpendicular to the longitudinal axis of the beam (figure 4.6(b)), the following approximate equation can be obtained,

$$Kv.b.dn_{1c}.fv_{1c} = A_w.f_w.\frac{x}{s}.\tan\alpha_{1c} \qquad (4.48)$$

Combining equation 4.47 with equation 4.48 to eliminate f_w,

and rearranging, an equation for ultimate torque in mode 1c can be formed,

$$T_{1c} = \frac{Kv.b.dn_{1c}.fv_{1c}.R_{1c} + Kv.b.dn_{1c}.fv_{1c}.(d_1-dn_{1c})}{1 + (\delta.x)/2}$$

If (d_1-dn_{1c}) can be approximated to the lever arm of the shear compression force of the concrete, R_{1c}, then

$$T_{1c} = \frac{2.Kv.b.dn_{1c}.fv_{1c}.R_{1c}}{1 + (\delta.x)/2} \qquad (4.49)$$

In the above equation the average shear stresses in the concrete, fv_{1c}, due to torsion and shear can be calculated from equation 4.23.

An expression for the depth of compression zone dn_{1c} can be deduced - using the same approach as in section 4.3, from the equilibrium of forces on a skew failure plane, assuming the elastic stress/strain relationships for both concrete and steel. It can be written in terms of the effective depth d_1 for mode 1c as follows:

$$\frac{dn_{1c}}{d_1} = \sqrt{(\frac{1}{2}.\frac{\rho_1.m}{Km_i} . C_{1c})^2 + 2.\frac{\rho_1.m}{Km_i} . C_{1c}} - \frac{1}{2} .\frac{\rho_1.m}{Km_i} . C_{1c} \qquad (4.50)$$

where

$$C_{1c} = \frac{(1 + r_{1c}.tan\alpha_{1c}.tan\theta_{1c})}{(1 + tan\alpha_{1c}.tan\theta_{1c})^2}$$

and

$$tan\theta_{1c} = tan\alpha_{1c}/[1 + Kd.(h/b)]$$

$$r_{1c} = \frac{A_w.f_w.x}{2.A_b.f_b.s}$$

$$f_w = f_b.tan^2\alpha_{1c}$$

Since dn_{1c} can now be calculated from equation 4.50, the lever arm for the shear force in the concrete R_{1c} may be calculated from the following expression - see figure 4.6(b);

$$R_{1c} = \sqrt{(d_1 - Ks.dn_{1c})^2 + (x/2)^2}$$

Substituting the values for fv_{1c}, dn_{1c} and R_{1c} from the expressions above, the ultimate torsional capacity T_{1c} resisted by an over-reinforced member under combined loadings failing in mode 1c, can be determined from equation 4.49.

4.5.2 Mode 2c Failure

An alternative failure mode for symmetrically over-reinforced beams is possible, when subject to moderate or low ratio of ψ. Due to the longitudinal component of the addative stresses from torsion and shear on one of the sides, the longitudinal bars experience a higher strain in this side, and forms a compression zone in the opposite side. Since the beam is over-reinforced, the concrete in this zone reaches its ultimate compressive strain before yielding any of the reinforcement at failure. The failure surface associated with this mode can be seen in figure 4.7(a).

Considering the equilibrium of external moments and internal moments about a longitudinal axis through point e_2 (see figure 4.7(b)) results;

$$T_{2c} - V.\frac{x}{2} = Kv.d.dn_{2c}.fv_{2c}.R_{2c} + A_w.f_w.\frac{(d_2 - dn_{2c})}{s}.y.\tan\alpha_{2c} \qquad 4.51)$$

Equating the forces in the compression zone to the forces in the stirrup legs of the tension side, crossing the failure section, in a direction perpendicular to the longitudinal axis of the beam;

$$Kv.d.dn_{2c}.fv_{2c} = A_w.f_w.\frac{y}{s}.\tan\alpha_{2c} \tag{4.52}$$

Combining equation 4.51 with 4.52 to eliminate the stress in the stirrup leg, f_w, and rearranging, an equation for the failure torque in mode 2c can be deduced, assuming that $(d_2 - dn_{2c})$ is approximately equal to R_{2c}.

$$T_{2c} = \frac{2.Kv.d.dn_{2c}.fv_{2c}.R_{2c}}{1 - (\delta.x)/2} \tag{4.53}$$

A value for fv_{2c} can be obtained from equation 4.23.

An expression can be derived for the depth of compression zone, dn_{2c}, from the equilibrium of forces perpendicular to the skew plane-figure 4.7(c), using the same approach as in mode 1c. It is a quadratic in dn_{2c}/d_2, and expressed as;

$$\frac{dn_{2c}}{d_2} = \sqrt{(\frac{1}{2}.\frac{\rho_2.m}{Km_i}.C_{2c})^2 + 2.\frac{\rho_2.m}{Km_i}.C_{2c}} - \frac{1}{2}.\frac{\rho_2.m}{Km_i}.C_{2c} \tag{4.54}$$

where

$$C_{2c} = \frac{(1 + r_{2c}.\tan\alpha_{2c}.\tan\theta_{2c})}{(1 + \tan\alpha_{2c}.\tan\theta_{2c})^2}$$

and

$$\tan\theta_{2c} = \tan\alpha_{2c}/[1 + Kd.(b/h)]$$

$$r_{2c} = \frac{A_w.f_w.y}{2.A_s.f_s.s}$$

$$f_w = f_s . \tan^2\alpha_{2c}$$

The lever arm to the shear force in the compression zone, R_{2c}, can be obtained from the following expression - see figure 4.7(b),

$$R_{2c} = \sqrt{(d_2 - Ks.dn_{2c})^2 + (y/4)^2}$$

4.5.3 Mode 3c Failure

Another mode of failure occurs when an over-reinforced member is subjected to a very small ratio of ψ. It gives a lower theoretical torque capacity where there is less top steel than in the bottom. At failure the concrete crushes near the bottom of the section before yielding of any of the reinforcement. The failure section resulting from this mode can be seen in figure 4.8(a).

Taking moment of forces about an axis perpendicular to the longitudinal axis of the beam through point e_3 (see figure 4.8(b)),

$$T_{3c} - V \cdot \frac{x}{2} = Kv \cdot b \cdot dn_{3c} \cdot fv_{3c} \cdot R_{3c} + A_w \cdot f_w \cdot \frac{(d_3 - dn_{3c})}{s} \cdot x \cdot \tan\alpha_{3c} \qquad (4.55)$$

Equating the shear force of the concrete in compression zone to the tensile forces in the top stirrup legs crossing the failure section, in a direction perpendicular to the longitudinal axis of the beam, the following equation can be obtained

$$Kv \cdot b \cdot dn_{3c} \cdot fv_{3c} = A_w \cdot f_w \cdot \frac{x}{s} \cdot \tan\alpha_{3c} \qquad (4.56)$$

Combining equation 4.55 with equation 4.56 to eliminate the tensile stress in the stirrup legs, f_w, and rearranging, an equation to calculate the ultimate torsional capacity in mode 3c can be obtained after approximating $(d_3 - dn_{3c})$ to R_{3c}

$$T_{3c} = \frac{2 \cdot Kv \cdot d \cdot dn_{3c} \cdot fv_{3c} \cdot R_{3c}}{1 - (\delta \cdot x)/2} \qquad (4.57)$$

Equation 4.23 can be used to obtain a value for the average shear stresses, fv_{3c}, in the concrete.

From the equilibrium of forces on the skew failure plane (see figure 4.8(c)), an expression for the depth of compression zone dn_{3c} can be derived using the same approach as for the previous

160

modes of this type. It can be expressed in terms of the effective depth, d_3, by,

$$\frac{dn_{3c}}{d_3} = \sqrt{(\frac{1}{2} \cdot \frac{\rho_3 \cdot m}{Km_i} \cdot C_{3c})^2 + 2 \cdot \frac{\rho_3 \cdot m}{Km_i} \cdot C_{3c}} - \frac{1}{2} \cdot \frac{\rho_3 \cdot m}{Km_i} \cdot C_{3c} \qquad (4.58)$$

where

$$C_3 = \frac{(1 + r_{3c} \cdot \tan\alpha_{3c} \cdot \tan\theta_{3c})}{(1 + \tan\alpha_{3c} \cdot \tan\theta_{3c})^2}$$

and

$$\tan\theta_{3c} = \tan\alpha_{3c} / [1 + kd \cdot (h/b)]$$

$$r_{3c} = \frac{A_w \cdot f_w \cdot x}{2 \cdot A_t \cdot f_t \cdot s}$$

$$f_w = f_t \cdot \tan^2\alpha_{3c}$$

From figure 4.8(b), the lever arm to the shear force in the compression zone, R_{3c}, can be expressed as,

$$R_{3c} = \sqrt{(d_3 - Ks \cdot dn_{3c})^2 + (x/2)^2}$$

CHAPTER FIVE

ANALYSIS OF THE TEST RESULTS AND COMPARISON

5.1 INTRODUCTION

The test results outlined in Chapter three are analysed first in
accordance with the theoretical solution proposed in the preceding
chapter. The analysis is followed by a discussion on the behaviour
and ultimate strength predicted by the theory. The proposed approach
will then be verified, and the accuracy of the theory will be checked
by direct comparison with the test results.

Using only one set of results for assessing a theory may be
criticised,because the variation in material properties is small.
The theory,therefore, is also compared with over 470 results of 20
different sets reported by other investigators in various countries.
This includes the experimental results by; Ernst [20], Hsu [10],
Swann [54], Evans and Sarkar [41], Gesund et al [40], Goode and Helmy
[11], Iyengar and Rangan [15], Jackson and Estanero [46], Kemp [66],
Pandit and Warwaruk [37], Collins [45], Elfgren [69], Laylin [9],
Lessig [35], McMullen and Warwaruk [52], Osburn [50], Staley [59],
Yudin [48].

The collected results are from tests of solid and hollow rect-
angular concrete members reinforced longitudinally and transversely
in the form of closed stirrups or open links - as in Lessig's -
and subjected to pure torsion or torsion in combination with bending
and shear. No limitations have been imposed on the applicability of
the theory and therefore all the results of the investigators above
have been considered, unless there are difficulties in obtaining
accurate data.

The theoretical analysis of the author's results and the comparison
were carried out using the computer. Programs were written in FORTRAN
and run on ICL 1904S main frame of the University of Aston's computer
centre. ICL Statistical Package (UASTATSXDS3) was used to determine
the coefficient of variation. Lists of the program used are given
in Appendix F.

5.2 ANALYSIS OF THE RESULTS

The solution of the ultimate torsional equations derived in the
preceding chapter for types of failure other than the yielding
requires a stress-strain relationship for the concrete to determine
Young's modulus of elasticity, E_c. Since it was not possible to
obtain an experimental value for all the test beams, a relationship
has to be adopted.

Considerable work has been carried out in investigating the
stress-strain relationship for concrete, but no general accurate
solution, applicable to all types of concrete, is yet available. The
nature of this relation is dependent upon many factors; the most
important is the compressive strength of the concrete.

The author's concrete varied from very low to very high compres-
sive strength (table 3.1), therefore, two relatively simple and
reasonable accurate empirical formulae for determining E_c have been
adopted from [70] and [71] respectively;

$$E_c = 1000 . f'_c \qquad \text{for } f'_c < 27.5 \text{ N/mm}^2$$

and

$$E_c = 6149.2 . \sqrt{f'_c} \qquad \text{for } f'_c \geq 27.5 \text{ N/mm}^2$$

The distribution of the shear stress in the compression zone is
parabolic, but the 'average stress' coefficient is assumed to be

1.0 (i.e. $K_V = 1.0$), and hence the 'depth to the resultant force' coefficient is equal to 0.5 (i.e. $K_s = 0.5$). Since a linear elastic stress distribution was assumed in the analysis for dn, the 'bending stress' coefficient for the concrete in the compression zone normal to θ-plane is equal to 0.5 (i.e. $K_{m_i} = 0.5$). The coefficient Kd is associated with the cracking of the failure section, and its magnitude is mainly a function of the depth of compression zone and possibly varies between 1 and 2 (i.e. $1.0 \leq Kd < 2.0$). In the present analysis the lower bound (i.e. $Kd = 1.0$) has been adopted because it agrees better with the test results. The standard value of 206.9 kN/mm^2 (i.e. 30,00,000 lb/in^2) for the modulus of elasticity of the steel has been used throughout.

In the analysis the torsional moment for each beam has been assumed as unknown, while the ratio of bending moment to torsional moment, ψ, and the ratio of shear force to torsional moments, δ, have been taken as their test values. The torque has been calculated theoretically using the equations for each principal mode (i.e. 1, 2 and 3) of each individual type of failure.

For mode 1 failure mechanism the theoretical torque has been determined from equations 4.1, 4.24, 4.35 and 4.49 and presented in table 5.1. Table 5.2 shows the theoretical torsional moment which has been computed from equations 4.11, 4.29, 4.41 and 4.53. The theoretical torque for mode 3 has been calculated using equations 4.18, 4.31, 4.45 and 4.57 and given in table 5.3.

In each of the preceding tables the lowest torsional moment has been recognised as a critical type of failure and stated in column 6. Table 5.4 consists of the values of column 6 from tables 5.1, 5.2 and 5.3. In this table also, the lowest torsional moment of the three

Beam	Theoretical torsional moments kN.m				Critical torque* kN.m
	Eq.(4.1)	Eq.(4.24)	Eq.(4.35)	Eq.(4.49)	
A1	1.624	1.433	1.683	1.691	1.433 (II)
A2	1.592	1.716	1.789	2.206	1.592 (I)
A3	1.602	1.839	1.865	2.437	1.602 (I)
A4	1.577	2.013	1.925	2.772	1.577 (I)
A5	1.694	2.031	2.087	2.782	1.694 (I)
A6	1.368	2.107	1.719	2.963	1.368 (I)
A7	1.647	2.210	2.119	3.133	1.647 (I)
A8	1.599	2.409	2.159	3.531	1.599 (I)
A9	1.630	2.624	2.318	3.955	1.630 (I)
AR4	3.648	2.708	3.982	2.896	2.708 (II)
AR5	3.649	2.769	4.038	3.007	2.769 (II)
AR9	3.655	3.871	5.079	5.115	3.655 (I)
B1	3.153	4.947	2.371	2.714	2.371 (III)
B2	2.489	3.733	2.186	2.813	2.186 (III)
B3	2.409	3.035	2.306	2.879	2.306 (III)
B4	2.104	2.574	2.149	2.748	2.104 (I)
B5	1.947	2.144	2.007	2.396	1.947 (I)
B6	2.149	2.185	2.471	2.765	2.149 (I)
B7	1.922	1.720	2.637	2.484	1.720 (II)
BR2	5.155	4.049	4.144	3.171	3.171 (IV)
BR4	3.327	2.512	3.346	2.641	2.512 (II)
BR7	2.185	1.849	3.394	2.711	1.849 (II)
C1	0.857	2.313	1.044	2.141	0.857 (I)
C2	1.260	2.568	1.462	2.631	1.260 (I)
C3	3.355	2.557	3.417	2.715	2.557 (II)
C4	4.187	2.803	4.821	3.231	2.803 (II)
C5	5.599	3.131	7.698	4.003	3.131 (II)
CR1	2.227	2.518	2.142	2.368	2.142 (III)
CR3	3.648	2.708	3.982	2.896	2.708 (II)
CR5	5.699	3.250	8.216	4.107	3.250 (II)
D1	1.317	1.153	1.432	1.381	1.153 (II)
D2	1.739	1.743	1.876	2.061	1.739 (I)
D3	2.111	2.236	2.236	2.616	2.111 (I)
D4	2.558	2.697	2.660	3.081	2.558 (I)
D5	2.447	3.156	2.566	3.598	2.447 (I)
DR1	1.805	1.264	2.355	1.558	1.264 (II)
DR3	3.278	2.433	4.021	2.894	2.433 (II)
DR5	4.313	3.658	5.090	4.329	3.658 (II)

* Inside the brackets identify the critical failure type

TABLE 5.1 Mode 1 failure analysis for the test beams

Beam	Theoretical torsional moment kN.m				Critical torque* kN.m
	Eq.(4.11)	Eq.(4.29)	Eq.(4.41)	Eq.(4.53)	
A1	1.886	1.313	2.181	1.386	1.313 (II)
A2	2.541	1.572	3.632	1.827	1.572 (II)
A3	2.539	1.689	3.737	2.033	1.689 (II)
A4	2.531	1.868	3.919	2.350	1.868 (II)
A5	2.538	1.884	3.917	2.353	1.884 (II)
A6	2.495	2.062	4.158	2.657	2.062 (II)
A7	2.539	2.037	4.066	2.650	2.037 (II)
A8	2.533	2.227	4.263	3.016	2.227 (II)
A9	2.535	2.411	4.443	3.377	2.411 (II)
AR4	3.089	2.223	2.819	1.952	1.952 (IV)
AR5	3.090	2.268	2.858	2.028	2.028 (IV)
AR9	3.094	3.046	3.585	3.465	3.046 (II)
B1	6.419	4.601	3.707	2.131	2.131 (IV)
B2	5.035	3.569	3.852	2.294	2.294 (IV)
B3	4.118	2.853	3.887	2.347	2.347 (IV)
B4	3.556	2.410	3.860	2.259	2.259 (IV)
B5	3.169	2.010	3.736	1.983	1.983 (IV)
B6	2.882	2.051	3.941	2.332	2.051 (II)
B7	2.224	1.591	3.851	2.113	1.591 (II)
BR2	4.370	3.491	2.931	2.199	2.199 (IV)
BR4	2.987	2.295	2.931	1.975	1.975 (IV)
BR7	1.904	1.496	2.888	1.915	1.496 (II)
C1	2.271	2.363	2.136	1.901	1.901 (IV)
C2	2.643	2.502	2.665	2.241	2.241 (IV)
C3	3.559	2.389	3.840	2.227	2.227 (IV)
C4	4.205	2.499	4.953	2.553	2.499 (II)
C5	5.553	2.663	7.802	3.068	2.663 (II)
CR1	2.376	2.233	2.016	1.828	1.828 (IV)
CR3	3.089	2.223	2.819	1.952	1.952 (IV)
CR5	4.364	2.397	4.790	2.445	2.397 (II)
D1	1.798	0.934	2.218	0.911	0.911 (IV)
D2	2.541	1.583	3.159	1.629	1.583 (II)
D3	3.212	2.182	3.970	2.332	2.182 (II)
D4	3.840	2.757	4.657	2.968	2.757 (II)
D5	4.368	3.520	5.519	3.868	3.520 (II)
DR1	1.554	0.920	1.647	0.861	0.861 (IV)
DR3	2.771	2.076	2.966	2.120	2.076 (II)
DR5	3.811	3.315	4.137	3.583	3.315 (II)

* Inside the brackets identify the critical failure type

TABLE 5.2: Mode 2 failure analysis for the test beams

Beam	Theoretical torsional moments kN.m				Critical torque* kN.m
	Eq.(4.18)	Eq.(4.31)	Eq.(4.45)	Eq.(4.57)	
A1	2.889	1.635	**	1.929	1.635 (II)
A2	4.352	1.948	**	2.505	1.948 (II)
A3	4.323	2.092	**	2.773	2.092 (II)
A4	4.383	2.314	**	3.185	2.314 (II)
A5	4.087	2.313	66.492	3.168	2.313 (II)
A6	5.002	2.542	**	3.574	2.542 (II)
A7	4.205	2.513	**	3.563	2.513 (II)
A8	4.325	2.762	**	4.048	2.762 (II)
A9	4.243	3.003	**	4.526	3.003 (II)
AR4	2.420	2.494	2.280	2.304	2.280 (III)
AR5	2.418	2.540	2.320	2.388	2.320 (III)
AR9	2.412	3.382	3.127	4.009	2.412 (I)
B1	13.738	5.385	14.313	2.954	2.954 (IV)
B2	10.843	4.166	34.925	3.139	3.139 (IV)
B3	7.476	3.368	19.841	3.195	3.195 (IV)
B4	6.410	2.883	37.659	3.078	2.883 (II)
B5	5.532	2.432	63.974	2.718	2.432 (II)
B6	4.168	2.507	11.777	3.173	2.507 (II)
B7	2.789	2.000	7.812	2.888	2.000 (II)
BR2	3.426	3.976	2.494	2.732	2.494 (III)
BR4	2.757	2.579	2.717	2.337	2.337 (IV)
BR7	1.652	1.635	2.556	2.125	1.635 (II)
C1	6.512	2.676	**	2.477	2.477 (IV)
C2	5.929	2.893	47.096	2.965	2.893 (II)
C3	4.021	2.858	4.967	3.035	2.858 (II)
C4	4.455	3.070	5.872	3.539	3.070 (II)
C5	5.821	3.442	9.263	4.401	3.442 (II)
CR1	2.541	2.529	2.418	2.379	2.397 (IV)
CR3	2.420	2.494	2.280	2.304	2.280 (III)
CR5	2.405	2.580	2.329	2.433	2.329 (III)
D1	2.590	1.250	7.705	1.496	1.250 (II)
D2	3.918	1.910	13.976	2.259	1.910 (II)
D3	5.160	2.484	21.261	2.906	2.484 (II)
D4	6.055	2.989	18.097	3.414	2.989 (II)
D5	8.300	3.688	**	4.204	3.688 (II)
DR1	1.241	1.100	1.341	1.160	1.100 (II)
DR3	2.169	2.184	2.283	2.252	2.169 (I)
DR5	3.160	3.274	3.327	3.399	3.160 (I)

*   Inside the brackets identify the critical failure type
** Indicates values close to infinity
     TABLE 5.3: Mode 3 failure analysis for the test beams

167

Beam	Critical torsional moments kN.m			Ulti. torq. kN.m	Predicted mode
	Mode 1	Mode 2	Mode 3		
A1	1.433 (II)	1.313 (II)	1.635 (II)	1.313	2.II
A2	1.592 (I)	1.572 (II)	1.948 (II)	1.572	2.II
A3	1.602 (I)	1.689 (II)	2.092 (II)	1.602	1.I
A4	1.577 (I)	1.868 (II)	2.314 (II)	1.577	1.I
A5	1.694 (I)	1.884 (II)	2.313 (II)	1.694	1.I
A6	1.368 (I)	2.062 (II)	2.542 (II)	1.368	1.I
A7	1.647 (I)	2.037 (II)	2.513 (II)	1.647	1.I
A8	1.599 (I)	2.227 (II)	2.762 (II)	1.599	1.I
A9	1.630 (I)	2.411 (II)	3.003 (II)	1.630	1.I
AR4	2.708 (II)	1.952 (IV)	2.280 (III)	1.952	2.IV
AR5	2.769 (II)	2.028 (IV)	2.320 (III)	2.028	2.IV
AR9	3.655 (I)	3.046 (II)	2.412 (I)	2.412	3.I
B1	2.371 (III)	2.131 (IV)	2.954 (IV)	2.131	2.IV
B2	2.186 (III)	2.294 (IV)	3.139 (IV)	2.186	1.III
B3	2.306 (III)	2.347 (IV)	3.195 (IV)	2.306	1.III
B4	2.104 (I)	2.259 (IV)	2.883 (II)	2.104	1.I
B5	1.947 (I)	1.983 (IV)	2.432 (II)	1.947	1.I
B6	2.149 (I)	2.051 (II)	2.507 (II)	2.051	2.II
B7	1.720 (II)	1.591 (II)	2.000 (II)	1.591	2.II
BR2	3.171 (IV)	2.199 (IV)	2.494 (III)	2.199	2.IV
BR4	2.512 (II)	1.975 (IV)	2.337 (IV)	1.975	2.IV
BR7	1.849 (II)	1.496 (II)	1.635 (II)	1.496	2.II
C1	0.857 (I)	1.901 (IV)	2.477 (IV)	0.857	1.I
C2	1.260 (I)	2.241 (IV)	2.893 (II)	1.260	1.I
C3	2.557 (II)	2.227 (IV)	2.858 (II)	2.227	2.IV
C4	2.803 (II)	2.499 (II)	3.070 (II)	2.499	2.II
C5	3.131 (II)	2.663 (II)	3.442 (II)	2.663	2.II
CR1	2.142 (III)	1.828 (IV)	2.397 (IV)	1.828	2.IV
CR3	2.708 (II)	1.952 (IV)	2.280 (III)	1.952	2.IV
CR5	3.250 (II)	2.397 (II)	2.329 (III)	2.329	3.III
D1	1.153 (II)	0.911 (IV)	1.250 (II)	0.911	2.IV
D2	1.739 (I)	1.583 (II)	1.910 (II)	1.583	2.II
D3	2.111 (I)	2.182 (II)	2.484 (II)	2.111	1.I
D4	2.558 (I)	2.757 (II)	2.989 (II)	2.558	1.I
D5	2.447 (I)	3.520 (II)	3.688 (II)	2.447	1.I
DR1	1.264 (II)	0.861 (IV)	1.100 (II)	0.861	2.IV
DR3	2.433 (II)	2.076 (II)	2.169 (I)	2.076	2.II
DR5	3.658 (II)	3.315 (II)	3.160 (I)	3.160	3.I

TABLE 5.4: Ultimate theoretical torque and predicted mode of failure

Beam	Observed (Test)		Predicted (Theory)	
	T_{test} kN.m	mode	T_{theory} kN.m	mode
A1	1.382	1	1.313	2.II
A2	1.409	1	1.572	2.II
A3	1.657	1	1.602	1.I
A4	1.792	1	1.577	1.I
A5	2.207	1	1.694	1.I
A6	1.519	1	1.368	1.I
A7	2.207	1	1.647	1.I
A8	2.345	1	1.599	1.I
A9	2.620	1	1.630	1.I
AR4	2.345	3	1.952	2.IV
AR5	2.441	3	2.028	2.IV
AR9	3.514	3	2.412	3.I
B1	2.936	1	2.131	2.IV
B2	2.276	1	2.186	1.III
B3	2.413	1	2.306	1.III
B4	2.207	1	2.104	1.I
B5	2.001	1	1.947	1.I
B6	1.932	2	2.052	2.II
B7	1.588	2	1.591	2.II
BR2	2.661	3,2	2.199	2.IV
BR4	2.386	3,2	1.975	2.IV
BR7	1.519	2	1.496	2.II
C1	1.244	1	0.857	1.I
C2	1.519	1	1.260	1.I
C3	1.932	2	2.227	2.IV
C4	2.400	2	2.499	2.II
C5	2.345	-	2.663	2.II
CR1	2.001	2	1.828	2.IV
CR3	2.345	3	1.952	2.IV
CR5	2.592	3	2.329	3.III
D1	1.313	-	0.911	2.IV
D2	2.028	1	1.585	2.II
D3	2.372	1	2.111	1.I
D4	3.032	1	2.558	1.I
D5	2.413	1	2.447	1.I
DR1	1.244	3	0.861	2.IV
DR3	2.042	2	2.076	2.II
DR5	3.280	2	3.160	3.I

TABLE 5.5: Observed and predicted ultimate torque, and behaviour of the test beams

principal modes (i.e. 1, 2 and 3) has been recognised as the theoretical ultimate torque according to the proposed analysis, and outlined in the fifth column of the table adjacent to the predicted mode and type of failure.

5.3 DISCUSSION OF THE ANALYSIS

Both the observed and predicted ultimate torque and modes of failure are presented in table 5.5. This table shows that the theory is reasonably accurate in the prediction of the ultimate torsional moment and the behaviour of the test beams.

As explained in section 5.2, both ψ and δ were taken as the experimental values and the torsional moment was calculated theoretically, therefore some of the difference between the test and the theoretical values must be attributed to amplified errors associated with the torsional moment.

It can be seen from table 5.5 that generally the theoretical torsional moments for the test beams are low - i.e. conservative, and the observed modes and types of failure are predicted with a reasonable degree of accuracy by the theory.

5.3.1 Beams of Series A

Series A beams were manufactured to investigate the effect of varying the strength of concrete. The effect on the torsional strength for beams of group A is shown in figure 5.1, and beams of group AR in figure 5.2.

For beams of group A, the theory predicts mode 1.I (i.e. yielding), except beams A1 and A2, but for all beams of this group the observed failure mechanism indicates mode 1 (see table 5.5).

Observed behaviour for the rest of the beams in this group,

170
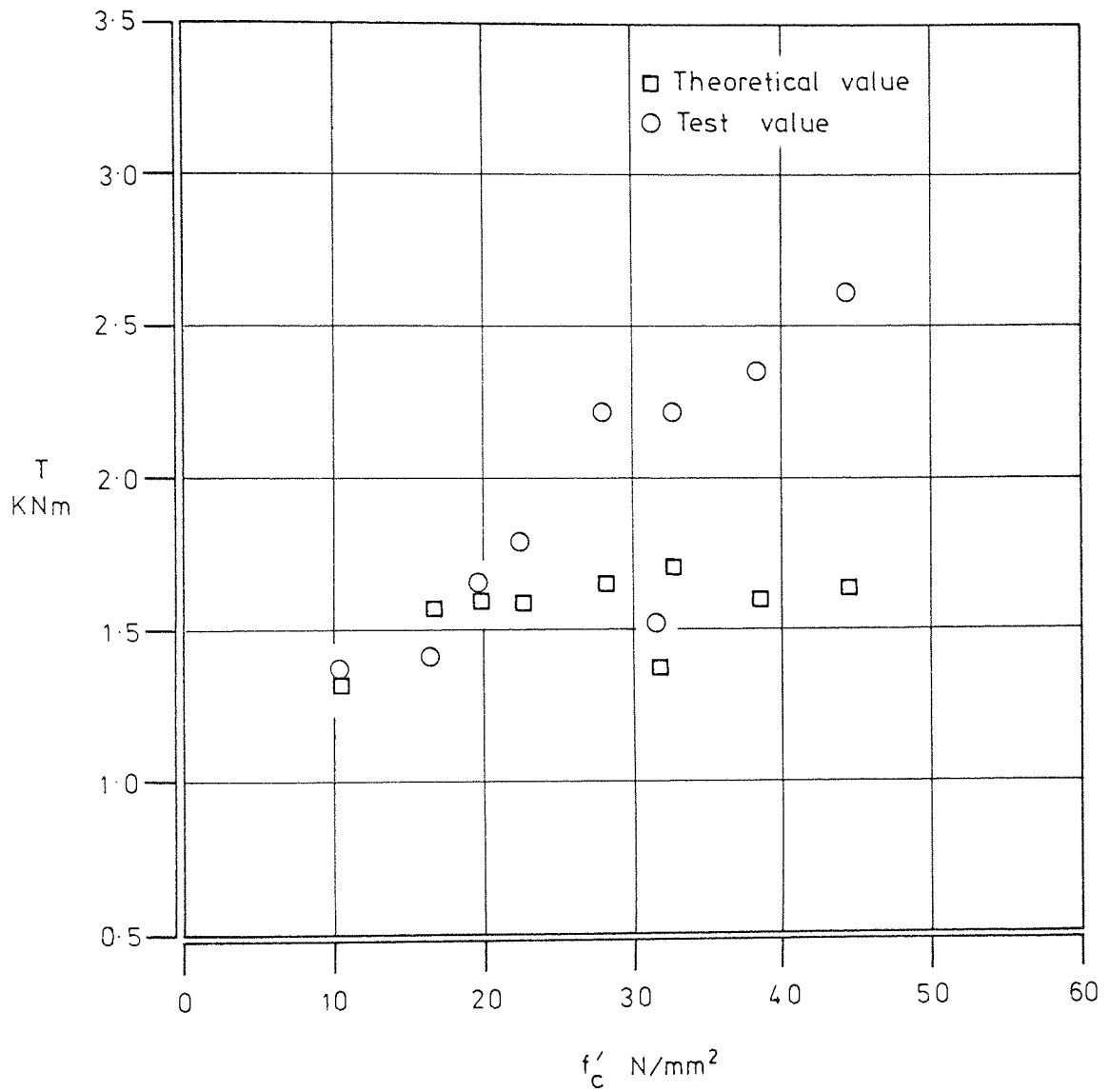
FIGURE 5.1: Ultimate torque versus cylinder compressive strength of the concrete for beams of group A

171
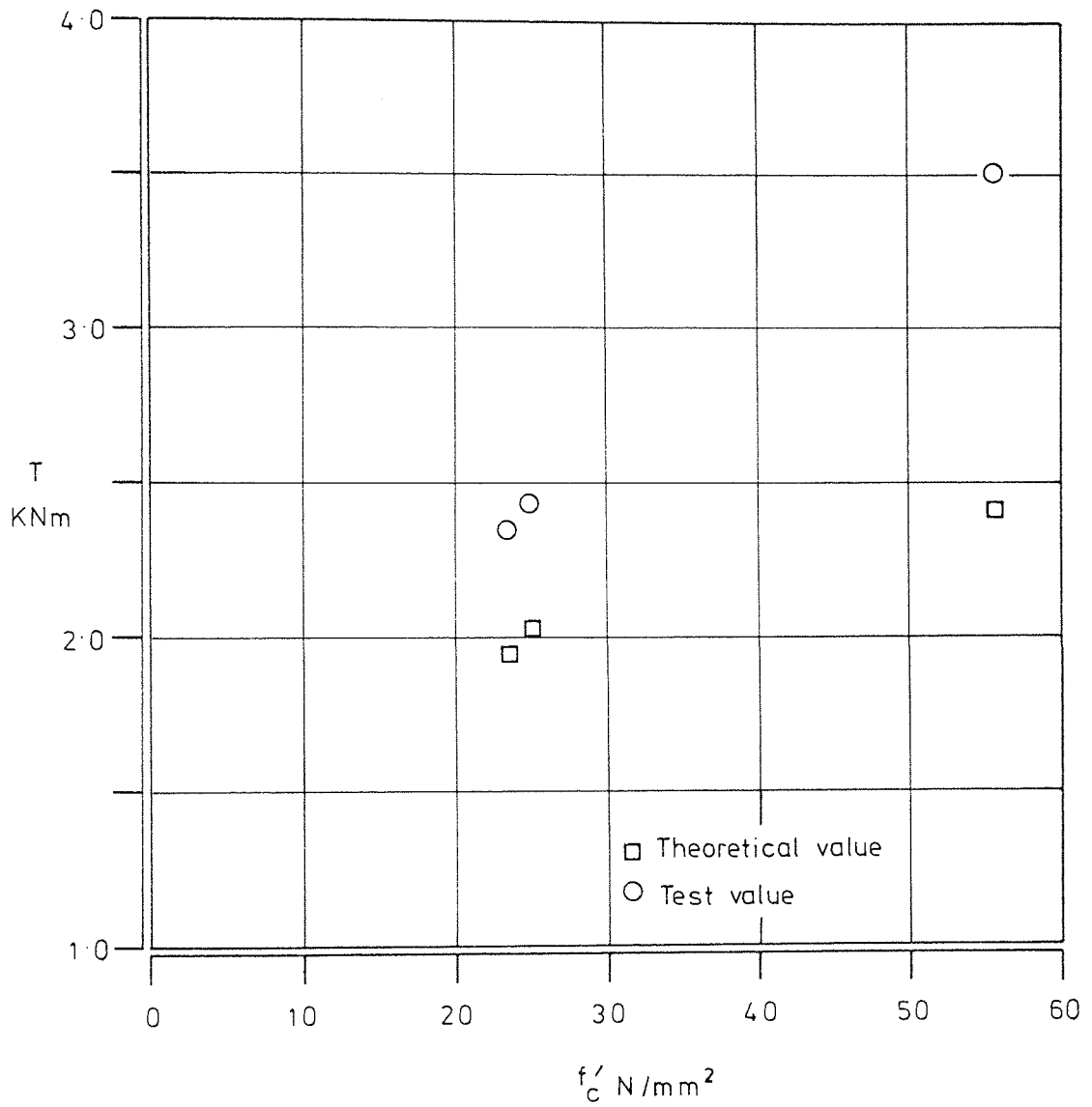
FIGURE 5.2 Ultimate torque versus cylinder compressive strength
of the concrete for beams of group AR

except A3, A7 and A9 indicate yielding of the longitudinal steel only (see table 3.4), which is not in agreement with that predicted by the theory. Table 2.5, however, shows that the position of the strain gauges was close to the location of the failure section for these beams. The strain gauge readings are affected by whether the failure cracks intercepted the strain gauges. In the author's tests only one single stirrup in the transverse plane was instrumented, although the failure section extended over a considerable distance along the longitudinal axis.

The mode and type of failure have been predicted correctly for beams A3, A7 and A9, although the predicted ultimate torques for beams A7 and A9 are rather low. This increase in the torsional strength for the beams were achieved by incorporating the higher strength concrete as can be seen from figure 5.1.

Beams of group AR were tested under approximately pure torsion (section 3.7.2). The predicted ultimate torques are considerably lower than the test values (see table 5.5). The predicted mode of failure for beams AR4 and AR5 shows mode 2.IV (crushing), but the observed failure mechanism for these two beams was thought to be cleavage at the bottom face. It is quite possible that the cleavage was a tensile crack at bottom which formed a part of the spiral tensile cracks of the failure surface for mode 2. Some crushing of the concrete on the north face can be traced from the crack pattern of the failure section of beam AR5 (see Appendix C), which supports the theoretical prediction. Analysing beams AR4 and AR5 as mode 3.III failure - which is the second critical mode for both beams (table 5.4), underestimates the strength by only 3% and 5% respectively compared with 20% of the predicted values by the theory. The

mode 3.I (yielding) of the reinforcement for beam AR9 is correctly predicted by the theory, but underestimates the torque by 46%, which is rather large.

Direct comparison of beams in group AR with their identical beams in group A (see table 5.5) leads to a conclusion that a moderate combination of bending and shear in conjunction with the applied torque on a reinforced concrete member reduces the ultimate torsional capacity. This reduction in the capacity is incorporated in the present analysis as can be seen again in the same table.

5.3.2 Beams of Series B

Beams of series B were tested in order to study the effect of stirrup spacing on the ultimate torsional capacity. This can be seen from figure 5.3 for group B, and figure 5.4 for group BR.

The ultimate torque and modes of failure for beams of group B are predicted by the theory with a reasonable degree of accuracy (see table 5.5). The theoretical ultimate torque for beam B1 is 38% below the experimental value, which is low. The theory predicts mode 2.IV (crushing) type of failure but the test result indicates mode 1 failure. If this beam were analysed as mode 1.III (longitudinal steel yielding) - which is the second critical mode - the theoretical torque would be only 24% below the test value, which is reasonable.

For the rest of the beams of this group, the theory overestimates the strength of beam B6 only, by 6%. In the test where failure section intercepted the position of the strain gauges the theory predicts the correct mechanism of failure and behaviour characteristics, as in beam B4.

The predicted torsional moment for the three beams of group BR
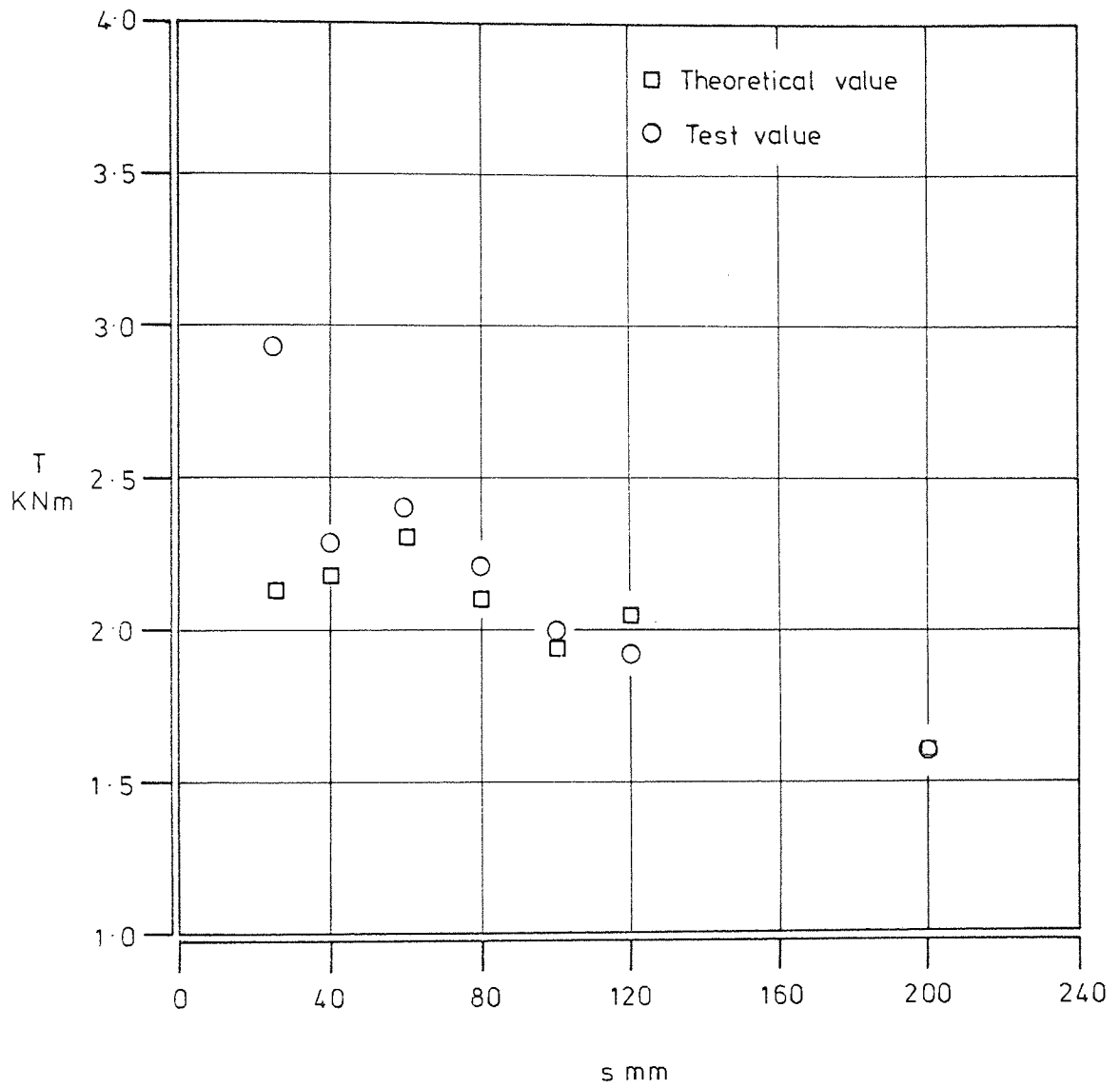
FIGURE 5.3: Ultimate torque versus the spacing of the stirrups for beams of group B
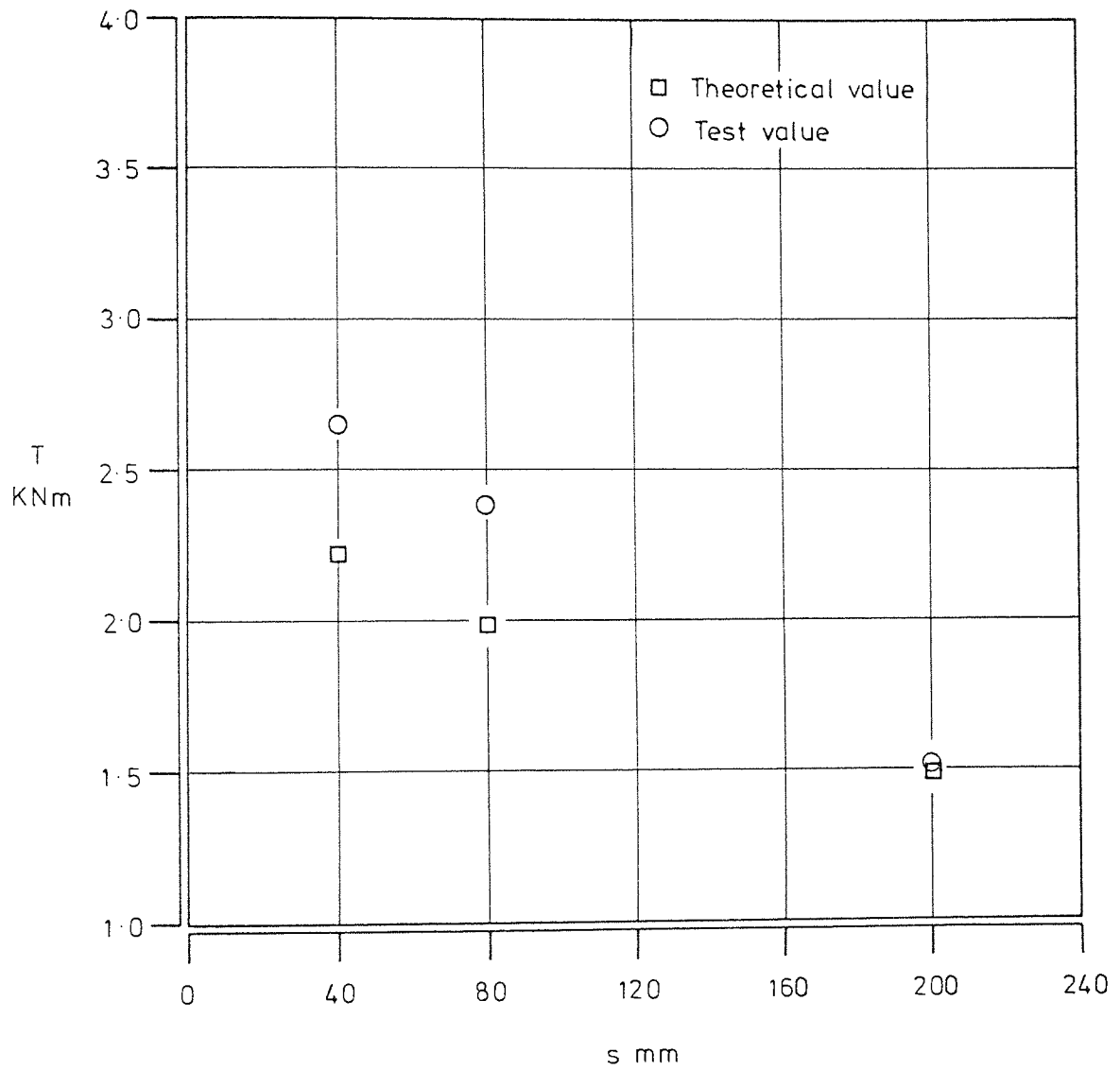
FIGURE 5.4 : Ultimate torque versus the spacing of the stirrups for

beams of group BR

are lower than the experimental values but the behaviour and theoretical modes have been predicted reasonably well. Beam BR2 showed an upward deflection (table 3.3) at the midspan upon failure, which implied mode 3, but from the location of the failure section (table 2.5) it is possible that the beam failed in mode 2 as predicted by the theory, since the upward deflection in this section is very small.

According to the theory beam BR4 failed in mode 2.IV (crushing), but the crack pattern of the failure surface (Appendix C) indicates no apparent crushing of the concrete, although mode 2 failure mechanism is possible.

It is interesting to note for the previous two beams mode 2.IV (crushing) dominated other modes by small differences in the estimated torque. If they were analysed in accordance to their second critical modes - 3.III for beam BR2 (table 5.3) and 2.II for beam BR4 (table 5.2) - the theory would underestimate the actual torsional strength by 7% and 4% respectively, compared with 21% predicted by mode 2.IV equation.

Comparing beam BR7 with beam B7, one may conclude that mode 3 failure mechanism governs mode 2 or mode 1 failure as the amount of top steel decreases. It can also be seen that only a small increase in bending and shear of a member subject to combined loads will increase the ultimate torsional strength. Figures 5.3 and 5.4 show that the ultimate torsional capacity of a reinforced concrete beam increases by increasing the amount of transverse steel.

5.3.3 Beams of Series C

Beams of series C were manufactured to investigate the effect of the amount of the longitudinal steel on the ultimate torsional strength. This effect is shown in figure 5.5 for beams of group C and figure
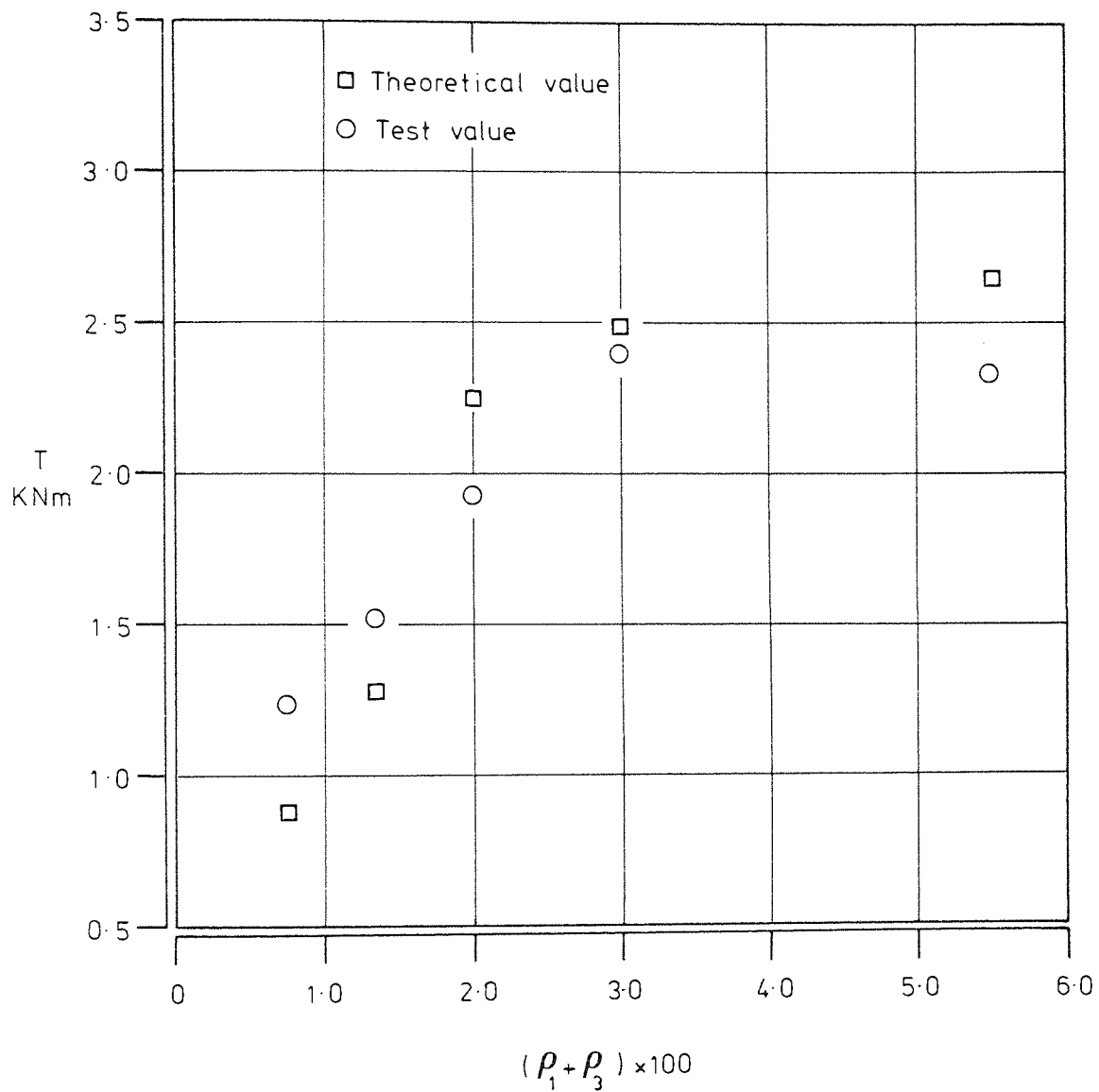
FIGURE 5.5: Ultimate torque versus the sum of tension and compression steel ratio for beams in group C
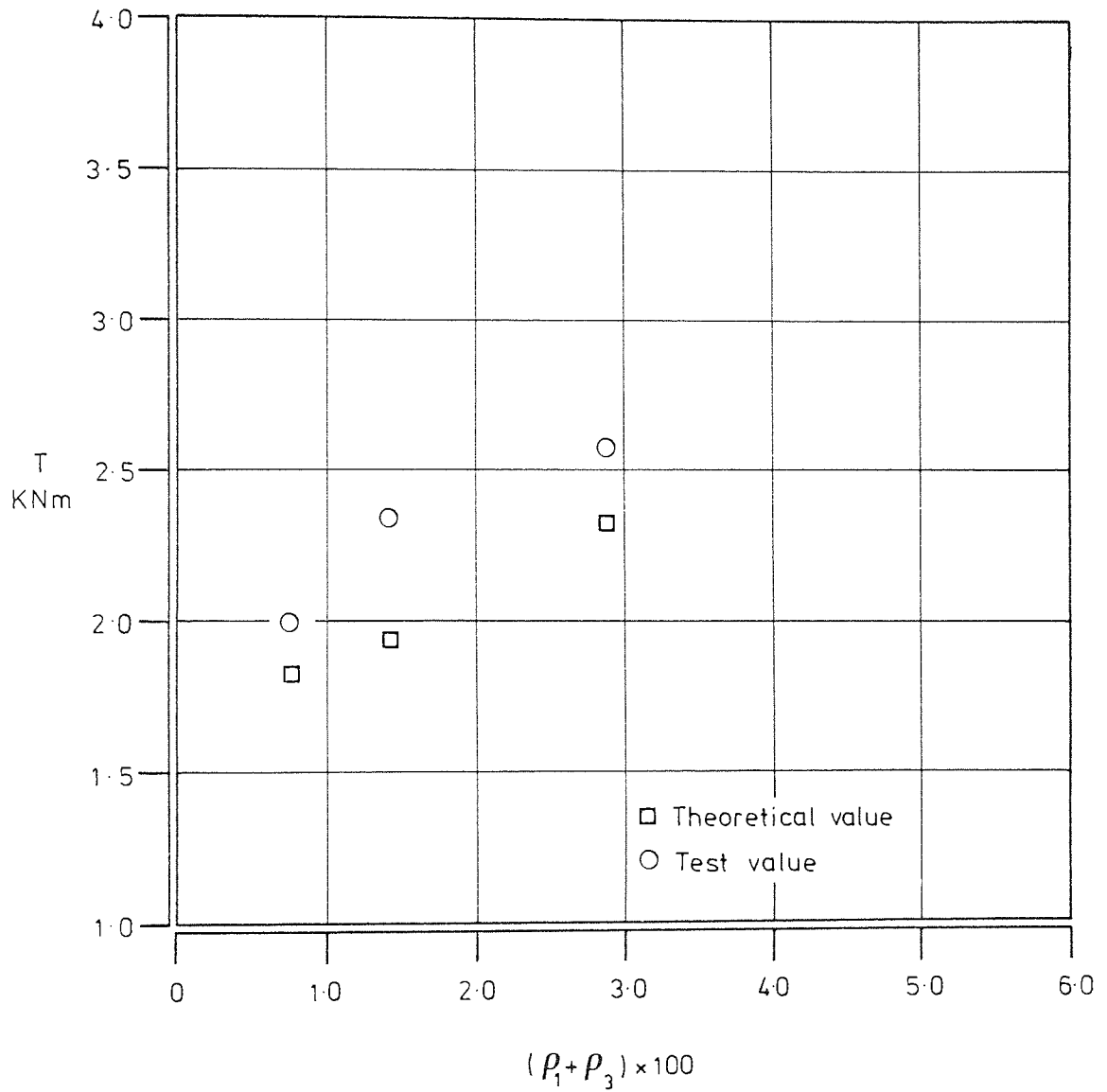
FIGURE 5.6 : Ultimate torque versus the sum of tension and

compression steel ratio for beams in group CR

179

5.6 for beams of group CR.

The predicted modes of failure for beams in group C show good agreement with the observed mechanism of failure. The test results of these beams varied between 13% below to 45% above the theoretical values (see table 5.5).

A conservative estimation of beam C1 by the theory seems to have been produced by a low value of $\tan\alpha_{1y}$, due to the high experimental ratio of the transverse to longitudinal steel, r_{1y}. This characteristic and the analysis of later beams of group A leads to a conclusion that for both low and high values of the ratio r_{1y} the theory is conservative. This is obviously advantageous for safety in design and a disadvantage for accuracy in analysis.

The unsafe estimation of the ultimate torsional capacity for beams C3, C4 and C5 may be attributed to the fact that these beams failed prematurely, as observed during the experimental investigation (see section 3.7.5). This fact may be supported by a direct comparison between beams C3 and B4 - which were identical. From table 3.3 the load ratio of M:T:Vh of beam C3 was approximately 0.4:1.0:0.3, while this ratio for beam B4 was 2.4:1.0:0.3, which suggests that beam C3 should have resisted higher applied loads.

The ultimate torque and modes of failure for beams of group CR have been reasonably determined by the theory. For beam CR1 the theory predicts mode 2.IV (crushing), while the observed mode of failure was between 3 and 2. It is quite reasonable that the absence of bending and shear in this beam - unlike its identical C1, might have initiated crushing of the concrete in one of the sides before yielding of the reinforcement. It is interesting to realize that by analysing beam CR1 in accordance to its second critical theoretical

180

mode (i.e. mode 2.III, see table 5.2), the critical ultimate torque would be 2.016 kNm against 2.001 kNm for the actual failure torque.

Supported by the strain readings of the longitudinal reinforcement it is reasonable to expect that beam CR5 failed by yielding of the steel at the top of the section, as predicted by the theory.

In general it appears that the ultimate torsional capacity of a reinforced concrete member under pure torsion (figure 5.6), or torsion with combined loads (figure 5.5) increases as the amount of longitudinal steel increases until it is over-reinforced.

5.3.4   Beams of Series D

Series D beams were manufactured in order to investigate the effect of varying the breadth of the section. The effect of the breadth to height ratio on the torsional capacity for beams in group D is shown in figure 5.7, and group DR in figure 5.8.

The theoretical solutions for beams in group D generally underestimate the test values. The theoretical predictions vary between 44% lower to 1% higher than the test values.

The mechanism of failure in the tests for beams D1 and D2 described in section 3.7.7 are not in agreement with the theoretical modes. For beam D1, careful examination of the crack pattern of the failure section (see Appendix C) shows that some crushing of the concrete on the north face occurred which supports the predicted failure mechanism. It can be seen from table 3.1 that the cylinder compressive strength, f'_c, for this beam is actually 20% lower than the design value. This fact and the low value for dn_{2c} produces a low estimation for the torsional capacity of mode 2.IV (crushing). The immaturity of the concrete seems to be related to the method by which the test beam and its control specimens were vibrated (see
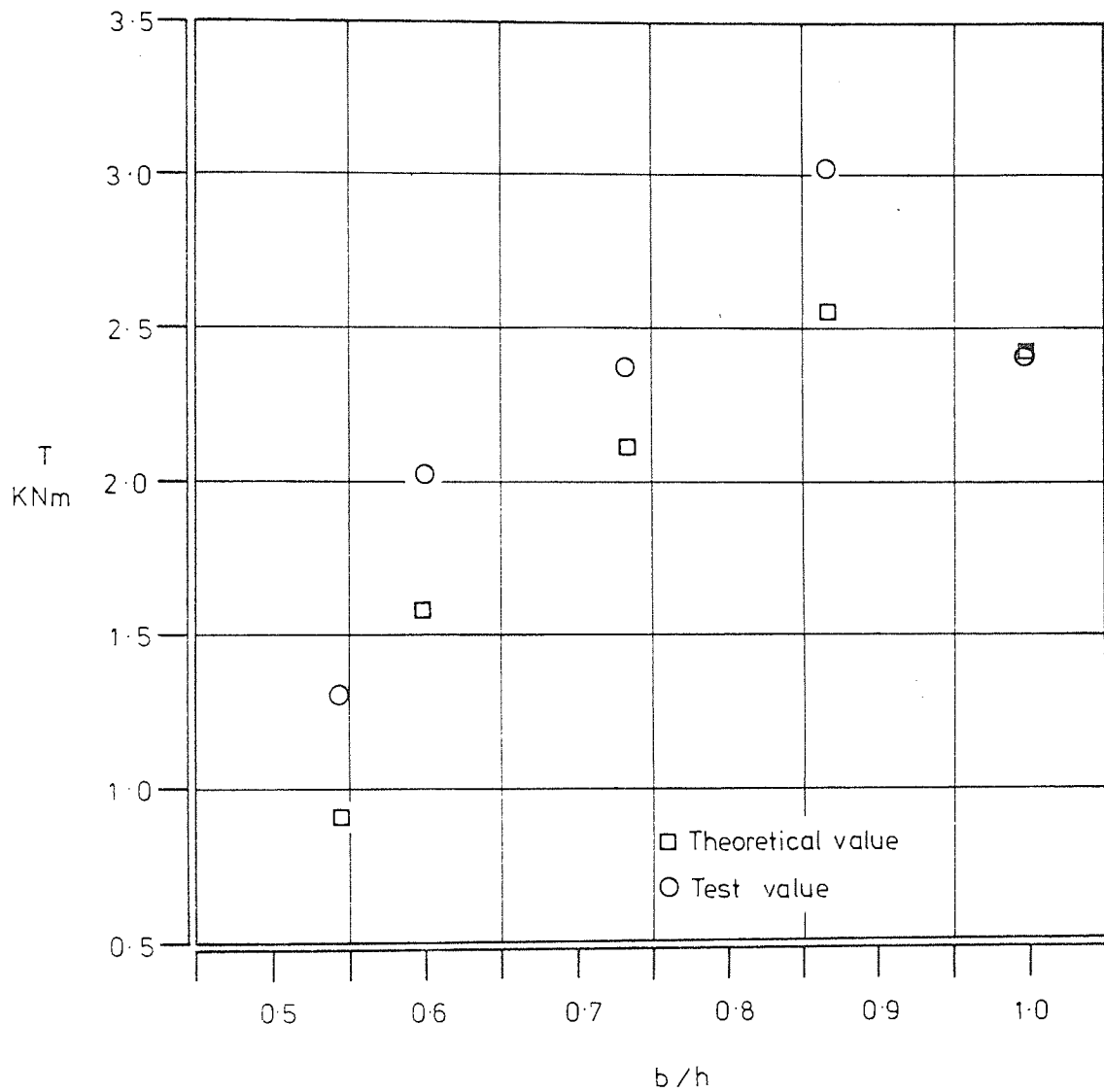
FIGURE 5.7 : Ultimate torque versus the breadth to height ratio
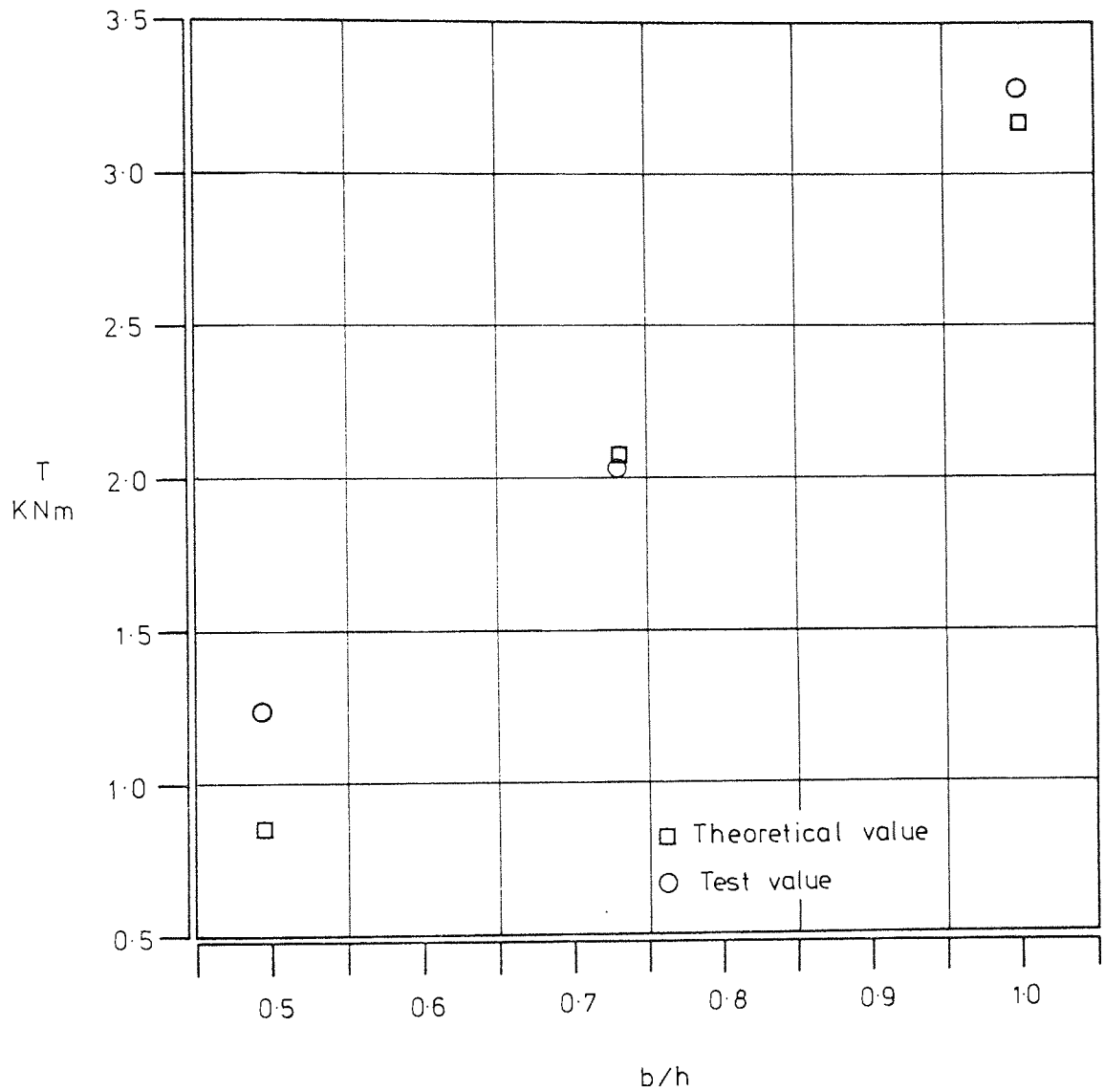
for beams of group D

FIGURE 5.8 : Ultimate torque versus the breadth to height ratio
for beams of group DR

ection 2.3.2). For beam D2, the described mode 1 of tensile failure seems to be mode 2 failure by yielding of the stirrups only according to the theoretical analysis. From the crack pattern of the failure section (Appendix C), it is quite reasonable to consider the tensile cracks on the top, described as cleavage in section 3.7.7, were infact a part of the spiralling tensile cracks on the top, south and bottom faces for a mode 2 failure mechanism. It has been noted, however, that the measured stresses in the longitudinal reinforcement (table 3.4) support mode 1 failure, but they are not entirely reliable.

The theoretical solution and the predicted mode of failure for the remaining beams of this group are in reasonable agreement with the tests.

The mechanism of failure for beam DR1 described in section 3.7.8 was observed to be mode 3, while the theory indicates mode 2.IV (crushing) failure. This may be due to the same reasons as described in the analysis for its identical beam (i.e. beam D1) above. The failure mode and the ultimate torque for beam DR3 is predicted by the theory with reasonable accuracy i.e. a 1.6% overestimation. In beam DR5 the observed failure mechanism was mode 2, but the theory predicts mode 3.I (yielding). The latter could in fact be the real case, since the beam is square in cross-section and contains less top steel. It is quite possible that the sort of crumbled con-crete on the bottom face (see plate 3.4) was the crushed compression zone. Mode 3 failure mechanism for this beam is further supported by the upward deflection at failure, as it can be seen from table 3.3.

Close examination of beams D1 and DR1 from tables 5.2 and 5.4, apart from confirming the high conservatism of mode 2.IV (crushing), as concluded earlier, also leads to another conclusion. A beam with a rectangular cross-section, where the height is twice or greater

than the breadth, mode 2.II (stirrup yielding) underestimates the ultimate torsional capacity.

Figure 5.7 shows that the ultimate torsional capacity of a rectangular reinforced concrete member under combined loads is increased by increasing the breadth of the section up to a certain limit, beyond which the flexural mechanism tends to dominate the nature of the failure. This limit can be defined by the ratio of breadth to height (b/h) to be about 0.85 for the test beams of group D. Figure 5.8 confirms that the torsional capacity of a rectangular reinforced beam under nearly pure torsion is increased by increasing the b/h ratio. The limit in this case seems to be associated with the state where the failure mechanism of a wide beam changes to one of a slab under torsion.

5.4 EVALUATION OF THE PROPOSED METHOD OF ANALYSIS

5.4.1 Deficiencies of the Theory

The theory proposed in Chapter four to predict the behaviour and ultimate strength of reinforced concrete members under combined torsion, bending and shear is not considered to be the final solution to the problem. It is apparent, however, that the test results support the proposed theory, although some deficiencies were noted in the discussion in the preceding section. These deficiencies could be summarised as follows:-

1   The theory seems to underestimate the ultimate strength of a member reinforced with steel of widely different yield strengths. It is possible therefore that dissimilar strengths of steel should be avoided.

2   In general mode 2.IV (crushing) tends to an excessive underestimation of the ultimate strength. This obviously increases the

185

safety factor but decreases the accuracy of the theory.

3   Mode 2.II (stirrup yielding) also tends to underestimate the ultimate strength in beams where h/b>2.

4   Mode 3.III (longitudinal steel yielding) in some cases estimates values for torsional strength close to infinity (see table 5.3). This is apparent from equation 4.45, where if ψ is close to 1.0 and δ is small the denominator will be nearly zero, thus the estimated torque will be very large, hence this mode will not generally be critical. Only beam CR5 of the author's test failed in this mode for which ψ = 0.028 (or ψ = 0 if the dead load is ignored).

5   It must be realised, however, that the present theory analyses the principal modes of failure only, and assumes a sudden change from one failure mechanism to another, which in fact is unlikely to occur.

5.4.2   Comparison of the Theory with the Author's Test Beams

The accuracy of the proposed analysis has been compared with the experimental results of the author's beams for each principal mode of failure (i.e. 1, 2 and 3) separately. For this purpose a comparative ratio (CRT) of T_{test}/T_{theory} - which idealy should be 1.0, has been used so that ratios of less than unity indicate unsafe results. For each beam T_{test} corresponds to the ultimate torsional moment which the beam can resist upon failure, and T_{theory} corresponds to the lowest (positive) theoretical torque calculated from the equations for the three principal modes of each type of failure. The mean value for the comparative ratio (CRT), and the coefficient of variation for each of the principal modes is presented in tables 5.6, 5.7 and 5.8.

Beam	Failure torque		$\dfrac{T_{test}}{T_{theory}}$
	Observed T_{test} kN.m	Predicted T_{theory} kN.m	
A3	1.657	1.602	1.03
A4	1.792	1.577	1.14
A5	2.207	1.694	1.30
A6	1.519	1.368	1.11
A7	2.207	1.647	1.34
A8	2.345	1.599	1.47
A9	2.620	1.630	1.61
B2	2.276	2.186	1.04
B3	2.413	2.306	1.05
B4	2.207	2.104	1.05
B5	2.001	1.945	1.03
C1	1.244	0.857	1.45
C2	1.519	1.260	1.21
D3	2.372	2.111	1.12
D4	3.032	2.558	1.19
D5	2.413	2.447	0.99

Average mean of T_{test}/T_{theory}	1.20
Coefficient of variation	0.15

TABLE 5.6: Comparison of author's results for mode 1 failure mechanism

187

Beam	Failure torque		$\dfrac{T_{test}}{T_{theory}}$
	Observed T_{test} kN.m	Predicted T_{theory} kN.m	
A1	1.382	1.313	1.05
A2	1.409	1.572	0.90
AR4	2.345	1.952	1.20
AR5	2.441	2.028	1.20
B1	2.936	2.131	1.38
B6	1.932	2.052	0.94
B7	1.588	1.591	1.00
BR2	2.661	2.199	1.21
BR4	2.386	1.975	1.21
BR7	1.519	1.496	1.02
C3	1.932	2.227	0.87
C4	2.400	2.499	0.96
C5	2.345	2.663	0.88
CR1	2.001	1.828	1.10
CR3	2.345	1.952	1.20
D1	1.313	0.199	1.44
D2	2.028	1.585	1.28
DR1	1.244	0.861	1.45
DR3	2.042	2.076	0.98

Average mean of T_{test}/T_{theory}	1.12
Coefficient of variation	0.17

TABLE 5.7: Comparison of author's results for mode 2 failure mechanism

Beam	Failure torque		$\dfrac{T_{test}}{T_{theory}}$
	Observed T_{test} kN.m	Predicted T_{theory} kN.m	
AR9	3.514	2.412	1.46
CR5	2.592	2.329	1.11
DR5	3.280	3.160	1.04

Average mean of T_{test}/T_{theory}	1.20
Coefficient of variation	0.15

TABLE 5.8: Comparison of author's results for mode 3 failure mechanism

Failure modes	T_{test}/T_{theory}			Coefficient of variations	Number of beams	Total
	Minimum	Maximum	Mean			
1	0.896	1.607	1.195	0.151	16	
2	0.868	1.445	1.117	0.166	19	38
3	1.038	1.457	1.203	0.155	3	

TABLE 5.9: Summary of the comparison for author's test beams

For those beams where the theory predicts mode 1 failure mechanism the ultimate torque are compared with the test values in table 5.6. The theory underestimates the test results by about 20% with a coefficient of variation of 0.15. The test results varying from 1% below to 61% above the theoretical values.

The beams where mode 2 failure mechanism was predicted, are compared in table 5.7. The theory underestimates the test results on average by nearly 12% with a coefficient of variation of 0.17. The actual torsional capacity for these beams vary between 13% below to 45% above the predicted values.

The three beams which failed theoretically in mode 3 are compared with the test results in table 5.8. The theory underestimates the results by 20% with a coefficient of variation of 0.16. The test results ranging from 4% to 46% above the theoretical values.

The comparison is summarized and presented in table 5.9, together with the lowest and the highest values of CRT (i.e. T_{test}/T_{theory}) and also the number of beams which failed in each mode.

The comparison of each individual group, however, can be seen in graphical representation from figures 5.1 through 5.8. Only fair agreement can be seen between the theory and the test results of group A beams (figure 5.1). This must be due to the fact that the transverse reinforcement for beams in this group had a lower yield strength than the main bars as discussed earlier. For the beams of group AR (figure 5.2), and the rest of the groups (figures 5.3 through 5.8), good correlation can be found between the theory and the experimental results.

5.5 COMPARISON OF THE THEORY WITH OTHERS' RESULTS

The proposed theoretical approach is also compared with a total

of 477 experimental results carried out by different research workers in various countries. The summary of the comparison is given in table 5.10. All the results used in the comparison were from tests of fully reinforced concrete (except Zia and Gardenas' [67]) beams subjected to pure torsion, or torsion in conjunction with bending and shear. The test results include those reported by the following investigators:

1	Ernst, G C [20]	15 tests
2	Hsu, T T C [10]	53 tests
3	Swann, R A [54]	12 tests
4	Evans, R S and Sarkar, S [41]	15 tests
5	Gesund, G et al [40]	12 tests
6	Goode, C D and Helmy, M A [11]	16 tests
7	Iyengar, K T and Rangan, V B [15]	37 tests
8	Jackson, N and Estanero, R A [46]	68 tests
9	Kemp, E L [66]	10 tests
10	Pandit, G S and Warwaruk, J [37]	14 tests
11	Zia, P and Gardenas, R [67]	31 plaster model beams
12	Klus, J P [68]	8 tests
13	Collins, M P et al [45]	15 tests
14	Elfgren, L [69]	35 tests
15	Lyalin, I M [9]	36 tests
16	Lessig, N N [35]	42 tests
17	McMullen, A E and Warwaruk, J [52]	18 tests
18	Osburn, D L [50]	10 tests
19	Staley, R F [59]	11 tests
20	Yudin, V K [48]	19 tests

As can be seen from table 5.10, the test results of each individual investigators have been analysed separately for the three

Investigator	Modes	CRT (T_{test}/T_{theory})			Coeff. of variation	No. of beams	Total
		Minimum	Maximum	Mean			
ERNST [20]	2	0.818	1.370	1.01	0.13	15	15
HSU [10]	2	0.875	1.390	1.15	0.11	53	53
SWANN [54]	2	0.806	1.192	0.93	0.11	12	12
EVANS AND SARKAR [41]	1	0.948	1.191	1.04	0.06	12	15
	2	0.762	0.762	0.76	-	1	
	3	0.845	1.010	0.93	-	2	
GESUND ET AL [40]	1	0.895	1.087	0.99	0.06	10	12
	2	0.957	1.035	1.00	-	2	
GOODE AND HELMY [11]	1	1.062	1.193	1.13	-	2	16
	2	1.121	1.360	1.22	0.11	4	
	3	1.020	1.723	1.39	0.17	10	
IYENGAR AND RANGAN [15]	1	0.906	1.148	1.03	0.08	15	37
	2	0.826	1.113	1.01	0.07	22	
JACKSON AND ESTANERO [46]	1	0.918	1.180	1.04	0.07	22	68
	2	0.879	1.201	1.03	0.09	36	
	3	0.719	1.179	0.95	0.15	10	
KEMP [66]	1	1.055	1.524	1.26	0.15	6	10
	2	1.232	1.553	1.41	0.10	4	
PANDIT AND WARWARUK [37]	1	0.995	1.031	1.01	0.01	3	14
	2	0.775	1.258	1.03	0.18	10	
	3	0.961	0.961	0.96	-	1	

TABLE 5.10: Summary of the comparison for the test beams of other investigators

Investigator	Modes	CRT (T_{test}/T_{theory})			Coeff. of variation	No. of beams	Total
		Minimum	Maximum	Mean			
ZIA AND GARDENAS [67]	1	1.137	1.489	1.30	0.08	21	
	2	1.039	1.580	1.33	0.12	10	31
	-	-	-	-	-	-	-
KLUS [68]	1	0.835	1.043	0.95	0.07	6	
	2	1.120	1.198	1.16	-	2	8
	-	-	-	-	-	-	
COLLINS ET AL [45]	1	0.939	1.097	1.04	0.05	7	
	2	0.901	1.282	1.01	0.14	6	15
	3	0.882	0.891	0.89	-	2	
ELFGREN [69]	1	0.769	1.349	1.13	0.10	20	
	2	0.893	2.114	1.42	0.21	13	35
	3	1.155	1.155	1.16	-	1	
LYALIN [9]	1	0.935	1.639	1.26	0.13	30	
	2	1.204	1.465	1.35	0.08	6	36
	-	-	-	-	-	-	
LESSIG [35]	1	1.000	1.414	1.21	0.09	27	
	2	1.122	1.649	1.38	0.13	15	42
	-	-	-	-	-	-	
McMULLEN AND WARWARUK [52]	1	0.936	1.156	1.01	0.07	6	
	2	0.891	1.340	1.05	0.16	10	18
	3	0.902	1.086	0.99	-	2	
OSBURN [50]	1	0.872	1.142	1.03	0.08	10	
	-	-	-	-	-	-	10
	-	-	-	-	-	-	
STALEY [59]	1	0.896	1.374	1.09	0.14	10	
	2	1.402	1.402	1.40	-	1	11
	-	-	-	-	-	-	
YUDIN [48]	1	0.800	1.491	1.11	0.20	19	
	-	-	-	-	-	-	19
	-	-	-	-	-	-	

TABLE 5.10 (CONTINUED): Summary of the comparison with the test beams of other investigators

principal mechanisms of failure (i.e. modes 1, 2 and 3). Also shown
is the mean values of the comparative ratio (CRT) - T_{test}/T_{theory},
the coefficient of variation, and the number of beams which have
failed in each particular mode. These results have been analysed
using the same computer program as for the author's test results,
unless an alteration was required for the system of units. The
experimental and theoretical torsional moments and modes of failure,
as well as the comparative ratio for each beam of each investigator
is given in the Appendix D.

The experimental work of these investigators is not described
here, but a list of details of experimental data required for the
analysis is given in the Appendix E.

The following points in relation to the preparation of the data
in Appendix E should be noted;

1   For those test results where only the cube compressive strength,
f_{cu}, has been reported, a coefficient of 0.8 was used to obtain the
cylinder compressive strength, f'_c, i.e. $f'_c = 0.8.f_{cu}$.

2   The present analysis is applicable to members where the longi-
tudinal steel is concentrated in the four corners around the inside
perimeter of the stirrups. In those test beams where the distri-
bution of the main bars did not comply with this condition, the
longitudinal steel along the faces was distributed to the existing
bars in the corners. In the case of bars with different yield
strength, the correction of the strength was also considered. This
was made in accordance to the proportion of the cross-sectional area
of the steel added to the corner bars.

3   The failure torque for Jackson and Estanero's [46] test beams
was obtained from the failure bending moment and the torsion to bend-
ing ratio ψ.

CHAPTER SIX

CONCLUSIONS AND SUGGESTIONS FOR FURTHER STUDY

6.1 CONCLUSIONS

From the experimental and theoretical investigation presented in the previous chapters the following is concluded:

(1) The instruments (except the Data Logger), and the performance of the test rig for applying the required combination of loads onto the test beams were found to be satisfactory.

(2) Upward deflection occurred in beams which contained weak top steel and were subjected to high torsion. This confirms the existence of mode 3 failure mechanism.

(3) Combined flexural moment and shear reduce the torque at which the first visible crack appears.

(4) The deflection of beams under combined torsion, bending and shear decreases with the amount of longitudinal steel inversely.

(5) The cracking torque in concrete members under pure torsion or combined loading increases with the compressive strength of the concrete.

(6) An increase in the amount of longitudinal steel is accompanied by an increase in the cracking torque for beams under combined torsion, bending and shear, but this effect for beams under pure torsion seems to be insignificant.

(7) The presence of bending moment reduces the ultimate torsional capacity of a concrete member reinforced with equal areas of longitudinal steel in the bottom and the top of the section.

(8) The presence of bending moment to a certain limit increases the torsional strength in a rectangular member reinforced

with less longitudinal steel at the top and subjects to high torsional moment, particularly when it fails by yielding of the reinforcement.

(9)   It is apparent from the result of series A test beams that the ultimate strength of reinforced concrete members under pure torsion or torsion with combined bending and shear, increases with compressive strength of the concrete.

(10)   Torsional capacity of reinforced concrete members, in pure torsion, or combined torsion bending and shear increase with the spacing of the stirrups inversely.

(11)   There is appreciable increase in the ultimate capacity in beams under pure torsion for an increase in the amount of longitudinal steel. This increase in beams under combined torsion, bending and shear is limited to the state of over-reinforcement.

(12)   The ultimate strength in beams subject to a high torsional moment increases with the breadth of the section. For beams under combined loads the increase is limited. This limit for the author's test beams was approximately 0.85 (i.e. $b/h = 0.85$).

(13)   The experimental results of the author's test beams, as well as the other investigators, indicate that a reinforced concrete member under combined torsion bending and shear may fail in one of the following types of failure:

I   -   Yielding of both categories of reinforcement at failure before crushing of the concrete in the shear-compression zone.

II -   Yielding of the transverse steel only at failure before crushing of the concrete in the shear-compression zone.

196

III - Yielding of the longitudinal steel only, at failure, before crushing the concrete in the shear-compression zone.

IV - Crushing of the concrete in the shear-compression zone, at failure, before yielding of any of the reinforcement.

(14) In any of the failure types above the beam may fail in one of the three principal modes (i.e. 1, 2 or 3), depending on the combination of the loads and the distribution of the steel.

(15) The hypothesis that torsion in reinforced concrete members is resisted partially by the concrete in the compression zone and partially by the reinforcement is further substantiated by the experimental work and the theoretical investigation of this thesis.

(16) The results of the experimental investigations confirm that the interaction curve for combined torsion bending and shear, $(T/T_u)^2 + (V/V_u)^2 + M/M_u = 1$, proposed by previous investigators predicts the ultimate strength accurately only when complete yielding has occurred.

(17) The direct and torsional shear stresses in the shear compression zone for a reinforced concrete member can be combined by Cowan's simplified failure criterion for concrete under tensile-compressive stresses. It can be further simplified to a relationship independent of the direct stress, fm, except for $0.75 \ f'_c < fm < f'_c$.

(18) Detail examination of the author's results shows the proposed theoretical approach describes the behaviour of the test beams with a reasonable degree of accuracy.

(19) Analytical interaction equations as well as design formulae

can be obtained from the proposed theoretical approach for combined torsion, bending and shear in reinforced concrete members.

(20) Reasonable agreement between the theory and test results was found not only for the beams of the author, but also for another 477 beams reported in the literature.

6.2 SUGGESTIONS FOR FURTHER RESEARCH

From the result of this investigation the following recommendations for future work, concerning combined torsion, bending and shear of reinforced concrete members, are proposed:

1 Experimental and theoretical work is required into a method by which the stresses in the reinforcement can be calculated for types of failure other than yielding.

2 Further experimental evidence is needed to clarify the nature and behaviour of combined stresses in concrete at failure.

3 Assuming $\tan \alpha = 1$ in the non-yielding types of failure affects the accuracy of the theory. Further experimental work is needed to obtain a more accurate value.

4 Theoretical and experimental investigation is required into the flexural and torsional stiffnesses of reinforced concrete beams under combined loads, particularly for cracked sections.

5 Further analysis is required in order to improve the accuracy of the expression for determining the depth of the compression zone.

6 Although some experimental work has been done to investigate the effect of the size, distribution and the yield strength of the reinforcement, further investigation is required

to optimize these effects in relation to the ultimate capacity of the member.

7 Although the present analysis ignores the dowel action and produce reasonable results, further investigation is still required in order to study the effect of the dowel action of the steel on the ultimate capacity of beams under combined loads.

8 The equations which are presented in this investigation need to be simplified further in order to serve as design formulae.

9 If only under-reinforced members are recommended in practice, further study is required in order to obtain the necessary conditions for full yielding of the reinforcement.

APPENDIX A

A METHOD TO DETERMINE THE MODULUS
OF ELASTICITY OF CONCRETE E_c

A.1 EXPERIMENTAL WORK

For each beam two cylinders from the control specimens were tested in order to determine the modulus of elasticity of the concrete E_c. On the day of casting, after the concrete had set in the moulds, the two cylinders were capped with a 10 mm thickness of concrete mortar to give a smooth end surface. On the day of the test they were removed from the curing tank and left in the air for some hours to dry the surface. The surface was then cleaned, and marked with two vertical lines each being the intersection with a vertical plane through the diameter of the bases. Two PL-60-11 strain gauges were then fixed at the mid-height of each of the intersection lines using F88 dental cement. Later electrical wires were soldered to the leads of the strain gauges.

A Dennison compression machine was used to test the cylinders with a standard rate of loading. Testing started by recording the initial readings, after the strain gauges were stablized; and thereafter the strain was recorded at each stage of loading upto failure.

A.2 ANALYSIS

The maximum stress (σ_{max}) and the corresponding strain ε_o for all the specimens are given in table A-1. A typical stress-strain curve is also presented in figure A-1.

To determine the modulus of elasticity, a relation between uniaxial compressive stress (σ) and strain (ε) for the concrete had

to be obtained. Desayi and Krishnan's equation [72] was found to be suitable for the purpose and can be expressed in the form of $E_{ci} = (\sigma/\varepsilon).[1.0+(\varepsilon/\varepsilon_o)^2]$, where E_{ci} is Young's modulus and ε_o is concrete strain at maximum stress.

At failure, σ reaches σ_{max}, thus ε will be equal to ε_o, and the above relationship is reduced to $E_{ci} = 2.\sigma_{max}/\varepsilon_o$. Since $\sigma_{max}/\varepsilon_o$ is the secant modulus of elasticity, E_{cs}, at the maximum stress, then the initial tangent modulus of elasticity of a concrete is equal to twice its secant modulus at maximum stress.

Using the test values for the maximum stress (σ_{max}) and its corresponding strain ε_o, both the initial tangent modulus (Young's modulus), and secant modulus at ultimate stress were determined. These values are presented in table 3.1 in the text.

Beam	Specimens 1		Specimens 2	
	σ_{max}. N/mm^2	ε_o x 10^{-6}	σ_{max}. N/mm^2	ε_o x 10^{-6}
A1	-	-	-	-
A2	15.538	1820	15.677	1300
A3	20.533	1760	19.090	1860
A4	24.778	1800	25.416	1900
A5	-	-	-	-
A6	-	-	-	-
A7	-	-	-	-
A8	-	-	-	-
A9	44.284	2120	44.673	2100
AR4	21.754	1600	25.027	1800
AR5	25.250	1720	24.750	2000
AR9	58.380	2340	52.831	2040
B1	-	-	-	-
B2	18.757	1500	20.810	1500
B3	24.334	1600	22.142	1400
B4	-	-	-	-
B5	19.562	1280	19.090	1240
B6	26.471	1700	25.583	1640
B7	24.584	1720	22.198	1600
BR2	22.198	1820	22.697	1600
BR4	21.310	1900	-	-
BR7	27.636	2300	-	-
C1	20.089	1400	27.049	1940
C2	-	-	-	-
C3	22.531	1700	22.864	1420
C4	22.642	1400	27.692	1880
C5	26.637	1900	27.192	2060
CR1	25.805	1620	24.251	1420
CR3	21.754	1600	25.027	1800
CR5	-	-	-	-
D1	19.811	1820	-	-
D2	24.584	1740	-	-
D3	26.249	1860	25.361	1820
D4	24.972	1640	-	-
D5	22.198	1620	27.470	1800
DR1	24.972	1700	-	-
DR3	33.130	1960	28.802	2060
DR5	30.522	2060	31.743	1880

TABLE A-1: Maximum stress and the corresponding strain for the test specimens
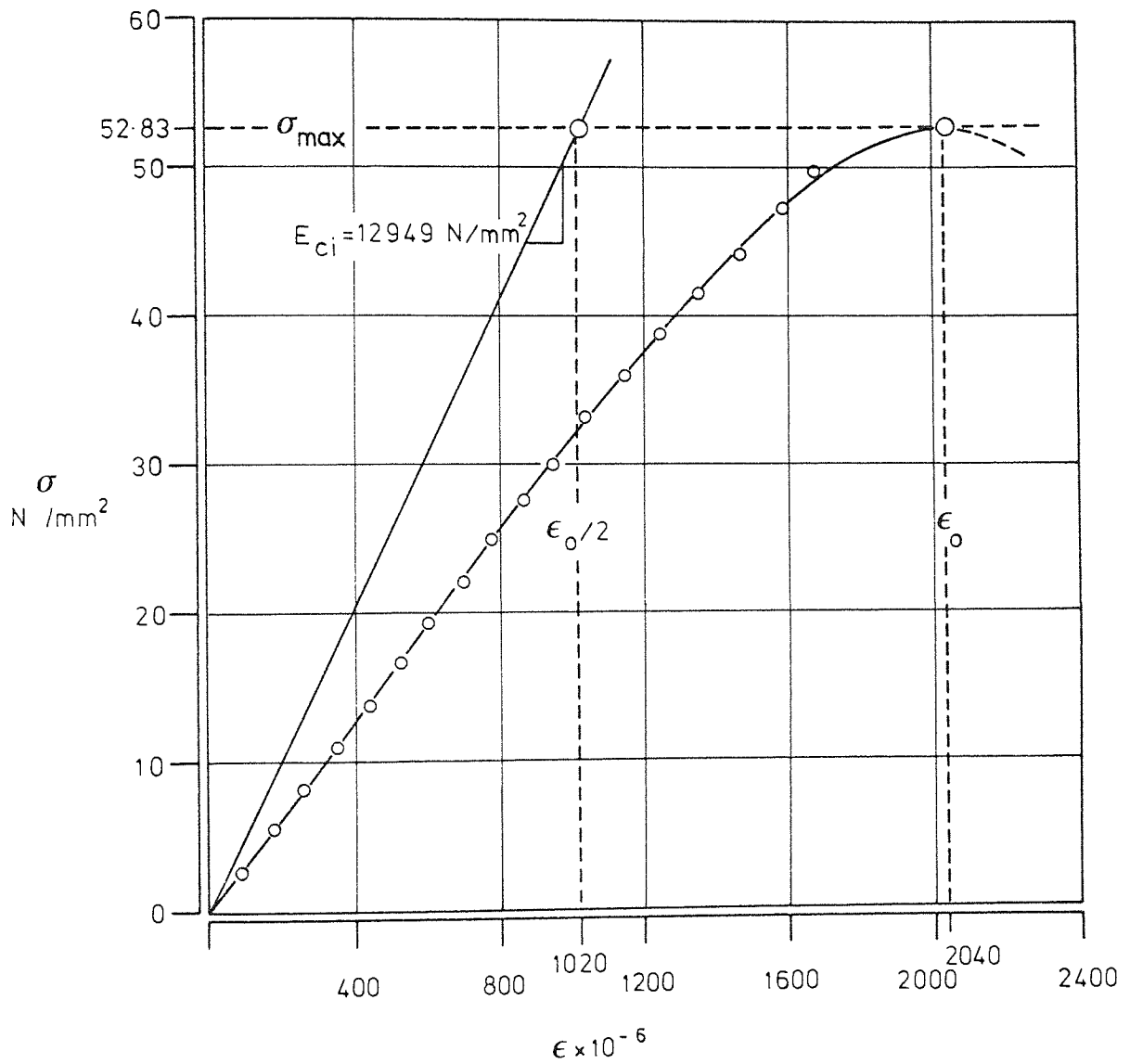
FIGURE A-1 : Experimental stress-strain curve for concrete in compression , for specimens 2 of beam AR9 given as a typical example.

APPENDIX B

BEHAVIOUR CHARACTERISTICS OF INDIVIDUAL

TEST BEAMS

The behaviour characteristics of the test beams from the first stage of loading until failure is presented sequentially in this appendix. In the tables, columns 7 through to 14 show the development of stresses in the reinforcement. These stresses are calculated from the recorded strains for the instrumented section in each test beam. The position of the strain gauges is shown in the following diagram.
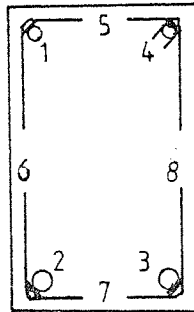
For the location of the gauges see table 2.5 in the text.

Applied load				Displacement		Stresses in the reinforcement N/mm^2							
P kN	M kNm	T kNm	V kN	A_r rad/km	d_m mm	1	2	3	4	5	6	7	8
1.450	0.585	0.144	0.103	–	–	–	–	–	–	–	–	–	–
2.431	1.296	0.419	0.593	2.30	0.82	-16.00	264.93	260.93	–	3.00	9.00	10.00	-1.00
3.411	2.007	0.694	1.084	6.16	2.32	-13.00	299.93	292.93	–	6.00	12.00	18.00	6.00
4.392	2.718	0.969	1.574	12.03	3.63	-16.00	324.13	323.92	–	9.00	16.00	30.99	18.00
5.373	3.429	1.244	2.065	25.20	5.76	-5.00	yield	yield	–	13.00	13.00	39.99	31.99
6.353	4.140	1.382	2.555	38.00	7.52	-29.00			–	33.99	6.00	53.99	53.99

A1

Applied load				Displacement		Stresses in the reinforcement N/mm²							
P kN	M kNm	T kNm	V kN	A_r rad/km	d_m mm	1	2	3	4	5	6	7	8
1.450	0.585	0.144	0.103	-	-	-	-	-	-	-	-	-	-
2.431	1.296	0.419	0.593	0.65	1.53	-	61.99	59.99	-172.96	-	10.00	-2.00	-3.00
3.411	2.007	0.694	1.084	5.59	3.15	-	103.98	95.98	-177.96	-	29.99	-3.00	0.00
4.392	2.778	0.969	1.574	10.48	4.88	-	145.97	133.97	-203.95	-	-141.97	1.00	13.00
5.373	3.429	1.244	2.065	16.54	6.55	-	177.96	163.96	-205.95	-	-106.98	-2.00	24.99
6.353	4.140	1.409	2.555	29.36	8.81	-	218.95	229.95	-222.95	-	-97.98	6.00	44.99

A2

Applied load				Displacement		Stresses in the reinforcement N/mm²							
P kN	M kNm	T kNm	V kN	A_r rad/km	d_m mm	1	2	3	4	5	6	7	8
1.450	0.585	0.144	0.103	-	-	-	-	-	-	-	-	-	-
2.431	1.296	0.419	0.593	3.68	1.79	-16.00	50.99	47.99	-22.00	-3.00	5.00	-4.00	-2.00
3.411	2.007	0.694	1.084	7.59	3.26	-22.00	99.98	93.99	-30.99	35.99	21.00	30.99	7.00
4.392	2.718	0.969	1.574	12.05	4.75	-32.99	129.97	114.97	-39.99	148.97	26.99	47.99	14.00
5.373	3.429	1.244	2.065	20.33	6.48	-33.99	155.96	149.97	-35.99	yield	42.99	64.99	20.00
6.353	4.140	1.519	2.555	39.36	8.86	-30.99	182.96	189.96	-31.99		66.98	97.98	25.99
7.334	4.851	1.657	3.045	72.97	12.92	-152.97	yield	-	25.99		156.96	160.96	48.99

A3

Applied load				Displacement		Stresses in the reinforcement N/mm^2							
P kN	M kNm	T kNm	V kN	A_r rad/km	d_m mm	1	2	3	4	5	6	7	8
1.450	0.585	0.144	0.103	-	-	-	-	-	-	-	-	-	-
2.431	1.296	0.419	0.593	2.56	1.05	-14.80	21.00	18.00	-16.00	-1.00	64.99	-2.00	-2.00
3.411	2.007	0.694	1.084	6.21	2.30	-23.39	67.98	53.99	-25.99	-1.00	80.98	8.00	6.00
4.392	2.718	0.969	1.574	10.28	3.84	-28.39	110.98	83.98	-31.99	0.00	-173.96	18.00	19.60
5.373	3.429	1.244	2.065	17.75	5.67	-32.39	151.97	125.97	-30.99	-1.00	-101.98	27.99	31.99
6.353	4.140	1.519	2.555	29.83	7.35	-35.99	194.96	158.96	-33.99	4.00	129.97	42.99	42.99
7.334	4.851	1.794	3.045	43.03	9.36	-45.39	241.95	205.95	-37.99	19.00	-	64.99	47.99
8.315	5.562	-	3.536	74.21	15.82	-22.39	262.94	-	-140.37	83.98	-	-	131.97

A4

Applied load				Displacement		Stresses in the reinforcement N/mm²							
P kN	M kNm	T kNm	V kN	A_r rad/km	d_m mm	1	2	3	4	5	6	7	8
1.450	0.585	0.144	0.103	-	-	-	-	-	-	-	-	-	-
2.431	1.296	0.419	0.593	3.26	1.07	-10.00	30.59	21.00	-11.00	2.00	4.00	3.00	6.60
3.411	2.007	0.694	1.084	7.36	2.19	-14.00	96.18	63.99	-22.00	3.00	34.59	10.00	-16.40
4.392	2.718	0.969	1.574	10.93	3.84	-22.00	141.57	115.97	-27.99	0.00	55.59	35.99	13.60
5.373	3.429	1.244	2.065	23.91	5.51	-27.59	175.56	142.77	-30.59	0.00	65.99	56.99	33.59
6.353	4.140	1.519	2.555	30.75	7.46	-35.99	212.55	179.56	-35.99	1.40	81.98	72.98	50.59
7.334	4.851	1.794	3.045	43.37	11.40	-47.99	258.54	233.95	-97.98	16.00	129.97	106.98	77.58
8.315	5.562	2.070	3.536	69.02	13.38	-82.98	269.54	254.94	-122.97	46.99	133.97	104.98	105.58
9.295	6.273	2.207	4.026	70.14	15.55	-112.97	285.54	272.94	-119.97	50.99	136.97	103.98	121.57

A5

	Applied load				Displacement		Stresses in the reinforcement N/mm²							
P kN	M kNm	T kNm	V kN		A_r rad/km	d_m mm	1	2	3	4	5	6	7	8
1.450	0.585	0.144	0.103		-	-	-	-	-	-	-	-	-	-
3.902	2.362	0.419	1.329		1.21	0.45	1.00	11.00	11.00	-3.00	0.00	6.00	3.00	4.00
6.353	4.140	0.694	2.555		2.30	2.48	-33.59	131.97	112.97	-20.99	-2.00	4.00	5.00	0.00
8.805	5.917	0.969	3.780		6.34	5.62	-55.39	202.55	166.96	-28.99	0.40	0.40	3.60	0.00
7.334	4.851	1.244	3.045		10.03	5.37	45.99	-205.95	156.96	-28.99	-2.20	-201.35	1.20	-3.60
8.315	5.562	1.519	3.536		21.21	7.21	-53.99	220.94	181.15	-38.79	-2.00	-1.40	1.00	-1.80
9.295	6.273	-	4.026		23.45	7.92	-65.98	266.93	215.55	-46.99	3.00	0.00	1.20	-2.00

A6

Applied load				Displacement		Stresses in the reinforcement N/mm²							
P kN	M kNm	T kNm	V kN	A_r rad/km	d_m mm	1	2	3	4	5	6	7	8
1.450	0.585	0.144	0.103	-	-	-	-	-	-	-	-	-	-
2.431	1.396	0.419	0.593	3.26	1.58	-28.99	78.98	42.99	-28.99	-3.00	3.00	-2.00	0.00
3.411	2.007	0.694	1.084	6.58	3.01	-43.99	159.96	79.98	-34.99	-4.00	6.00	27.99	4.00
4.392	2.718	0.969	1.574	9.80	4.54	-54.99	225.95	113.97	-39.99	-5.00	10.00	36.99	3.00
5.373	3.429	1.244	2.065	14.13	6.29	-66.98	284.94	141.97	-49.99	-10.00	20.00	91.98	0.00
6.353	4.140	1.519	2.555	23.32	7.97	-66.98	yield	176.96	-48.99	-5.00	29.00	108.98	5.00
7.334	4.851	1.794	3.045	30.90	9.74	-75.98		206.95	-48.99	-2.00	38.99	115.97	5.00
8.315	5.562	2.070	3.536	58.18	12.35	-63.99		268.94	-26.99	36.99	60.99	yield	20.00
9.295	6.273	2.207	4.026	77.52	21.54	-		-	-	-	69.98	-	-

A7

Applied load				Displacement		Stresses in the reinforcement N/mm²							
P kN	M kNm	T kNm	V kN	A_r rad/km	d_m mm	1	2	3	4	5	6	7	8
1.450	0.585	0.144	0.103	-	-	-	-	-	-	-	-	-	-
2.431	1.396	0.419	0.593	1.55	0.42	-5.40	6.80	6.20	-6.40	0.80	-0.60	-0.40	0.40
3.411	2.007	0.694	1.084	3.51	0.85	-9.60	13.40	17.40	-12.60	2.20	1.00	5.40	2.20
4.392	2.718	0.969	1.574	4.33	1.50	-14.40	40.79	53.19	-19.60	6.00	0.40	12.60	10.00
5.373	3.429	1.244	2.065	9.38	2.82	-14.40	108.78	99.98	-26.59	6.80	0.20	24.59	32.99
6.353	4.140	1.519	2.555	17.13	4.50	-16.00	143.97	142.37	-29.79	8.00	-1.60	30.39	49.59
7.334	4.851	1.794	3.045	24.38	6.09	-13.60	181.76	173.96	-24.79	11.60	-0.80	36.59	64.79
8.315	5.562	2.070	3.536	37.00	8.42	-11.60	229.55	204.75	-22.20	10.60	-4.80	25.19	77.18
9.295	6.273	2.345	4.026	51.62	12.01	-7.80	277.14	239.55	-26.99	22.00	-3.00	20.40	76.55
10.276	6.984	-	4.516	64.05	23.08	-	294.93	267.54	-108.78	10.20	-5.00	12.00	72.78

A8

Applied load				Displacement		Stresses in the reinforcement N/mm^2							
P kN	M kNm	T kNm	V kN	A_r rad/km	d_m mm	1	2	3	4	5	6	7	8
1.450	0.585	0.144	0.103	-	-	-	-	-	-	-	-	-	-
2.431	1.396	0.419	0.593	1.46	0.70	-12.00	14.00	-	-11.00	4.00	2.00	0.00	1.00
3.411	2.007	0.694	1.084	3.17	1.19	-16.00	23.99	-	-12.00	6.00	2.00	4.00	3.00
4.392	2.718	0.969	1.574	5.14	2.07	-26.00	90.98	-	-22.99	3.00	10.00	36.00	-3.00
5.373	3.429	1.244	2.065	7.45	3.28	-29.00	121.97	-	-23.99	4.00	14.00	32.99	0.00
6.353	4.140	1.519	2.555	10.45	4.64	-32.00	155.96	-	-26.99	4.00	18.00	-7.00	-1.00
7.334	4.851	1.794	3.045	14.78	6.35	-31.00	193.96	-	-26.99	4.00	25.99	-35.99	3.00
8.315	5.562	2.070	3.536	21.06	7.98	-24.00	238.95	-	-22.99	10.00	33.99	-30.99	4.00
9.295	6.273	2.345	4.026	30.67	12.44	-32.00	yield	-	-18.00	61.99	61.99	106.98	12.00
10.276	6.984	2.620	4.516	30.92	17.78	-54.99	-	-	-33.99	22.99	188.95	yield	29.99
11.257	7.695	-	5.007	31.12	26.04	-8.99	-	-	-50.99	-21.00	-	.	36.99

A9

Applied load				Displacement		Stresses in the reinforcement N/mm^2							
P kN	M kNm	T kNm	V kN	A_r rad/km	d_m mm	1	2	3	4	5	6	7	8
1.244	0.436	0.144	0.00	-	-	-	-	-	-	-	-	-	-
		0.419		0.99	0.03	-6.00	-0.60	-2.20	-1.40	-0.60	-1.80	-4.40	-2.40
		0.694		2.66	0.08	-3.40	-1.80	-2.80	-0.80	0.40	0.40	-4.00	1.20
		0.969		4.50	0.10	-10.60	-2.80	-2.40	-0.20	0.40	1.60	-11.40	2.40
		1.244		5.93	0.13	-0.60	-1.40	-3.00	-1.00	-0.20	2.40	-17.00	-1.00
		1.519		7.98	0.18	-24.59	2.00	-1.60	-2.20	-0.20	7.60	16.00	16.80
		1.794		11.46	0.38	-19.40	0.80	28.19	8.60	4.40	17.20	-	-112.97
		2.070		38.97	-0.99	-	111.97	41.99	134.57	67.18	3.20	-	-356.11
		2.345		55.02	-2.18	-	163.76	20.19	195.95	98.38	71.38	-	190.75

AR4

214

Stresses in the reinforcement N/mm²

Applied load				Displacement		Stresses in the reinforcement N/mm²							
P kN	M KNm	T kNm	V kN	A_r rad/Km	d_m mm	1	2	3	4	5	6	7	8
1.244	0.436	0.144	0.00	-	-	-	-	-	-	-	-	-	-
		0.419		0.86	0.00	-2.60	-20.19	-0.20	-0.20	-1.00	-1.00	-1.60	-1.00
		0.694		2.05	-0.03	-2.80	-20.79	1.60	-1.20	-1.60	-0.40	-1.80	-0.60
		0.969		3.27	-0.03	-4.80	-22.39	-5.20	-1.00	-2.00	-0.60	-1.80	0.00
		1.244		4.75	-0.03	-3.00	-19.80	-5.40	-1.80	-1.40	-1.80	-2.80	1.20
		1.519		6.35	-0.05	-1.60	-15.20	-3.20	1.00	0.60	0.60	-3.40	6.40
		1.794		17.08	-0.08	57.39	39.39	15.20	78.78	28.19	19.99	-7.20	24.79
		2.070		43.00	-1.80	110.17	81.38	101.37	182.75	70.78	29.79	66.18	45.79
		2.345		65.04	-3.73	149.16	111.37	118.37	279.73	107.17	31.79	105.96	43.39
		2.441		74.08	0.50	132.17	94.38	96.18	254.34	107.57	-3.00	140.36	73.78

AR5

Applied load				Displacement		Stresses in the reinforcement N/mm^2							
P kN	M kNm	T kNm	V kN	A_r rad/km	d_m mm	1	2	3	4	5	6	7	8
1.244	0.436	0.144	0.00	-	-	-	-	-	-	-	-	-	-
		0.419		0.44	0.03	-0.20	39.79	-0.20	0.00	1.00	0.80	-0.40	3.00
		0.694		1.44	0.03	-0.20	37.19	-0.60	0.80	0.60	-0.40	0.00	0.80
		0.969		2.22	0.03	-0.60	-1.20	-0.80	0.20	0.80	-1.40	0.40	-6.20
		1.244		2.98	0.03	-1.20	-59.19	-1.80	0.40	0.60	-2.80	0.60	-15.40
		1.519		3.91	0.03	-2.20	-91.98	-2.20	0.20	0.60	-3.20	-0.20	-22.19
		1.794		4.96	0.03	-3.00	-95.98	-2.20	1.20	1.20	-2.60	0.40	-23.79
		2.070		6.10	0.03	-2.80	-91.98	-2.00	1.20	1.60	-3.20	1.20	-22.59
		2.345		7.30	0.03	82.78	287.13	11.60	5.60	6.80	0.20	66.18	34.19
		2.620		9.90	0.02	266.13	219.15	29.59	21.19	5.20	-47.19	103.37	47.99
		2.895		10.77	0.15	331.32	186.15	31.39	22.99	7.20	-44.39	119.17	58.19
		3.170		15.79	-0.03	yield	216.15	34.99	31.19	7.00	-42.39	194.75	70.58
		3.445		53.52	-2.59	-	-	149.16	275.33	-5.60	-1.40	307.72	72.58
				61.98	-1.02	-	-	-	-	-	-	-	-

AR9

Applied load				Displacement		Stresses in the reinforcement N/mm²							
P kN	M kNm	T kNm	V kN	A_r rad/km	d_m mm	1	2	3	4	5	6	7	8
1.450	0.585	0.144	0.103	-	-	-	-	-	-	-	-	-	-
2.431	1.296	0.419	0.593	2.13	0.76	-1.00	52.99	-81.99	-107.97	0.00	-4.00	-1.00	-3.00
3.411	2.007	0.694	1.084	4.18	2.16	-8.00	114.97	-11.00	-74.98	3.00	3.00	4.00	1.00
4.392	2.718	0.969	1.574	7.49	3.43	-10.00	155.96	27.99	-41.99	2.00	1.00	0.00	8.00
5.373	3.429	1.244	2.065	12.92	5.26	-15.00	197.95	68.98	-65.98	-9.00	-7.00	-7.00	13.00
6.353	4.140	1.519	2.555	18.20	7.26	-29.99	237.94	125.97	-68.98	1.00	42.99	0.00	30.99
7.334	4.851	1.794	3.045	24.27	8.33	-31.99	273.93	156.96	-79.98	4.00	11.00	2.00	42.99
8.315	5.562	2.070	3.536	30.10	10.13	-39.99	yield	208.95	-83.98	8.00	19.00	2.00	52.99
		2.345		36.37	10.49	-41.99		225.94	-49.99	11.00	28.99	2.00	58.99
		2.620		52.80	11.00	-32.99		297.93	-29.99	28.99	42.99	12.00	72.98
		2.895		69.97	12.78	-13.00		308.92	-103.97	38.99	90.98	39.99	82.98
		2.936		101.69	17.83	-		-	-	-	-	-	-

B1

	Applied Load				Displacement		Stresses in the reinforcement N/mm²							
P kN	M kNm	T kNm	V kN		A_r rad/km	d_m mm	1	2	3	4	5	6	7	8
1.450	0.585	0.144	0.103		-	-	-	-	-	-	-	-	-	-
2.431	1.296	0.419	0.593		2.59	1.15	-16.00	15.00	25.99	-15.00	-2.00	4.00	0.00	-1.00
3.411	2.007	0.694	1.084		6.21	2.52	-35.99	32.99	90.98	-29.99	-6.00	8.00	10.00	7.00
4.392	2.718	0.969	1.514		11.82	4.27	-48.99	45.99	134.97	-29.99	-8.00	6.00	14.00	14.00
5.373	3.429	1.244	2.065		18.66	6.17	-67.98	54.99	172.96	-11.00	-20.99	11.00	21.99	22.99
6.353	4.140	1.519	2.555		27.24	8.21	-121.97	98.98	210.95	-3.00	-15.00	13.00	26.99	26.99
7.334	4.851	1.794	3.045		37.41	9.76	-89.98	128.97	246.94	-15.00	-20.00	17.00	30.99	34.99
8.315	5.562	2.070	3.536		45.54	12.13	-193.95	243.94	yield	-11.00	-13.00	27.99	36.99	57.99
		2.276			70.03	14.48	-	-		-	-117.97	59.99	27.99	96.98

B2

Applied load				Displacement		Stresses in the reinforcement N/mm²							
P kN	M kNm	T kNm	V kN	A_r rad/km	d_m mm	1	2	3	4	5	6	7	8
1.450	0.585	0.144	0.103	–	–	–	–	–	–	–	–	–	–
2.431	1.296	0.419	0.593	1.60	2.15	-14.00	–	45.99	-9.00	3.00	1.00	2.00	8.00
3.411	2.007	0.694	1.084	4.66	2.39	-23.99	–	92.98	-16.00	3.00	1.00	3.00	28.99
4.392	2.718	0.969	1.574	9.30	3.76	-29.99	–	123.97	-16.99	7.00	3.00	2.00	39.99
5.373	3.429	1.244	2.065	14.33	5.45	-37.99	–	155.96	-18.00	11.00	4.00	1.00	53.99
6.353	4.140	1.519	2.555	21.44	6.99	-39.99	–	157.96	-24.99	20.99	7.00	0.00	65.98
7.334	4.851	1.794	3.045	33.00	10.15	-48.99	–	193.95	-31.99	33.99	11.00	11.00	80.98
8.315	5.562	2.070	3.536	43.62	11.44	-44.99	–	215.95	-30.99	-196.95	14.00	31.99	118.97
		2.345		53.98	13.05	-50.99	–	199.95	-25.99	–	6.00	109.97	52.99
		2.413		78.87	23.38	–	–	–	–	–	240.94	88.98	–

B3

Applied Load				Displacement		Stresses in the reinforcement N/mm²							
P kN	M kNm	T kNm	V kN	A_r rad/km	d_m mm	1	2	3	4	5	6	7	8
1.450	0.585	0.144	0.103	-	-	-	-	-	-	-	-	-	-
2.431	1.296	0.419	0.594	1.63	0.74	-11.00	53.99	31.99	-20.00	0.00	-4.00	176.96	-3.00
3.411	2.007	0.694	1.084	4.08	1.84	-20.99	87.98	61.98	-29.99	0.00	-3.00	175.96	-9.00
4.392	2.718	0.969	1.574	8.00	3.33	-28.99	121.97	88.98	-34.99	1.00	1.00	175.96	-10.00
5.373	3.429	1.244	2.065	13.77	4.97	-34.99	156.96	117.97	-34.99	5.00	8.00	175.96	-10.00
6.353	4.140	1.519	2.555	21.93	6.68	-40.99	195.95	144.96	-40.99	11.00	16.00	175.96	-8.00
7.334	4.851	1.794	3.045	34.67	8.57	-45.99	248.94	171.96	-48.99	23.99	20.00	175.96	-3.00
8.315	5.562	2.070	3.536	52.52	10.43	-43.99	yield	213.95	-60.98	48.99	58.99	178.96	9.00
		2.207		78.62	23.23	-49.99		-	-	-	333.92	368.91	-

B4

Applied Load				Displacement		Stresses in the reinforcement N/mm^2							
P kN	M kNm	T kNm	V kN	A$_r$ rad/km	d$_m$ mm	1	2	3	4	5	6	7	8
1.450	0.585	0.144	0.103	-	-	-	-	-	-	-	-	-	-
2.431	1.296	0.419	0.593	1.88	1.08	-16.00	40.99	29.99	-22.99	-44.99	-35.99	-	68.98
3.411	2.007	0.694	1.084	4.55	2.35	-20.99	79.98	72.98	-12.00	-35.99	-23.99	-	70.98
4.392	2.718	0.969	1.574	7.56	3.41	-124.97	-2.00	-22.99	-131.97	-162.96	-152.96	-	-67.98
5.373	3.429	1.244	2.065	12.86	6.16	-153.96	19.00	7.00	-109.97	-140.96	-119.97	-	-41.99
6.353	4.140	1.519	2.555	19.11	7.08	-119.97	84.98	69.98	-76.98	-109.97	-56.99	-	-20.00
7.334	4.851	1.794	3.045	29.46	8.97	-89.98	132.97	136.97	-30.99	-76.98	7.00	-	6.00
8.315	5.562	2.001	3.536	37.36	27.85	-	-	-	-104.97	-	207.95	-	68.98

B5

Applied Load				Displacement		Stresses in the reinforcement N/mm²							
P kN	M kNm	T kNm	V kN	A_r rad/km	d_m mm	1	2	3	4	5	6	7	8
1.450	0.585	0.144	0.103	-	-	-	-	-	-	-	-	-	-
2.431	1.296	0.419	0.593	1.51	0.90	-12.00	22.00	19.00	-16.00	2.00	21.00	-1.00	0.00
3.411	2.007	0.694	1.084	4.09	1.87	-21.00	65.99	56.99	-28.99	6.00	20.00	3.00	-1.00
4.392	2.718	0.969	1.574	6.43	3.03	-29.99	112.97	101.98	-34.99	9.00	18.00	-19.00	4.00
5.373	3.429	1.244	2.065	12.98	5.37	-36.99	145.97	125.97	-36.99	18.00	24.99	-11.00	8.00
6.353	4.140	1.519	2.555	21.63	6.80	-41.99	192.96	151.97	-34.99	43.99	44.99	-2.00	15.00
7.334	4.851	1.794	3.045	32.31	8.67	-47.99	239.95	187.96	-41.99	81.98	72.98	22.99	32.99
8.315	5.562	1.932	3.536	42.86	21.98	-55.99	282.94	208.95	-56.99	159.96	83.98	40.99	48.99

B6

Applied Load				Displacement		Stresses in the reinforcement N/mm^2							
P kN	M kNm	T kNm	V kN	A_r rad/km	d_m mm	1	2	3	4	5	6	7	8
1.450	0.585	0.144	0.103	-	-	-	-	-	-	-	-	-	-
2.431	1.296	0.419	0.593	1.77	0.76	-17.00	15.00	13.00	-	2.00	-2.00	0.00	0.00
3.411	2.007	0.694	1.084	4.33	1.88	-30.00	68.99	69.99	-	3.00	0.00	2.00	2.00
4.392	2.718	0.969	1.574	8.59	2.82	-34.00	101.99	98.99	-	-1.00	-2.00	2.00	9.00
5.373	3.429	1.244	2.065	17.73	5.49	-47.38	161.98	158.98	-	5.00	4.00	20.00	23.00
6.353	4.140	1.519	2.555	36.25	7.42	-38.00	195.98	187.98	-	42.00	14.00	24.00	37.00
7.334	4.851	1.588	3.045	62.57	10.46	-48.00	237.98	213.98	-	105.99	24.00	14.00	53.99

B7

| Applied Load | | | | Displacement | | Stresses in the reinforcement N/mm² | | | | | | | |
P kN	M kNm	T kNm	V kN	A_r rad/km	d_m mm	1	2	3	4	5	6	7	8
1.244	0.436	0.144	0.0	-	-	-	-	-	-	-	-	-	-
		0.419		1.63	-0.03	-	-	-	-	-	-	-	-
		0.694		3.44	-0.04	-	-	-	-	-	-	-	-
		0.969		5.04	-0.06	-	-	-	-	-	-	-	-
		1.244		6.48	-0.19	-	-	-	-	-	-	-	-
		1.519		8.11	-0.20	-	-	-	-	-	-	-	-
		1.794		11.13	-0.25	-	-	-	-	-	-	-	-
		2.070		19.86	-1.05	-	-	-	-	-	-	-	-
		2.345		34.75	-2.54	-	-	-	-	-	-	-	-
		2.620		47.99	-3.59	-	-	-	-	-	-	-	-
		2.661		61.33	-4.24	-	-	-	-	-	-	-	-

BR2

Applied Load				Displacement		Stresses in the reinforcement N/mm^2							
P kN	M kNm	T kNm	V kN	A_r rad/km	d_m mm	1	2	3	4	5	6	7	8
1.450	0.585	0.144	0.103	-	-	-	-	-	-	-	-	-	-
2.431	1.296	0.419	0.593	2.21	1.00	-	-	-	-	-	-	-	-
3.411	2.007	0.694	1.084	4.22	1.85	-	-	-	-	-	-	-	-
4.392	2.718	0.969	1.574	7.68	2.77	-	-	-	-	-	-	-	-
5.373	3.429	1.244	2.065	11.54	3.63	:	-	-	-	-	-	-	-
6.353	4.140	1.519	2.555	18.01	5.44	-	-	-	-	-	-	-	-
7.334	4.851	1.794	3.045	26.87	7.04	-	-	-	-	-	-	-	-
8.315	5.562	2.070	3.536	39.87	8.81	-	-	-	-	-	-	-	-
		2.345		71.91	9.60	-	-	-	-	-	-	-	-
		2.386		99.60	9.88	-	-	-	-	-	-	-	-

BR4

Applied Load				Displacement		Stresses in the reinforcement N/mm^2							
P kN	M kNm	T kNm	V kN	A$_r$ rad/km	d$_m$ mm	1	2	3	4	5	6	7	8
1.450	0.585	0.144	0.103	-	-	-	-	-	-	-	-	-	-
2.431	1.296	0.419	0.593	1.89	0.99	-	-	-	-	-	-	-	-
3.411	2.007	0.694	1.084	4.65	1.88	-	-	-	-	-	-	-	-
4.392	2.718	0.969	1.574	8.08	3.30	-	-	-	-	-	-	-	-
		1.244		11.15	3.51	-	-	-	-	-	-	-	-
		1.579		67.06	4.49	-	-	-	-	-	-	-	-

BR7

Applied Load				Displacement		Stresses in the reinforcement N/mm^2								
P kN	M kNm	T kNm	V kN	A_r rad/km	d_m mm	1	2	3	4	5	6	7	8	
1.450	0.585	0.144	0.103	-	-	-	-	-	-	-	-	-	-	
2.431	1.296	0.419	0.593	2.72	2.01	-21.99	153.96	137.97	-13.00	-7.00	32.99	3.00	-6.20	
3.411	2.007	0.694	1.084	6.42	4.06	-14.00	219.95	185.95	-5.00	-4.00	34.99	12.00	-8.20	
4.392	2.718	0.969	1.574	14.14	9.93	63.98	319.92		13.00	103.97	-5.00	41.99	-4.20	
5.373	3.429	1.244	2.065	37.82	37.72	-154.96	yield	-	-368.91	299.93	4.00	132.97	16.80	
6.353	4.140	-	2.555	-	-	-	-	-	-	303.92	-	-	-	C1

227

Applied Load				Displacement		Stresses in the reinforcement N/mm²							
P kN	M kNm	T kNm	V kN	A_r rad/km	d_m mm	1	2	3	4	5	6	7	8
1.450	0.585	0.144	0.103	-	-	-	-	-	-	-	-	-	-
2.431	1.296	0.419	0.593	1.37	2.50	-35.99	116.97	103.97	-31.99	-	-	10.00	11.00
3.411	2.007	0.694	1.084	4.27	4.54	-51.99	171.96	161.96	-43.99	-	-	14.00	6.00
4.392	2.718	0.969	1.574	9.57	7.54	-47.99	250.94	267.93	-53.99	-	-	29.99	11.00
5.373	3.429	1.244	2.065	22.42	21.86	9.00	186.95	119.97	-89.98	-	-	-	25.99
6.353	4.140	1.519	2.555	39.24	41.00	-293.93	150.96	129.97	-85.98	-	-	-	37.99

C2

Applied Load				Displacement		Stresses in the reinforcement N/mm^2							
P kN	M kNm	T kNm	V kN	A_r rad/k_m	d_m mm	1	2	3	4	5	6	7	8
1.450	0.585	0.144	0.103	-	-	-	-	-	-	-	-	-	-
2.431	1.296	0.419	0.593	1.97	0.38	-2.00	0.00	8.00	-4.00	-3.00	0.00	1.00	4.00
3.411	2.007	0.694	1.084	4.33	1.07	-17.00	43.99	60.00	-12.00	-2.00	3.00	1.00	1.00
4.392	2.718	0.969	1.574	7.76	2.24	-28.99	73.98	95.98	-18.00	-6.00	4.00	-2.00	-1.00
5.373	3.429	1.244	2.065	13.71	4.06	-23.99	111.97	139.97	-17.00	-1.00	23.99	2.00	1.00
6.353	4.140	1.519	2.555	22.10	6.58	-33.99	157.96	194.95	-26.99	6.00	40.99	3.00	1.00
		1.794		36.13	7.67	-23.99	179.96	203.95	-23.99	24.99	59.99	7.00	-1.00
		1.932		70.41	7.80	-8.00	175.96	184.95	-20.00	33.99	62.98	9.00	3.00

C3

Applied Load				Displacement		Stresses in the reinforcement N/mm²							
P kN	M kNm	T kNm	V kN	A_r rad/km	d_m mm	1	2	3	4	5	6	7	8
1.450	0.585	0.144	0.103	-	-	-	-	-	-	-	-	-	-
2.431	1.296	0.419	0.593	2.48	1.09	-29.99	20.99	57.99	-16.00	-12.00	2.00	14.00	0.00
3.411	2.007	0.694	1.084	5.44	1.80	-27.99	49.99	101.97	8.00	-1.00	13.00	31.99	18.00
4.392	2.718	0.969	1.574	9.66	3.12	-47.99	75.98	159.96	14.00	-10.60	16.00	33.99	136.97
5.373	3.429	1.244	2.065	16.08	4.70	-59.99	107.97	200.95	-42.99	3.00	25.99	31.99	275.93
6.353	4.140	1.519	2.555	23.21	5.92	-67.98	131.97	220.94	-57.99	12.00	23.99	29.99	352.91
		1.794		35.02	6.43	-59.99	137.97	225.94	-14.00	23.99	29.99	28.99	yield
		2.070		50.98	6.93	-51.99	143.96	234.94	-2.00	38.99	31.99	26.99	
		2.345		78.92	7.57	-30.99	160.96	223.94	-66.98	78.98	35.99	20.00	
		2.400			8.69	-	165.96	217.95	-12.00	93.98	40.99	22.99	

C4

Stresses in the reinforcement N/mm²

Applied Load				Displacement		Stresses in the reinforcement N/mm²							
P kN	M kNm	T kNm	V kN	A_r rad/km	d_m mm	1	2	3	4	5	6	7	8
1.534	0.614	0.144	0.103	-	-	-	-	-	-	-	-	-	-
2.515	1.325	0.419	0.593	0.83	0.69	-76.98	7.00	-16.00	-13.00	-23.99	5.00	-3.00	0.00
3.495	2.036	0.694	1.084	3.59	1.27	-133.97	43.99	28.99	-19.00	-24.99	7.00	21.99	6.00
4.475	2.747	0.969	1.574	6.94	1.98	-105.97	46.99	39.99	-21.99	-29.99	10.00	40.99	7.00
5.457	3.458	1.244	2.065	12.38	2.77	50.99	44.99	50.99	-22.99	-29.99	19.00	56.99	11.00
6.457	4.169	1.519	2.555	18.89	3.53	-134.97	-14.00	62.98	-29.99	-27.99	32.99	73.98	10.00
		1.794		27.81	3.86	-146.96	-14.00	62.98	-28.99	-19.00	48.99	79.98	29.99
		2.070		41.93	4.11	-137.97	22.99	65.98	-23.99	71.98	78.98	124.97	79.98
		2.345		57.15	4.67	-146.96	39.99	74.98	-24.99	102.97	127.97	145.96	99.98

C5

Applied Load				Displacement		Stresses in the reinforcement N/mm²							
P kN	M kNm	T kNm	V kN	A_r rad/km	d_m mm	1	2	3	4	5	6	7	8
1.244	0.436	0.144	0.0	-	-	-	-	-	-	-	-	-	-
		0.419		1.20	0.03	-1.00	0.00	0.00	1.00	7.00	-1.00	10.00	0.00
		0.694		2.72	0.05	0.00	0.00	1.00	2.00	10.00	1.00	15.00	1.00
		0.969		4.24	0.08	0.00	0.00	0.00	2.00	11.00	1.00	17.00	3.00
		1.244		5.95	0.10	2.00	2.00	2.00	3.00	17.00	2.00	19.00	5.00
		1.519		7.89	0.18	6.00	2.00	2.00	3.00	21.99	1.00	20.99	16.00
		1.794		20.01	1.04	196.95	63.98	73.95	59.99	30.99	14.00	122.97	160.96
		2.001		55.59	4.29	273.93	101.97	77.98	166.96	45.99	46.99	119.97	238.94

CR1

Applied Load				Displacement		Stresses in the reinforcement N/mm^2							
P kN	M kNm	T kNm	V kN	A_r rad/km	d_m mm	1	2	3	4	5	6	7	8
1.244	0.436	0.144	0.0	-	-	-	-	-	-	-	-	-	-
		0.419		0.99	0.03	-6.00	-0.60	-2.20	-1.40	-0.60	-1.80	-4.40	-2.40
		0.694		2.66	0.08	-3.40	-1.80	-2.80	-0.80	0.40	0.40	-4.00	1.20
		0.969		4.50	0.10	-10.60	-2.80	-2.40	-0.20	0.40	1.60	-11.40	2.40
		1.244		5.93	0.13	-0.60	-1.40	-3.00	-1.00	-0.20	2.40	-17.00	-1.00
		1.519		7.98	0.18	-24.59	2.00	-1.60	-0.20	-0.20	7.60	16.00	16.80
		1.794		11.46	0.38	-19.40	0.80	28.19	8.60	4.40	17.20	-	-112.97
		2.070		38.97	-0.99	-	111.97	41.99	134.57	67.18	3.20	-	-356.11
		2.345		55.02	-2.18	-	163.97	20.19	195.95	98.38	71.38	-	190.75

CR3

Applied Load				Displacement		Stresses in the reinforcement N/mm^2							
P kN	M kNm	T kNm	V kN	A$_r$ rad/km	d$_m$ mm	1	2	3	4	5	6	7	8
1.244	0.436	0.144	0.00	-	-	-	-	-	-	-	-	-	-
		0.419		0.87	0.03	-3.00	-	3.00	2.00	-8.00	16.00	2.00	-
		0.694		1.88	0.08	-6.00	-	0.00	5.00	16.00	6.00	20.00	-
		0.969		3.12	0.08	-9.00	-	4.00	7.00	-47.99	13.00	25.99	-
		1.244		4.26	0.08	-7.00	-	5.00	9.00	-8.00	28.99	27.99	-
		1.519		6.76	0.13	-1.00	-	8.00	10.00	-30.00	59.99	29.99	-
		1.794		11.91	0.13	148.96	-	8.00	63.98	-29.99	-160.96	29.99	-
		2.070		26.81	-2.26	228.94	-	25.99	135.97	-80.98	-347.91	52.99	-
		2.345		39.12	-3.99	yield	-	13.00	190.95	-189.95	-272.93	-29.99	-
		2.592		74.31	-4.55	-	-	-104.97	295.93	-140.96	-	-	-

CR5

Applied Load				Displacement		Stresses in the reinforcement N/mm^2							
P kN	M kNm	T kNm	V kN	A_r rad/km	d_m mm	1	2	3	4	5	6	7	8
0.953	0.411	0.144	0.103	-	-	-	-	-	-	-	-	-	-
1.934	1.122	0.419	0.593	4.53	2.85	-	-	-	-	-	-	-	-
2.914	1.833	0.694	1.084	18.91	4.85	-	-	-	-	-	-	-	-
3.895	2.544	0.969	1.574	40.03	7.24	-	-	-	-	-	-	-	-
4.877	3.255	1.244	2.065	51.81	8.76	-	-	-	-	-	-	-	-
5.856	3.966	1.313	2.555	102.48	14.05	-	-	-	-	-	-	-	-

D1

Applied Load				Displacement		Stresses in the reinforcement N/mm^2							
P kN	M kNm	T kNm	V kN	A_r rad/km	d_m mm	1	2	3	4	5	6	7	8
1.167	0.485	0.144	0.103	-	-	-	-	-	-	-	-	-	-
2.148	1.196	0.419	0.593	3.43	1.65	-52.00	46.00	50.00	-18.00	1.00	2.00	-	9.00
3.128	1.907	0.694	1.084	9.98	3.89	-57.00	113.00	119.00	-31.00	2.00	17.00	-	23.00
4.109	2.618	0.969	1.574	21.73	6.12	-64.00	166.00	165.00	-36.00	3.00	32.00	-	30.00
5.090	3.329	1.244	2.065	45.71	8.26	-62.00	223.00	193.00	-41.00	14.00	57.00	-	-38.00
6.070	4.040	1.519	2.555	56.52	9.80	-43.40	260.00	223.00	-45.00	33.00	46.00	-	46.00
7.051	4.751	1.794	3.045	88.11	13.44	-197.00	yield	274.00	-72.00	139.00	-100.00	-	59.00
		2.028		109.53	16.48	-155.00		269.00	-67.00	316.00	-111.00	-	53.00

D2

Applied Load				Displacement		Stresses in the reinforcement N/mm²							
P kN	M kNm	T kNm	V kN	A_r rad/km	d_m mm	1	2	3	4	5	6	7	8
1.379	0.560	0.144	0.103	-	-	-	-	-	-	-	-	-	-
2.360	1.271	0.419	0.593	0.71	1.35	-	-	-	-	-	-	-	-
3.340	1.982	0.694	1.084	3.15	2.95	-	-	-	-	-	-	-	-
4.321	2.693	0.969	1.574	6.86	5.13	-	-	-	-	-	-	-	-
5.302	3.404	1.244	2.065	11.87	7.04	-	-	-	-	-	-	-	-
6.282	4.115	1.519	2.555	18.26	9.09	-	-	-	-	-	-	-	-
7.263	4.826	1.794	3.045	28.12	11.63	-	-	-	-	-	-	-	-
		2.070		47.45	13.18	-	-	-	-	-	-	-	-
		2.345		74.43	17.91	-	-	-	-	-	-	-	-
		2.372		79.08	24.21	-	-	-	-	-	-	-	-

D3

Applied Load				Displacement		Stresses in the reinforcement N/mm²							
P kN	M kNm	T kNm	V kN	A_r rad/km	d_m mm	1	2	3	4	5	6	7	8
1.592	0.635	0.144	0.103	—	—	—	—	—	—	—	—	—	—
2.574	1.346	0.419	0.593	0.91	1.04	-16.00	49.99	-8.00	-4.00	20.00	-2.00	-13.00	-10.00
3.553	2.057	0.694	1.084	2.84	2.16	-12.00	95.98	20.00	1.00	20.99	5.00	-8.00	4.00
4.534	2.768	0.969	1.574	5.05	3.40	-21.99	112.97	74.98	4.00	25.99	8.00	9.00	12.00
5.515	3.479	1.244	2.065	7.38	4.83	-43.99	140.96	119.97	-8.00	21.99	1.00	12.00	8.00
6.495	4.190	1.519	2.555	10.06	7.47	-69.98	198.95	202.95	-8.00	18.00	2.00	16.00	18.00
7.476	4.901	1.794	3.045	14.32	8.81	-83.98	223.94	249.94	-20.00	15.00	-8.00	23.99	16.00
		2.070		20.43	9.55	-80.98	251.94	270.93	-135.97	-14.00	-54.99	-2.00	-8.00
		2.345		26.98	10.31	-75.98	261.93	325.92	-203.95	-10.00	-43.99	13.00	14.00
		2.620		37.07	11.05	-87.98	245.94	yield	-302.92	10.00	-8.00	31.99	36.99
		2.895		53.25	12.90	-99.98	249.94		-340.42	24.99	-6.00	30.99	37.99
		3.032		81.60	18.14	-90.98	293.93			29.99	13.00	39.99	50.99

D4

238

	Applied Load			Displacement		Stresses in the reinforcement N/mm^2							
P kN	M kNm	T kNm	V kN	A_r rad/km	d_m mm	1	2	3	4	5	6	7	8
1.806	0.710	0.144	0.103	-	-	-	-	-	-	-	-	-	-
2.787	1.421	0.419	0.593	0.91	0.61	-69.98	-18.00	9.00	-24.99	-8.00	-5.00	2.00	0.00
3.767	2.132	0.694	1.084	2.45	2.01	-29.99	41.99	178.96	-73.98	-67.98	13.00	23.99	46.99
4.748	2.843	0.969	1.574	5.40	4.32	-43.99	59.99	288.93	-123.97	-111.97	11.00	31.99	62.98
5.729	3.554	1.244	2.065	8.68	6.20	-53.99	81.98	yield	-185.95	-151.96	17.00	43.99	88.98
6.709	4.265	1.519	2.555	.13.41	8.84	-63.98	85.98		-199.95	-105.97	22.99	59.99	150.96
7.690	4.976	1.794	3.045	19.48	11.81	-	173.96			-259.94	20.99	57.99	72.98
		2.070		25.75	14.07	-	227.94			-	19.00	69.98	130.97
		2.345		33.64	16.03	-	245.94			-	22.99	81.98	146.96
		2.413		51.98	29.95	-	-			-	-	-	287.93

D5

239

Applied Load				Displacement		Stresses in the reinforcement N/mm²							
P kN	M kNm	T kNm	V kN	A_r rad/km	d_m mm	1	2	3	4	5	6	7	8
0.953	0.262	0.144	0.0	-	-	-	-	-	-	-	-	-	-
		0.419		2.00	0.00	-1.00	2.00	-1.00	-	2.00	5.00	-10.00	2.00
		0.694		5.59	0.13	9.00	4.00	0.00	-	1.00	8.00	-32.99	2.00
		0.969		19.40	-	238.94	27.99	-131.97	-	319.92	-99.98	215.95	-82.98
		1.244		45.90	-0.10	281.93	55.99	-289.93	-	yield	-72.98	192.95	-79.98
													DR1

240

Applied Load				Displacement		Stresses in the reinforcement N/mm²							
P kN	M kNm	T kNm	V kN	A_r rad/km	d_m mm	1	2	3	4	5	6	7	8
1.379	0.411	0.144	0.0	-	-	-	-	-	-	-	-	-	-
		0.419		0.67	0.00	4.00	0.00	-1.00	0.00	0.00	9.00	4.00	4.00
		0.694		2.45	-0.10	11.00	1.00	-1.00	1.00	-1.00	11.00	19.00	6.00
		0.969		4.03	-0.08	16.00	1.00	0.00	1.00	-2.00	12.00	23.99	8.00
		1.244		5.83	-0.08	19.20	4.00	2.00	2.00	-2.00	13.00	24.99	12.00
		1.519		7.85	-0.05	20.00	11.00	6.00	5.00	-6.00	16.00	25.99	21.00
		1.794		13.07	-0.38	-19.00	79.98	77.98	125.97	137.97	105.97	26.99	-87.98
		2.042		37.41	-1.12	45.99	89.98	76.98	118.97	134.97	79.98	11.00	-56.99

DR3

Applied Load				Displacement		Stresses in the reinforcement N/mm²							
P KN	M kNm	T kNm	V kN	A_r rad/km	d_m mm	1	2	3	4	5	6	7	8
1.806	0.561	0.144	0.0	–	–	–	–	–	–	–	–	–	–
		0.419		0.46	0.03	0.00	1.00	–	1.00	2.00	-2.00	3.00	0.00
		0.694		1.10	0.05	1.00	1.00	–	2.00	6.00	-1.00	2.00	2.00
		0.969		1.94	0.13	1.00	3.00	–	2.00	9.00	0.00	2.00	4.00
		1.244		2.70	0.13	1.00	4.00	–	3.00	15.00	0.00	3.00	7.00
		1.519		3.57	0.18	2.00	7.00	–	6.00	21.99	1.00	4.00	10.00
		1.794		4.47	0.20	2.00	9.00	–	6.00	15.00	1.00	6.00	12.00
		2.070		5.15	0.25	3.00	11.00	–	8.00	21.99	4.00	9.00	16.00
		2.354		5.83	0.33	4.00	12.00	–	10.00	29.99	5.00	11.00	17.00
		2.620		7.64	0.30	65.98	35.99	–	119.97	13.00	-17.00	-19.00	-7.00
		2.895		9.10	0.36	119.97	10.00	–	153.96	-20.99	-136.97	-52.99	-6.00
		3.170		14.06	0.25	46.99	-79.98	–	182.95	-35.99	-229.94	-54.99	6.00
		3.280		31.20	-1.22	34.99	-79.98	–	183.95	-20.99	-220.94	-57.99	8.00

DR5

APPENDIX C

CRACK PATTERN OF THE FAILURE SECTION

FOR THE TEST BEAMS

This appendix contains the crack pattern of the failure section over a distance of 1000 mm for all the test beams.

The legend:
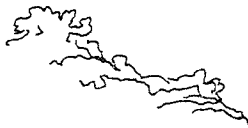
crushing of the concrete
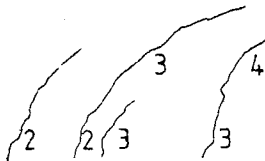
tensile cracks; the numbers refer to the loading stage at which the part of the crack has developed.

missing part of the beam
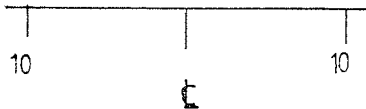
distance to the right or left of the centre line in mm
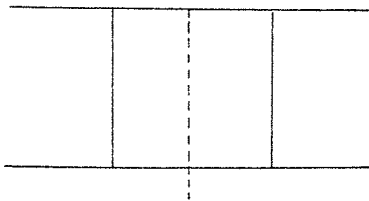
position of the bearing pads for the applied bending load.

The developed surfaces for all the beams from top to bottom are in the same order as in plates 3.1, 3.2, 3.3 and 3.4, for which:

TF   top face

NF   north face

BF   bottom face

SF   south face
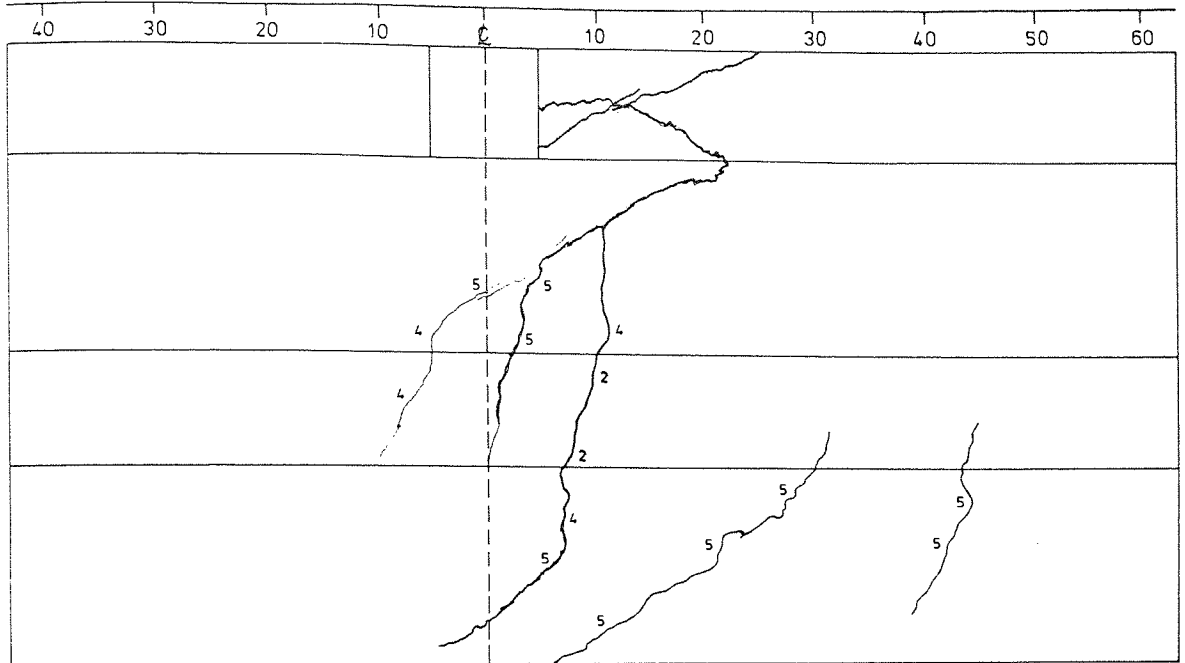
BEAM A1
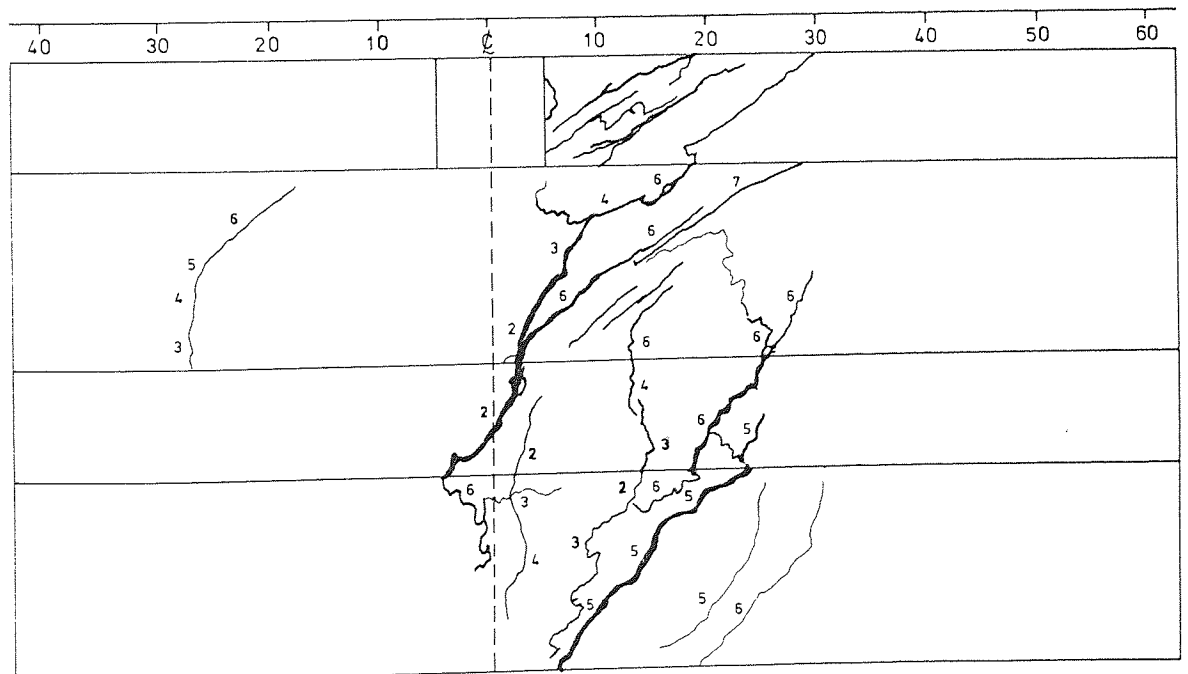
BEAM A2

BEAM A4

BEAM AR4

245
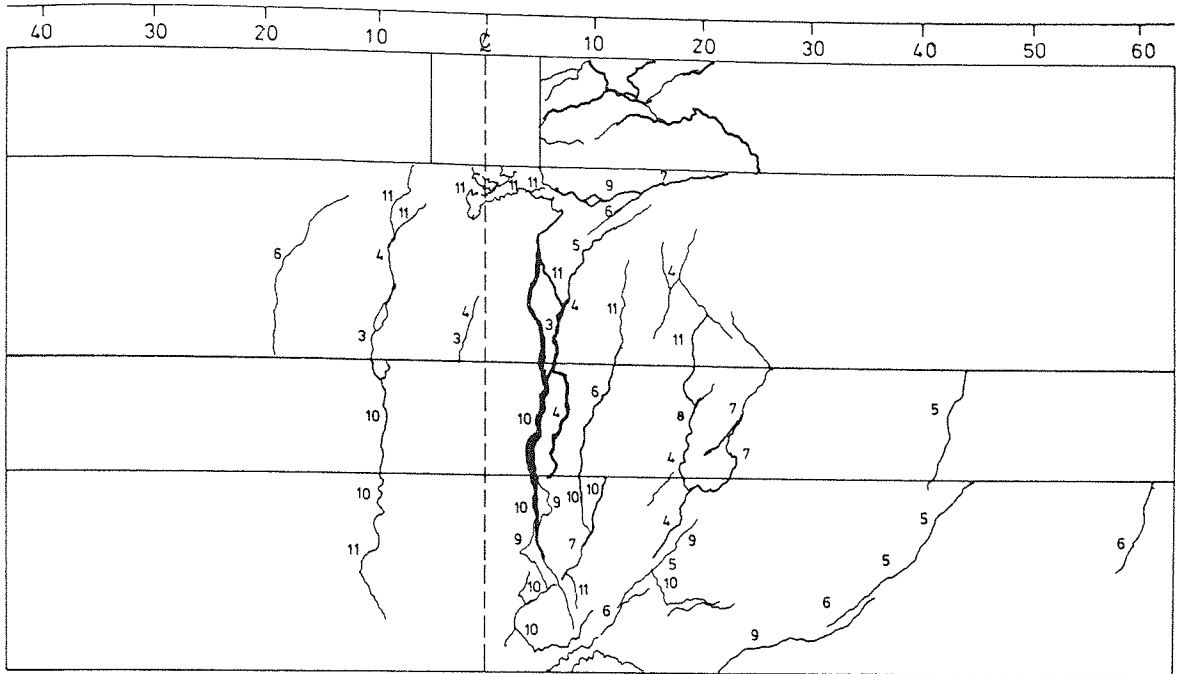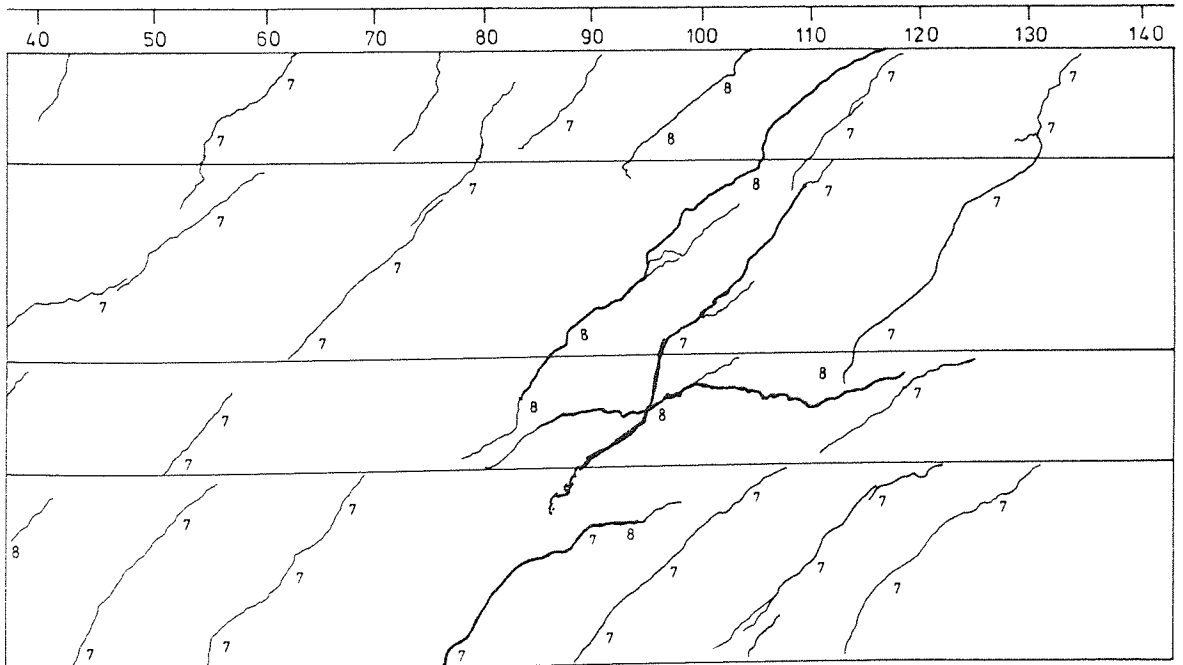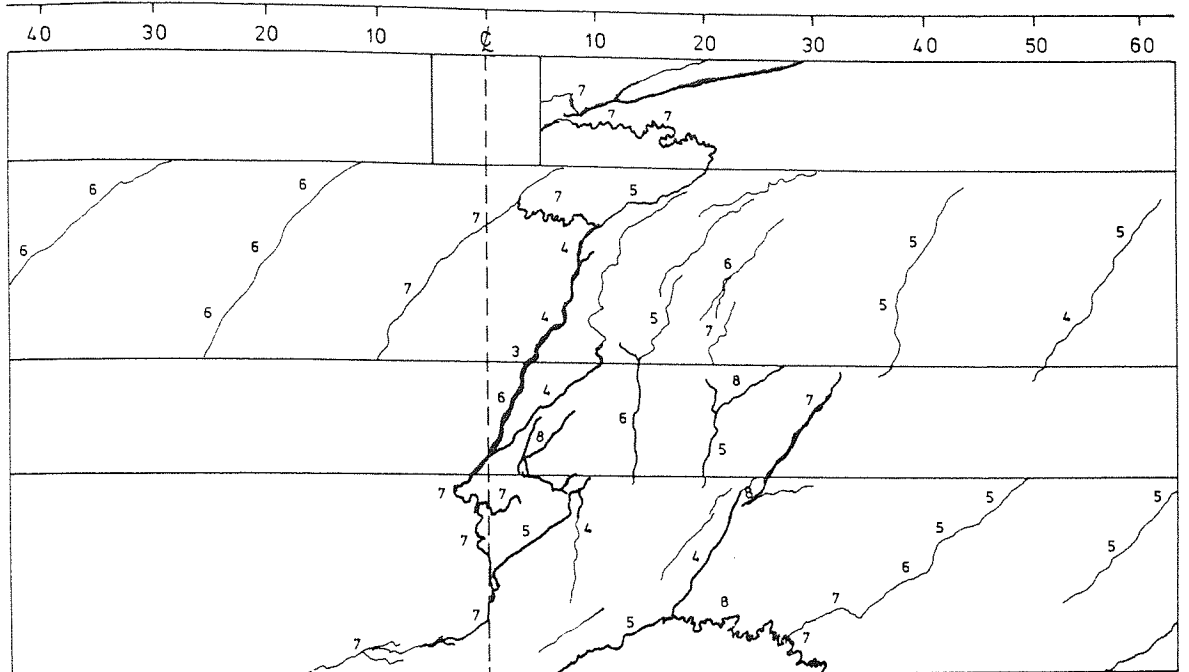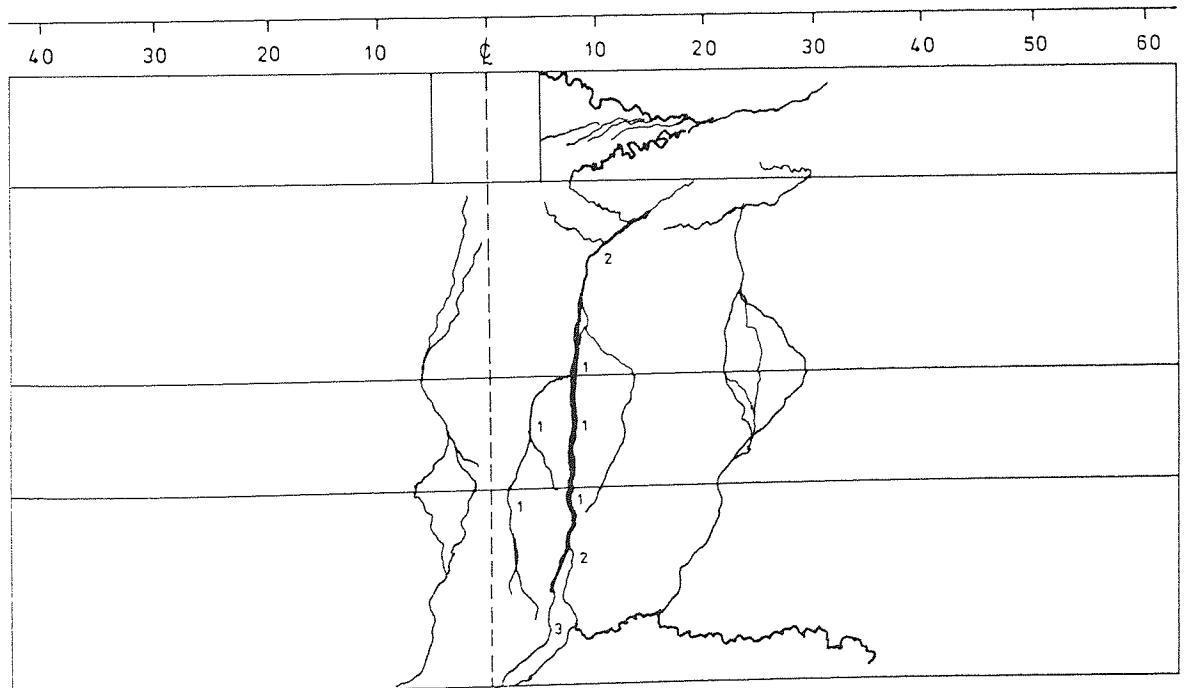
BEAM A3

BEAM A6

BEAM A5

BEAM AR5

247
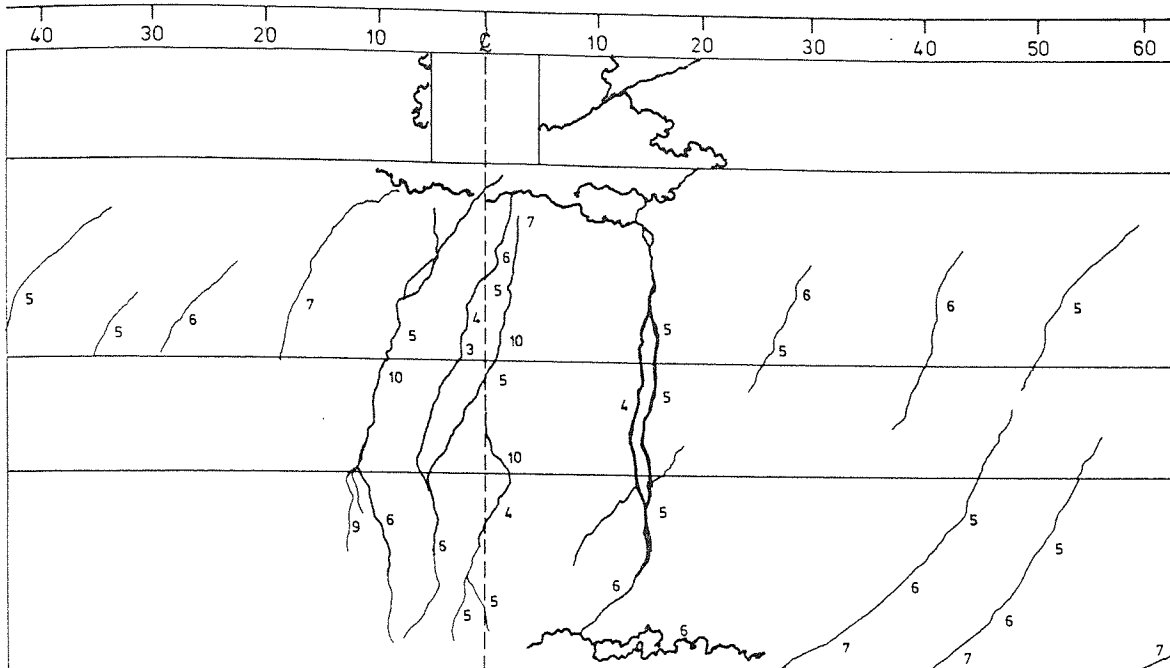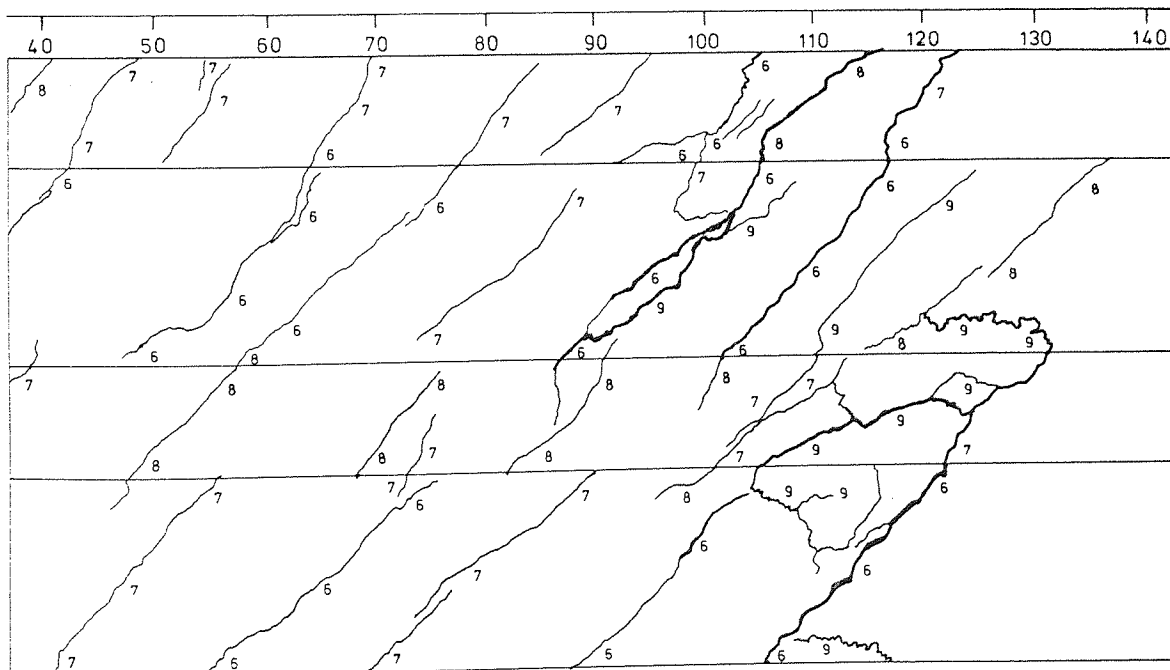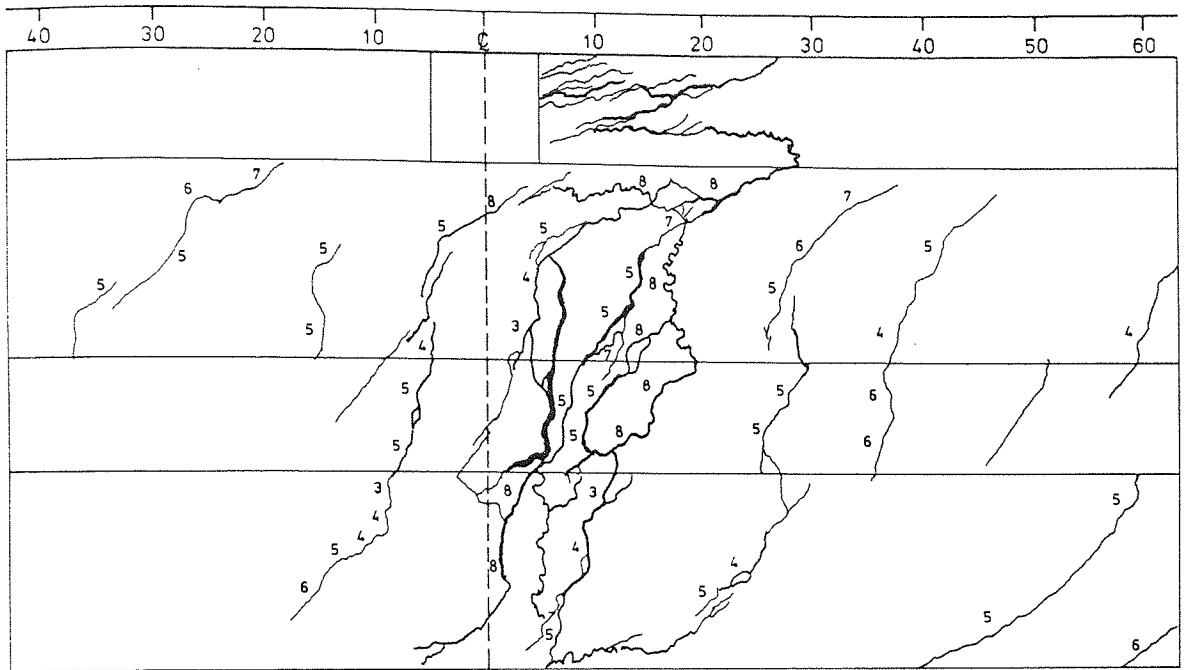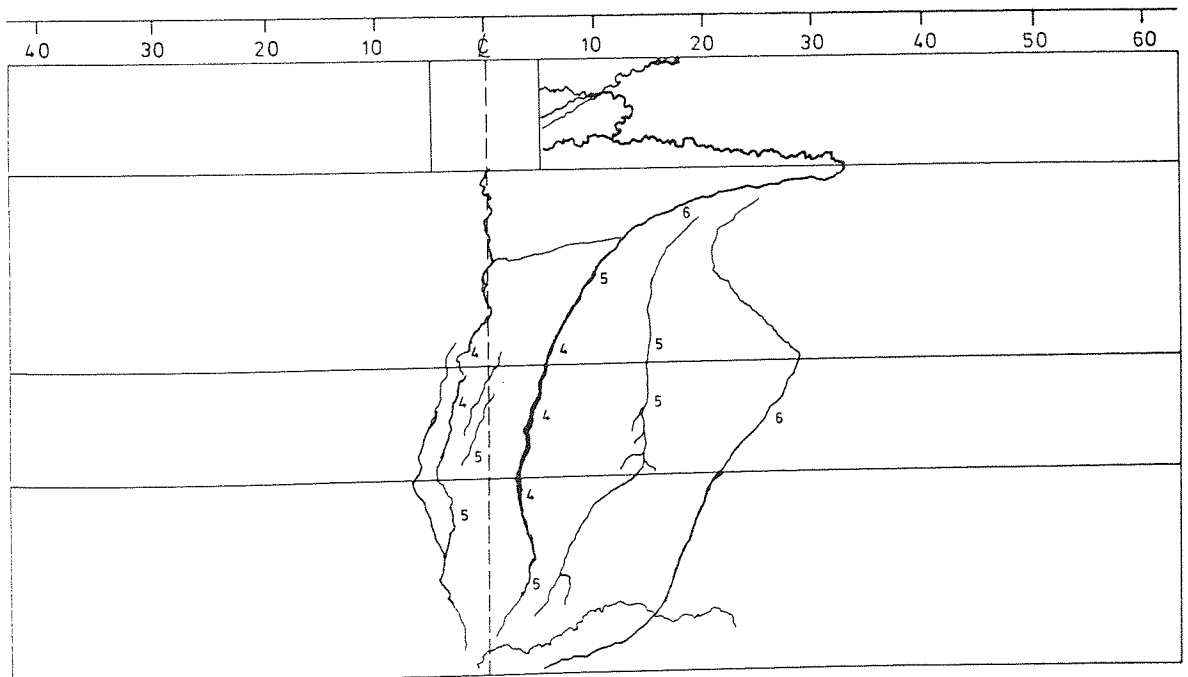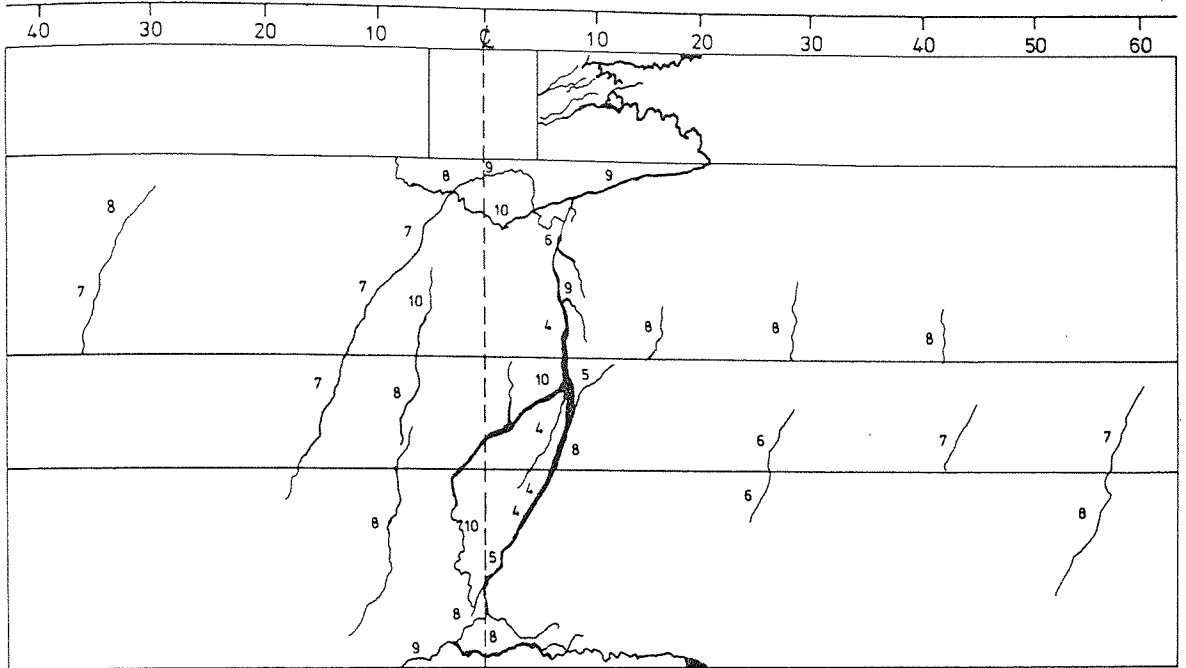
BEAM A7

BEAM A8

BEAM A9
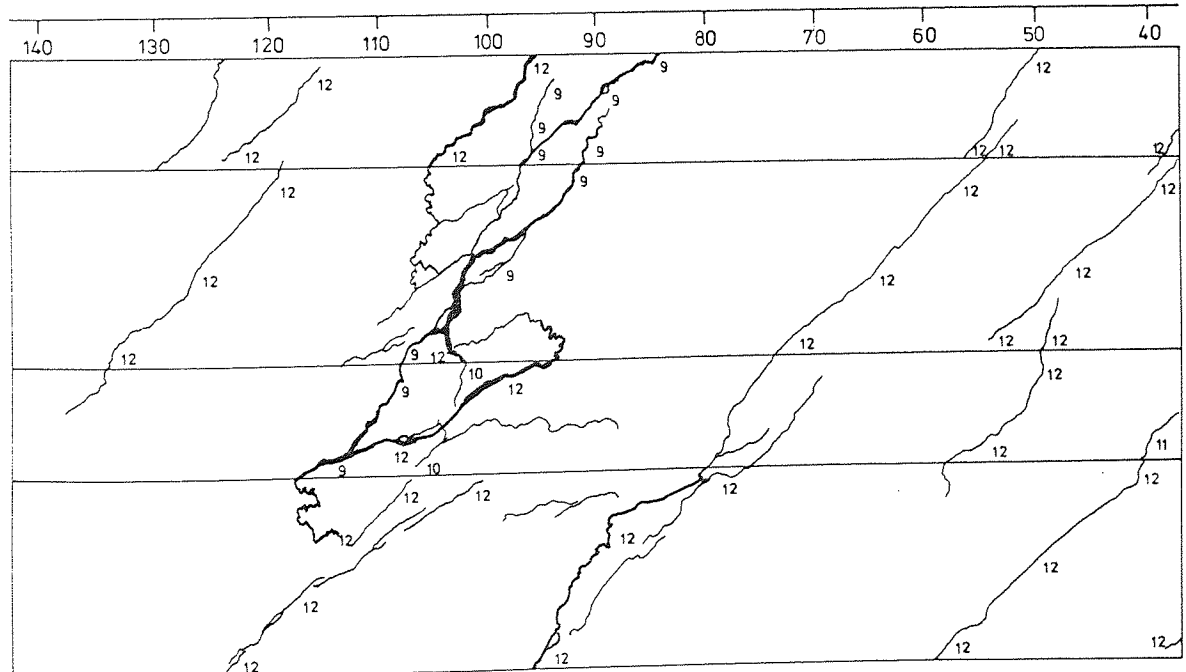
BEAM AR9

BEAM B1

BEAM B3

250
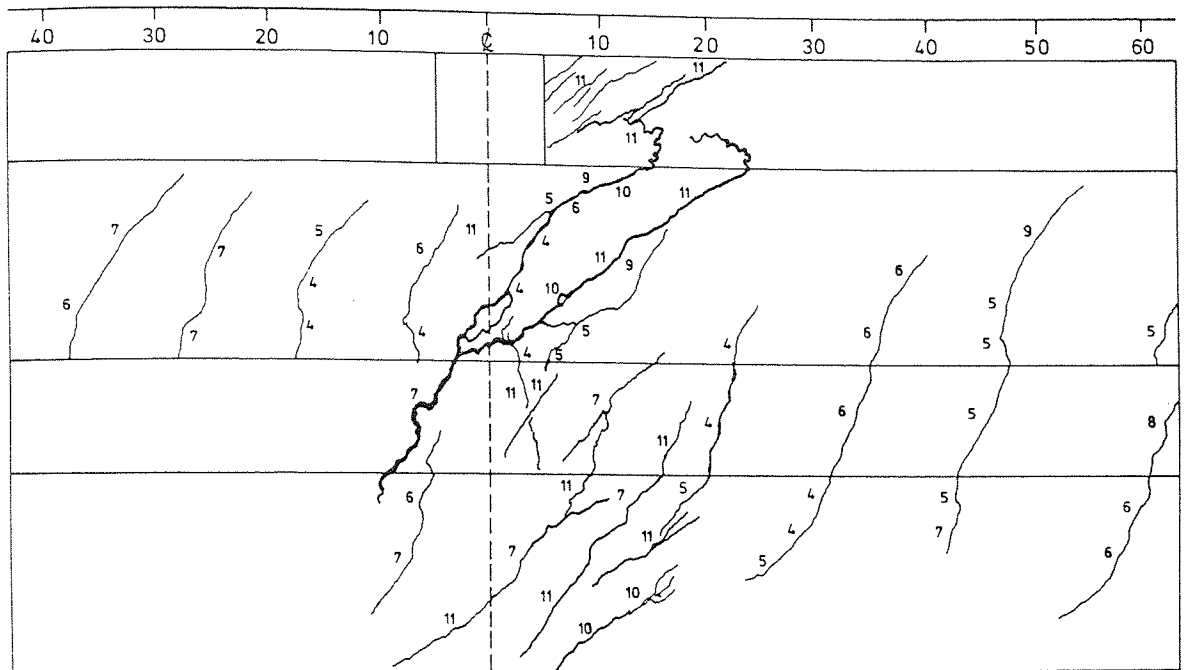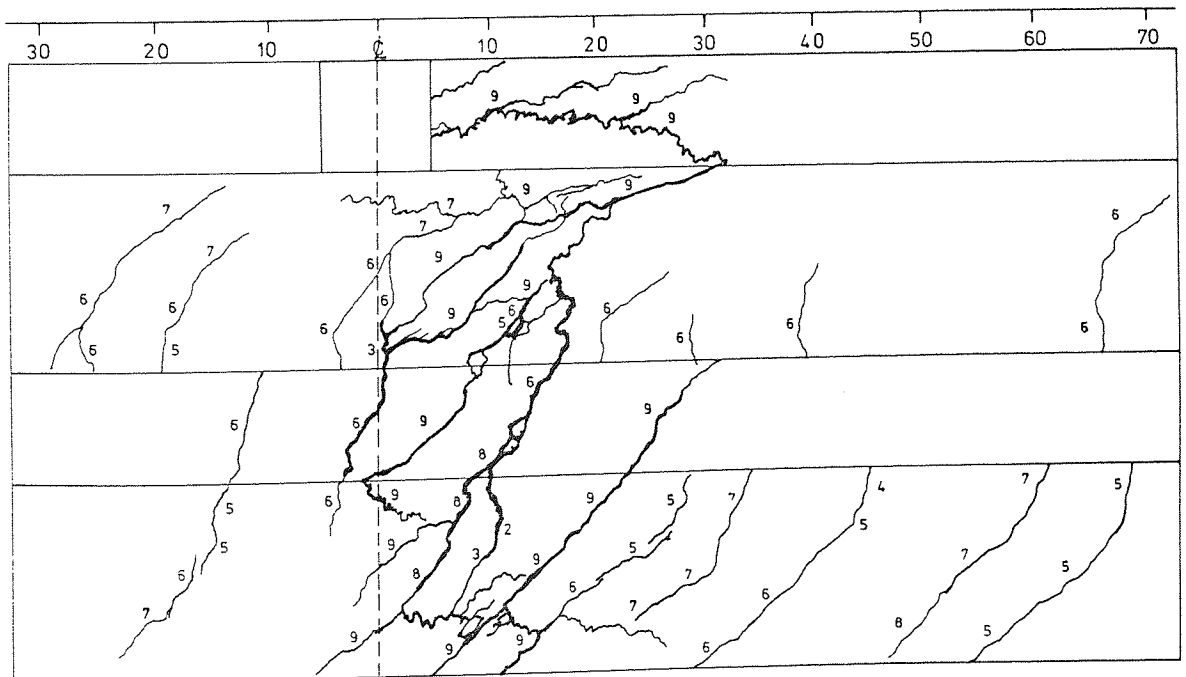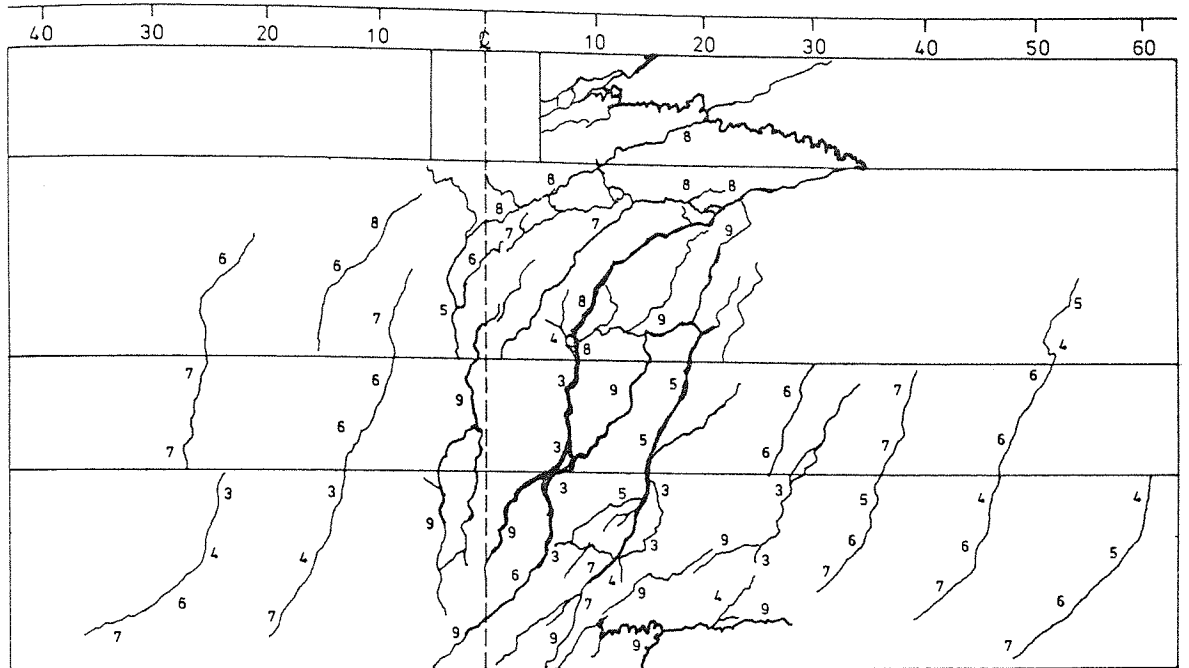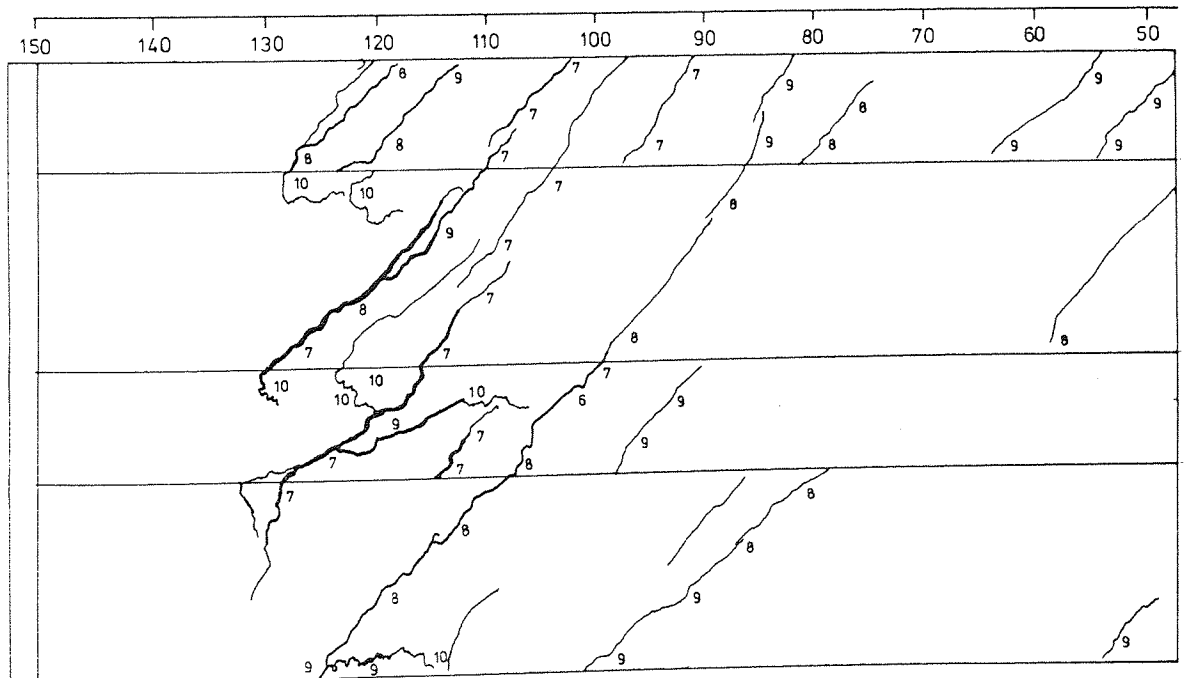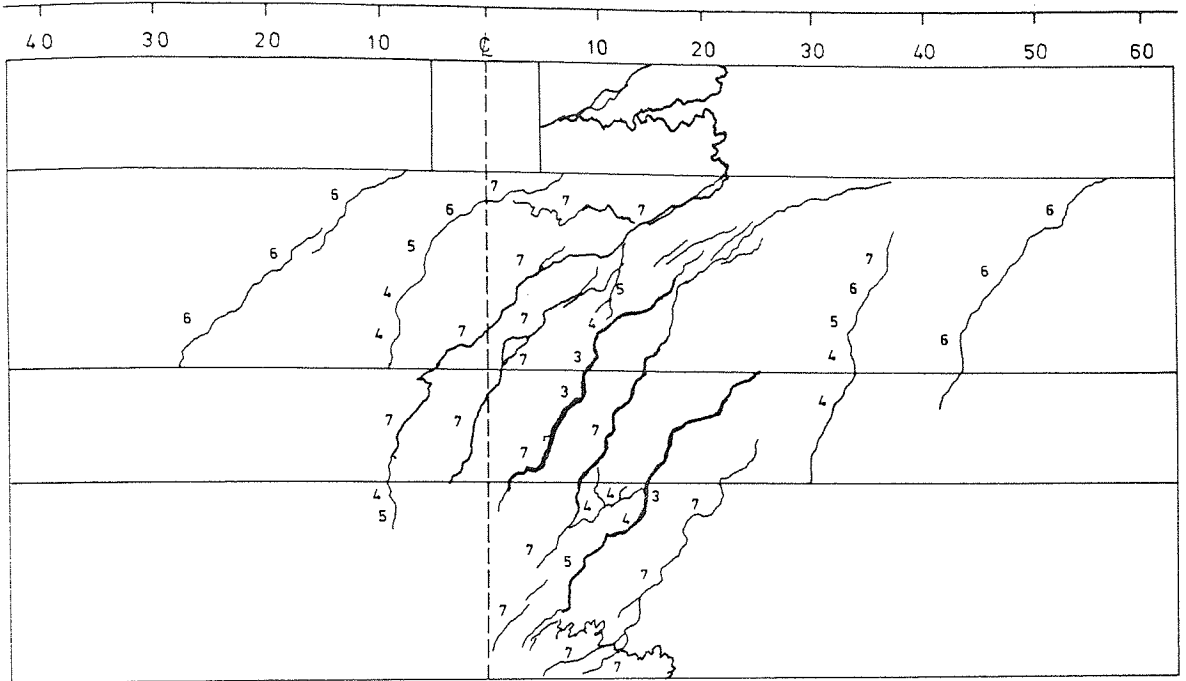
BEAM B2

BEAM BR2

BEAM B4
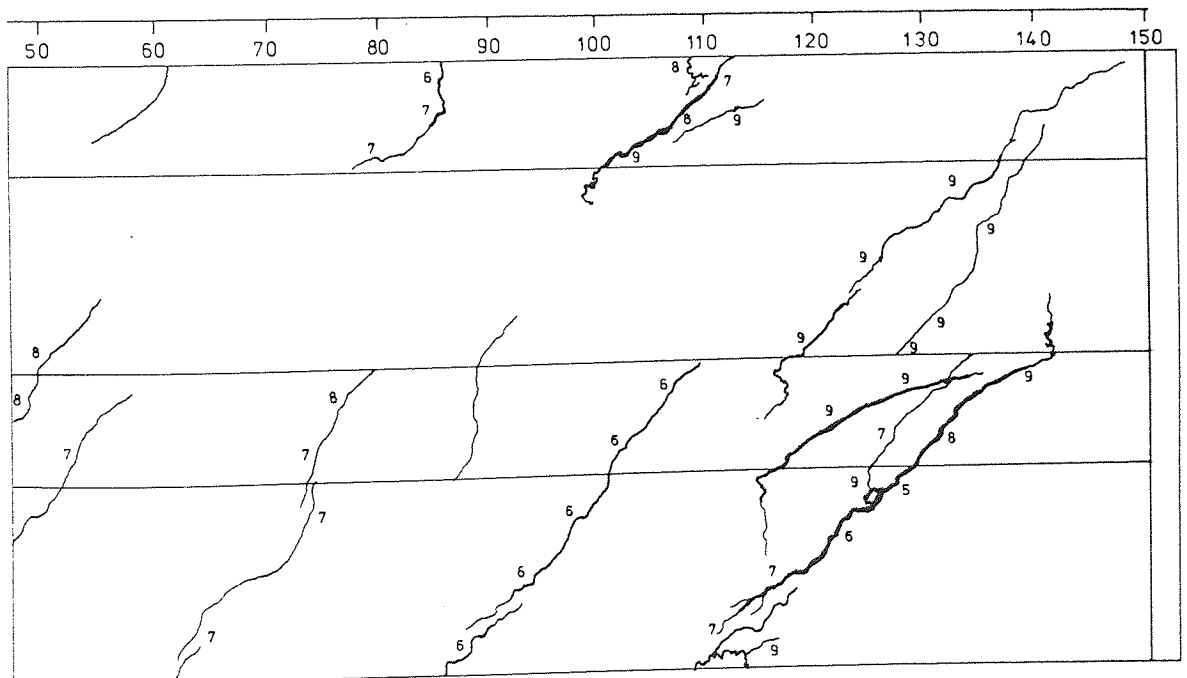
BEAM BR4
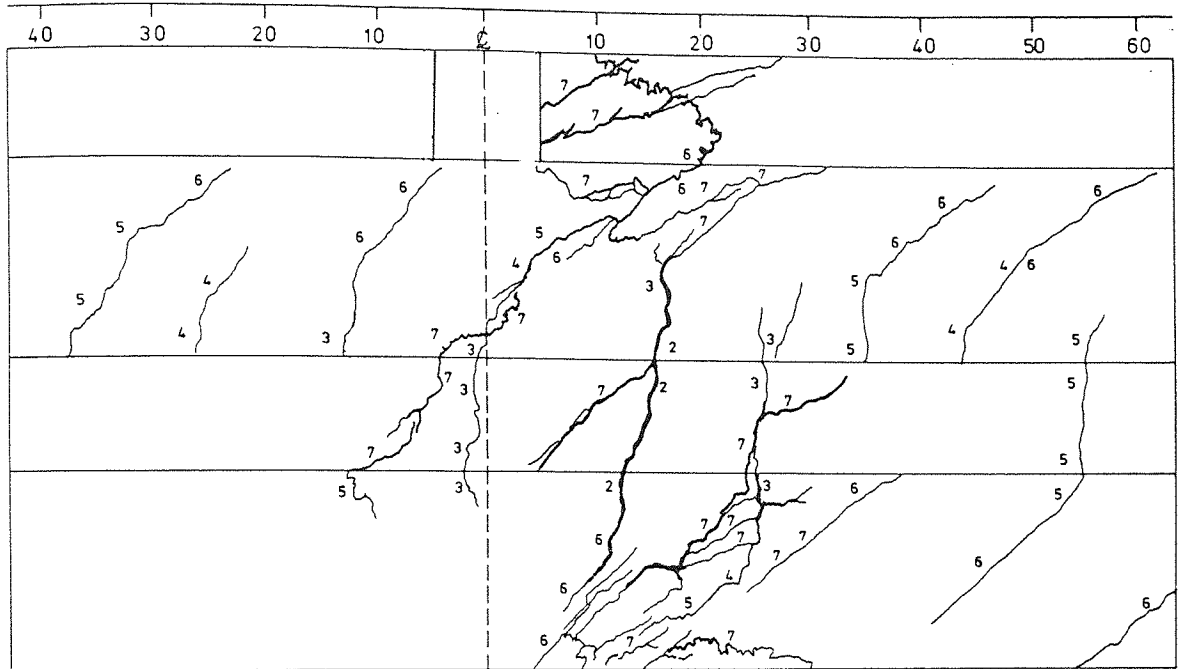
BEAM B5
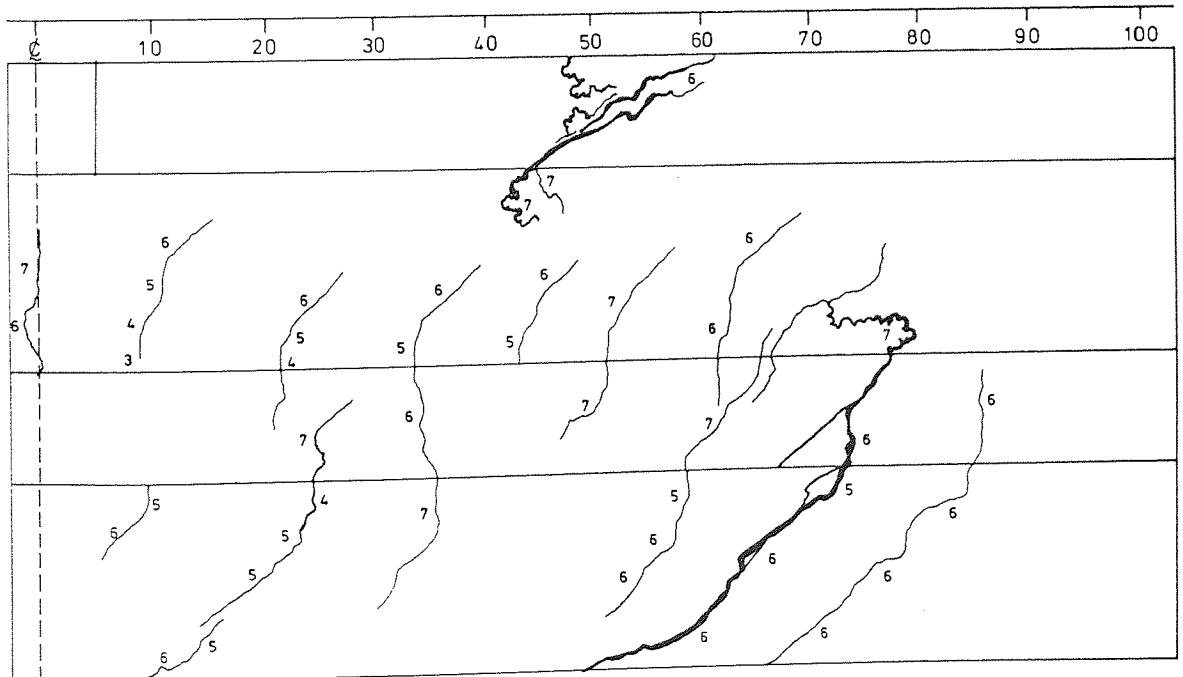
BEAM B6
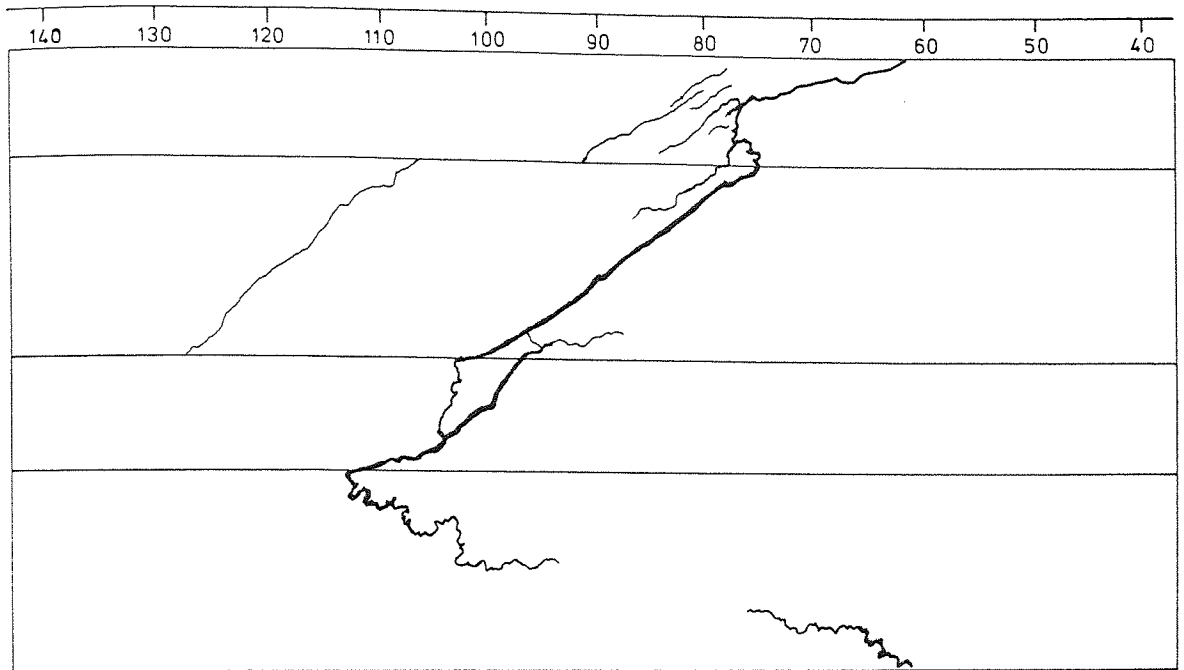
BEAM B7
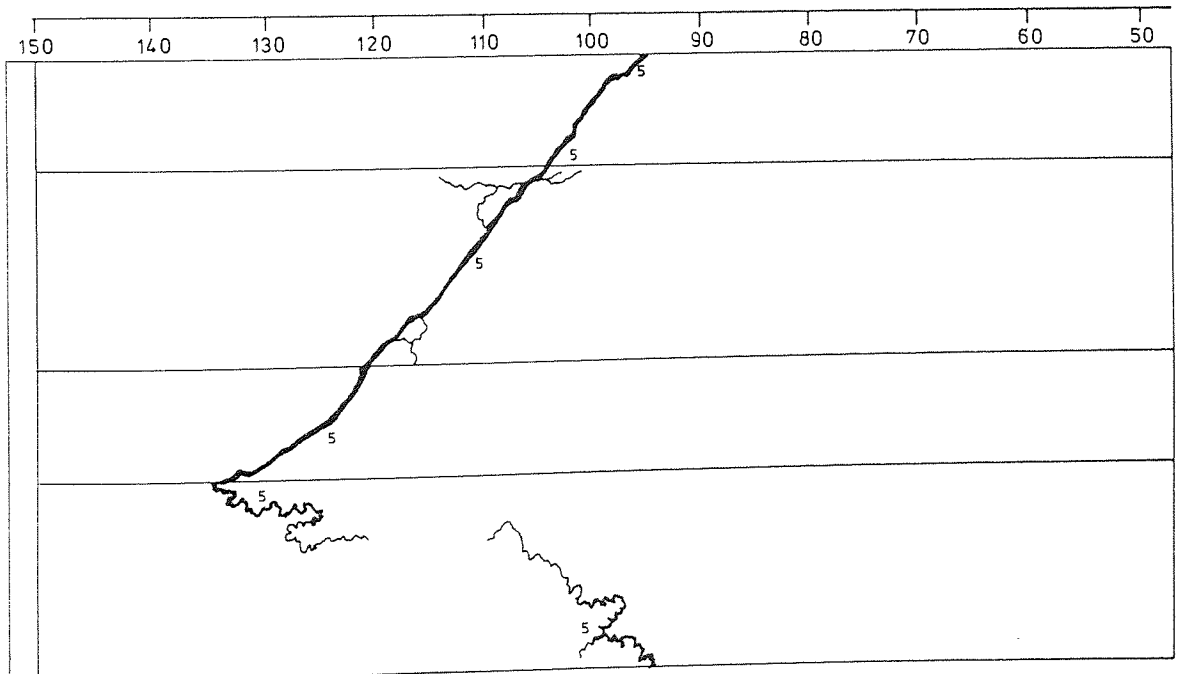
BEAM BR7
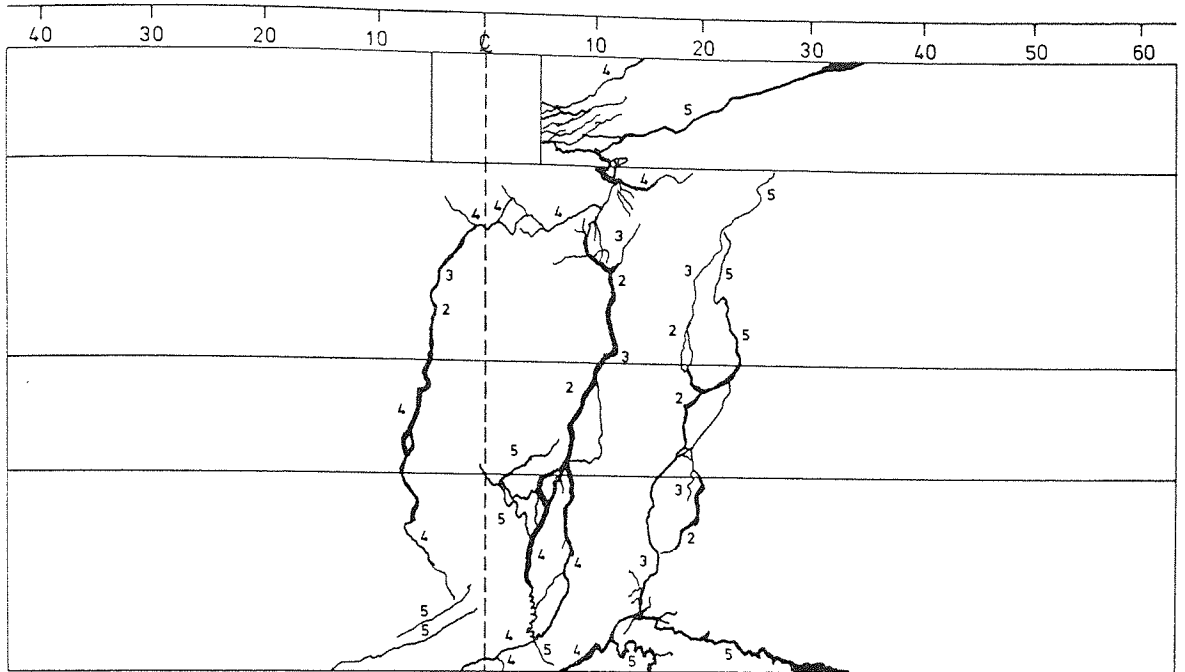
BEAM C1
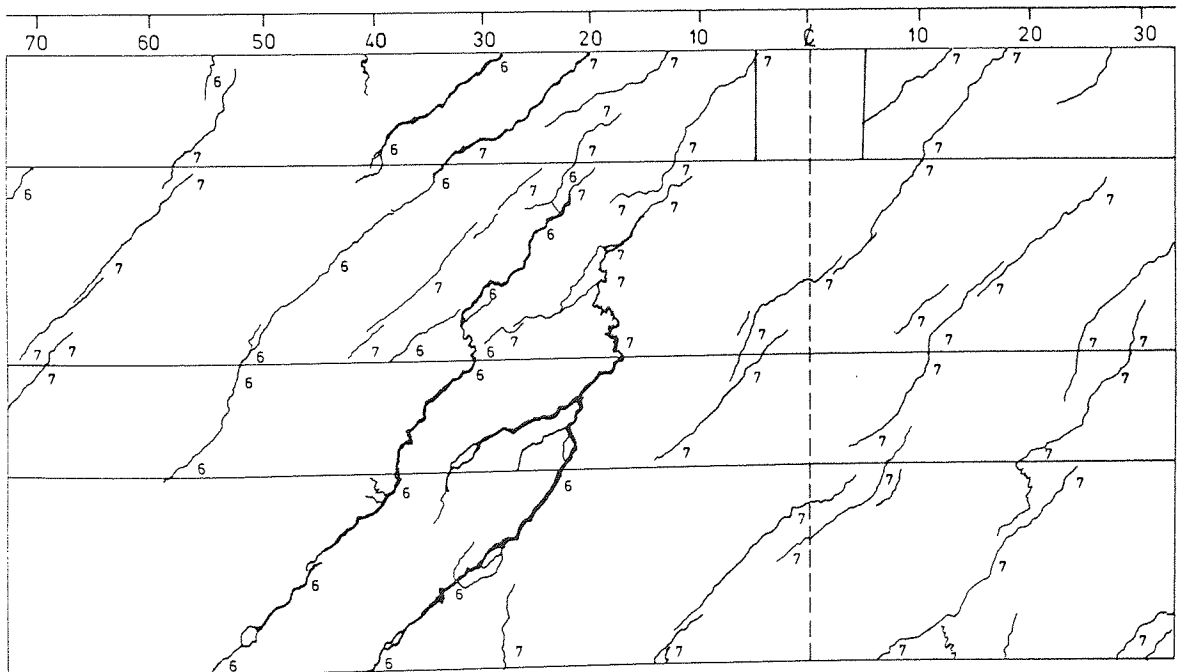
BEAM CR1
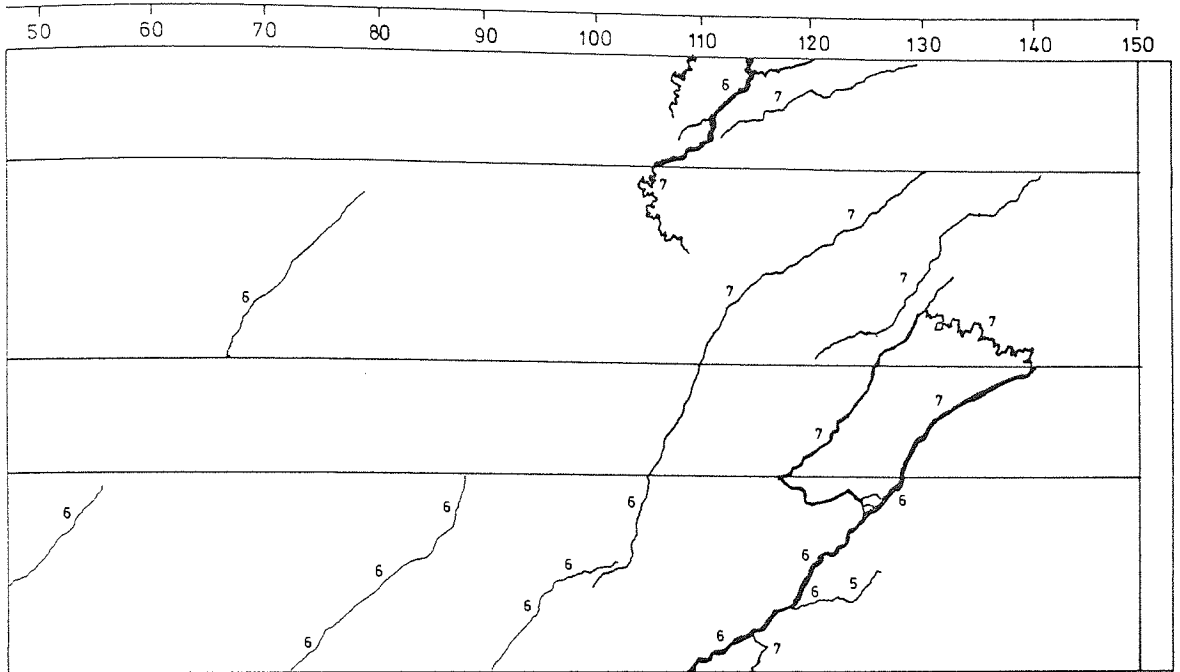
BEAM C3
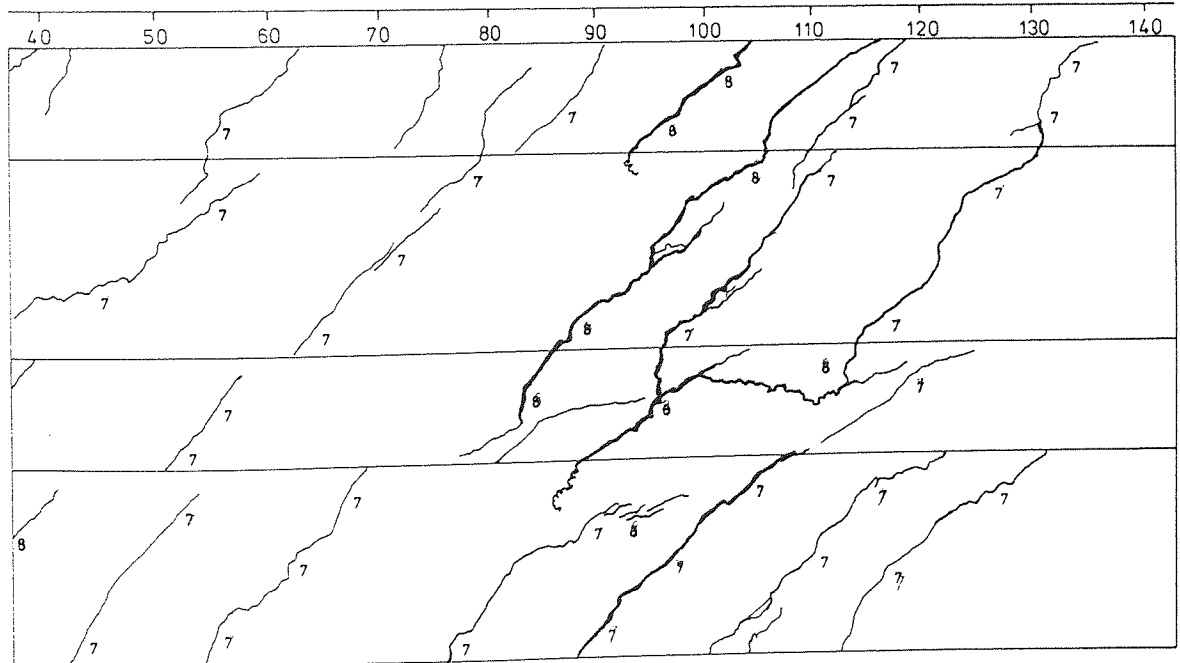
BEAM CR3

BEAM C2

BEAM C4

257
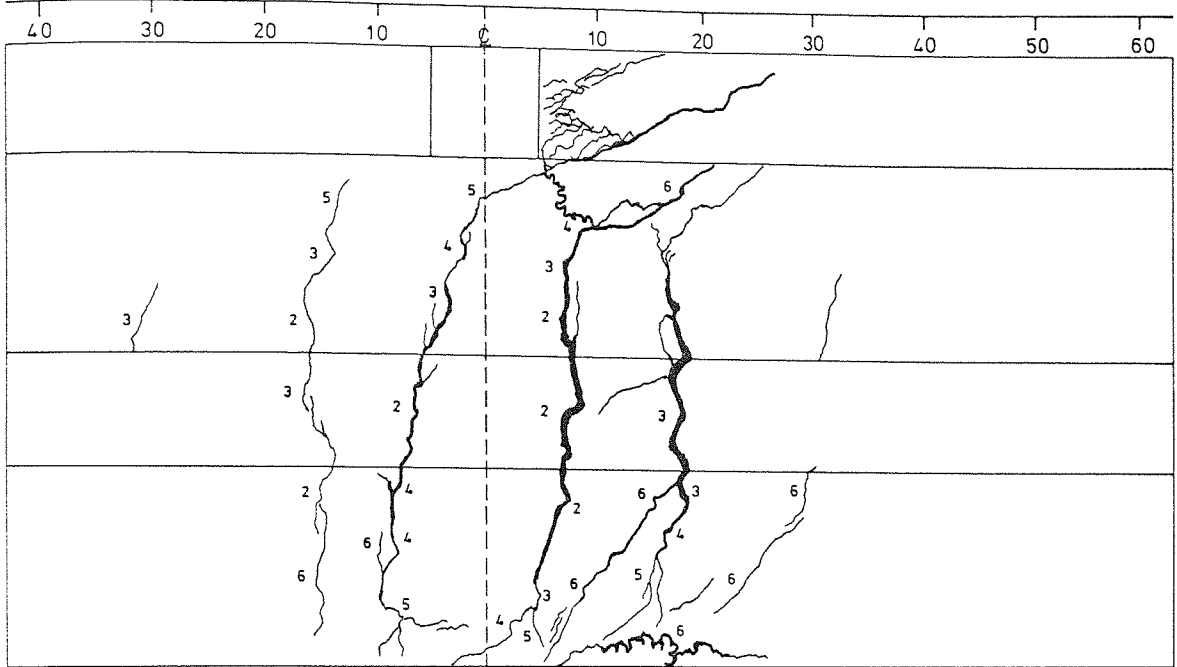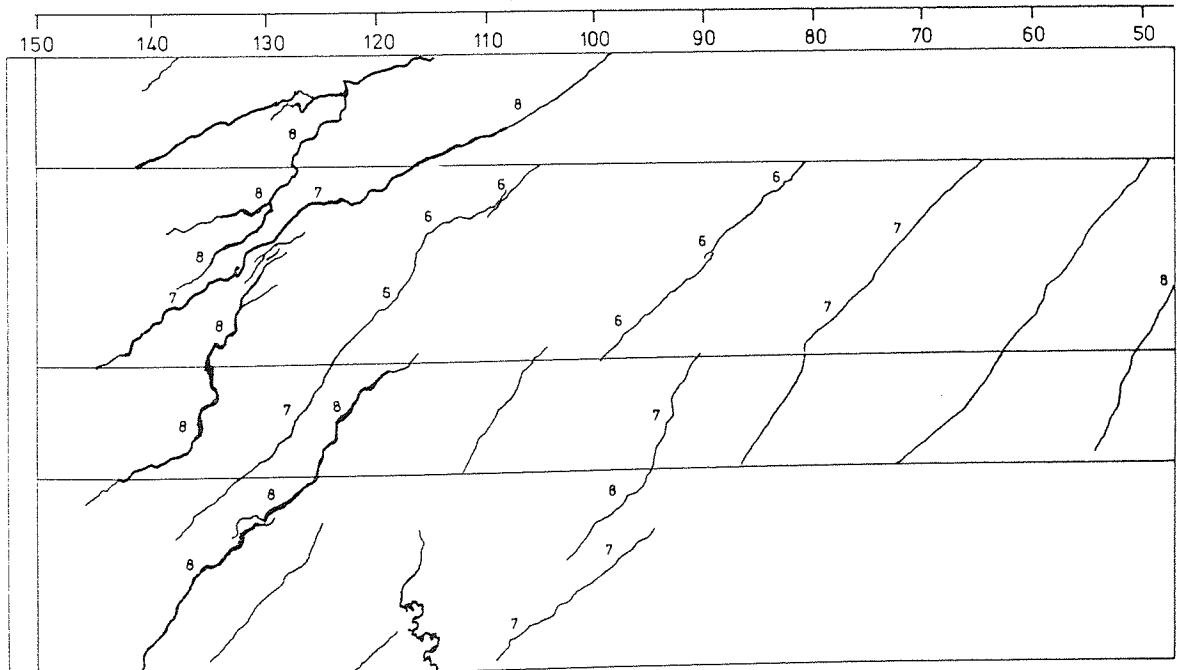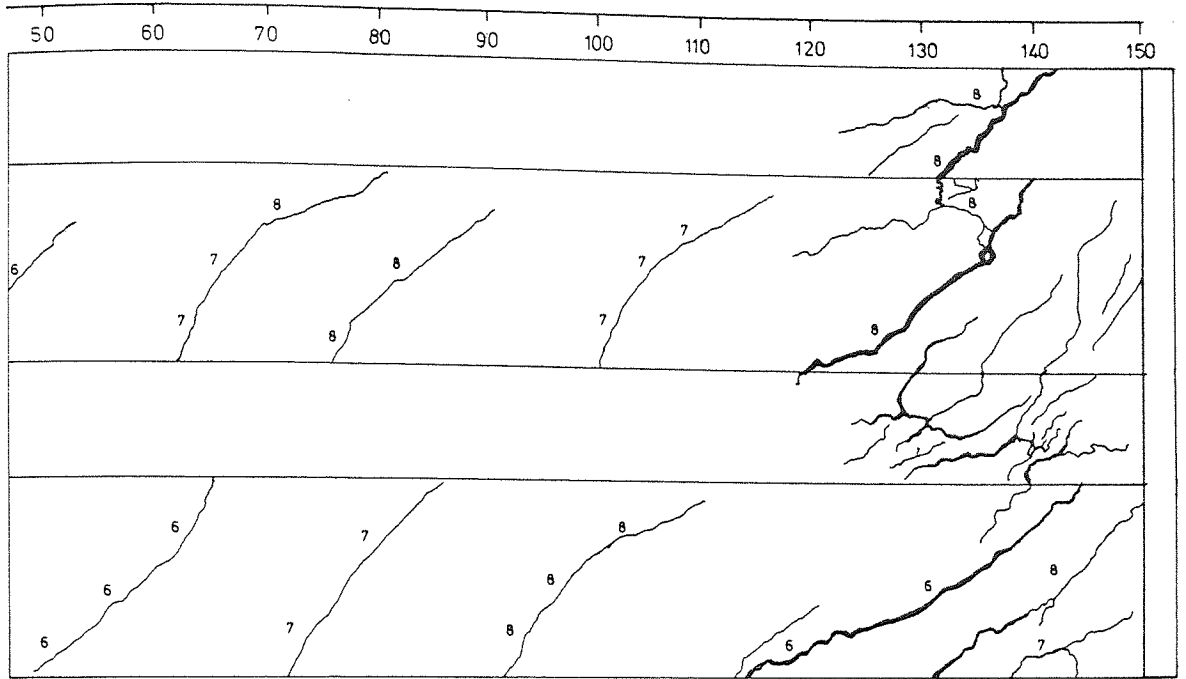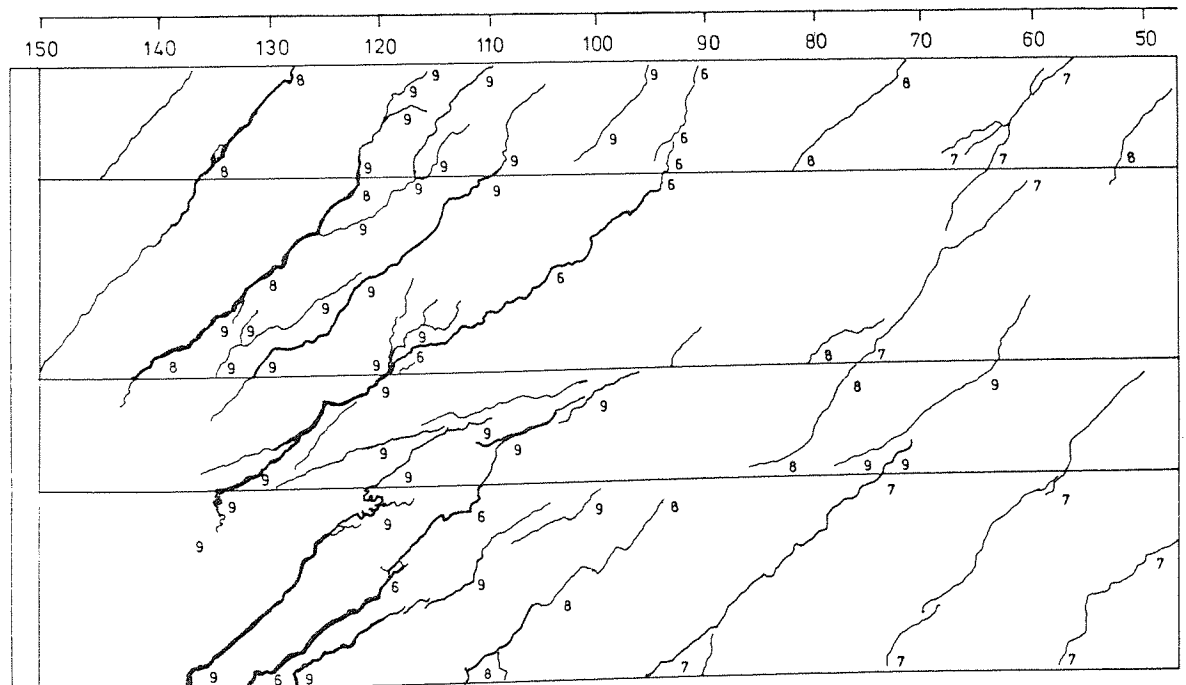
BEAM C5

BEAM CR5
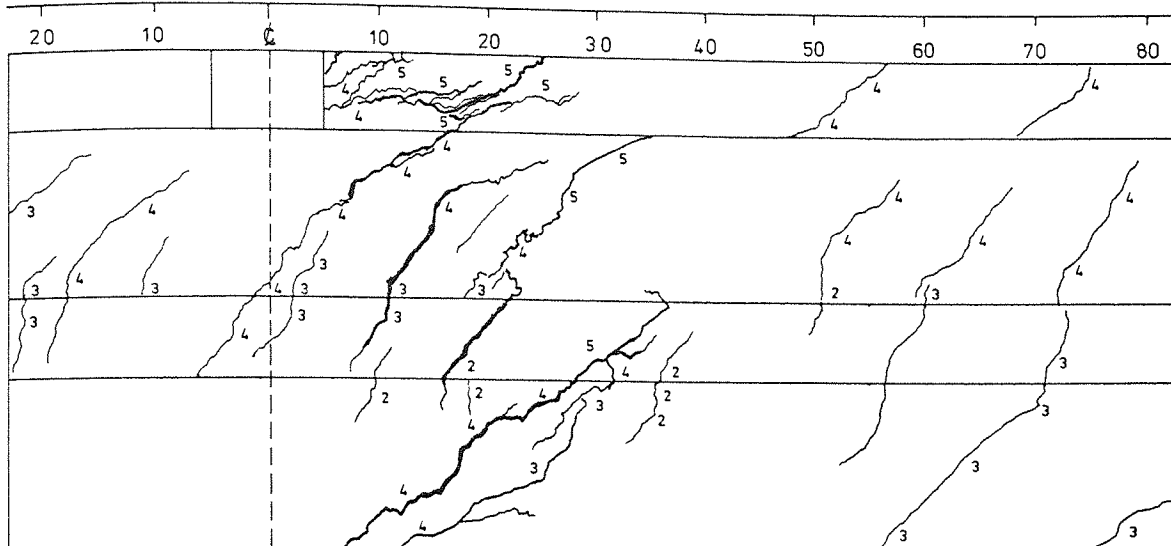
BEAM DI
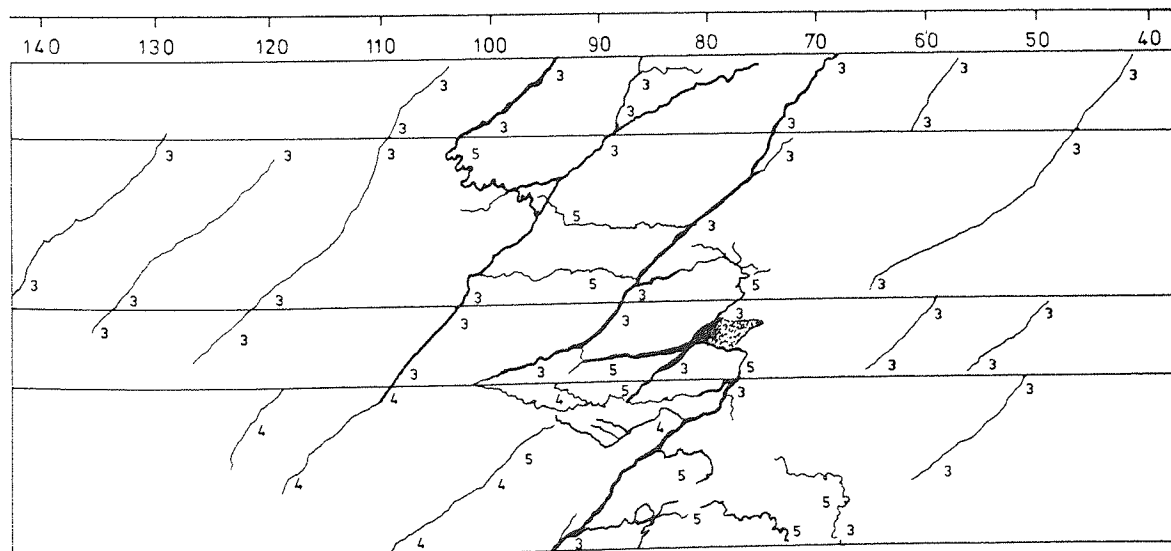
BEAM DRI

BEAM D3

BEAM DR3

260

BEAM D2

BEAM D4

261
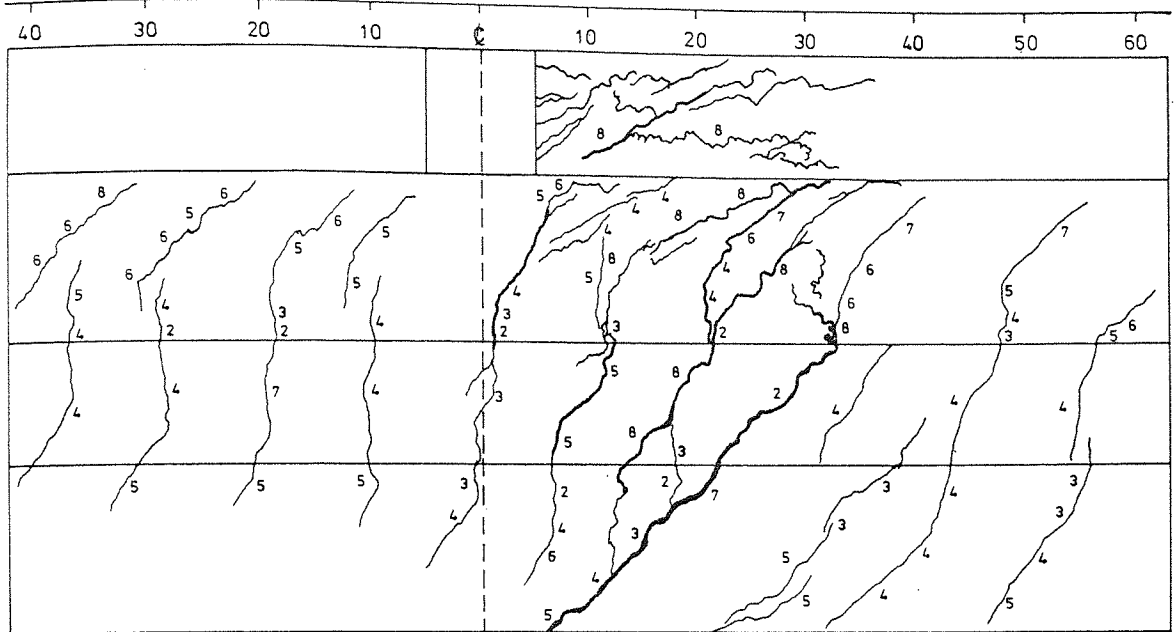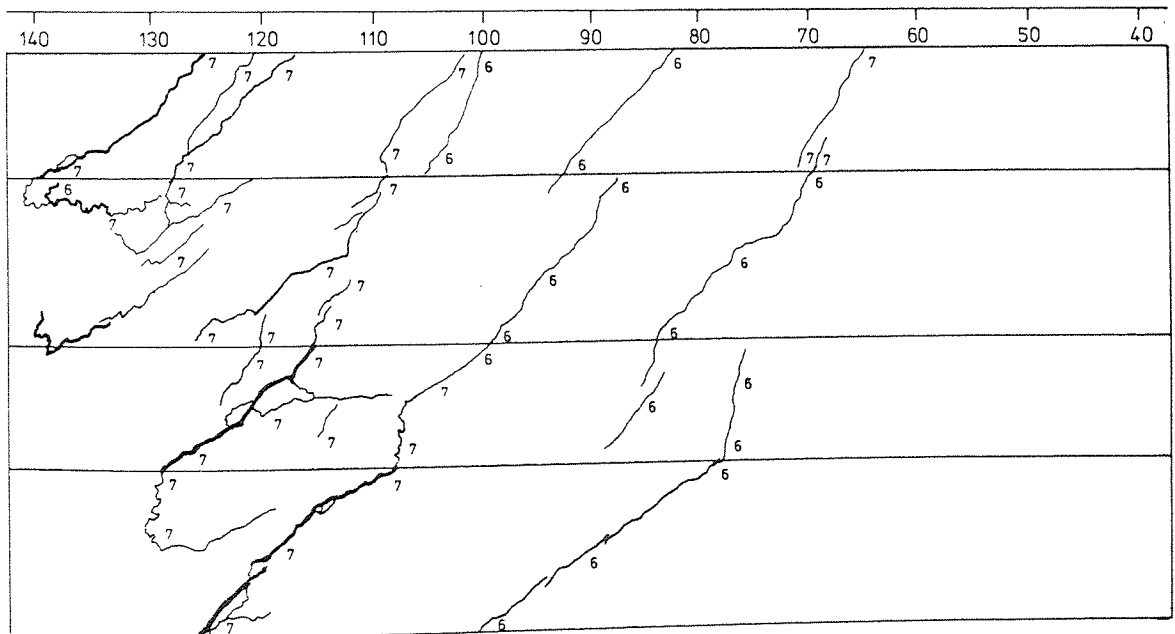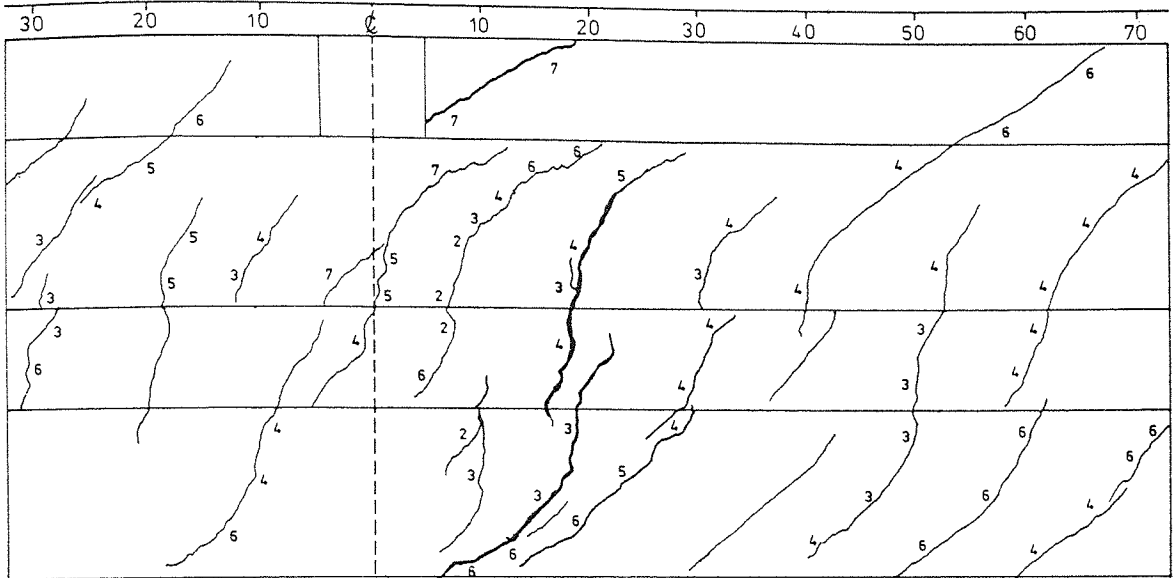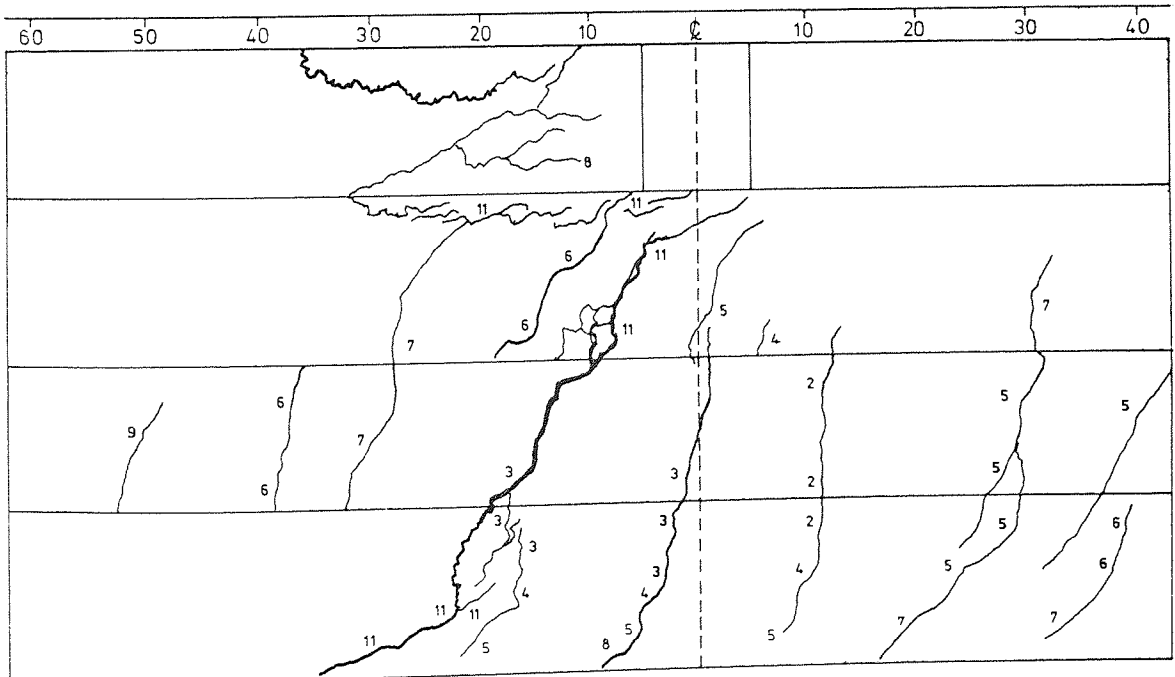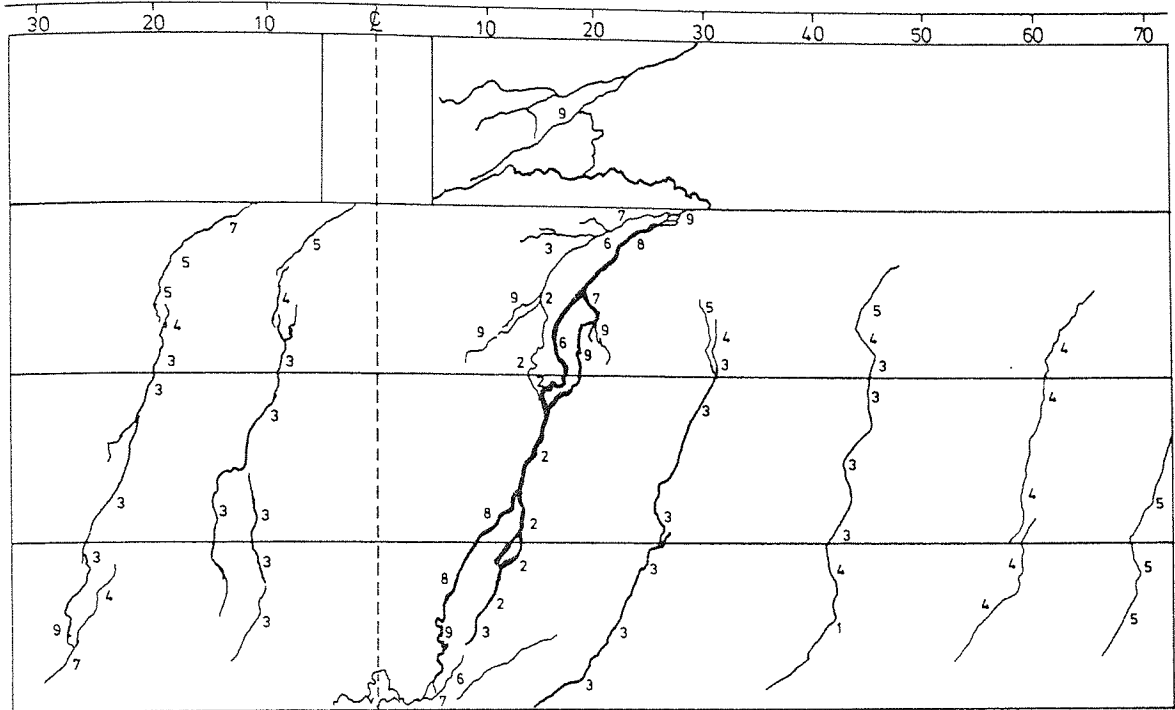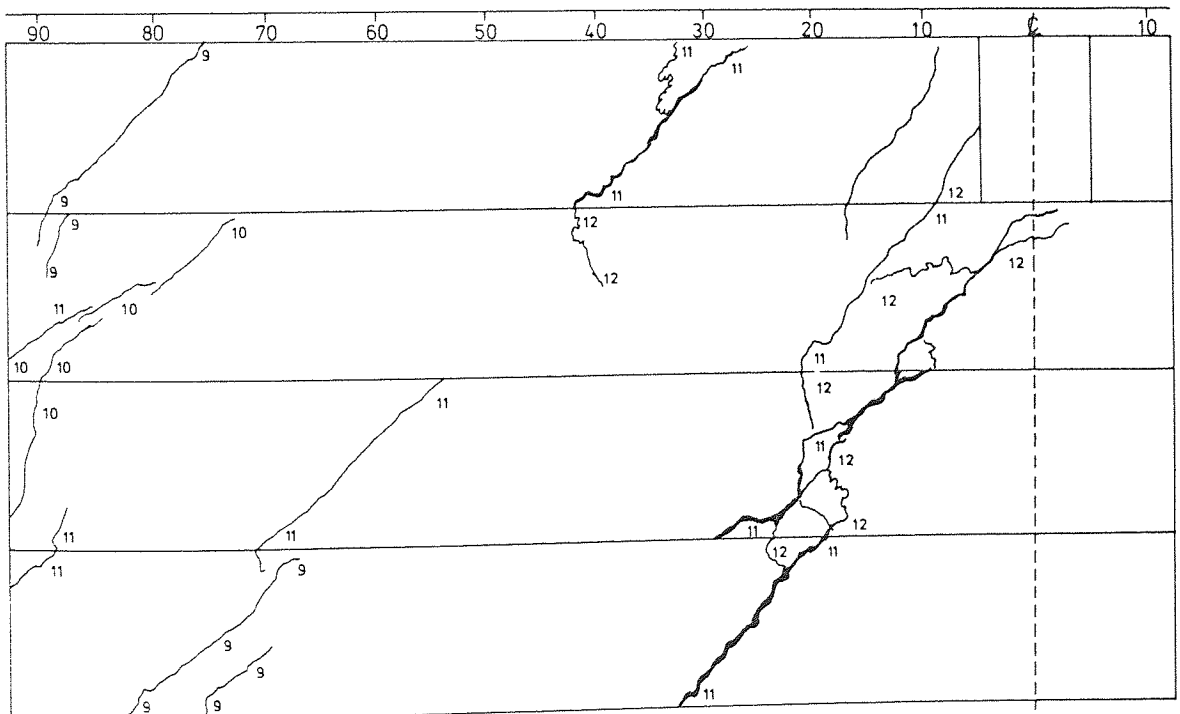
BEAM D5

BEAM DR5

APPENDIX D

DETAILS OF THE COMPARISON WITH THE TEST
RESULTS OF OTHER INVESTIGATORS

The observed and predicted torsional moments as well as the comparative ratio $CRT(T_{test}/T_{theory})$ for all the results used in the comparison are given in this appendix from table D-1 through to D-20. The result of each investigator is given separately, and in the same order as their appearance in table 5.10.

Beam	Observed		Predicted		CRT
	T in-kips	mode	T in kips	mode	
3TR-1	35.00	–	25.55	2.I	1.37
3TR-3	34.30	–	36.13	2.I	0.95
3TR-7	49.70	–	51.10	2.I	1.04
3TR-15	61.70	–	63.56	2.II	0.97
3TR-30	76.00	–	76.65	2.III	0.99
4TR-1	32.10	–	30.13	2.I	1.07
4TR-3	35.00	–	42.61	2.I	0.82
4TR-7	54.80	–	52.92	2.II	1.04
4TR-15	74.00	–	67.52	2.II	1.10
4TR-30	85.00	–	85.74	2.IV	0.99
5TR-1	33.40	–	40.84	2.I	0.82
5TR-3	43.00	–	48.33	2.II	0.89
5TR-7	59.70	–	57.61	2.II	1.04
5TR-15	76.50	–	71.24	2.II	1.08
5TR-30	92.60	–	93.58	2.IV	0.99

TABLE D-1: Comparison with the test beams of
Ernst [20]

Beam	Observed		Predicted		CRT
	T in-kips	Mode	T in-kips	Mode	
B1	197.00	2	198.85	2.I	0.99
B2	259.00	2	262.19	2.IV	0.99
B3	332.00	2	298.15	2.IV	1.11
B4	419.00	2	360.83	2.IV	1.16
B5	497.00	2	384.34	2.IV	1.29
B6	546.00	2	412.88	2.IV	1.32
B7	238.00	2	232.54	2.III	1.02
B8	288.00	2	275.78	2.III	1.04
B9	264.00	2	227.48	2.II	1.16
B10	304.00	2	255.96	2.II	1.19
D1	198.00	2	203.84	2.I	0.97
D2	245.00	2	261.66	2.IV	0.94
D3	346.00	2	301.02	2.IV	1.15
D4	424.00	2	361.47	2.IV	1.17
M1	269.00	2	226.89	2.II	1.19
M2	359.00	2	289.57	2.II	1.24
M3	388.00	2	322.57	2.IV	1.20
M4	439.00	2	356.62	2.IV	1.23
M5	493.00	2	377.20	2.IV	1.31
M6	532.00	2	416.11	2.IV	1.28
I2	319.00	2	317.23	2.I	1.01
I3	404.00	2	410.88	2.II	0.98
I4	514.00	2	489.27	2.IV	1.05
I5	626.00	2	544.50	2.IV	1.15
I6	679.00	2	597.41	2.IV	1.14
J1	190.00	2	159.45	2.IV	1.19
J2	258.00	2	191.58	2.IV	1.35
J3	312.00	2	236.22	2.IV	1.32
J4	360.00	2	263.74	2.IV	1.37
G1	237.00	2	224.09	2.I	1.06
G2	357.00	2	345.17	2.I	1.03
G3	439.00	2	411.28	2.IV	1.07
G4	574.00	2	450.42	2.IV	1.27
G5	637.00	2	518.34	2.IV	1.23
G6	346.00	2	339.06	2.II	1.02
G7	466.00	2	437.95	2.IV	1.06
G8	650.00	2	467.67	2.IV	1.39

TABLE D-2: Comparison with the test beams of Hsu [10]

Beam	Observed		Predicted		CRT
	T in-kips	Mode	T in-kips	Mode	
N1	80.50	2	74.12	2.IV	1.09
N1a	79.60	2	73.60	2.II	1.08
N2	128.00	2	101.34	2.IV	1.26
N2a	117.00	2	94.14	2.IV	1.24
N3	108.00	2	92.39	2.IV	1.17
N4	139.00	2	105.48	2.IV	1.32
K1	136.00	2	120.57	2.I	1.13
K2	210.00	2	185.34	2.IV	1.13
K3	252.00	2	207.65	2.IV	1.21
K4	310.00	2	234.38	2.IV	1.32
C1	100.00	2	92.57	2.I	1.08
C2	135.00	2	154.25	2.IV	0.88
C3	177.00	2	183.37	2.IV	0.97
C4	224.00	2	211.54	2.IV	1.06
C5	263.00	2	237.23	2.IV	1.11
C6	303.00	2	248.95	2.IV	1.22

TABLE D-2 (CONTINUED): Comparison with the test beams
of Hsu [10]

Beam	Observed		Predicted		CRT
	T kNm	Mode	T kNm	Mode	
11	14.600	-	15.487	2.IV	0.94
12	12.300	-	14.144	2.IV	0.87
13	14.300	-	15.978	2.IV	0.90
14	15.500	-	18.035	2.IV	0.86
15	4.500	-	3.775	2.I	1.19
16	5.900	-	5.928	2.I	1.00
17	11.600	-	14.383	2.IV	0.81
18	10.900	-	12.457	2.IV	0.88
51	10.000	-	9.647	2.IV	1.04
52	9.200	-	10.484	2.IV	0.88
53	10.700	-	11.720	2.IV	0.91
54	12.000	-	13.043	2.IV	0.92

TABLE D-3:   Comparison with the test beams of Swann [54]

Beam	Observed		Predicted		CRT
	T in-kips	Mode	T in-kips	Mode	
HB1	44.10	1	43.68	3.I	1.01
HB2	33.90	1	28.47	1.I	1.19
HB3	20.40	1	18.75	1.I	1.09
HB4	15.70	1	14.85	1.I	1.06
HB5	13.20	1	12.31	1.I	1.07
HB7	36.10	1	47.36	2.II	0.76
HB8	21.40	1	20.88	1.I	1.03
HB9	18.30	1	19.18	1.I	0.95
HB10	17.30	1	17.57	1.I	0.98
HB11	14.10	1	14.16	1.I	1.00
HB13	51.30	1	60.70	3.I	0.85
HB14	41.70	1	44.00	1.I	0.95
HB15	29.90	1	28.07	1.I	1.07
HB16	23.50	1	22.91	1.I	1.03
HB17	19.40	1	18.42	1.I	1.05

TABLE D-4:   Comparison with the test beams of
Evans and Sarkar [41]

Beam	Observed		Predicted		CRT
	T in-kips	Mode	T in-kips	Mode	
1	79.00	1	82.54	2.II	0.96
2	102.00	1	104.55	1.III	0.98
3	61.00	1	63.42	1.I	0.96
4	67.00	1	74.85	1.III	0.90
5	49.00	1	49.28	1.I	0.99
6	56.00	1	54.69	1.I	1.02
7	43.00	1	39.57	1.I	1.09
8	44.00	1	42.57	1.I	1.03
9	60.00	1	57.94	2.II	1.04
10	44.00	1	45.30	1.I	0.97
11	68.00	1	74.16	1.I	0.92
12	53.00	1	52.49	1.I	1.01

TABLE D-5: Comparison with test beams of Gesund [40]

Beams	Observed		Predicted		CRT
	T in-kips	Mode	T in-kips	Mode	
III.1	24.50	–	20.85	3.I	1.18
III.2	39.50	–	22.93	3.II	1.72
III.3	34.00	–	22.49	3.II	1.51
III.4	36.80	–	22.42	3.II	1.64
IV.1	34.30	–	26.07	3.III	1.31
IV.2	43.50	–	30.83	3.IV	1.41
IV.3	46.00	–	30.97	3.IV	1.49
IV.4	42.50	–	30.10	3.IV	1.41
V.I	25.50	–	20.80	3.I	1.23
V.2	24.00	–	20.87	2.II	1.15
V.3	28.50	–	20.96	2.II	1.36
V.4	24.00	–	20.12	1.I	1.19
VI.1	27.00	–	26.47	3.III	1.02
VI.2	31.00	–	27.67	2.IV	1.12
IV.3	25.00	–	23.53	1.I	1.06
IV.4	36.00	–	28.59	2.IV	1.26

TABLE D-6: Comparison with the test beams of Goode and Helmy [11]

Beam	Observed		Predicted		CRT
	T in-kips	Mode	T in-kips	Mode	
V1	41.00	-	38.68	2.II	1.06
V2	36.00	-	36.09	2.II	1.00
V3	25.00	-	27.61	1.I	0.91
V4I	33.00	-	35.80	2.II	0.92
V5	39.00	-	35.05	2.II	1.11
V6	34.00	-	33.96	2.II	1.00
S1II	24.00	-	20.91	1.I	1.15
S2I	16.00	-	15.18	1.I	1.05
S2II	31.00	-	27.57	1.I	1.12
S3	29.00	-	29.81	2.II	0.97
S4I	12.00	-	12.23	1.I	0.98
S41I	31.00	-	27.33	1.I	1.13
S5I	20.00	-	18.79	1.I	1.06
S5II	28.00	-	25.73	1.I	1.09
S6	30.00	-	30.31	2.II	0.99
R1	25.00	-	30.26	2.IV	0.83
R2	28.00	-	24.82	1.I	1.13
R4	30.00	-	35.31	2.II	0.85
R6	33.00	-	35.31	2.II	0.94
L1-1	29.00	-	28.19	2.II	1.03
L1-2II	32.00	-	30.05	2.II	1.07
L2-1I	10.00	-	10.36	1.I	0.97
L2-1II	33.00	-	31.67	2.II	1.04
L2-2I	10.00	-	10.36	1.I	0.97
L2-2II	33.00	-	31.67	2.II	1.04
L3-1I	20.00	-	20.74	1.I	0.97
L3-1II	30.00	-	28.54	2.II	1.05
L3-2I	20.00	-	20.74	1.I	0.97
L3-2II	30.00	-	27.18	2.II	1.10
L4-1	30.00	-	29.71	2.II	1.01
L4-2	27.00	-	27.33	2.II	0.99
L5-1	27.00	-	26.73	2.II	1.01
L5-2	29.00	-	26.88	2.II	1.08
L6-1I	20.00	-	20.74	1.I	0.97
L6-1II	25.00	-	23.41	2.II	1.07
L6-2I	22.00	-	23.02	1.I	0.97
L6-2II	25.00	-	23.41	2.II	1.07

TABLE D-7: Comparison with the test beams of
Iyengar and Rangan [15]

Beam	Observed		Predicted		CRT
	T kNm	Mode	T kNm	Mode	
A5-3	2.916	-	2.671	2.II	1.09
A5-5	2.928	-	2.730	2.II	1.07
A5-8	2.420	-	2.707	2.II	0.89
B4-3	2.076	-	2.179	2.II	0.95
B4-5	1.984	-	2.130	2.II	0.93
B4-8	1.900	-	2.152	2.II	0.88
C4-2	3.754	-	3.760	1.I	1.00
C4-3	5.300	-	5.382	2.II	0.99
C4-4	6.360	-	5.492	2.II	1.16
C4-5	5.696	-	5.475	2.II	1.04
C4-6	5.410	-	5.163	2.II	1.05
C4-7	5.940	-	5.535	2.II	1.07
C4-8	5.470	-	5.420	2.II	1.01
D4-2	2.648	-	2.649	1.I	1.00
D4-3	3.692	-	4.056	2.II	0.91
D4-4	4.140	-	3.865	2.II	1.07
D4-5	3.848	-	3.806	2.II	1.01
D4-6	3.700	-	3.720	2.II	1.00
D4-7	3.615	-	3.680	2.II	0.98
D4-8	3.160	-	3.596	2.II	0.88
E4-2	2.832	-	2.772	1.I	1.02
E4-3	4.152	-	4.450	1.I	0.93
E4-4	5.340	-	5.491	1.I	0.97
E4-5	5.624	-	5.626	2.II	1.00
E4-6	5.860	-	5.560	2.II	1.05
E4-7	4.980	-	5.588	2.II	0.89
E4-8	4.860	-	5.454	2.II	0.89
F3-2	1.664	-	1.711	1.I	0.97
F3-3	2.720	-	2.964	1.I	0.92
F3-4	3.120	-	3.623	3.II	0.86
F3-5	3.384	-	3.808	3.II	0.89
F3-6	3.360	-	3.715	3.II	0.91
F3-7	.3.270	-	3.715	3.II	0.88
F3-8	2.710	-	3.768	3.II	0.72
G2-3	3.012	-	2.580	1.II	1.17
G2-5	4.408	-	3.877	1.I	1.14

TABLE D-8: Comparison with the test beams of Jackson and Estanero [46]

270

Beam	Observed		Predicted		CRT
	T kNm	Mode	T KNm	Mode	
G2-6	4.990	-	4.305	1.I	1.16
G2-7	5.440	-	5.175	1.I	1.04
G2-8	5.790	-	6.265	2.IV	0.92
AU-3	3.140	-	2.614	2.II	1.20
AU-5	2.928	-	2.539	2.II	1.15
AU-8	2.490	-	2.637	2.II	0.94
CU-2	3.166	-	3.242	1.I	0.98
CU-3	5.052	-	5.078	1.I	1.00
CU-4	6.294	-	5.262	2.II	1.20
CU-5	5.808	-	5.160	2.II	1.13
CU-6	6.040	-	5.136	2.II	1.18
CU-7	6.000	-	5.199	2.II	1.15
CU-8	4.920	-	5.009	2.II	0.98
DU-2	2.410	-	2.321	1.I	1.04
DU-3	3.760	-	3.762	1.I	1.00
DU-4	4.284	-	3.909	2.II	1.10
DU-5	4.168	-	3.871	2.II	1.08
DU-6	4.020	-	3.797	2.II	1.06
DU-7	4.125	-	3.781	2.II	1.09
DU-8	3.570	-	3.686	2.II	0.97
EU-2	2.560	-	2.454	1.I	1.04
EU-3	4.424	-	4.163	1.I	1.06
EU-4	5.466	-	5.210	1.I	1.05
EU-5	5.760	-	5.539	3.II	1.04
EU-6	6.350	-	5.414	3.II	1.17
EU-7	6.570	-	5.572	3.II	1.18
EU-8	5.110	-	5.520	3.II	0.93
GU-3	3.032	-	2.656	1.I	1.14
GU-5	4.608	-	3.903	1.I	1.18
GU-6	4.820	-	4.470	1.I	1.08
GU-7	5.265	-	4.999	1.I	1.05
GU-8	4.110	-	4.556	3.III	0.90

TABLE D-8 (CONTINUED): Comparison with the test
beams of Jackson and Estanero [46]

Beam	Observed		Predicted		CRT
	T in-kips	Mode	T in-kips	Mode	
BT2	39.18	-	25.71	1.I	1.52
BT3	61.20	-	43.42	1.I	1.41
BT4	78.36	-	57.32	1.I	1.37
BT5	85.72	-	62.26	2.II	1.38
TT6	79.92	-	64.86	2.II	1.23
BT1	143.40	-	92.31	2.II	1.55
BBT3	70.10	-	65.93	1.I	1.06
BBT4	72.60	-	68.84	1.I	1.06
BBT5	17.00	-	14.78	1.I	1.15
BBT6	138.00	-	92.31	2.II	1.50

TABLE D-9: Comparison with the test beams of Kemp [66]

Beam	Observed		Predicted		CRT
	T in-kips	Mode	T in-kips	Mode	
B-2	72.00	-	69.80	1.I	1.03
B-3	95.00	-	92.00	2.IV	1.03
B-4	85.00	-	98.30	2.IV	0.87
C-1	78.00	-	76.93	1.I	1.01
C-2	105.00	-	106.48	2.IV	0.99
C-3	111.00	-	114.73	2.IV	0.97
C-4	111.00	-	115.56	3.I	0.96
D-1	99.00	-	127.77	2.II	0.76
D-2	164.00	-	130.32	2.II	1.26
D-3	156.00	-	125.06	2.II	1.25
D-4	146.00	-	130.09	2.II	1.12
E-1	76.00	-	76.37	1.I	1.00
E-2	101.00	-	112.50	2.IV	0.90
E-3	121.00	-	105.34	2.IV	1.15

TABLE D-10: Comparison with test beams of Pandit
and Warwaruk [37]

Beam	Observed		Predicted		CRT
	T in-kips	Mode	T in-kips	Mode	
R-1	1.464	2	0.997	2.IV	1.47
R-2	1.575	2	0.997	2.IV	1.58
R-3	1.429	1	0.997	2.IV	1.43
R-4	1.230	1	0.954	1.I	1.29
R-5	0.958	1	0.736	1.I	1.30
R-6	0.585	1	0.501	1.I	1.17
RA-2	1.440	2	0.980	2.IV	1.47
RA-3	1.415	1	0.950	1.I	1.49
RA-4	1.187	1	0.943	1-I	1.26
RA-5	0.958	1	0.746	1.I	1.28
RA-6	0.574	1	0.505	1.I	1.14
RB-1	1.248	2	1.061	2.IV	1.18
RB-2	1.404	2	1.061	2.IV	1.32
RB-3	1.368	1	0.973	1.I	1.41
RB-4	1.008	1	0.706	1.I	1.43
RB-5	0.802	1	0.539	1.I	1.49
RB-6	0.466	1	0.355	1.I	1.31
RC-1	1.103	2	1.061	2.IV	1.04
RC-2	1.225	2	1.061	2.IV	1.15
RC-3	1.150	1	0.973	1.I	1.18
RC-4	1.023	1	0.707	1.I	1.45
RC-4A	0.960	1	0.706	1.I	1.36
RC-5	0.698	1	0.538	1.I	1.30
RC-5A	0.682	1	0.508	1.I	1.34
RC-6	0.466	1	0.355	1.I	1.31
RD-1	1.320	2	1.057	2.IV	1.25
RD-2	1.440	2	1.057	2.IV	1.36
RD-3	1.248	1	1.039	1.I	1.20
RD-4	0.840	1	0.734	1.I	1.14
RD-5	0.672	1	0.552	1.I	1.22
RD-6	0.432	1	0.359	1.I	1.20

TABLE D-11:   Comparison with the model beams of Zia and Gardenas [67]

Beam	Observed		Predicted		CRT
	T t.cm	Mode	T t.cm	Mode	
3	155.00	-	129.44	2.II	1.20
4	145.00	-	129.44	2.II	1.12
5	90.00	-	89.41	1.II	1.01
6	60.00	-	64.35	1.II	0.93
7	118.00	-	113.16	1.II	1.04
8	127.50	-	134.12	1.II	0.95
9	75.50	-	79.32	1.II	0.95
10	33.70	-	40.34	1.II	0.84

Table D-12:   Comparison with the test beams of Klus [68]

Beam	Observed		Predicted		CRT
	T in-kips	Mode	T in-kips	Mode	
RE1	81.40	2	87.93	2.IV	0.93
RE2	83.40	1	89.50	2.IV	0.93
RE3	81.50	1	86.78	1.III	0.94
RE4	74.60	1	71.52	1.III	1.04
RE5	66.00	1	60.96	1.I	1.08
RE4*	38.00	1	34.65	1.I	1.10
RU	73.30	3	82.27	3.III	0.89
RU3A*	76.00	3	86.16	3.III	0.88
RU2	84.90	3	82.81	2.IV	1.03
RU3	105.00	3	81.88	2.IV	1.28
RU3A	89.40	1	91.35	2.IV	0.98
RU4	85.50	-	94.87	2.IV	0.90
RU5	75.40	1	72.06	1.III	1.05
RU5A	68.30	1	66.13	1.I	1.03
RU6	59.10	1	56.57	1.III	1.05

TABLE D-13:   Comparison with the test beams of
               Collins et al [45]

Beam	Observed		Predicted		CRT
	T $M_p$cm	Mode	T $M_p$cm	Mode	
1-1	153.00	-	99.64	2.IV	1.54
1-1A	165.00	-	126.14	2.IV	1.31
1-2	128.00	-	103.09	1.III	1.24
1-3	68.00	-	59.43	1.III	1.14
1-4	131.00	-	101.56	2.IV	1.29
1-5	128.00	-	116.23	2.IV	1.10
1-6	67.00	-	61.06	1.III	1.10
2-1	108.00	-	71.76	2.II	1.51
2-1A	157.00	-	88.17	2.II	1.78
2-2	94.00	-	89.70	1.II	1.05
2-2A	128.00	-	101.20	1.I	1.27
2-3	67.00	-	57.81	1.I	1.16
3-1	190.00	-	89.87	2.IV	2.11
3-2	123.00	-	92.39	2.IV	1.33
3-3	68.00	-	62.92	1.I	1.08
3-4	136.00	-	108.35	1.I	1.26
4-1	141.00	-	94.17	2.IV	1.50
4-2	122.00	-	105.23	1.III	1.16
4-3	71.00	-	65.31	1.I	1.09
5-1	145.00	-	116.26	2.IV	1.25
5-1A	144.00	-	103.04	2.IV	1.40
5-2	146.00	-	102.67	2.IV	1.42
5-3	124.00	-	106.24	1.III	1.17
5-4	73.00	-	64.15	1.III	1.14
6-1	491.00	-	549.74	2.II	0.89
6-2	603.00	-	505.00	1.I	1.19
6-3	493.00	-	502.70	1.III	0.98
6-4	281.00	-	267.52	1.I	1.05
6-5	391.00	-	326.78	1.I	1.20
7-1	644.00	-	557.59	3.II	1.16
7-2	469.00	-	404.65	1.I	1.16
7-3	545.00	-	403.97	1.I	1.35
7-4	402.00	-	372.09	1.I	1.08
7-5	191.00	-	248.26	1.II	0.77
7-5A	332.00	-	318.21	1.II	1.04

TABLE D-14: Comparison with the test beams of
        Elfgren [69]

Beam	Observed		Predicted		CRT
	T t.cm	Mode	T t.cm	Mode	
B-8-K	144.00	-	98.67	2.IV	1.46
B-8-Ka	176.00	-	140.60	2.IV	1.27
B-8-0,1	60.00	-	55.54	1.III	1.08
B-8-0,1a	64.00	-	58.52	1.III	1.09
B-8-0,2	104.00	-	94.99	1.III	1.10
B-8-0,2a	112.00	-	95.66	1.III	1.17
B-8-0,4	152.00	2	121.68	1.II	1.25
B-8-0,4a	160.00	2	131.49	1.II	1.22
B-7-0,2	108.00	-	82.72	1.II	1.31
B-7-0,2a	104.00	-	90.32	1.II	1.15
B-10,0,2	120.00	1	98.14	1.III	1.22
B-10-0,2a	120.00	1	102.31	1.III	1.17
B-1	104.00	1	84.08	1.III	1.24
B-1a	104.00	1	87.28	1.III	1.19
B-2	160.00	1	139.27	1.III	1.15
B-2a	160.00	-	131.10	1.III	1.22
B-3	224.00	1,2	182.63	1.II	1.23
B-3a	224.00	1,2	183.40	1.II	1.22
B-4	301.00	2	189.27	1.II	1.59
B-4a	320.00	2	195.19	1.II	1.64
B-5	224.00	1	196.87	1.I	1.14
B-5a	224.00	1	181.27	1.I	1.24
B-6	192.00	1	161.34	1.I	1.19
B-6a	208.00	1	163.45	1.I	1.27
B-7	255.00	2	179.06	2.IV	1.42
B-7a	240.00	2	163.80	2.IV	1.47
B-8	180.00	2	144.24	2.II	1.25
B-8a	180.00	2	149.47	2.II	1.20
B-9	45.00	2	31.54	1.IV	1.43
B-9a	54.00	2	33.31	1.II	1.62
B-10	42.00	2	34.68	1.II	1.21
B-10a	48.00	2	32.56	1.II	1.47
B-11	42.00	1	28.49	1.IV	1.47
B-11a	42.00	1	29.28	1.IV	1.44
B-12	28.00	2	29.96	1.IV	0.94
B-12a	36.00	2	30.90	1.IV	1.17

TABLE D-15: Comparison with the test beams of Lyalin [9]

Beam	Observed		Predicted		CRT
	T t.cm	Mode	T t.cm	Mode	
BK-1	140.00	2	114.24	2.IV	1.23
BK-1a	120.00	2	101.35	2.IV	1.18
BK-2	170.00	2	109.29	2.IV	1.56
BK-2a	176.00	2	113.17	2.IV	1.56
BK-3	202.00	2	122.49	2.IV	1.65
BK-3a	172.00	2	109.07	2.IV	1.58
BN-4	128.00	1	81.43	2.IV	1.57
BN-4a	120.00	1	78.89	2.IV	1.52
BN-5	80.00	2	64.05	2.IV	1.25
BN-5a	78.00	2	68.00	2.IV	1.18
BN-6	80.00	2	62.00	2.IV	1.29
BN-6a	84.00	2	64.42	2.IV	1.30
Bπ-7	72.00	-	58.97	1.I	1.22
Bπ-7a	72.00	-	63.02	1.I	1.14
Bπ-8	84.00	-	66.51	1.IV	1.26
Bπ-8a	85.00	-	74.12	1.III	1.15
Bπ-9	102.00	-	77.31	2.IV	1.32
Bπ-9a	108.00	-	79.38	2.IV	1.36
Bπ-10	158.00	-	114.59	1.IV	1.38
Bπ-10a	144.00	-	115.89	1.IV	1.24
Bπ-11	140.00	-	124.24	1.IV	1.13
Bπ-11a	132.00	-	119.68	1.IV	1.10
Bπ-12	168.00	-	122.78	1.II	1.37
Bπ-12a	174.00	-	125.06	1.II	1.39
Bπ-13	108.00	-	93.64	1.II	1.15
Bπ-13a	144.00	-	101.82	1.II	1.41
Bπ-14	96.00	-	94.81	1.II	1.01
Bπ-14a	130.00	-	98.96	1.II	1.31
Bπ-15	180.00	-	135.22	1.III	1.33
Bπ-15a	174.00	-	133.00	1.III	1.31
Bπ-16	106.00	1	87.87	1.III	1.21
Bπ-16a	96.00	1	83.47	1.III	1.15
Bπ-17	96.00	1	87.09	1.I	1.10
Bπ17a	104.00	1	85.03	1.I	1.22
Bπ-18	132.00	2	117.68	2.IV	1.12
Bπ-18a	128.00	2	122.16	1.III	1.05

TABLE D-16: Comparison with the test beams of Lessig [35]

Beam	Observed		Predicted		CRT
	T t.cm	Mode	T t.cm	Mode	
Bπ-19	90.00	1	77.97	1.III	1.15
Bπ-19a	91.00	1	76.89	1.III	1.18
Bπ-20	144.00	-	144.43	1.1V	1.26
Bπ-20a	150.00	-	120.96	1.II	1.24
Bπ-21	139.00	-	111.27	1.II	1.25
Bπ-21a	114.00	-	114.01	1.II	1.00

TABLE D-16:(CONTINUED)   Comparison with the test beams
of Lessig [35]

Beam	Observed		Predicted		CRT
	T in-kips	Mode	T in-kips	Mode	
1-1	122.00	3	112.36	3.III	1.09
1-2	138.00	3	108.52	2.IV	1.27
1-3	140.00	3	120.30	2.IV	1.16
1-4	159.00	2,1	118.61	2.IV	1.34
1-5	131.00	1	115.78	2.IV	1.13
1-6	90.00	1	94.94	1.I	0.95
5-1	128.00	3	134.31	2.IV	0.95
5-2	141.00	2,3	149.21	2.IV	0.95
5-3	130.00	1	138.95	1.I	0.94
5-4	99.00	1	95.84	1.I	1.03
6-1	129.00	3	139.96	2.IV	0.92
6-2	145.00	3,2	147.15	2.IV	0.99
6-3	132.00	1	134.50	1.III	0.98
6-4	107.00	1	92.58	1.I	1.16
7-1	112.00	3	124.12	3.I	0.90
7-2	115.00	3	129.06	2.II	0.89
7-3	132.00	3,2	147.48	2.II	0.90
7-4	125.00	1,2	127.08	1.I	0.98

TABLE D-17: Comparison with the test beams of McMullen
and Warwaruk [52]

Beam	Observed		Predicted		CRT
	T in-kips	Mode	T in-kips	Mode	
A1	59.52	-	57.29	1.I	1.04
A2	64.15	-	61.62	1.I	1.04
A3	70.41	-	74.84	1.III	0.94
A4	77.33	-	82.58	1.III	0.94
A5	90.74	-	104.09	1.III	0.87
B1	78.51	-	68.74	1.I	1.14
B2	82.06	-	76.13	1.I	1.08
B3	93.32	-	84.96	1.III	1.10
B4	100.56	-	94.50	1.III	1.06
B5	115.48	-	106.36	1.III	1.09

TABLE D-18: Comparison with the test beams of Osburn [50]

Beam	Observed		Predicted		CRT
	T kNm	Mode	T kNm	Mode	
TM1	54.130	2	38.612	2.II	1.40
TM2	41.290	1	40.108	1.I	1.03
TM3	24.690	1	22.603	1.I	1.09
TMV1	40.460	2	40.281	1.II	1.00
TMV2	33.870	-	34.715	1.I	0.99
TMV3	22.590	-	16.942	1.I	1.33
TMV4	44.280	2	39.330	1.II	1.13
TMV5	39.460	-	35.775	1.II	1.10
TMV6	23.600	-	17.176	1.I	1.37
TMV7	43.620	2	43.691	1.II	1.00
TMV8	33.430	2	37.329	1.II	0.90

TABLE D-19: Comparison with the test beams of Staley [59]

Beam	Observed		Predicted		CRT
	T t.cm	Mode	T t.cm	Mode	
B-1	8.30	-	8.26	1.II	1.01
B-2	8.20	-	8.26	1.II	0.99
B-3	13.70	-	10.06	1.III	1.36
B-4	13.70	-	10.06	1.III	1.36
B-5	6.40	-	5.69	1.I	1.13
B-6	5.30	-	5.67	1.I	0.93
B-7	11.30	-	8.26	1.II	1.37
B-8	15.00	-	10.06	1.III	1.49
B-9	15.00	-	10.06	1.III	1.49
B-10	6.80	-	5.70	1.I	1.19
B-11	16.60	-	13.45	1.II	1.23
B-12	12.80	-	13.45	1.II	0.95
B-13	12.80	-	13.45	1.II	0.95
B-17	8.30	-	10.37	1.II	0.80
B-18	9.10	-	10.37	1.II	0.88
B-19	9.10	-	10.37	1.II	0.88
B-20	10.50	-	10.37	1.II	1.01
B-21	9.10	-	10.37	1.II	0.88
B-22	7.50	-	6.14	1.I	1.22

TABLE D-20: Comparison with the test beams of Yudin [48]

APPENDIX E

EXPERIMENTAL DATA USED IN THE COMPARISON

The experimental data used in the comparison for each investi-
gator is given in this appendix from table E-1 through to E-20 in
the same order as in Appendix D. This means that for example,
table E-1 is the experimental data used for table D-1, and DATA 01
in table E-1 is the experimental data for beam 3TR-1 in table D-1
of Ernst [20]. The points which should be noted in relation to the
preparation of these data can be recalled from section 5.5 of the
text.
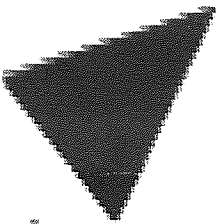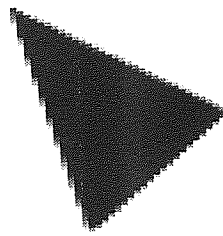
Illustration removed for copyright restrictions

TABLE E-1:   The experimental data of Ernst [20]
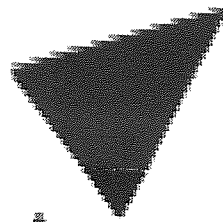
TABLE E-2: The experimental data of Hsu [10]

TABLE E-2 (CONTINUED): The experimental data of Hsu [10]

Aston University

Illustration removed for copyright restrictions
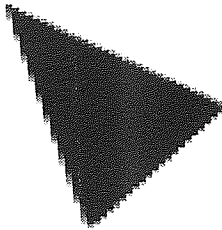
Aston University

Illustration removed for copyright restrictions

TABLE E-3: The experimental data of Swann [54].
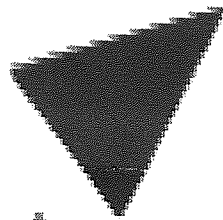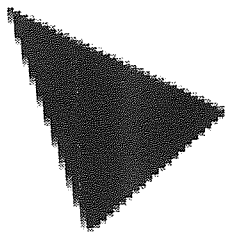
TABLE E-4: The experimental data of Evans and Sarkar [41]
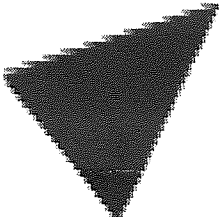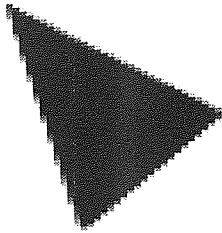
TABLE E-5: The experimental data of Gesund [40]
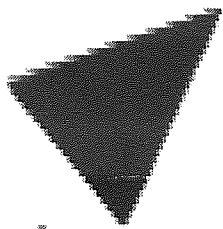
Illustration removed for copyright restrictions
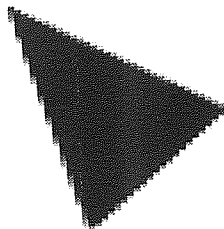
Illustration removed for copyright restrictions

TABLE E-6: The experimental data of Goode and Helmy [11]
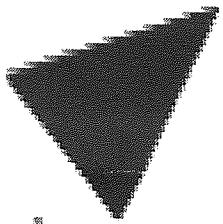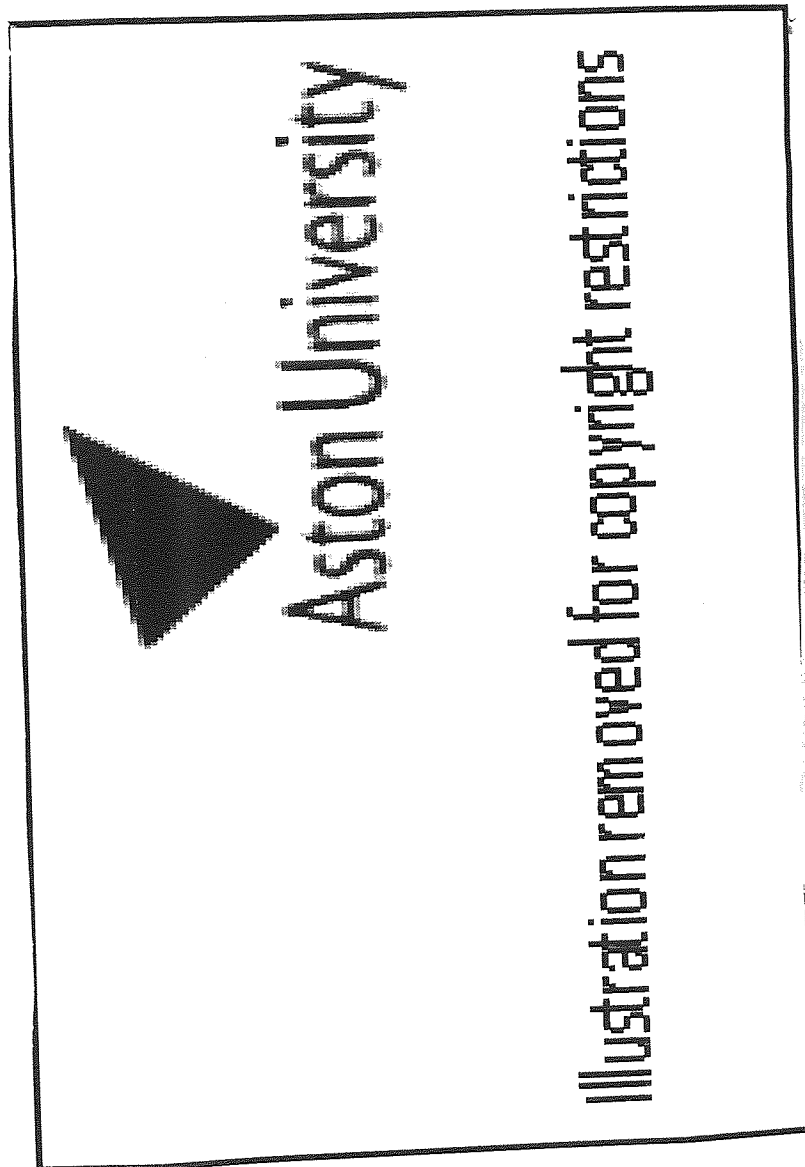
TABLE E-7: The experimental data of Iyengar and Rangan [15]
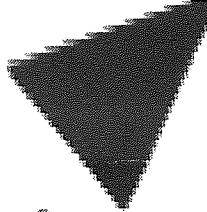
Aston University

Illustration removed for copyright restrictions
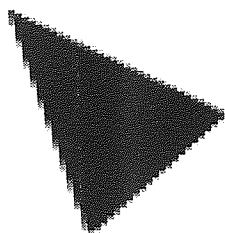
Aston University

Illustration removed for copyright restrictions

TABLE E-7 (CONTINUED): The experimental data of Iyengar and Rangan [15]

TABLE E-8: The experimental data of Jackson and Estanero [46]

TABLE E-8 (CONTINUED): The experimental data of Jackson and Estanero [46]
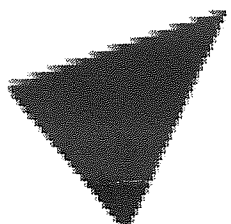
Aston University

Illustration removed for copyright restrictions
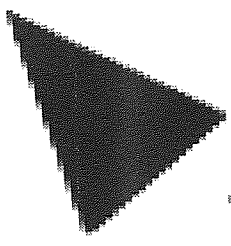
Aston University

Illustration removed for copyright restrictions

TABLE E-9: The experimental data of Kemp [66]
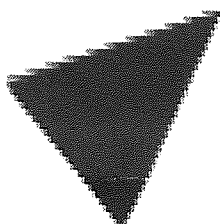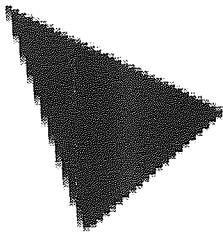
TABLE E-10: The experimental data of Pandit and Warwaruk [37]

TABLE E-11: The experimental data of Zia and Gardenas [67]
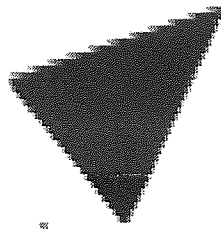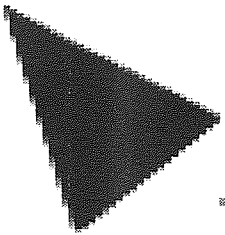
TABLE E-12: The experimental data of Klus [68]
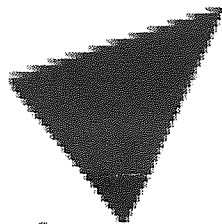
Aston University

Illustration removed for copyright restrictions
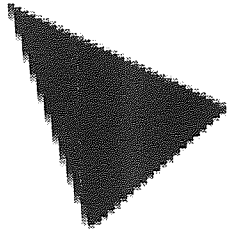
Aston University

Illustration removed for copyright restrictions

TABLE E-13:   The experimental data of Collins et al [45]
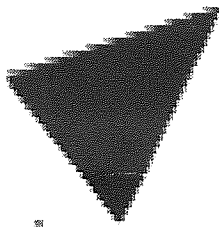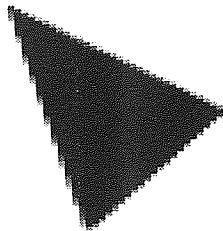
TABLE E-14: The experimental data of Elfgren [69]
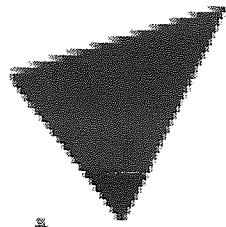
Aston University

Illustration removed for copyright restrictions
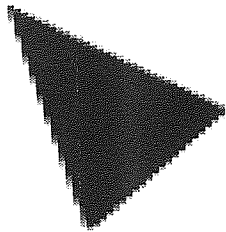
Aston University

Illustration removed for copyright restrictions

TABLE E-14 (CONTINUED): The experimental data of Elfgren [69]
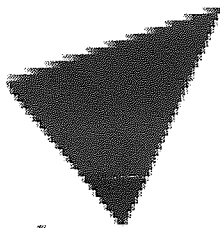
Aston University

Illustration removed for copyright restrictions
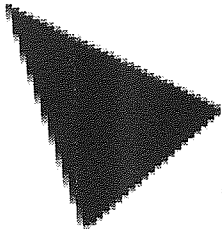
Aston University

Illustration removed for copyright restrictions

TABLE E-15:   The experimental data of Lyalin [9]
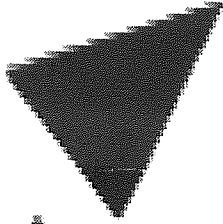
Aston University

Illustration removed for copyright restrictions
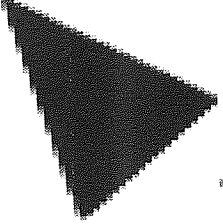
Aston University

Illustration removed for copyright restrictions

TABLE E-15 (CONTINUED): The experimental data of Lyalin [9]

Aston University

Illustration removed for copyright restrictions
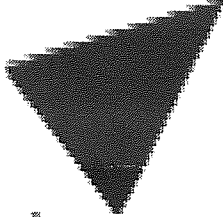
Aston University

Illustration removed for copyright restrictions
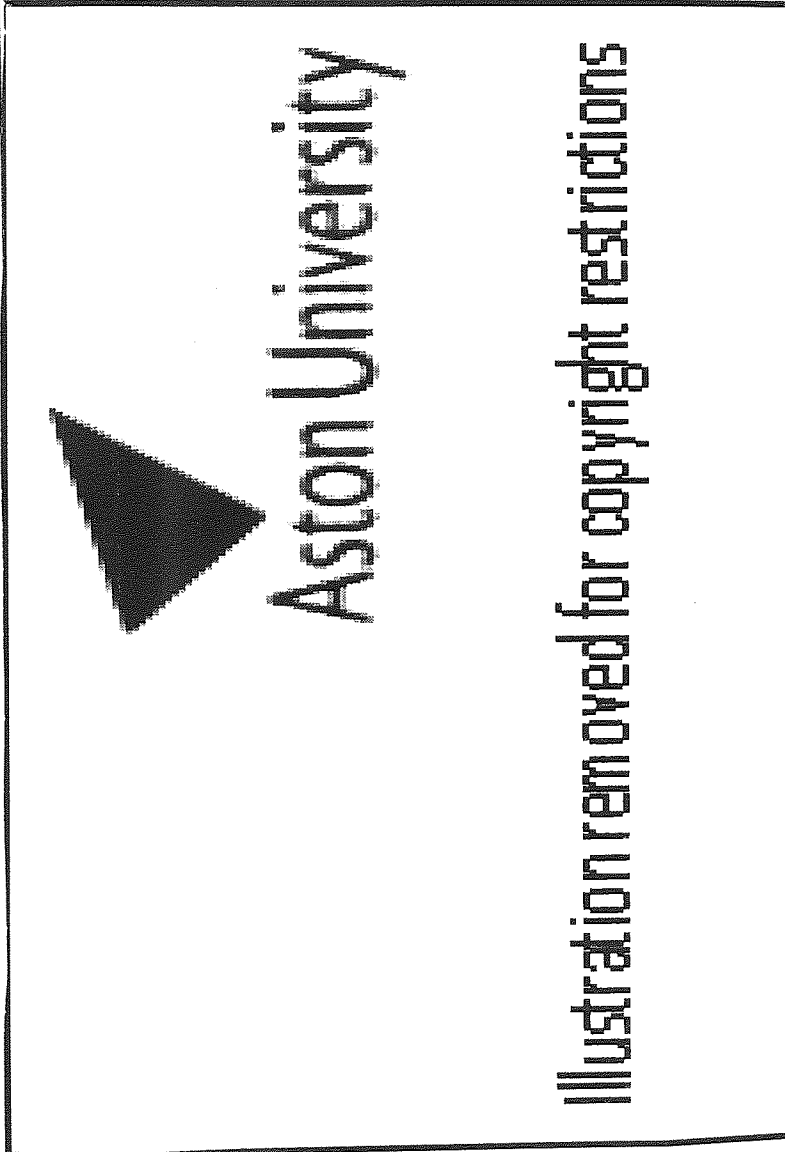
TABLE E-16:   The experimental data of Lessig [35]
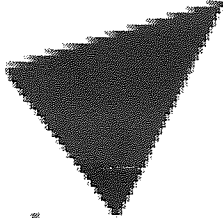
TABLE E-16 (CONTINUED): The experimental data of Lessig [35]
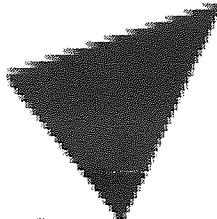
Aston University
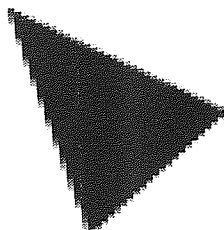
Illustration removed for copyright restrictions

TABLE E-17: The experimental data of McMullen and Warwaruk [52]
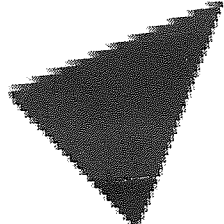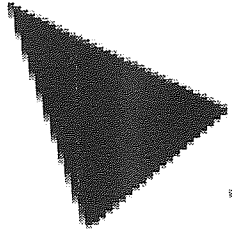
TABLE E-18: The experimental data of Osburn [50]
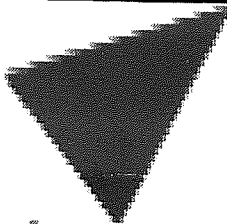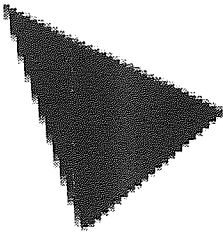
TABLE E-19: The experimental data of Staley [59]
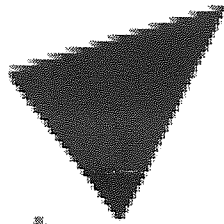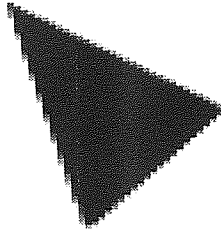
TABLE E-20: The experimental data of Yudin [48]

APPENDIX F

'FORTRAN LANGUAGE' LIST OF THE PROGRAMS

In this appendix the list of the program used in the analysis of the author's test beams is given first, followed by the list of the program used for the comparison of the author and other investigator's test results. For those sets of test data where the units differ from the author's, the program required an alteration for the values of E_c and E_s only, as follows;

metric units -

$E_c = 19636.0 . \sqrt{f'_c}$ where f'_c is in kgf/cm^2

$E_s = 2110344.8 \ kgf/cm^2$

imperial units -

$E_c = 74046.0 . \sqrt{f'_c}$ where f'_c is in lbf/in^2

$E_s = 30000000 \ lbf/in^2$

LIST F-1: Listing of the program used for the analysis
LIST(LF)
PROGRAM (FXXX)
INPUT 1=CRD
OUTPUT 2=LPD
COMPRESS INTEGER AND LOGICAL
TRACE 2
EXTENDED DATA
END
MASTER ANALYSIS
REAL M,KNI,KD,KS,KV,MY,K1,K2,K3
REAL KA1,KA2,KA3,KB1,KB2,KBB
REAL LL1W,LL2W,LL3W,L1W,L2W,L3W
REAL LL1L,LL2L,LL3L,L1L,L2L,L3L
REAL LL1C,LL2C,LL3C,L1C,L2C,L3C
WRITE (2,1)
1 FORMAT (1H1,/////,4X,'BEAM',5X,'TRY1',4X,'TRY2',
*4X,'TRY3',5X,'TSY1',4X,'TSY2',4X,'TSY3',5X,
*'TLY1',4X,'TLY2',4X,'TLY3',5X,'TCR1',4X,'TCR2',
*4X,'TCR3',5X,'TEST',//)
READ (1,10) N
10 FORMAT (I3)
L=1
3 READ (1,40)M,T,V,AS,FL,Y,AW,FW,X,S,AT,FT,H,D,FC
4 FORMAT (15F0.0)
M=1000.*M
T=1000.*T
WSI=W/T
DEL=V/T
KNI=0.5
KD=1.0
KS=1.5
KV=1.0
RW=SQRT(AW/3.1415927)
RD=SQRT(AD/3.1415927)
RT=SQRT(AT/3.1415927)
A1=(B-K)/2.
A2W=A1+RW+RB
A2T=A1+RW+RT
A3=(D-K)/2.
A4W=A3+RW+RB
A4T=A3+RW+RT
D1=H-A2W
D2=H-A2T
D3=H-A4T
F1=(2.*AD)/(H*D1)
F2=(AT+AT)/(H*D2)
F3=(2.*AT)/(S*D3)
K1=(AW*X)/(2.*AB*S)
K2=(AW*Y)/((AB+AT)*S)
K3=(AW*X)/(2.*AT*S)
WD=H/A

```
C   TYPE I FAILURE
C   -YIELDING OF BOTH SETS OF REINFORCEMENT
      EL1=1.0+(Y/X)
      EL2=1.0+(X/Y)
      EL3=1.0+(Y/X)
      R1Y=R1*(FW/FB)
      R2Y=(AW*FW*Y)/(((R3*FB)+(RT*FT))*S)
      R3Y=R3*(FW/FT)
      ELR1=EL1/R1Y
      ELR2=EL2/R2Y
      ELR3=EL3/R3Y
      ELQ1=EL1/(X*Y)
      ELQ2=EL2/X
      ELQ3=EL3/(X*Y)
      AY1=SQRT(ELQ1)
      AY2=ELQ2
      AY3=SQRT(ELQ3)
      ELRS1=SQRT(ELR1)
      ELRS2=SQRT(ELR2)
      ELRS3=SQRT(ELR3)
      BE1=0.5*ELRS1
      BE2=0.5*ELRS2
      BE3=0.5*ELRS3
      BOA1=BE1/AY1
      BOA2=BE2**2/AY2
      BOA3=BE3/AY3
      BOAS1=(BOA1*DEL)**2
      BOAS2=BOA2*DEL
      BOAS3=(BOA3*DEL)**2
      BES1=BE1**2
      BES2=BE2**2
      BES3=BE3**2
      BBR1=BES1+BOAS1
      BBR2=BES2+BOAS2
      BBR3=BES3+BOAS3
      KA1=1.0+(KD*HOB)
      KA2=1.0+(KD*BOD)
      KA3=1.0+(KD*HOB)
      KB1=4.0*BBR1
      KB2=4.0*BBR2
      KB3=4.0*BBR3
      K1=1.0/(KB1*R1Y)
      K2=1.0/(KB2*R2Y)
      K3=1.0/(KB3*R3Y)
      RS1=SQRT((PSI**2)+KB1)-PSI
      RS2=SQRT(KB2)
      RS3=SQRT((PSI**2)+KB3)+PSI
      TAN1Y=K1*RS1
      TAN2Y=K2*RS2
      TAN3Y=K3*RS3
```

310

```
      AFW=AW*FW
      G=AFW/S
      GW=G*X*Y
      TRY1=2.0*GW*TAN1Y
      TRY2=2.0*GW*TAN2Y
      TRY3=2.0*GW*TAN3Y
C   PARTIAL-YIELD OF THE REINFORCEMENT
      FC13=SQRT(FC)
      IF (FC.LT.27.5) GO TO 913
      EC=6149.2*FC13
      GO TO 914
  913 EC=1000.0*FC
  914 ES=206896.55
      SN=ES/EC
      MK=SN/(2.*KMI)
      DELP=1.+(DEL*(X/2.))
      DELN=1.-(DEL*(X/2.))
C   TYPE II FAILURE
C   -YIELDING OF THE WEB STEEL ONLY
      TAN1W=1.0
      TAN2W=1.0
      TAN3W=1.0
      TAT1W=KA1*TAN1W
      TAT2W=KA2*TAN2W
      TAT3W=KA3*TAN3W
      R1W=R1*TAN1W*TAN1W
      R2W=R2*TAN2W*TAN2W
      R3W=R3*TAN3W*TAN3W
      PA1W=R1W*TAN1W*TAT1W
      PA2W=R2W*TAN2W*TAT2W
      PA3W=R3W*TAN3W*TAT3W
      PB1W=PA1W/R1W
      PB2W=PA2W/R2W
      PB3W=PA3W/R3W
      PC1W=1.+PA1W
      PC2W=1.+PA2W
      PC3W=1.+PA3W
      PD1W=1.+PB1W
      PD2W=1.+PB2W
      PD3W=1.+PB3W
      PD1W=PD1W**2
      PD2W=PD2W**2
      PD3W=PD3W**2
      PE1W=PC1W/PD1W
      PE2W=PC2W/PD2W
      PE3W=PC3W/PD3W
      PF1W=P1*PE1W
      PF2W=P2*PE2W
      PF3W=P3*PE3W
```

311

```
D4W=NK*PF1W
D5W=NK*PF2W
D6W=NK*PF3W
D8W=D4W**2
D10W=D5W**2
D12W=D6W**2
DA1W=D8W+(2.*D4W)
DA2W=D10W+(2.*D5W)
DA3W=D12W+(2.*D6W)
DS1W=SQRT(DA1W)
DS2W=SQRT(DA2W)
DS3W=SQRT(DA3W)
DA4W=DS1W-D4W
DA5W=DS2W-D5W
DA6W=DS3W-D6W
DN1W=D1*DA4W
DN2W=D2*DA5W
DN3W=D3*DA6W
LL1W=D1-(KS*DN1W)
LL2W=D2-(KS*DN2W)
LL3W=D3-(KS*DN3W)
L1W=LL1W**2
L2W=LL2W**2
L3W=LL3W**2
DB1W=(X/2.)**2
DB2W=(Y/4.)**2
DB3W=(Y/2.)**2
RA1W=SQRT(L1W+DB1W)
RA2W=SQRT(L2W+DB2W)
RA3W=SQRT(L3W+DB3W)
FV1W=0.225*FC
FV2W=0.225*FC
FV3W=0.225*FC
TC1W=KV*8*DN1W*FV1W*RA1W
TC2W=KV*H*DN2W*FV2W*RA2W
TC3W=KV*8*DN3W*FV3W*RA3W
GW1W=G*X*(D1-DN1W)
GW2W=G*Y*(D2-DN2W)
GW3W=G*X*(D3-DN3W)
TSY1=(TC1W+GW1W)/DELP
TSY2=(TC2W+GW2W)/DELP
TSY3=(TC3W+GW3W)/DELM
```
C   TYPE III FAILURE
C   -YIELDIG OF THE LONGITUDINAL STEEL ONLY
C   STEEL ONLY
```
TAN1L=1.0
TAN2L=1.0
TAN3L=1.0
TAT1L=KA1*TAN1L
TAT2L=KA2*TAN2L
TAT3L=KA3*TAN3L
```

312

```
R1L=R1*TAN1L*TAN1L
R2L=R2*TAN2L*TAN2L
R3L=R3*TAN3L*TAN3L
PA1L=R1L*TAN1L*TAT1L
PA2L=R2L*TAN2L*TAT2L
PA3L=R3L*TAN3L*TAT3L
PB1L=PA1L/R1L
PB2L=PA2L/R2L
PB3L=PA3L/R3L
PC1L=1.+PA1L
PC2L=1.+PA2L
PC3L=1.+PA3L
PD1L=1.+PB1L
PD2L=1.+PB2L
PD3L=1.+PB3L
PD1L=PD1L**2
PD2L=PD2L**2
PD3L=PD3L**2
PE1L=PC1L/PD1L
PE2L=PC2L/PD2L
PE3L=PC3L/PD3L
PF1L=P1*PE1L
PF2L=P2*PE2L
PF3L=P3*PE3L
D4L=MK*PF1L
D5L=MK*PF2L
D6L=MK*PF3L
D9L=D4L**2
D10L=D5L**2
D12L=D6L**2
DA1L=D9L+(2.*D4L)
DA2L=D10L+(2.*D5L)
DA3L=D12L+(2.*D6L)
DS1L=SQRT(DA1L)
DS2L=SQRT(DA2L)
DS3L=SQRT(DA3L)
DA4L=DS1L-D4L
DA5L=DS2L-D5L
DA6L=DS3L-D6L
DN1L=D1*DA4L
DN2L=D2*DA5L
DN3L=D3*DA6L
LL1L=D1-(KS*DN1L)
LL2L=D2-(KS*DN2L)
LL3L=D3-(KS*DN3L)
L1L=LL1L**2
L2L=LL2L**2
L3L=LL3L**2
```

```
      DB1L=(Y/2.)**2
      DB2L=(Y/4.)**2
      DB3L=(X/2.)**2
      RA1L=SQRT(L1L+DB1L)
      RA2L=SQRT(L2L+DB2L)
      RA3L=SQRT(L3L+DB3L)
      FV1L=0.225*FC
      FV2L=0.225*FC
      FV3L=0.225*FC
      TC1L=KV*B*DN1L*FV1L*RA1L
      TC2L=KV*H*DN2L*FV2L*RA2L
      TC3L=KV*B*DN3L*FV3L*RA3L
      XY1=1./(1.+((D1-DN1L)/X))
      XY2=1./(1.+((D2-DN2L)/Y))
      XY3=1./(1.+((D3-DN3L)/X))
      GL1L=2.*AB*FB*LL1L*XY1
      GL2L=((AB*FB)+(AT*FT))*LL2L*XY2
      GL3L=2.*AT*FT*LL3L*XY3
      TLY1=(TC1L+GL1L)/(DELF+(PSI*XY1))
      TLY2=(TC2L+GL2L)/(DELF)
      TLY3=(TC3L+GL3L)/(DELA-(PSI*XY3))
C  NON-YIELDING OF THE REINFORCEMENT
C  TYPE IV FAILURE
C   -CRUSHING OF THE CONCRETE
      TAN1C=1.0
      TAN2C=1.0
      TAN3C=1.0
      TAT1C=KA1*TAN1C
      TAT2C=KA2*TAN2C
      TAT3C=KA3*TAN3C
      R1C=R1*TAN1C*TAN1C
      R2C=R2*TAN2C*TAN2C
      R3C=R3*TAN3C*TAN3C
      PA1C=R1C*TAN1C*TAT1C
      PA2C=R2C*TAN2C*TAT2C
      PA3C=R3C*TAN3C*TAT3C
      PB1C=PA1C/R1C
      PB2C=PA2C/R2C
      PB3C=PA3C/R3C
      PC1C=1.+PA1C
      PC2C=1.+PA2C
      PC3C=1.+PA3C
      PD1C=1.+PB1C
      PD2C=1.+PB2C
      PD3C=1.+PB3C
      PD1C=PD1C**2
      PD2C=PD2C**2
      PD3C=PD3C**2
      PE1C=PC1C/PD1C
      PE2C=PC2C/PD2C
      PE3C=PC3C/PD3C
```

314

```
PF1C=P1*PE1C
PF2C=P2*PE2C
PF3C=P3*PE3C
D4C=MK*PF1C
D5C=MK*PF2C
D6C=MK*PF3C
D8C=D4C**2
D10C=D5C**2
D12C=D6C**2
DA1C=D8C+(2.*D4C)
DA2C=D10C+(2.*D5C)
DA3C=D12C+(2.*D6C)
DS1C=SQRT(DA1C)
DS2C=SQRT(DA2C)
DS3C=SQRT(DA3C)
DA4C=DS1C-D4C
DA5C=DS2C-D5C
DA6C=DS3C-D6C
DN1C=D1*DA4C
DN2C=D2*DA5C
DN3C=D3*DA6C
LL1C=D1-(KS*DN1C)
LL2C=D2-(KS*DN2C)
LL3C=D3-(KS*DN3C)
L1C=LL1C**2
L2C=LL2C**2
L3C=LL3C**2
DB1C=(X/2.)**2
DB2C=(Y/4.)**2
DB3C=(X/2.)**2
RA1C=SQRT(L1C+DB1C)
RA2C=SQRT(L2C+DB2C)
RA3C=SQRT(L3C+DB3C)
FV1C=0.225*FC
FV2C=0.225*FC
FV3C=0.225*FC
TC1C=KV*6*DN1C*FV1C*RA1C
TC2C=KV*8*DN2C*FV2C*RA2C
TC3C=KV*8*DN3C*FV3C*RA3C
TOR1=2.*TC1C/DELP
TOR2=2.*TC2C/DELM
TOR3=2.*TC3C/DELM
TY1=T/TRY1
TY2=T/TRY2
TY3=T/TRY3
TS1=T/TSY1
TS2=T/TSY2
TS3=T/TSY3
TL1=T/TLY1
TL2=T/TLY2
TL3=T/TLY3
```

```
      TO1=T/TOR1
      TO2=T/TOR2
      TO3=T/TOR3
      T=T/1000000.
      TRY1=TRY1/1000000.
      TRY2=TRY2/1000000.
      TRY3=TRY3/1000000.
      TSY1=TSY1/1000000.
      TSY2=TSY2/1000000.
      TSY3=TSY3/1000000.
      TLY1=TLY1/1000000.
      TLY2=TLY2/1000000.
      TLY3=TLY3/1000000.
      TOR1=TOR1/1000000.
      TOR2=TOR2/1000000.
      TOR3=TOR3/1000000.
      IF (L.GT.9) GO TO 203
      WRITE (2,31)L,TRY1,TRY2,TRY3,TSY1,TSY2,TSY3,TLY1
     *,TLY2,TLY3,TOR1,TOR2,TOR3,T
   31 FORMAT (5X,'ROO',I1,1F9.3,2F8.3,1F9.3,2F8.3,1F9.
     *3,2F8.3,1F9.3,2F8.3,1F9.3)
      GO TO 190
  203 IF (L.GT.99) GO TO 204
      WRITE (2,32)L,TRY1,TRY2,TRY3,TSY1,TSY2,TSY3,TLY1,
     *TLY2,TLY3,TOR1,TOR2,TOR3,T
   32 FORMAT (5X,'RO',I2,1F9.3,2F8.3,1F9.3,2F8.3,1F9.3
     *,2F8.3,1F9.3,2F8.3,1F9.3)
      GO TO 190
  204 WRITE (2,33)L,TRY1,TRY2,TRY3,TSY1,TSY2,TSY3,TLY1,
     *TLY2,TLY3,TOR1,TOR2,TOR3,T
   33 FORMAT (5X,'R',I3,1F9.3,2F8.3,1F9.3,2F8.3,1F9.3,
     *2F8.3,1F9.3,2F8.3,1F9.3)
      GO TO 190
  190 L=L+1
      IF (L.GT.N) GO TO 200
      GO TO 30
  200 STOP
      END
      FINISH
```

```
NOLIST
PROGRAM(FXXX)
INPUT 1=CRD
OUTPUT 2=LPD
COMPRESS INTEGER AND LOGICAL
TRACE 2
EXTENDED DATA
END
MASTER COMPARISON
REAL M,KMI,KD,KS,KV,MK,K1,K2,K3
REAL KA1,KA2,KA3,KB1,KB2,KB3
REAL LL1W,LL2W,LL3W,L1W,L2W,L3W
REAL LL1L,LL2L,LL3L,L1L,L2L,L3L
REAL LL1C,LL2C,LL3C,L1C,L2C,L3C
WRITE (2,1)
1 FORMAT (1X,'TEST 1LP')
WRITE (2,2)
2 FORMAT (1X,'OBSERVATION MATRIX',8X,'W1')
WRITE (2,3)
3 FORMAT (1X,'MATRIX',14X,'S',5X,'W1',7X,'M')
READ (1,10) N
10 FORMAT (I3)
L=1
30 READ (1,40)M,T,V,AB,FB,Y,AW,FW,X,S,AT,FT,H,B,FC
40 FORMAT (15F0.0)
M=1000.*M
T=1000.*T
PSI=M/T
DEL=V/T
KMI=0.5
KD=1.0
KS=0.5
KV=1.0
RW=SQRT(AW/3.1415927)
RB=SQRT(AB/3.1415927)
RT=SQRT(AT/3.1415927)
A1=(B-X)/2.
A1B=A1+RW+RB
A2T=A1+RW+RT
A3=(D-Y)/2.
A4B=A3+RW+RB
A4T=A3+RW+RT
D1=H-A4B
D2=H-A2B
D3=H-A4T
P1=(2.*AB)/(B*D1)
P2=(AB+AT)/(H*D2)
P3=(2.*AT)/(B*D3)
R1=(AW*X)/(2.*AB*S)
R2=(AW*Y)/((AB+AT)*S)
R3=(AW*X)/(2.*AT*S)
```

```fortran
      HOB=H/B
      BOH=B/H
C  TYPE I FAILURE
C  -YIELDING OF BOTH SETS OF REINFORCEMENT
      EL1=1.0+(Y/X)
      EL2=1.0+(X/Y)
      EL3=1.0+(Y/X)
      R1Y=R1*(FW/FB)
      R2Y=(AW*FW*Y)/(((AB*FB)+(AT*FT))*S)
      R3Y=R3*(FW/FT)
      ELR1=EL1/R1Y
      ELR2=EL2/R2Y
      ELR3=EL3/R3Y
      ELG1=EL1/(Y*Y)
      ELG2=EL2/X
      ELG3=EL3/(X*Y)
      AY1=SQRT(ELG1)
      AY2=ELG2
      AY3=SQRT(ELG3)
      ELRS1=SQRT(ELR1)
      ELRS2=SQRT(ELR2)
      ELRS3=SQRT(ELR3)
      BE1=0.5*ELRS1
      BE2=0.5*ELRS2
      BE3=0.5*ELRS3
      BOA1=BE1/AY1
      BOA2=BE2**2/AY2
      BOA3=BE3/AY3
      BOAS1=(BOA1*DEL)**2
      BOAS2=BOA2*DEL
      BOAS3=(BOA3*DEL)**2
      BES1=BE1**2
      BES2=BE2**2
      BES3=BE3**2
      BBR1=BES1+BOAS1
      BBR2=BES2+BOAS2
      BBR3=BES3+BOAS3
      KA1=1.0+(KD*HOB)
      KA2=1.0+(KD*BOB)
      KA3=1.0+(KD*HOB)
      KB1=4.0*BBR1
      KB2=4.0*BBR2
      KB3=4.0*BBR3
      K1=1.0/(KB1*R1Y)
      K2=1.0/(KB2*R2Y)
      K3=1.0/(KB3*R3Y)
      RS1=SQRT((PSI**2)+KU1)-PSI
      RS2=SQRT(KB2)
      RS3=SQRT((PSI**2)+KU3)+PSI
```

318

```
      TAN1Y=K1*RS1
      TAN2Y=K2*RS2
      TAN3Y=K3*RS3
      AFW=AW*FW
      G=AFW/S
      GW=G*X*Y
      TRY1=2.0*GW*TAN1Y
      TRY2=2.0*GW*TAN2Y
      TRY3=2.0*GW*TAN3Y
C   PARTIAL-YIELD OF THE REINFORCEMENT
      FC13=SQRT(FC)
      IF (FC.LT.27.5) GO TO 913
      EC=6149.2*FC13
      GO TO 914
  913 EC=1000.0*FC
  914 ES=206896.55
      SM=ES/EC
      UK=SM/(2.*KMI)
      DELF=1.+(DEL*(X/2.))
      DELM=1.-(DEL*(X/2.))
C   TYPE II FAILURE
C   -YIELDING OF THE WEB STEEL ONLY
      TAN1W=1.0
      TAN2W=1.0
      TAN3W=1.0
      TAT1W=KA1*TAN1W
      TAT2W=KA2*TAN2W
      TAT3W=KA3*TAN3W
      R1W=R1*TAN1W*TAN1W
      R2W=R2*TAN2W*TAN2W
      R3W=R3*TAN3W*TAN3W
      PA1W=R1W*TAN1W*TAT1W
      PA2W=R2W*TAN2W*TAT2W
      PA3W=R3W*TAN3W*TAT3W
      PB1W=PA1W/R1W
      PB2W=PA2W/R2W
      PB3W=PA3W/R3W
      PC1W=1.+PA1W
      PC2W=1.+PA2W
      PC3W=1.+PA3W
      PD1W=1.+PB1W
      PD2W=1.+PB2W
      PD3W=1.+PB3W
      PD1W=PD1W**2
      PD2W=PD2W**2
      PD3W=PD3W**2
      PE1W=PC1W/PD1W
      PE2W=PC2W/PD2W
      PE3W=PC3W/PD3W
```

```
      PF1W=P1*PE1W
      PF2W=P2*PE2W
      PF3W=P3*PE3W
      D4W=MK*PF1W
      D5W=MK*PF2W
      D6W=MK*PF3W
      D8W=D4W**2
      D10W=D5W**2
      D12W=D6W**2
      DA1W=D8W+(2.*D4W)
      DA2W=D10W+(2.*D5W)
      DA3W=D12W+(2.*D6W)
      DS1W=SQRT(DA1W)
      DS2W=SQRT(DA2W)
      DS3W=SQRT(DA3W)
      DA4W=DS1W-D4W
      DA5W=DS2W-D5W
      DA6W=DS3W-D6W
      DN1W=D1*DA4W
      DN2W=D2*DA5W
      DN3W=D3*DA6W
      LL1W=D1-(KS*DN1W)
      LL2W=D2-(KS*DN2W)
      LL3W=D3-(KS*DN3W)
      L1W=LL1W**2
      L2W=LL2W**2
      L3W=LL3W**2
      DB1W=(X/2.)**2
      DB2W=(Y/4.)**2
      DB3W=(X/2.)**2
      RA1W=SQRT(L1W+DB1W)
      RA2W=SQRT(L2W+DB2W)
      RA3W=SQRT(L3W+DB3W)
      FV1W=0.225*FC
      FV2W=0.225*FC
      FV3W=0.225*FC
      TC1W=KV*2*DN1W*FV1W*RA1W
      TC2W=KV*H*DN2W*FV2W*RA2W
      TC3W=KV*2*DN3W*FV3W*RA3W
      GW1W=G*X*(D1-DN1W)
      GW2W=G*Y*(D2-DN2W)
      GW3W=G*X*(D3-DN3W)
      TSY1=(TC1W+GW1W)/DELP
      TSY2=(TC2W+GW2W)/DELM
      TSY3=(TC3W+GW3W)/DELM
C   TYPE III FAILURE
C   -YIELDIG OF THE LONGITUDINAL STEEL ONLY
C        STEEL ONLY
      TAN1L=1.0
      TAN2L=1.0
      TAN3L=1.0
```

```
TAT1L=KA1*TAN1L
TAT2L=KA2*TAN2L
TAT3L=KA3*TAN3L
R1L=R1*TAN1L*TAN1L
R2L=R2*TAN2L*TAN2L
R3L=R3*TAN3L*TAN3L
PA1L=R1L*TAN1L*TAT1L
PA2L=R2L*TAN2L*TAT2L
PA3L=R3L*TAN3L*TAT3L
PB1L=PA1L/R1L
PB2L=PA2L/R2L
PB3L=PA3L/R3L
PC1L=1.+PA1L
PC2L=1.+PA2L
PC3L=1.+PA3L
PD1L=1.+PB1L
PD2L=1.+PB2L
PD3L=1.+PB3L
PD1L=PD1L**2
PD2L=PD2L**2
PD3L=PD3L**2
PE1L=PC1L/PD1L
PE2L=PC2L/PD2L
PE3L=PC3L/PD3L
PF1L=P1*PE1L
PF2L=P2*PE2L
PF3L=P3*PE3L
D4L=NK*PF1L
D5L=NK*PF2L
D6L=NK*PF3L
D8L=D4L**2
D10L=D5L**2
D12L=D6L**2
DA1L=D8L+(2.*D4L)
DA2L=D10L+(2.*D5L)
DA3L=D12L+(2.*D6L)
DS1L=SQRT(DA1L)
DS2L=SQRT(DA2L)
DS3L=SQRT(DA3L)
DA4L=DS1L-D4L
DA5L=DS2L-D5L
DA6L=DS3L-D6L
DN1L=D1*DA4L
DN2L=D2*DA5L
DN3L=D3*DA6L
LL1L=D1-(KS*DN1L)
LL2L=D2-(KS*DN2L)
LL3L=D3-(KS*DN3L)
L1L=LL1L**2
L2L=LL2L**2
L3L=LL3L**2
```

```
      DB1L=(X/2.)**2
      DB2L=(Y/4.)**2
      DB3L=(X/2.)**2
      RA1L=SQRT(L1L+DB1L)
      RA2L=SQRT(L2L+DB2L)
      RA3L=SQRT(L3L+DB3L)
      FV1L=0.225*FC
      FV2L=0.225*FC
      FV3L=0.225*FC
      TC1L=KV*B*DN1L*FV1L*RA1L
      TC2L=KV*H*DN2L*FV2L*RA2L
      TC3L=KV*B*DN3L*FV3L*RA3L
      XY1=1./(1.+((D1-DN1L)/X))
      XY2=1./(1.+((D2-DN2L)/Y))
      XY3=1./(1.+((D3-DN3L)/X))
      GL1L=2.*AB*FB*LL1L*XY1
      GL2L=((AB*FB)+(AT*FT))*LL2L*XY2
      GL3L=2.*AT*FT*LL3L*XY3
      TLY1=(TC1L+GL1L)/(DELP+(PSI*XY1))
      TLY2=(TC2L+GL2L)/DELM
      TLY3=(TC3L+GL3L)/(DELM-(PSI*XY3))
C   NON-YIELDING OF THE REINFORCEMENT
C   TYPE IV FAILURE
C   -CRUSHING OF THE CONCRETE
      TAN1C=1.0
      TAN2C=1.0
      TAN3C=1.0
      TAT1C=KA1*TAN1C
      TAT2C=KA2*TAN2C
      TAT3C=KA3*TAN3C
      R1C=R1*TAN1C*TAN1C
      R2C=R2*TAN2C*TAN2C
      R3C=R3*TAN3C*TAN3C
      PA1C=R1C*TAN1C*TAT1C
      PA2C=R2C*TAN2C*TAT2C
      PA3C=R3C*TAN3C*TAT3C
      PB1C=PA1C/R1C
      PB2C=PA2C/R2C
      PB3C=PA3C/R3C
      PC1C=1.+PA1C
      PC2C=1.+PA2C
      PC3C=1.+PA3C
      PD1C=1.+PB1C
      PD2C=1.+PB2C
      PD3C=1.+PB3C
      PD1C=PD1C**2
      PD2C=PD2C**2
      PD3C=PD3C**2
      PE1C=PC1C/PD1C
      PE2C=PC2C/PD2C
      PE3C=PC3C/PD3C
```

```
PF1C=P1*PE1C
PF2C=P2*PE2C
PF3C=P3*PE3C
D4C=MK*PF1C
D5C=MK*PF2C
D6C=MK*PF3C
D8C=D4C**2
D10C=D5C**2
D12C=D6C**2
DA1C=D8C+(2.*D4C)
DA2C=D10C+(2.+D5C)
DA3C=D12C+(2.*D6C)
DS1C=SQRT(DA1C)
DS2C=SQRT(DA2C)
DS3C=SQRT(DA3C)
DA4C=DS1C-D4C
DA5C=DS2C-D5C
DA6C=DS3C-D6C
DN1C=D1*DA4C
DN2C=D2*DA5C
DN3C=D3*DA6C
LL1C=D1-(KS*DN1C)
LL2C=D2-(KS*DN2C)
LL3C=D3-(KS*DN3C)
L1C=LL1C**2
L2C=LL2C**2
L3C=LL3C**2
DB1C=(X/2.)**2
DB2C=(Y/4.)**2
DB3C=(X/2.)**2
RA1C=SQRT(L1C+DB1C)
RA2C=SQRT(L2C+DB2C)
RA3C=SQRT(L3C+DB3C)
FV1C=0.225*FC
FV2C=0.225*FC
FV3C=0.225*FC
TC1C=KV*B*DN1C*FV1C*RA1C
TC2C=KV*H*DN2C*FV2C*RA2C
TC3C=KV*B*DN3C*FV3C*RA3C
TOR1=2.*TC1C/DELP
TOR2=2.*TC2C/DELM
TOR3=2.*TC3C/DELM
TY1=T/TRY1
TY2=T/TRY2
TY3=T/TRY3
TS1=T/TSY1
TS2=T/TSY2
TS3=T/TSY3
TL1=T/TLY1
TL2=T/TLY2
TL3=T/TLY3
```

```
      TO1=T/TOR1
      TO2=T/TOR2
      TO3=T/TOR3
      IF (TY1.GE.TS1) GO TO 325
      GO TO 330
325   IF (TY1.GE.TL1) GO TO 335
      GO TO 330
335   IF (TY1.GE.TO1) GO TO 340
      GO TO 330
340   T1=TY1
      GO TO 420
330   IF (TS1.GE.TY1) GO TO 345
      GO TO 355
345   IF (TS1.GE.TL1) GO TO 355
      GO TO 355
355   IF (TS1.GE.TO1) GO TO 360
      GO TO 350
360   T1=TS1
      GO TO 420
350   IF (TL1.GE.TY1) GO TO 365
      GO TO 370
365   IF (TL1.GE.TS1) GO TO 375
      GO TO 370
375   IF (TL1.GE.TO1) GO TO 380
      GO TO 370
380   T1=TL1
      GO TO 420
370   T1=TO1
      GO TO 420
420   IF (TY2.GE.TS2) GO TO 425
      GO TO 430
425   IF (TY2.GE.TL2) GO TO 435
      GO TO 430
435   IF (TY2.GE.TO2) GO TO 440
      GO TO 430
440   T2=TY2
      GO TO 520
430   IF (TS2.GE.TY2) GO TO 445
      GO TO 450
445   IF (TS2.GE.TL2) GO TO 455
      GO TO 450
455   IF (TS2.GE.TO2) GO TO 460
      GO TO 450
460   T2=TS2
      GO TO 520
450   IF (TL2.GE.TY2) GO TO 465
      GO TO 470
465   IF (TL2.GE.TS2) GO TO 475
      GO TO 470
```

```
475 IF (TL2.GE.TO2) GO TO 480
    GO TO 470
480 T2=TL2
    GO TO 520
470 T2=TO2
    GO TO 520
520 IF (TY3.GE.TS3) GO TO 525
    GO TO 530
525 IF (TY3.GE.TL3) GO TO 535
    GO TO 530
535 IF (TY3.GE.TO3) GO TO 540
    GO TO 530
540 T3=TY3
    GO TO 50
530 IF (TS3.GE.TY3) GO TO 545
    GO TO 550
545 IF (TS3.GE.TL3) GO TO 555
    GO TO 550
555 IF (TS3.GE.TO3) GO TO 560
    GO TO 550
560 T3=TS3
    GO TO 50
550 IF (TL3.GE.TY3) GO TO 565
    GO TO 570
565 IF (TL3.GE.TS3) GO TO 575
    GO TO 570
575 IF (TL3.GE.TO3) GO TO 580
    GO TO 570
580 T3=TL3
    GO TO 50
570 T3=TO3
    GO TO 50
50  IF (T1.GT.T2) GO TO 60
    GO TO 90
60  IF (T1.GT.T3) GO TO 70
    GO TO 90
70  IF (L.GT.9) GO TO 203
    WRITE (2,31)L,T1
31  FORMAT (5X,'ROO',I1,1F8.3,4X,'*',7X,'*')
    GO TO 190
203 IF (L.GT.99) GO TO 204
    WRITE (2,32)L,T1
32  FORMAT (5X,'RO',I2,1F8.3,4X,'*',7X,'*')
    GO TO 190
204 WRITE (2,33)L,T1
33  FORMAT (5X,'R',I3,1F8.3,4X,'*',7X,'*')
    GO TO 190
90  IF (T2.GT.T1) GO TO 100
    GO TO 130
100 IF (T2.GT.T3) GO TO 110
```

```
      GO TO 130
113   IF (L.GT.9) GO TO 205
      WRITE (2,34)L,T2
 34   FORMAT (5X,'R.0',I1,4X,'*',1F11.3,4X,'*')
      GO TO 190
205   IF (L.GT.99) GO TO 206
      WRITE (2,35)L,T2
 35   FORMAT (5X,'R0',I2,4X,'*',1F11.3,4X,'*')
      GO TO 190
206   WRITE (2,36)L,T2
 36   FORMAT (5X,'R',I3,4X,'*',1F11.3,4X,'*')
      GO TO 190
130   IF (T3.GT.T1) GO TO 140
      GO TO 810
140   IF (T3.GT.T2) GO TO 150
      GO TO 811
150   IF (L.GT.9) GO TO 207
      WRITE (2,37)L,T3
 37   FORMAT (5X,'R.0',I1,4X,'*',7X,'*',1F11.3)
      GO TO 190
207   IF (L.GT.99) GO TO 208
      WRITE (2,38)L,T3
 38   FORMAT (5X,'R0',I2,4X,'*',7X,'*',1F11.3)
      GO TO 190
208   WRITE (2,39)L,T3
 39   FORMAT (5X,'R',I3,4X,'*',7X,'*',1F11.3)
      GO TO 190
810   IF (T1.EQ.T2) GO TO 900
      GO TO 811
811   IF (T2.EQ.T3) GO TO 901
      GO TO 812
812   IF (T3.EQ.T1) GO TO 902
      GO TO 900
900   IF (T2.GE.T3) GO TO 110
      GO TO 150
901   IF (T2.GE.T1) GO TO 110
      GO TO 70
902   IF (T2.GE.T3) GO TO 110
      GO TO 150
190   L=L+1
      IF (L.GT.N) GO TO 999
      GO TO 50
999   WRITE (2,4)
  4   FORMAT (1X,'END OF DATA')
      WRITE (2,6)
  6   FORMAT (1X,'PRINT MEANS',11X,'13  W1')
      WRITE (2,7)
  7   FORMAT (1X,'PRINT MEANS',11X,'13  W1',11X,'S')
      WRITE (2,8)
      FORMAT (1X,'GET OFF')
200   STOP
      END
      FINISH
```

REFERENCES

The abbreviations appearing in the references are explained below;

SP-18   Special Publication No 18

ACI   American Concrete Institute

ICE   Institution of Civil Engineers, London

ASCE   American Society of Civil Engineers

MCR   Magazine of Concrete Research, London

CCE   Concrete and Constructional Engineering, London

NSW   New South Wales, Australia

TSE   The Structural Engineer

TIE   The Institution of Engineers, Australia

CCA   Cement and Concrete Association, London

[1]   PUBLICATION SP-18

        Torsion of Structural Concrete

        American Concrete Institute, Detroit, Michigan, 1968

[2]   FISHER, G P and ZIA, P

        Review of code requirements for torsion design

        ACI Journal, Jan. 1964, Proceedings V 61, No 1, pp 1-44

[3]   TURNER, L and DAVIES, V C

        Plain and reinforced concrete in torsion

        ICE Selected Engineering Paper No 165, 1934

[4]   ZIA, P

        Torsion theories for concrete members

        ACI SP 18-4, 1968, pp 103-132

[5]   SANDEGREN, D S and YU, C W

        An equilibrium-compatability approach to the determination

        of the strength of reinforced concrete rectangular beams

        under combined bending and torsion.

        MCR March 1978, V 30, No 102, pp 3-10

[6]   ANDERSON, P

        Experiments with concrete in torsion

        ASCE Transaction, 1935, V 100, pp 949-983

[7]   COWAN, H J

        The strength of plain, reinforced and prestressed concrete

        under the action of combined stresses, with particular

        reference to the combined bending and torsion of rect-

        angular sections.

        MCR, Dec. 1953, V 5, No 14, pp 75-86

[8]   LESSIG, N N

        Theoretical and experimental investigation of reinforced

        concrete elements subjected to combined bending and

        torsion.

        Theory for Design and Construction of Reinforced Concrete

        Structures, Moscow, USSR, 1958, pp 73-84

[9]   LYALIN, I M

        Experimental studies of the behaviour of reinforced con-

        crete beams rectangular cross-section subjected to the

        combined action of transverse force, flexural and tor-

        sional moment.

        Concrete and Reinforced Concrete Institute, Moscow, USSR

        1959, Trudy No 5, pp 54-77. (Translated from Russian by

        Margarete Corbin, Foreign Literature Study No 402, for

        the PCA).

[10]   HSU, C T T

        Torsion of structural concrete -behaviour of reinforced

        rectangular concrete members.

        ACI SP 18-10, 1968, pp 261-306

[11]   GOODE, C D and HELMY, M A

        Ultimate strength of reinforced concrete beams in com-

        bined bending and torsion.

        ACI SP 18-13, 1968, pp 357-377

[12]   RAUSCH, E

        Berechnung des eisenbetons gegen verdrehung

        Julius Springer, Berlin, 1929.

[13]   MARSHALL, W T

        The torsional resistance of plastic materials with special

        reference to concrete

        CCE, April 1944, V 39, No 4, pp 83-88

[14]   COWAN, H J

            An elastic theory for the torsional strength of rectan-

            gular reinforced beams.

            MCR, July 1950, V 2, No 4, pp 3-7

[15]   IYENGAR, K T and RANGAN, B

            Strength and stiffness of reinforced concrete beams under

            combined bending and torsion

            ACI SP 18-15, 1968, pp 403-440

[15]   HALL, A S and ARCHER, F E

            The strength of reinforced concrete beams in torsion,

            bending and shear

            The Unviersity of NSW, UNICIV Report No R-31, March 1968

[17]   HSU, C T T

            Torsion of structural concrete - Plain concrete rectangular

            sections

            ACI SP 18-8, 1968, pp 203-238

[18]   MARTIN, L H

            A theoretical investigation into the ultimate strength in

            bending and torsion of plain and reinforced concrete

            members.

            PhD thesis, The University of Aston in Birmingham 1973

[19]   WALSH, P F, COLLINS, M P, ARCHER, F E and HALL, A S

            Experiments on the strength of concrete beams in combined

            flexural and torsion.

            The University of NSW, UNICIV Report No r-15, Feb. 1966

[20]   ERNST, G C

            Ultimate torsional properties of rectangular reinforced

            concrete beams.

            ACI Journal, Oct. 1957, Proceedings V 54, No 18, pp 341-356

[21]   BIRKELAND, C J

Strength of rectangular beams with longitudinal reinforce-

ment in combined torsion, bending and shear

MSc thesis, University of Washington, 1965

[22]   GESUND, H and BOSTON, L A

Ultimate strength in combined bending and torsion of con-

crete beams containing only longitudinal reinforcement.

ACI Journal, Nov. 1964, Proceedings V 61, No 11, pp 1453-1472

[23]   HSU, T T C

Torsion of structural concrete. A summary on pure torsion

ACI SP 18-6, 1968, pp 165-178

[24]   RANGAN, V

Discussion on Ref [22]

ACI Journal, Part 2, June 1965, Proceedings V 61, pp 1813-1815

[25]   NYLANDER, H

Vridning och vridningsinspaning vid betog konstructioner.

Statens Kommitee for Byggnadsferskning, Stockholm 1945,

Bulletin No 3.

[26]   COLLINS, M P, WALSH, P F, ARCHER, F E and HALL, A S

Reinforced concrete beams subjected to combined torsion

bending and shear.

The University of NSW, UNICIV Report R-14, Oct. 1965

[27]   HSU, T T C

Torsion of structural concrete - Interaction surface for

combined torsion, shear and bending in beams without

stirrups.

ACI Journal, Jan. 1968, Proceedings V 65, No 1, pp 51-60

[28]   MIRZA M S and McCUTCHEON, J O

The behaviour of reinforced concrete beams under combined

bending, shear and torsion

ACI Journal, May 1969, Proceedings V 66, No 5, pp 421-427

[29]   MATTOCK, A H, BIRKELAND, C J and HAMILTON, M E
         Strength of reinforced concrete beams without web rein-
         forcement in combined torsion, shear and bending.
         The Trend in Engineering. University of Washington,
         Oct. 1967, V 19, No 4, pp 8-12 and 29

[30]   ACI-ASCE COMMITTEE 328
         Shear and diagonal tension
         ACI Journal, Jan.-March 1962, Proceedings V59, Nos 1-3,
         Parts 1-3 pp 1-30, 277-334 and 353-396

[31]   ANDERSON, P
         Rectangular concrete sections under torsion
         ACI Journal, Sep. 1937, Proceedings V 34, No 1, pp 1-11

[32]   HSU, T T C
         Ultimate torque of reinforced rectangular beams
         ASCE Journal, Feb. 1968, Proceedings V 94, No ST2, pp 485-510

[33]   COWAN, H J and ARMSTRONG, S
         Experiments on the strength of reinforced and prestressed
         concrete-encased steel joists in combined bending and
         torsion.
         MCR, March 1955, V 7, No 19, pp 3-20

[34]   LESSIG, N N
         Determination of load carrying capacity of reinforced con-
         crete element with rectangular cross-section subjected to
         flexure with torsion.
         Concrete and Reinforced Concrete Institute, Moscow, USSR,
         1959, Trudy No 5, pp 5-28

[35]   LESSIG, N N
         Study of cases of failure of concrete in reinforced concrete
         elements with rectangular cross-section subjected to com-
         bined flexure and torsion.

Design of Reinforced Concrete Structures, Moscow, USSR, 1961, pp 229-271. (Translated from Russian by Margaret Corbin, Foreign Literature Study No 398, for PCA)

[36] KEMP, E L

An analytical and experimental study of torsion in reinforced concrete beams.

PhD thesis, University of Illinois, Urbana, 1962

[37] PANDIT, G S and WARWARUK, J

Reinforced concrete beams in combined bending and torsion

ACI SP 18-5, 1968, pp 133-163

[38] ELFGREN, L, KARLSSON, I and LOSBERG, A

Torsion-bending-shear interaction for concrete beams.

ASCE Journal, Aug. 1974, Proceedings V 100, No ST8, pp 1657-1676

[39] LAMPERT, P and COLLINS, M P

Torsion, bending and confusion - An attempt to establish the facts.

ACI Journal, Aug. 1972, Proceedings V 69, No 45, pp 500-504

[40] GESUND, H, SCHUETTE, F J, BUCHANAN, G R and GRAY, G A

Ultimate strength in combined bending and torsion of concrete beams containing both longitudinal and transverse reinforcement.

ACI Journal, Dec. 1964, Proceedings V 61, No 12, pp 1509-1521

[41] EVANS, R H and SARKAR, S

A method of ultimate strength design of reinforced concrete beams in combined bending and torsion.

TSE, Oct. 1965, V 43, No 10, pp 337-344

[42] COLLINS, M P, WALSH, P F, ARCHER, F E and HALL, A S

The design of rectangular reinforced concrete beams subjected to combined torsion, bending and shear.

The University of NSW, UNICIV Report No R-16, Aug. 1966

[43]   WALSH, P F, COLLINS, M P and ARCHER, F E

The flexural-torsion and shear-torsion interaction

behaviour of rectangular reinforced concrete beams.

TIE Civil Engineering Transactions, Oct. 1967, pp 313-317

[44]   FAIRBURN, D R and DAVIES, S R

Combined bending and torsion in reinforced concrete beams.

TSE, April 1969, V 47, No 4, pp 151-156

[45]   COLLINS, M P, WALSH, P F, ARCHER, F E and HALL, A S

Ultimate strength of reinforced concrete beams subjected

to combined torsion and bending.

ACI SP 18-14, 1968, pp 379-402

[46]   JACKSON, N and ESTANERO, R A

The plastic flow law for reinforced concrete beams under

combined flexure and torsion

MCR, Dec.1971, V 23, No 77, pp 169-180

[47]   YUDIN, V K

Determination of the load-carrying capacity of rectangular

reinforced concrete elements subjected to combined torsion

and bending.

Concrete and Reinforced Concrete, Moscow, USSR, June 1962,

No 6, pp 265-268

[48]   YUDIN, V K

Behaviour of reinforced concrete beams with rectangular

cross-section subjected to combined torsion and flexure.

Concrete and Reinforced Concrete, Moscow, USSR, Jan. 1964,

pp 30-35. (Translated from Russian by Margaret Corbin,

Foreign Literature Study No 431, for the PCA)

[49]   WALSH, P E, COLLINS, M P, ARCHER, F E and HALL, A S

The ultimate strength design of rectangular reinforced

concrete beams subjected to combined torsion, bending and shear.

TIE Civil Engineering Transaction, Oct. 1966, pp 143-157

[50]   OSBURN, D L

Strength of rectangular reinforced concrete beams with

web reinforcement in combined torsion, bending and shear.

MSc thesis, University of Washington, 1966

[51]   MATTOCK, A H

How to design for torsion

ACI SP 18-18, 1968, pp 469-495

[52]   McMULLEN, E A and WARWARUK, J

Concrete beams in bending, torsion and shear

ASCE Journal, May 1970, Proceedings V 96, No ST5, pp 885-903

[53]   ELFGREN, L, KARLSSON, I and LOSBERG, A

Discussion on Ref [52]

ASCE Journal, Feb. 1971, Proceedings V 97, No ST2, pp 729-731

[54]   SWANN, R A

Experimental basis for a design method for rectangular

reinforced concrete beams in torsion.

CCA, Dec. 1970, Technical Report No 42-452

[55]   WAINWRIGHT, P J

Ultimate strength in bending and torsion of prestressed

beams reinforced with longitudinal steel only.

PhD thesis, The University of Aston in Birmingham, 1972

[56]   ALLOS, A E

Prestressed concrete T-beams subjected to torsion, bending

and shear

PhD thesis, The University of Aston in Birmingham, 1977

335

[57]   COOPER M J

        Prestressed concrete beams in torsion, bending and shear.

        PhD thesis, The University of Aston in Birmingham, 1976

[58]   ELFGREN, L and KARLSSON, I

        Tests on rectangular reinforced concrete beams in combined

        bending, torsion and shear

        Chalmers University of Technology, Goteborg, SWEDEN,

        Oct. 1970, Division of Concrete Structures, Report 70-5

[59]   STALEY, R F

        Torsion, bending and shear in rectangular reinforced

        concrete beams - An experimental study.

        The University of NSW, UNICIV Report No R-178, Nov. 1978

[60]   HUGHES, B P

        Limit state theory for reinforced concrete design.

        2nd Edition, Pitman, London 1976

[61]   GOODE, C D and HELMY, M A

        Bending and torsion of reinforced concrete beams.

        MCR, Sept. 1968, V 20, No 64, pp 155-166

[62]   MARTIN, L H and WAINWRIGHT, P J

        Torsion and bending of prestressed concrete beams

        ASCE Journal, Nov. 1973, ProceedingsV 99, No ST11, pp 2229-2244

[63]   COOPER, M J and MARTIN, L H

        Prestressed concrete beams with no stirrups in torsion,

        bending and shear.

        ICE Proceedings, Part 2, June 1977, V 63, pp 455-468

[64]   ALLOS, A E and MARTIN, L H

        Longitudinally prestressed concrete T-beams subjected to

        torsion, bending and shear.

        ICE Proceedings, Part 2, June 1978, V 65, pp 359-380

[65]   BELOW, K D, RANGAN, B V and HALL, A S

         Theory for concrete beams in torsion and bending.

         ASCE Journal, Aug. 1975, Proceedings V 101, No ST8, pp

         1645-1660

[66]   KEMP, E L

         Behaviour of concrete members subjected to torsion and to

         combined torsion, bending and shear

         ACI SP 18-7, 1968, pp 179-201

[67]   ZIA, P and GARDENAS, R

         Combined bending and torsion of reinforced plaster model

         beams.

         ACI SP 18-12, 1968, pp 337-356

[68]   KLUS, J P

         Ultimate strength of reinforced concrete beams in combined

         torsion and shear

         ACI Journal, March 1968, pp 210-215

[69]   ELFGREN, L

         Reinforced concrete beams loaded in combined torsion

         bending and shear.

         Thesis presented to Chalmers University of Technology at

         Goteborg, SWEDEN, in 1972, for the degree of Doctor of

         Engineering (Division of Concrete Structures Publication

         71-3)

[70]   ACI COMMITTEE 318

         Building code requirements for reinforced concrete (ACI

         318-63).

         ACI, Detroit, 1963

[71]   CP 110:1972

         The structural use of concrete, Part 1.

         British Standards Institution, London

[72]   DESAYI, P and KRISHNAN, S

Equation of the stress-strain curve of concrete

ACI Journal, March 1964, V 61, No 22, pp 345-350